CONCENTRATIONS AND DEPOSITION OF ATMOSPHERIC SPECIES AT REGIONAL SITES IN SOUTHERN AFRICA

JACOBUS JOHANNES MARTINS
(M.Sc.)

Thesis submitted in fulfillment of the requirements for the degree of Philosophiae Doctor in Chemistry at the North-West University (Potchefstroom campus)

Supervisor: Prof. J.J. Pienaar (North-West University, Potchefstroom campus, SA)
Co-supervisor: Dr. C. Galy-Lacaux (Laboratoire d'Aérologie, Université Paul Sabatier, Toulouse, France)

Potchefstroom
2009

ABSTRACT

Increasing atmospheric emissions of trace gases as a result of fast-growing economies like South Africa, especially those of SO_2 and NO_2, are a major environmental concern. The air quality and thus air chemistry of a region ultimately determines the composition of the deposition taking place. The air quality of a region is determined by many factors, including transportation processes of neighbouring regions that remove, disperse and transform gas to aerosol and *vice versa*. All chemical processes from emission to removal of all the trace species within a region and the rate thereof are key factors in understanding the air quality of a region. Air quality on regional and multi-regional level needs to be determined in order to ensure sustainable development. By determining atmospheric depositions using ambient concentrations data, the air quality of regions can be better understood, leading to improved decision-making processes for sustainable development. For this study, regional air quality was determined using dry deposition estimates calculated from the ambient concentrations of gases and aerosols. This was done by creating a long-term data set of inorganic trace gases of interest, as well as data sets of aerosol species. Data of both gas and aerosol species were measured to coincide with each other in different regions to enable the modelling of atmospheric processes.

The measurements of monthly mean gaseous concentrations of sulphur dioxide (SO_2), nitrogen dioxide (NO_2), ammonia (NH_3), nitric acid (HNO_3) and ozone (O_3) at four remote sites — Louis Trichardt (South Africa), Cape Point (South Africa), Amersfoort (South Africa) and Okaukuejo (Namibia) — in southern Africa, over a period of nine to 11 years, were done by using a diffusive (passive) sampling technique. The average ambient SO_2 and NO_2 concentrations at Amersfoort were by far higher than any of the other sites and are characteristic of the highly industrialised region it is situated in. The O_3 concentrations were the most constant for all the sites during the sampling period, except at the Louis Trichardt site where it was slightly higher than at the other sites. The annual concentrations of all gaseous species measured decreased from 1995 to 2001, after which they increased somewhat. Strong inter-annual variations were observed, which proves the scientific value of decision-making based on long-term observations. The 10-year mean concentrations provided the highest mean ambient concentrations for SO_2 (2.8 ppb), NO_2 (2.5 ppb)

and HNO_3 (0.9 ppb) at the Amersfoort site, while the highest ambient concentrations of O_3 were found at Louis Trichardt (35 ppb) and for NH_3 (1.5 ppb) at Cape Point. Deposition estimates were made for the gaseous species using results from the inferential technique.

The organic and ionic compositions of ambient aerosol measured on a daily basis during seasonal campaigns at Amersfoort (AF) and Louis Trichardt (LT) in South Africa were determined for 2005-2007. The average aerosol measured during all four campaigns at Amersfoort consisted of a carbonaceous fraction of between 45-60% in winter and 33-36% for the summer season. The ionic fraction of the Amersfoort aerosol mainly consisted of sulphate, ammonia, nitrate and minerals/organic acids making up a total of 25%, 10%, 7% and 6% for winter and 44%, 15%, 3% and 4 % for summer, respectively. The aerosol measured at the Louis Trichardt site consisted of a carbonaceous fraction of between 31-56% in winter and 23-31% for summer. The ionic fraction of the Louis Trichardt aerosol species of sulphate, ammonia, nitrate and minerals/organic acids consisted of 23%, 7%, 6% and 16% for winter and 44%, 17%, 3% and 9 % for summer, respectively. High correlations were found between the inorganic species of SO_4^-, NH_4^+, and NO_3^- suggesting that they originate from the same sources. Wind trajectories were calculated using the HYPSPLIT model, which suggests the transport of aerosol species from the same sources over the Amersfoort and the Louis Trichardt regions. By using similar methods as *Guazzotti et al., 2003* during the INDOEX experiment, possible regional sources were identified through the organic and ionic composition of the measured aerosols. It was concluded from these results that complete combustion processes of fossil fuels dominate the ionic composition of aerosols over both these regions as well as the transformation reactions during transport. Only the formation of nitrate has different influences. The carbonaceous composition over the Amersfoort region is mainly influenced by incomplete biofuel and fossil fuel combustion processes. The carbonaceous content over the Louis Trichardt region is mainly influenced by incomplete biofuel combustion processes, of which biomass burning is the main contributor. The deposition rates of the inorganic aerosol species were calculated using results from the inferential technique, and this, together with the deposition rates of the gaseous species, was used to determine the total dry deposition of nitrogen and sulphate. It was found that approximately 30% of the atmospheric sulphur get deposited in the Amersfoort region through dry deposition, while 45% are deposited at Louis Trichardt. For total

atmospheric nitrogen, only 27% get deposited through dry deposition in the Amersfoort region, while 45% get deposited in the Louis Trichardt region.

The ORISAM-TM4 model was used to simulate secondary aerosol production over both the Amersfoort and Louis Trichardt sites. The measured gas and aerosol concentrations were compared with the ORISAM-TM4 model results. The model's simulation for the winter periods in general at both sites seems to be consistent and good for all secondary aerosols when no real temperature influences are present. Well correlating simulations were made when optimum conditions for key parameters (temperature, humidity, and precursor gas and aerosol concentrations) are present, as for the winter of 2006 campaign. The model, as well as the experimental results, shows more aerosol production during winter at both sites for all aerosol species. The model simulations are not too accurate during summer periods for both sites. The experimental BC/OC_{tot} ratios at the Amersfoort site compared well with those in literature. $OC_p/OC_p + OC_{sec}$ and BC/OCtot ratios of both sites in South African conditions again show the poor simulations of the model during summer. All the parameters for which the model were sensitive, as found in development testing, were found to be applicable for southern African conditions, which are as follows: temperature < gas concentrations < humidity < aerosol concentrations. Particle size does not seem to have any real effect on the secondary aerosol simulated by the model.

OPSOMMING (ABSTRACT)

Die toenemende vrystelling van spoorgasse deur ontwikkelende lande soos Suid-Afrika, is 'n groot omgewings kwelling, veral ten opsigte van swaweldioksied (SO_2) en stikstofdioksied (NO_2). Die lugkwaliteit van 'n bepaalde streek, en dus die chemie daarvan, bepaal ook die samestelling van die deposisie wat plaasvind. Verskeie faktore dra by tot die lugkwaliteit van 'n betrokke streek wat die lugtransportprosesse van naburige streke, die verwydering, verspreiding en tansformasie van gasse na aërosols en omgekeerd insluit. Alle betrokke chemiese prosesse, vanaf die vrystelling van atmosferiese spesies tot die verwydering daarvan in 'n streek, sowel as die tempo daarvan, is van belang wanneer die lugkwaliteit van 'n streek verstaan wil word. Indien die lugkwaliteit op streeksvlak of in geheel beheer wil word, moet dit eers bepaal word. Deur gebruik te maak van agtergrondkonsentrasies vir die bepaling van atmosferiese deposisies, kan die lugkwaliteit van 'n bepaalde streek bepaal en verstaan word, wat dan lei tot beter besluitneming ten opsigte van volhoubare ontwikkeling. Vir hierdie studie is 'n bepaalde streek se lugkwaliteit bepaal deur droë deposisiewaardes te bereken deur gebruik te maak van agtergrondkonsentrasies van gasse en aërosols. Dit is bereik deur langtermyn data vir die konsentrasie van gasse asook chemiese data vir aërosol-samestelling te bepaal. Die data is ook van so aard dat dit periodies ooreenkom vir beide gasse en aërosols en verskillende streke om die modellering van atmosferiese prosesse moontlik te maak.

Die gas-spesies van swaweldioksied (SO_2), stikstofdioksied (NO_2), ammoniak (NH_3), salpetersuur (HNO_3) en osoon (O_3) is op 'n maandelikse basis by die vier stasies — Louis Trichardt (Suid-Afrika), Kaappunt (Suid-Afrika), Amersfoort (Suid-Afrika) en Okaukuejo (Namibië) — in suider-Afrika, oor 'n tydperk van nege tot 11 jaar gemeet deur van 'n diffusie (passiewe) metingsmetode gebruik te maak. Die hoogste gemiddelde agtergrondkonsentrasies van SO_2 en NO_2 is by Amersfoort gemeet, wat kenmerkend is van die uitgebreide industriële streek waarin dit geleë is. Die O_3-konsentrasies was konstant vir al die stasies gedurende die metingsperiode, behalwe by Louis Trichardt waar dit hoër as by die ander stasies was. Die jaarlikse konsentrasies van al die gasse wat gemeet is, het afgeneem gedurende die 1995-2001 tydperk, waarna dit weer effens verhoog het. Groot variasies in konsentrasies tussen die jare is waargeneem, wat die belangrikheid van besluitneming op grond van

lang-termyn data toon. Die hoogste konsentrasies vir die tien-jaar gemiddeld was by Amersfoort en is SO_2 (2.8 ppb), NO_2 (2.5 ppb) en HNO_3 (0.9 ppb), terwyl die hoogste gemiddelde O_3-konsentrasies van 35 ppb by Louis Trichardt gemeet is. Die hoogste gemiddelde NH_3-konsentrasie van 1.5 ppb is by Kaappunt gemeet. Die deposisiewaardes vir die gasse is bepaal deur van resultate van die inferensiële tegniek gebruik te maak.

Deur daaglikse aërosol-metings in seisoenale metingsondersoeke gedurende 2005-2007, is die organiese en anorganiese aërosol-komponent vir beide Amersfoort (AF) en Louis Trichardt (LT) in Suid-Afrika bepaal. Die aërosol gemeet gedurende die vier ondersoeke by Amersfoort bestaan uit 'n gemiddelde koolstofkomponent van tussen 45-60% in die winter en 33-36% vir die somer. Die ioniese komponent van die Amersfoort aërosol bestaan hoofsaaklik uit sulfaat, ammoniak, nitraat en minerale/organiese sure wat, 'n onderskeidelike gemiddeld van 25%, 10%, 7% en 6% vir die winter en 'n gemiddeld van 44%, 15%, 3% en 4% vir somer van die totale inhoud van die aërosol opmaak. Die aërosol by Louis Trichardt bestaan uit 'n gemiddelde koolstofkomponent van tussen 31-56% vir die winter en 23-31% vir die somer. Die ioniese komponent van die Louis Trichardt aërosol bestaan hoofsaaklik uit sulfaat, ammoniak, nitraat en minerale/organiese sure wat 'n onderskeidelike gemiddeld van 23%, 7%, 6% en 16% vir die winter en 'n gemiddeld van 44%, 17%, 3% en 9% vir die somer van die totale inhoud van die aërosol opmaak. Die hoë korrelasies wat telkens tussen SO_4^{2-}, NH_4^+, en NO_3^- bestaan, dui daarop dat dit vanaf dieselfde besoedelingsbronne afkomstig is. Die wind-trajektor-simulasies wat met behulp van die HYPSPLIT model gemaak is, dui aan dat die aërosol-spesies vervoer word vanaf dieselfde besoedelingsbronne oor beide die Amersfoort en Louis Trichardt gebiede. Deur gebruik te maak van dieselfde metodes as *Guazzott et al., 2003* gedurende die INDOEX eksperiment, is moontlike besoedelingsbronne geïdentifiseer op grond van die gemete organiese en ioniese komponente van die aërosol. Vanuit hierdie resultate is afgelei dat volledige verbrandingsprosesse van fossielbrandstowwe die ioniese komponent van die aërosol in beide hierdie gebiede, sowel as die transformasie reaksies gedurende transport domineer. Net die onstaan van nitraat het ander invloede. Die koolstofinhoud van die aërosol oor die Amersfoort-streek word hoofsaaklik beïnvloed deur die onvolledige verbrandingsprosesse van bio- en fossielbrandstof. Die koolstofinhoud van die aërosol oor die Louis Trichardt-streek word hoofsaaklik beïnvloed word deur onvolledige biobrandstof

verbrandingsprosesse waarvan die hoofbron biomassaverbranding is. Deposisiewaardes vir die ioniese spesies in die aërosol is uit resultate van die inferensiële tegniek bereken. Hierdie aërosol-waardes is dan saam met die gas-deposisie waardes gebruik om die totale stikstof en sulfaat droë-deposisie te bepaal. Daar is gevind dat in totaal net 30% van die atmosferiese sulfaat in die Amersfoort-streek deur droë deposisie neerslaan, waarvan 45% in Louis Trichardt plaasvind. Die totale droë deposisie van atmosferiese stikstof is slegs 27% in die Amersfoort-streek, terwyl 44% in die Louis Trichardt-gebied neerslaan.

Die ORISAM-TM4 model is gebruik om die sekondêre aërosol-produksie vir beide Amersfoort en Louis Trichardt te simuleer. Die gemete gas en aërosol-data is ook met die ORISAM-TM4 model vergelyk. Die modelsimulasies gedurende die winter-periodes korreleer oor die algemeen goed met gemete waardes in albei gebiede en is deurgaans goed vir alle sekondêre aërosol vorming wanneer daar geen temperatuurinvloede teenwoordig is nie. Die simulasies is baie goed wanneer sleutel parameters toestande (temperatuur, humiditeit, voorlopergas en aërosol-konsentrasies) bekend is, soos in die winter van 2006. Beide die model- en eksperimentele resultate toon hoër aërosol-produksie tydens die winter vir alle aërosol-spesies by albei stasies. Die moduleringsimulasies tydens die somer vergelyk nie goed met gemete waardes nie. Die eksperimentele BC/OC_{tot} verhouding in Amersfoort vergelyk goed met die in literatuur. Die swak $OC_p/OC_p + OC_{sec}$ en BC/OC_{tot} verhoudings by beide stasies wys weer op 'n tekortkoming in die model om tydens somerkondisies in Suid-Afrika akkurate simulasies te lewer. Al die parameters waarvoor die model tydens ontwikkeling om voor sensitief gevind is, is ook gevind tydens die studie onder suider-Afrikaanse kondisies en is: temperatuur < gaskonsentrasie < humiditeit < aërosol-konsentrasies. Die partikelgrootte self het geen werklike invloed gehad op die sekondêre aërosol-simulering deur die model nie.

CONTENTS PAGE

CHAPTER 1 Motivation and goals

1.1 Motivation of the study from a global perspective 1

1.1.1 Motivation of the study from a South African perspective 3

1.1.2 Role of inorganic gases in atmospheric chemistry 3

1.1.3 Role of aerosols in atmospheric chemistry 4

1.1.4 Long range transport and chemical transformations 5

1.2 Study goals 7

CHAPTER 2 Literature survey

2.1 Introduction 9

2.1.1 Introduction to atmospheric pollution 10

2.1.2 Historical perspective 11

2.1.2.1 Historical perspective on atmospheric trace gases 11

2.1.2.2 Historical perspective on aerosols 14

2.2 Selection of species monitored 15

2.2.1 Gaseous species 15

2.2.2 Aerosols 16

2.3 Gaseous species 17

2.3.1 Sources and atmospheric processes of selected gaseous species 17

2.3.1.1 Sources and atmospheric processes of sulphur dioxide 17

2.3.1.2 Sources and atmospheric processes of ozone 20

2.3.1.3 Sources and atmospheric processes of nitrogen dioxide 24

2.3.1.4 Sources and atmospheric processes of nitric acid 29

2.3.1.5 Sources and atmospheric processes of ammonia 31

2.3.2 Health and environmental impacts of selected gaseous species 32

2.3.2.1 Impacts of sulphur dioxide 33

2.3.2.2 Impacts of ozone 34

2.3.2.3 Impacts of nitrogen dioxide 34

2.3.2.4 Impacts of nitric acid 35

2.3.2.5 Impacts of ammonia 35

2.4 Aerosols 35

2.4.1 Sources and atmospheric processes of aerosols 35

2.4.1.1 Primary particulate matter 36

2.4.1.2 Secondary particulate matter 36

2.4.1.3 Formation and growth of atmospheric aerosols 38

2.4.1.4 Removal of aerosols from the atmosphere 40

2.4.2 Health and environmental impacts of selected aerosols 41

2.4.2.1 Health impacts of aerosols 42

2.4.2.2 Climatic and other environmental impacts of aerosols 42

2.5 Dry deposition estimates of gaseous and aerosol species 44

2.6 Heterogeneous reactions between gases and aerosols 46

2.7 An overview of heterogeneous modelling 52

2.8 Climatology of the sub-continent 55

2.9 Conclusion 59

CHAPTER 3 Experimental Design

3.1 Introduction and choice of sampling sites 61

3.2 Important considerations when monitoring air pollutants 66

3.3 Selection of monitoring methods 67

3.3.1 Selection of gas monitoring method 67

3.3.2 Selection of aerosol monitoring method 67

3.4 Apparatus used in analysing samples 68

3.4.1 Dionex 100 Ion Chromatograph 68

3.4.2 UV-visible spectrophotometer 69

3.4.3 The DX 100 Ion Chromatograph 69

3.4.4 The DX 500 Ion Chromatograph 70

3.4.5 The Thermal/Optical Carbon Analyser 71

3.5 The gas monitoring method 72

3.5.1 Theory and functioning of passive (diffusive) samplers 72

3.5.1.1 Concentration calculations of passive sampling method 74

3.5.2 Species specific preparation of samplers prior to exposure 77

3.5.2.1 Preparation of sulphur dioxide samplers 78

3.5.2.2 Preparation of ozone samplers 78

3.5.2.3 Preparation of nitrogen dioxide samplers 79

3.5.2.4 Preparation of nitric acid samplers 79

3.5.2.5 Preparation of ammonia samplers 80

3.5.3 Quality control procedures 80

3.5.4 Preparing and analysing samples and standards 81

3.5.4.1 Preparing and analysing sulphur dioxide 81

3.5.4.2 Preparing and analysing ozone 82

3.5.4.3 Preparing and analysing nitrogen dioxide 82

3.5.4.4 Preparing and analysing nitric acid 83

3.5.4.5 Preparing and analysing ammonia 84

3.5.5 Inter-comparison and quality control for passive samplers 84

3.6 Aerosol monitoring method 88

3.6.1 Theory and functioning of the Air metric MiniVol sampler 88

3.6.2 Filter selection 92

3.6.2.1 Carbonaceous aerosol collection 92

3.6.2.2 Ionic aerosol collection 92

3.6.3 Quality control procedures 93

3.6.4 Preparation of samples for analysis 94

3.6.4.1 Preparing and analysing samples and standards 94

3.6.4.2 Preparation and analysis of carbonaceous sample filters 94

3.6.4.3 Preparation and analysis of ionic sample filters 95

3.6.4.4 Quality control for aerosol sampling 95

CHAPTER 4 Results of gaseous measurements

4.1 Introduction **97**

4.2 Results **98**

4.3 Monthly averages **99**

4.3.1 Sulphur dioxide 99

4.3.2 Nitrogen dioxide 100

4.3.3 Ozone 101

4.3.4 Ammonia 102

4.3.5 Nitric acid 103

4.4 Annual averages **104**

4.4.1 Sulphur dioxide 104

4.4.2 Nitrogen dioxide 105

4.4.3 Ozone 106

4.4.4 Ammonia 107

4.4.5 Nitric acid 108

4.5 Dependences and linkages **109**

4.6 Gaseous deposition estimates **112**

CHAPTER 5 Results of aerosol measurements

5.1 Introduction **123**

5.2 Averaged aerosol composition ($PM_{2.5}$ and PM_{10}) and possible regional sources **124**

5.2.1 Identification of possible regional sources contributing to the carbonaceous aerosol composition 124
5.2.2 Possible regional sources contributing to the ionic aerosol composition 135

5.3 Source related regional aerosol composition correlations 139

5.4 Tracking characteristic species within plumes from possible source regions 143

5.5 Source group estimations based on the ionic content of $PM_{2.5}$ and PM_{10} aerosols of the sampling campaigns 160

5.6 Comparison of aerosol concentration data with similar work done in South Africa 164

5.7 Dependences and linkages 165

5.8 Aerosol deposition estimates 166

CHAPTER 6 Modelling heterogeneous atmospheric processes

6.1 Introduction 171

6.2 Modelling results 172

6.3 Secondary aerosol formation and its validation 178

6.4 Dependences and linkages 179

CHAPTER 7 Critical evaluations

7.1 Evaluation of study objectives reached 180

7.2 Disappointments of study 182

7.3 Future research opportunities 182

BIBLIOGRAPHY

References 184

Appendix A Gas concentration data 212

Appendix B Aerosol concentration data 217

Acknowledgements 224

CHAPTER 1

Motivation and goals

In this chapter the motivation and relevancy of this study from a global perspective are discussed alongside its main goals. The importance of concentration and deposition of atmospheric species to air quality and the impacts of it on the environment are also discussed.

1.1 Motivation of the study from a global perspective

Since precipitation (deposition) scavenges airborne gases and particles, trends in precipitation chemistry will indicate changes in air quality and the chemical composition of the earth's atmosphere. These trends also reflect the combined effects of pollutant emissions (naturally or by human activities), physical and chemical transformations and climate.[1] As fast growing economies like southern Africa emits large quantities of these pollutants, it becomes important to find ways to study these emissions and its chemistry in order to quantify its impacts on the surrounding ecosystems and stability thereof. Long-term precipitation chemistry data represents a means to do just that. Similar studies in Europe where primary gases and wet deposition was monitored, led to a decrease of sulphur and oxidised nitrogen emissions over the last two decades.[2] Climate is also directly influenced by the atmospheric abundance of greenhouse gases and aerosols as changes in it can alter the energy balance of the earth's climatic system causing radiative forcing (RF).[3] Trace gases and aerosols have a significant RF effect that can either result in cooling or heating of the atmosphere (see Figure 1.1). Atmospheric chemistry controls the regional distribution of natural and anthropogenic pollutant species of gases and aerosols.[4] The climate and atmospheric chemical composition of a region directly influence the ecosystem stability and is therefore a very important consideration in sustainable development planning. The abundance of gases and aerosols is intimately linked to atmospheric chemistry and climate change, which is linked to the precipitation chemistry in each specific region. Determining the seasonal and annual

average ambient concentrations of selected pollution related species on a regional scale and linking it to deposition is the main aim of this study.

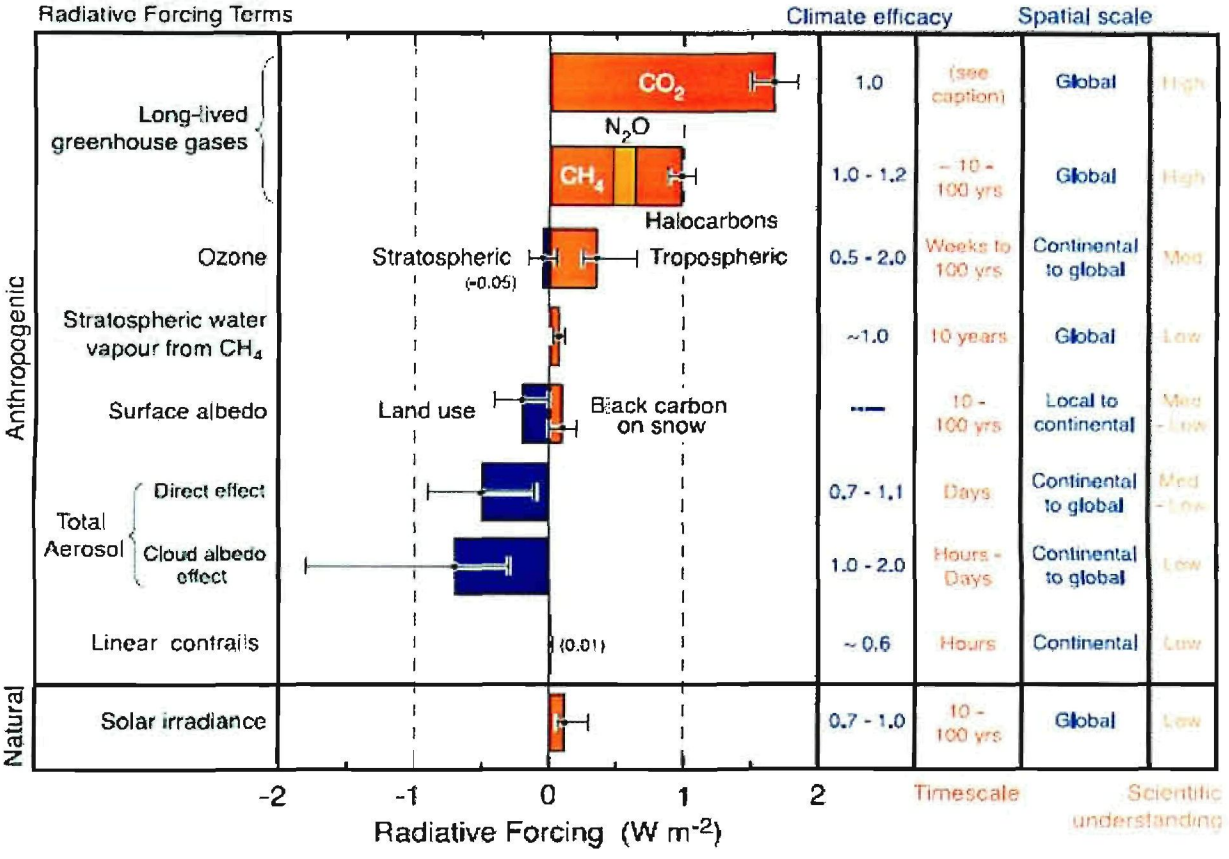


Figure 1.1: *The change in the global mean radiative forcing (RF) of atmospheric species between 1750 and 2005*[3]

The chemical compositions of aerosols in the atmosphere also have an important impact on its radiative forcing (RF) properties. Figure 1.1 gives an overview of the current understanding of RF changes since 1750. It is clear from this figure that a large uncertainty of the impact of aerosols on RF still exists. This uncertainty is to a large extent linked to uncertainties in the composition of aerosols. Gases and aerosols therefore need to be studied from a regional and multi-regionally perspective since its introduction into the atmosphere until its final deposition from it in order to better understand its chemistry and thus the climatic effects it will have in the region.

1.1.1 Motivation of the study from a South African perspective

Approximately 72% of South Africa's energy is produced from coal combustion[5] of which the highly industrialised region of the Mpumalanga Highveld and Gauteng (Johannesburg) accounts for 90% of South Africa's scheduled emissions of 2 million t/year SO_2, 1 million t/year NO_2 and 0.3 million t/year of particulates.[5] Consequently, rain quality in South Africa has been monitored intensely since 1985 by *Turner*[6,7] and *Held*[8] continued for 2000-2002 by *Held*[9] and *Mphepya*[10], while studies of dry deposition only started in 1994/95 by *Turner*[11] and *Zunckel*[12,13] and only for SO_2/SO_4^{2-} species. Continuous monitoring to calculate wet and dry deposition fluxes for mainly acids containing sulphur and nitrogen and its precursors aerosol and gases (SO_2 and SO_4^{2-}; NO_2 and NO_3^-) commenced in March 1996 by *Mphepya*[10, 14] and *Held.*[9] This study focuses only on the dry deposition of SO_2, NO_2, O_3, HNO_3 and NH_3 together with all the water soluble species in aerosols at selected sites in southern Africa during multiple years and seasons. The study also aims to incorporate the concentration data of both gases and aerosols into a suitable atmospheric model to predict secondary species formation during chemical reactions thereof. Thus tracking these atmospheric species from its emission into the atmosphere until it is finally removed by deposition.

1.1.2 Role of inorganic gases in atmospheric chemistry

The earth's atmosphere consists mainly of N ~ (78%), O_2 ~ (21%) and Ar ~ (1%) of which the concentrations are controlled by the biosphere over geological timescales, as well as the uptake and release from crustal material and degassing of the interior.[15] The remaining gaseous constituents are called the trace gases and represent less than 1% of the atmosphere, but play a crucial role in the earth's radiative balance as well as the chemical properties of the atmosphere.[15] Trace gases are produced by biological and geochemical processes on continents and in the ocean.[16] As seen in Figure 1.1, the scientific level of understanding of long-lived gases (highest positive RF (warming) effect) in the atmosphere is good, while only a medium level of scientific understanding exists for shorter lived gases like ozone (positive (warming) effect in troposphere and negative (cooling) effect in stratosphere). In order to improve the level of understanding of ozone (O_3), the atmospheric chemistry of inorganic precursor gases of O_3 like NO_2 and O_3 itself needs to be improved. In this study the main focus is key environmental inorganic gases that can ultimately also affect the formation of

secondary aerosols during transport. These inorganic gases include SO_2, NO_2, O_3, HNO_3 and NH_3. The effect of man-made emissions on the atmosphere is assessed by its RF properties.[3] A good understanding of the atmospheric cycles including natural and anthropogenic sources of the pollutant gases and their removal mechanisms is thus necessary.[17] Dry deposition removes gaseous substances from the atmosphere and represents an important sink in the atmospheric budget of many trace gas species.[18]

As many sources and sinks of gases in the atmosphere are a direct result of chemical reactions, a clear understanding of gas phase reaction rates is important. Chemical kinetics is concerned not only with the rate at which chemical processes take place, but also the mechanisms through which chemical change occurs,[19] which can easily be modelled with the necessary data input. For the evaluation and justification of any theoretical model, it must be compared to data physically collected in that specified region of the specific chemical species of interest. In this study, the seasonal and annual distribution of the inorganic gases mentioned is one of the main data inputs that will be collected.

1.1.3 Role of aerosols in atmospheric chemistry

The impacts of aerosols on the atmosphere are closely related to their chemical composition and size, which is very complex due to its chemical diversity and evolution in the atmosphere.[20] Aerosols are known to impact on gaseous chemistry[21] as well as being essential for the closure of radiative budgets.[22,23,24] Aerosols present in the atmosphere have two main origins:

i) primary aerosols emitted naturally and directly from the dispersal of solids from the earth's surface (i.e. through volcanoes and erosion) and anthropogenically (through industry and human activity); and

ii) the production of secondary aerosols as a direct result of transformation reactions between primary aerosols itself and with gases in the atmosphere.[25]

Aerosol particles have a short residence time in the atmosphere compared to gases, suggesting lower concentrations per unit mass emitted. This, however, does not influence their impact on the environment, which may be comparable to that of the long-lived gases due to their indirect effects on the concentrations of other pollutants through the heterogeneous chemistry that takes place on aerosol surfaces.[26] The

biggest uncertainties in climate change today are due to aerosol effects on the RF of the atmosphere as a direct result of the poor scientific understanding at this point in time, as indicated by the large uncertainties in Figure 1.1. Aerosols have a direct negative RF effect (cooling) by scattering incoming radiation and indirect negative RF effect (cooling) through cloud albedo. Aerosols potentially modify cloud size, lifetime, brightness, precipitation,[27] and the concentrations of trace gases.[26] The radiative, chemical and physical effects all ultimately depend on the aerosol composition and size, making it difficult to easily determine its radiative effect on biogeochemical cycles.[28,27,29] Until the mechanisms leading to background and anthropogenic aerosol formation and the removal thereof are fully understood within a theoretical framework (model), their influence on atmospheric chemistry and thus climate will not be fully understood.[30]

The effects of aerosols are dependent on the phase state of the particles (solid or liquid), their water content, and the partitioning of volatile components between the aerosol and vapour phases. Models are needed that can quickly and accurately predict the composition and state of the aerosol over wide ranges of temperature and relative humidities from the lower troposphere to the winter polar stratosphere.[31] Experimental data is needed not only to evaluate these models, but also to incorporated it as emission data in order to accurately model atmospheric processes. Improving the information on aerosol composition is one of the aims of this study.

1.1.4 Long-range transport and chemical transformations

Aerosols (natural or anthropogenic) can be transported over great distances and eventually be incorporated into each other.[32,33,26,34] Aerosols can serve as an active reaction site for chemical reactions (heterogeneous) and influence not only the partitioning of materials between the gas and aerosol phases,[26,34] but also the aerosol particle itself as inorganic gases emitted in each specific region are incorporated into the aerosol when it is transported over the region. This process is called aging of the aerosol and was previously studied in Asia by *Nishikawa,*[35,36] *Nishikawa* and *Kanamori,*[37] *Horai*[38] and *Harkel*[39] who reported that particulate sulphate and nitrate substitute volatile inorganic components in this region (hydrochloric acid in the case of sea-salt aerosol and carbonate/bicarbonate in the case of mineral aerosol) during the aging process. These interactions are dependent on the availability of gas-phase pollutants in the atmosphere as reported by *Lacaux,*[40] where dust particles emitted

from the Sahara desert are aged largely by formic and acetic acid products of the gas-phase reactions between isoprene and terpene formed during biomass burning. The need remains to more fully understand how primary aerosols age and how man-made pollutants are incorporated into natural aerosol particles.[41]

Southern Africa is an excellent geographical location for studying aerosol transformations consisting of all the primary factors involved in aerosol and gas-phase interactions, namely continental aerosol from arid areas, marine aerosol from the sea as well as the fossil-fuel combustion derived pollutants (SO_2 and NO_x). Biomass burning is one of the most intense sources of aerosol particles[42] and in Africa more biomass burning occurs than on any other continent[43] leading to massive, thick aerosol layers covering most of southern Africa during the dry season.[44] These plumes originate from biomass burning from central Africa to as far as plumes from South America through long-range transport.[45] Meteorological conditions in spring also favour the long-range transport of plumes of biomass combustion from central southern-Africa to South Africa.[46] The Southern African Research Science Initiative (SAFARI) has therefore launched several campaigns in the past in order to better understand the relationships between the physical, chemical, biological and anthropogenic processes that underlie the biogeophysical and biogeochemical systems of southern Africa and to predict regional sensitivities to atmospheric change.[45] SAFARI 2000 found that the haze layer has undergone significant modification during atmospheric transport, due to coagulation and condensation within 1-2 days from emission, through the two-fold increase in particle mass and elevated concentrations of secondary species such as SO_4^{2-}, NH_4^+ and NO_3^-.[47] Integrated stack coordinated measurements within these aerosol layers yielded large negative radiative forcing for both the surface and top atmosphere.[45] It is thus important to study these transformation processes of the aerosol from its emission into the atmosphere and during its transport until it reaches the region of interest and to compare it to modelling results.

In this study, modelling will be done using a combined ORISAM-0-D (Organic and Inorganic Spectral Aerosol Model,[48,49,20,50]) and Global CTM TM4 chemistry transport model[52,53] called the ORISAM-TM4 model. This model is able to accommodate size-differentiated chemistry in a selectable number of particle sizes and optional gas phase chemistry schemes to describe the composition change of aerosol particles due to strong and persistent interaction between the gas-phase anthropogenic pollutants

(SO_2, NO_X, HCl and NH_3) and aerosol particles.[41] The model focuses on the formation of secondary aerosols and especially secondary organic aerosols (SOA). This will also be relevant for the South African atmosphere where biomass/biofuel/fossil fuel all contribute to most of the aerosols formed, especially biofuel during dry season, when high inorganic gaseous emissions due to energy production are also taking place.

1.2 Study goals

Long-term air pollution measurements play a critical role in assessing the impact of the evolution and sustainability of ecosystems. This information is needed to improve our understanding of the behaviour of the atmosphere and its interactions with the biosphere.[8] The chemical content of atmospheric deposition is the product of numerous physical and chemical mechanisms that include emission, transport, chemical reactions and removal processes.[40] The long-term study of concentration, composition, transformation and deposition of atmospheric species consequently enables tracking the temporal and spatial evolution of atmospheric chemistry, and is a pertinent indicator of natural and anthropogenic influences on atmospheric conditions. Modelling of the formation/removal and aging processes of atmospheric species is the only way that allows the tracking of the species life cycle in the atmosphere and is an important tool in evaluating natural and anthropogenic influences. To enable such a study requires the monitoring of ambient air quality over a reasonable period of time[51] and is one of the main objectives in this study. The overall aims of this study are to:

i) Determine the ambient concentrations of the inorganic gases (SO_2, NO_2, O_3, HNO_3 and NH_3) and the water soluble fraction of aerosols (CH_3COO^-, $HCOO^-$, Cl^-, NO_3^-, SO_4^{2-}, $C_2O_4^{2-}$, Na^{2+}, NH_4^+, K^+, Mg^{2+} and Ca^{2+}) at selected sites in southern Africa.

ii) Validate all the analytical results by comparing them with standard quality check and control techniques of the US EPA (United States Environmental Protection Agency), WMO (World Meteorological Organization) and DEBITS (Deposition and Emission of Biogeochemical Important Trace Species) as well as participating in the development of new quality control procedures for diffusive samplers.

iii) Determining the total organic composition of aerosols (organic carbon (OC) and elemental carbon (BC)).

iv) Using the combined ORISAM-0-D (Organic and Inorganic Spectral Aerosol Model[48,49,20,50]) and Global CTM TM4 chemistry transport model[52,53] (called the ORISAM-TM4 model) to accommodate size-differentiated chemistry in a selectable number of particle sizes and optional gas phase chemistry schemes to model the fate of gas and aerosol species once they are emitted into the atmosphere.

v) Identifying possible sources that contribute to both inorganic (gas and aerosol) and organic (aerosol) composition and explaining the seasonal trends of the above-mentioned species at selected sites in southern Africa.

CHAPTER 2

Literature survey

This chapter gives a short general introduction to what air pollution is, its global extent, as well as the history of its main contributors. This is followed by the selection of specific gas and aerosol species important to this study. The selected gas and aerosol species are then discussed according to their sources and atmospheric processes, as well as their impacts on health and the environment. The method used to make dry deposition estimations for the selected gases and aerosols are also discussed. Heterogeneous reactions between the selected gases and aerosols are discussed, followed by a review of atmospheric modelling methods used to simulate these heterogeneous reactions. The climatology of southern Africa, which is extraordinary in its location and conditions influencing its air quality and the meteorology promoting it, is also discussed. Lastly, all the aspects that need to be addressed in such a study are briefly mentioned.

2.1 Introduction

It is difficult to imagine a modern society without the benefits of chemicals and industry. Pharmaceuticals, petrochemicals, agrochemicals, and industrial and consumer production processes, which contribute to modern lifestyles, all give entry for potentially harmful substances into the environment at any stage of its life cycle.[54] The introduction of harmful substances into the environment has been shown to have many adverse effects on human health, agricultural productivity and natural ecosystems.[55] The rise of industrialised economies producing harmful substances increased the public concern and awareness regarding the presence and impacts of these substances.

2.1.1 Introduction to atmospheric pollution

Air pollution can be defined as:

> i) a state in which substances are present in the atmosphere as a direct result of anthropogenic activities
> ii) in concentrations significantly higher than its normal ambient levels
> iii) producing measurable effects on humans, animals, vegetation and materials.[15]

Air pollution causes many environmental problems, such as the increase of tropospheric oxidants, changes in the self-cleaning ability of the atmosphere, perturbation of biogeochemical cycles, acid precipitation, radiative effects due to an increase in greenhouse gases and aerosols, the depletion of stratospheric ozone, as well as the related environmental impacts that all force global environmental changes.[16]

It is estimated that around six million chemical compounds have been created by humans during their history, of which most was created during the 20th century. At present, approximately 1000 new compounds are synthesised each year. Today, approximately 60 000 to 95 000 chemicals are used commercially[55] in industrial processes. Many of these compounds are introduced into the environment. Most sources of air pollutants are located within the troposphere, which extends 15 km in altitude over the equator into the 300 km thick atmosphere and 10 km over the poles.[56] The tropospheric boundary layer (in contact with earth's surface) is separated from the free troposphere by a temperature inversion (a horizontal band, in which temperature increases with height), through which little exchange of air can occur. Therefore, most of the air pollutants emitted into the tropospheric boundary layer are trapped within it.[54]

Chemical elements are circulated through the global environment within a biogeochemical cycle that can be described as exchange fluxes between reservoirs (atmosphere, terrestrial ecosystems and ocean).[16] The biogeochemical cycles of natural gas and aerosol species in the earth's systems are disturbed by means of socio-economic factors such as resource use, industrial activity, and land conversion (e.g., agricultural activity, deforestation and biomass burning), which release large quantities of pollutant species in regions of high energy production and/or high

population density, such as North America, Europe, Eastern Asia[16] and also South Africa. These cycles of atmospheric pollutants mainly involve two processes:

i) the formation of pollutants by means of chemical processes within the atmosphere itself (secondary pollutants), biological activity, volcanic exhalation, radioactive decay and man's industrial activities (primary pollutants); and
ii) the removal of pollutants from the atmosphere, which involves chemical reactions in the atmosphere, biological activity and physical processes in the atmosphere (such as particle formation), leading to the deposition of pollutant species and the uptake of it by oceans and the earth.[17]

The introduction of new chemical compounds, as well as the continued release of large quantities of already existing pollutants into the atmosphere, will adversely affect both processes of the biogeochemical cycle of atmospheric species (natural and anthropogenic). This will lead to significant impacts on both human health and the sustainability of the environment.

2.1.2 Historical perspective

Since the beginning of the industrial era, and even before it, gases and aerosols have been emitted from various natural and human activities, ranging from agricultural and mining activities to production processes involving large quantities of chemical compounds and combustion processes. As a result, many of these gases and aerosols are accumulating due to insufficient removal processes and therefore leads to environmental changes. The major gas and aerosol species that are accumulating and causing environmental problems are discussed briefly in the following paragraphs.

2.1.2.1 Historical perspective on atmospheric trace gases

The atmosphere is composed primarily of nitrogen (78%), oxygen (21%), and several noble gases (<1%), of which the concentrations stay remarkably constant over time.[15] They share the atmosphere with a variety of trace gases, which can occur either in small or high variable amounts,[15] and represent less than 1% of the atmosphere. The abundances of the trace gases have changed remarkably over the last two centuries. Although they represent only a small quantity of the atmosphere, they play a crucial role in atmospheric chemistry and the earth's radiative budget.[15]

Since the industrialisation era, carbon dioxide (CO_2) concentrations, of all trace gases, have increased the most, as can be seen in Figure 2.1 (ppm).[3] This is mainly due to emissions from fossil fuel combustion and biomass burning activities.[16] Carbon dioxide is the single most important waste product of the industrialised society,[15] making it the most important greenhouse gas (earth warming gas) as shown in Figure 1.1 (Chapter 1, Paragraph 1.1). This is mainly due to its relatively high concentration and its ability to absorb radiation reflected back from the earth's surface.

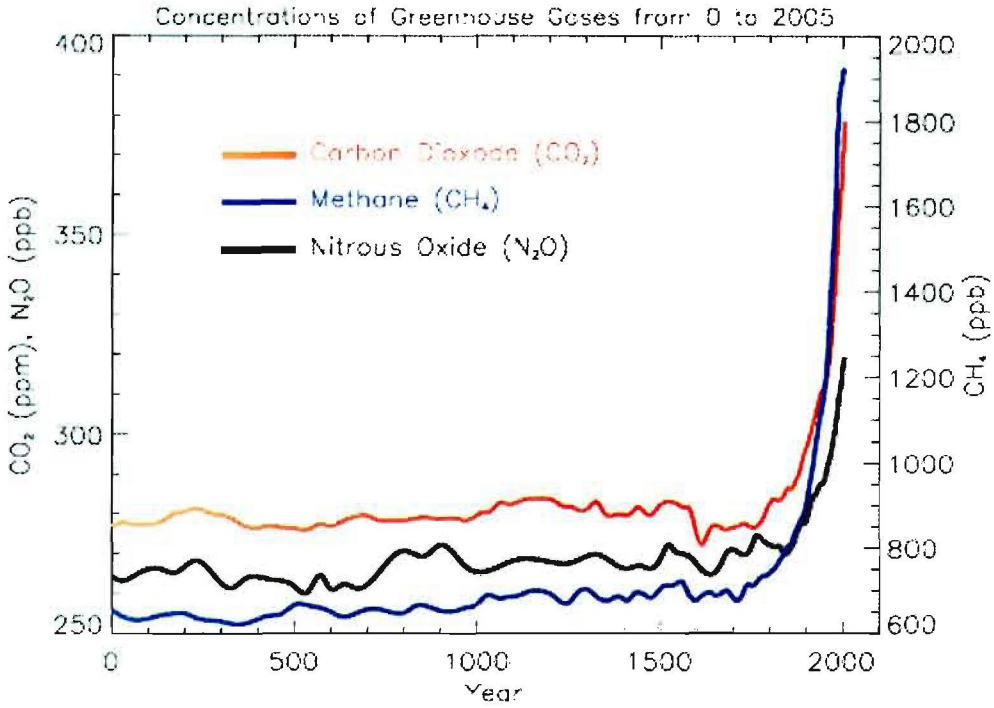


Figure 2.1: *The atmospheric concentrations of important long-lived greenhouse gases over the last 2 000 years. Increases since 1750 are attributed to human activities in the industrial era*[3]

Methane (CH_4) is another significant trace gas that has increased significantly since the industrial era, as seen in Figure 2.1.[3] Methane is also the second most important greenhouse gas as was shown in Figure 1.1 (Chapter 1, Paragraph 1.1). It is produced mainly by means of biogenic processes (wetlands, live stock, landfills, biomass burning), as well as the leakage of gas distribution systems.[16] Theoretically, four ozone (O_3) molecules are produced by the oxidation of one CH_4 molecule, if enough NO_x is present.[15] Methane therefore plays an important role in the photochemistry of the troposphere and stratosphere,[16] since it indirectly contributes to the production of O_3 within both atmospheric layers. Methane therefore indirectly

contributes to the environmental impacts that O_3 might have. Ozone and its impacts will be discussed later.

Progressive modification and fertilisation of the terrestrial biosphere are believed to have caused the increase of nitrous oxide (N_2O),[16] which is shown in Figure 2.1.[3] Nitrous oxide is a relatively inert gas in the troposphere, where its impacts are mainly climatic, having an absorbing potential 300 times stronger than that of CO_2.[15] In the stratosphere, N_2O is a major source of the ozone depleting species of NO and NO_2.[16] By being a source of these O_3 depleting species, it indirectly plays a significant role in the climatic impacts the depletion of stratospheric O_3 will have on health and the environment.

In the last two decades, the increase in tropospheric ozone (O_3) concentration has been surpassed only by the gases of carbon dioxide and methane.[3] Ozone is also regarded as the third most important greenhouse gas, as was shown in Figure 1.1 (Chapter 1, Paragraph 1.1). It is difficult to estimate the long-term trend of ozone concentrations, due to the lack of representative observational sites with long-term records. However, ozone in the free troposphere in Europe has increased from the early 20th century until the late 1980s. Thereafter its concentration began to level off and even showing a possible decline. A 33-year study of ozone data from Japan also showed ozone in the lower troposphere to have increased from 1970 to 2002.[3] Ozone is produced by photochemical processes involving industrial and biogenic emissions of nitrogen oxides, hydrocarbons and certain organic compounds.[16]

Other important trace pollutant gases include the human-made perfluorinatedcarbons (PFCs), hydroflouronatedcarbons (HFCs) and sulphurhexafluoride (SF_6). Hydroflouronatedcarbons sharply increased since the 1990s, as they were the replacement for chlorfluorocarbons (CFCs) as refrigerants, propellants and solvents. Perfluorinatedcarbon concentrations have been increasing linear since the 1960s.[3] It is produced as a by-product of aluminium production and also has considerable natural sources. Sulphurhexafluoride is produced for use as an electrical insulation fluid in power distribution equipment and is deliberately released as an essential inert tracer to study atmospheric and oceanic transport processes. Its concentration has also increased linearly for the last two decades. The gases of perfluorinatedcarbons and hydroflouronatedcarbons are responsible for ozone depletion in the stratosphere,[57] thus playing a role in the effects stratospheric ozone depletion has on

health and the environment. PFCs, HFCs and SF_6 all have significant positive RF effects on climate due to their ability to absorb radiation, although their concentrations are very low.[57] Similar to carbon dioxide, methane and nitrous oxide, PFCs, HFCs and SF_6 are all long-lived gases in the atmosphere,[3] thus making their contribution to atmospheric chemistry and environmental impacts more important.

Other important atmospheric gases, which have much shorter residence times, but play critical roles in atmospheric chemistry and climatic impacts due to their reactivity, include ozone, as well as sulphur and nitrogen-containing gas species. Nitrogen and sulphate containing trace gases (e.g. SO_2, NO_2, NH_3 and HNO_3) are produced by a variety of natural as well as anthropogenic activities. These gas species concentrations, in general, are on the decrease in developed countries, since restrictions are in place to control industrial activities resulting in their emissions. This is in contrast to developing countries, where their concentrations are on the increase due to emission control equipment not being utilised. All nitrogen-containing species are directly, or indirectly, involved in ozone formation or destruction, and thus responsible for its environmental and health impacts. Most nitrogen and sulphur containing gas species have too short residence times (no real vertical mixing possible) in the atmosphere to have a measurable RF effect themselves, but do form aerosol particles, which mostly have a negative RF effect (cooling). This negative RF effect can change to a positive RF effect, depending on the composition of the aerosol.

In this study, the trace gases ozone, the nitrogen containing species of NO_2, NH_3 and HNO_3, as well as the sulphur containing species of SO_2 were monitored. All aspects of their chemical characteristics and impacts are discussed in the subsequent paragraphs.

2.1.2.2 Historical perspective on aerosols

Aerosols, also called particulate matter or PM, are a complex mixture of chemical elements and liquid droplets in air. They have been emitted as primary aerosols from a variety of natural and human activities since the beginning of time. Aerosols are also formed in the atmosphere as secondary products of gaseous reactions. Thus, an increase in the concentration of gaseous compounds may also lead to a certain level of accumulation of new aerosols. Aerosols on average have shorter atmospheric

lifetimes than most gases, and will deposit more readily by dry as well as wet deposition. This, however, increases its potential impacts on health and the environment, especially regional ones. As mentioned in Chapter 1, only a medium to low scientific understanding of aerosols and their impacts on climate change exists, mainly due to the large uncertainties of its chemical composition. Most aerosols seem to have a negative RF influence, thus a cooling effect on the earth's climate. Only black carbon and aerosols containing larges quantities of it will have a positive RF effect by absorbing radiation from the sun and the earth's surface.

2.2 Selection of species monitored

The preceding paragraphs showed a range of biogeochemical important trace gas and aerosol species. It is beyond the scope of this study to focus on all the important species mentioned. Thus, only the species required to achieve the objectives, as stated in Chapter 1, will be discussed in greater detail in the following paragraphs. The selected species were chosen due to their importance in heterogeneous atmospheric reactions, as well as the direct influence they have on health and the environment.

2.2.1 Gaseous species

The US EPA (United States Environmental Protection Agency) regards SO_2, NO_2, O_3, Pb, CO and PM (i.e. particulate matter with an aerodynamic diameter less than or equal to 10 μm) as criteria pollutants.[58]. A criteria pollutant is a pollutant for which there is a NAAQS (National Ambient Air Quality Standard) set.[59] South Africa also has incorporated standards for all the above-mentioned species, with monthly averages of 30 and 50 ppb for SO_2 and NO_2, respectively. O_3 has an hourly average of 120 ppb and Pb a monthly average concentration of 2.5 $\mu g/m^3$. These are the most important and commonly monitored species in the atmosphere due to their impacts on human health and the environment, as well as their importance in atmospheric chemistry. Of these criteria pollutants, gases of SO_2, NO_2 and O_3 were selected for monitoring in this study. However, in order to estimate the total nitrogen deposition, as many as possible nitrogen containing gas species have to be included, as they all take part in the nitrogen cycle. For this reason, the gaseous species of NH_3 and HNO_3 were also included in this study. The following paragraphs (specifically Paragraph 2.3) will focus on the importance of these species, their sources, characteristics and most commonly occurring chemical mechanisms and processes (transformations in the atmosphere).

This will also involve intermediate species and precursors on a regional scale, which will improve the knowledge of their natural cycles (sources and sinks, regionally). This is important to better understand the chemistry of the sub-continent and the heterogeneous reactions involved. The latter aspect is of importance to this study.

2.2.2 Aerosols

Particle matter can be inhaled and transported deep into the lungs. Exposure to ambient particle pollution is therefore linked to a variety of health problems.[60] In setting particle standards, two categories of particle pollution are addressed:

i) fine particles ($PM_{2.5}$) that are 2.5 micrometers in diameter and smaller; and
ii) inhalable coarse particles (PM_{10}) that are smaller than 10 micrometers.

For both fine and coarse particles, the US EPA sets two types of standards: Primary standards to protect human health; and secondary standards, to protect the public welfare from effects including visibility, vegetation, and damage to buildings, monuments and other ecosystems. The primary standards were set based on studies showing association between exposure to particulate matter and significant health problems, including aggravated asthma, chronic bronchitis, reducing lung function, irregular heartbeat, heart attack, and premature death in people with heart or lung disease.[60]

The US EPA national air quality standard for particle pollution as on 21 September 2006 is as follows:

i) The 24-hour fine particle standard of 35 $\mu g/m^3$ for the primary, as well as the secondary standard, and the annual fine particle standard of 15 $\mu g/m^3$ for the primary, as well as the secondary standard;[60] and
ii) The 24-hour coarse (PM_{10}) standard of 150 $\mu g/m^3$ is retained for the primary as well as the secondary standard, while the annual PM_{10} standard is revoked as there is no evidence to suggest that long-term exposure to current levels of coarse particles leads to any health problems.

Both $PM_{2.5}$ and PM_{10} particle sizes are sampled in this study based on the regulations set for particulate pollution by the US EPA. The South African guidelines were also noted, which set a PM_{10} annual average of 60 $\mu g/m^3$. These regulations were not the only reason for the aerosol selections, as their data inputs are required for the specific atmospheric modelling done within this study.

2.3 Gaseous species

2.3.1 Sources and atmospheric processes of selected gaseous species

All gaseous species have a specific role to play within the natural cycles of elements within the atmosphere. These cycles are perturbed when an excess of trace species is present, which changes the natural processes and chemistry, leading to a response from the atmosphere. This response is either removal of the species or climate change, each leading to their respective impacts. The most important atmospheric processes of the selected gas pollutant species will be discussed.

2.3.1.1 Sources and atmospheric processes of sulphur dioxide

Sulphur is a chemical element essential to life on earth as all living organisms and plants assimilate sulphur. All living organisms release it in some form, since it is an end product of metabolism. The major sulphur containing compounds present in the atmosphere include carbonyl sulphide, carbon disulphide, dimethyl sulphide, hydrogen sulphide, sulphur dioxide and sulphate.[61]

Anthropogenic emissions of sulphur are primarily in the form of SO_2 emitted in great quantities by fossil fuel combustion, smelters and other industrial processes. The main natural sources, which contribute to the global sulphur budget, are the biological oxidation and reduction of sulphide and sulphate, respectively, found in the aquatic and the terrestrial environment as mineral species or produced by decomposition of organic matter (carbon-bonded compounds of the amino acid cysteine).[62] Elemental sulphur is rarely found in the terrestrial and aquatic environment. Oceans have a sulphate content of around 28 mmol per litre globally and sea spray is therefore an important natural source of sulphate in the atmosphere. In South Africa, the effect of point sources such as bio-fuel combustion used for cooking and heating is reflected in the diurnal variation of SO_2 of highly urbanised areas with reported maximum values around 08:00 am and 08:00 pm.[63] *Annegarn et al.*[46] and *Rorich et al.*[64] report SO_2 maximums around midday in the vicinity of power plants in the Mpumalanga Highveld. The seasonal variations show higher SO_2 levels in winter over most of South Africa. This is associated with combustion products emitted during increased burning of biofuels for heating when the ambient temperature drops.[63] The stable meteorological conditions during winter[10] do not favour the removal of pollutants from the atmosphere

(e.g. strong inversion layers, low humidity and very few rain events), thus contributing to these elevated winter levels. However, the exact pollutant levels that are determined by the factors affecting the dispersion and deposition thereof are region specific and will differ accordingly.

The approximate residence time of SO_2 in the atmosphere can vary between 12 hours and 6 days.[65] At present, anthropogenic emissions contribute to almost 75% of the total sulphur emitted globally with 90% of it occurring in the Northern Hemisphere. Approximately 24% are natural emissions (marine, terrestrial and volcanic), representing a 13% Northern Hemisphere and 11% Southern Hemisphere contribution if biomass burning is excluded.[16] In South Africa, anthropogenic emissions of SO_2 represent around 25% of the total flux of S into the atmosphere, of which more than 50% of the total SO_2 emitted into the atmosphere originates from anthropogenic sources.[61] The major sources of SO_2, which are centred around the Mpumalanga Highveld and Gauteng (Johannesburg) regions, include coal-fired power stations, petrochemical plants, various other industries (e.g. metallurgical, mineral mining, brick works, ferro-alloy smelters, steel works and fertilizer plants) and biomass burning.

Once SO_2 is emitted into the atmosphere, it can be oxidised to a sulphuric acid or sulphates by reactions occurring in the gas phase, liquid phase, on solid surfaces, or combinations of all three. SO_2 is readily dry deposited, while it is relatively insoluble in cloud water due to the acidity equilibrium present in its dissolved form in cloud water.[66] However, the photochemical transformation of SO_2 to the soluble sulphate aerosol and the subsequent reactions within cloud droplets, ultimately lead to the wet deposition thereof. From a thermodynamic point of view, SO_2 has a strong tendency to react with oxygen in the air, as presented in Equation 2.1.

$$2SO_2 + O_2 \leftrightarrow 2SO_3 \qquad 2.1$$

The rate of this reaction, however, is so slow under catalyst-free conditions in the gas phase, that it can be neglected as a source of SO_3.[67] If formed, SO_3 reacts rapidly with water vapour to form H_2SO_4. Figure 2.1 shows the ultimate fate of sulphur emissions produced naturally or anthropogenically.

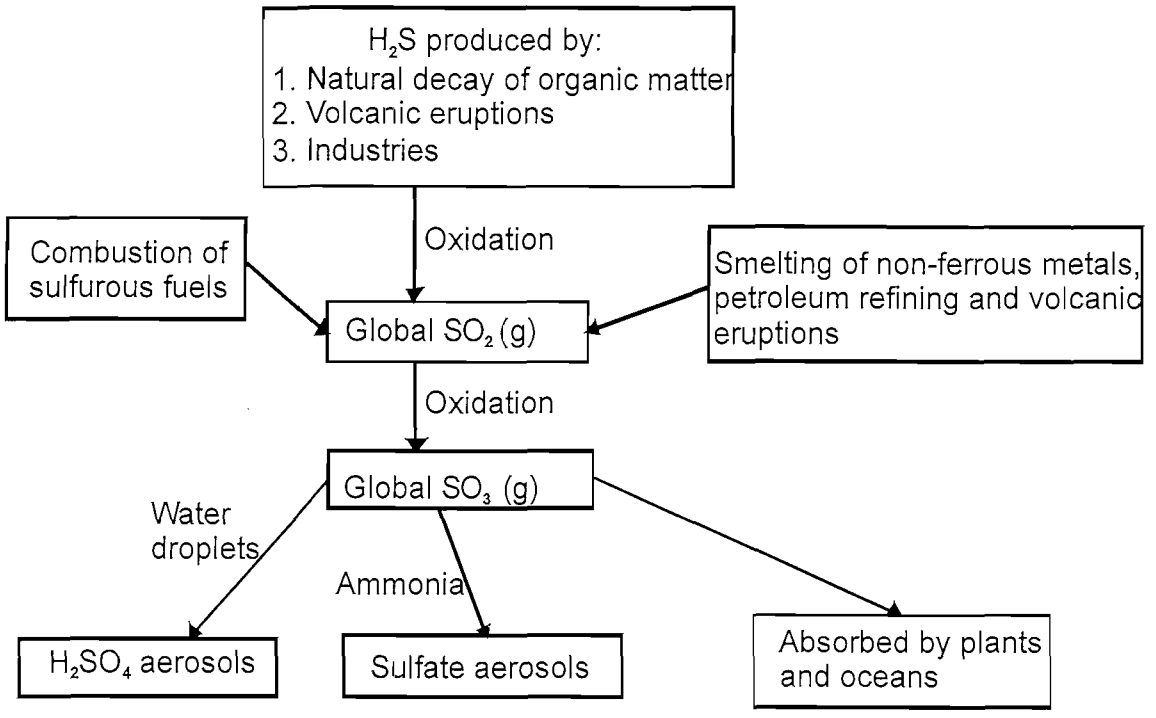


Figure 2.1: *Atmospheric fate of sulphur compounds*[68]

Photochemical oxidation in the gas phase is driven by the HO$^{\bullet}$ radical. In *Seinfeld and Pandis*,[15] *Calvert et. al.* demonstrated that the oxidation of SO_2 by photo oxidation is not a predominant mechanism. The major oxidation pathway remains through the reaction of SO_2 with HO$^{\bullet}$ radicals represented in Equation 2.2.[15]

$$HO^{\bullet} + SO_2 \rightarrow HOSO^{\bullet}{}_2$$
$$HOSO^{\bullet}{}_2 + O_2 \rightarrow HO^{\bullet}{}_2 + SO_3$$
$$SO_3 + H_2O \rightarrow H_2SO_4 \qquad 2.2$$

Sulphuric acid formed by Equation 2.2 can be neutralised by forming $(NH_4)_2SO_4$ or NH_4HSO_4. Rates of these reactions are higher during the day than at night, and in summer compared to winter.[67] Intensity of sunlight, the presence of oxidants and/or oxidant precursors, relative humidity and the presence of fog and clouds all appear to affect the reaction rates for the transformation of SO_2.[69,70] Many oxidising agents (O_3, H_2O_2, PAN, methylhydroperoxide and peroxyacetic acid) formed in the gas phase do not react with gaseous SO_2 at measurable rates. However, when these species are dissolved in the cloud water, they readily oxidise dissolved SO_2.[71] SO_2 can be oxidised to sulphate in heterogeneous reactions on fly ash[72], ferric oxide particles and free atmospheric dust.[73]

2.3.1.2 Sources and atmospheric processes of ozone

Ozone is the only major trace gas in the stratosphere that almost fully absorbs ultraviolet radiation between 240-290 nm from the sun. The stratosphere contains 90% of the earth's ozone, which is responsible for shielding the earth's surface from incoming harmful ultraviolet-β radiation from the sun.[15] It is thus critical in shielding the earth from radiation, which is particularly harmful to unicellular organisms and the surface cells of higher plants, animals and humans.[15]

The only significant source of ozone (O_3) in both the strato- and troposphere (due to the slow vertical mixing rate between the layers) is the photochemical production of it as a secondary trace gas in both these layers. In the stratosphere ozone formation occurs above 30km altitude, where UV radiation of less than 242 nm slowly dissociates molecular oxygen.[15] The oxygen atoms formed react with oxygen in the presence of a third molecule M (mainly N_2 or O_2 that act as a stabilising molecule by absorbing the excess vibrational energy) to produce O_3 as is shown in Equations 2.3 and 2.4.

$$O_2 + h\nu \rightarrow O + O \qquad 2.3$$

$$O + O_2 + M \rightarrow O_3 + M \qquad 2.4$$

Equation 2.4 is the only source of O_3 production in the atmosphere. The O_3 formed in this reaction strongly absorbs radiation between 240-320 nm to decompose back to O_2 and an excited singlet O atom as presented in Equation 2.5, which is considered as the trigger of most oxidation reactions occurring in the troposphere,[74] since $HO^{\bullet}$ radicals are formed in a subsequent reaction (see Equation 2.7).

$$O_3 + h\nu\ (\lambda < 320\ nm) \rightarrow O\ (^1D) + O_2 \qquad 2.5$$

Apart from Equations 2.3 and 2.4, ozone is also produced primarily in the troposphere when NO_2 is photolysed, as is shown in Equation 2.6.[15] The singlet O atom produced reacts with oxygen in the presence of a third body (N_2 or O_3) to form ozone, as is shown in Equation 2.4.

$$NO_2 + h\nu\ (\lambda < 424\ nm) \rightarrow NO + O_3 \qquad 2.6$$

An increase in the ambient levels of CO and CH_4 in NO_x-rich environments directly results in an increase in tropospheric O_3 concentrations.[75,16] Hydrocarbons of natural origin are the largest single contributing source of O_3 in NO_x rich environments. *Blake*

and Roland[76] reported extremely high O_3 concentrations in Mexico City caused by alkane hydrocarbons present in unburned liquid petroleum gas leaking into the atmosphere from numerous urban sources. In *Brasseur and Orlando,*[16] *Crutzen* and also *Chameides and Walker* suggested that the oxidation of CH_4 and CO in the presence of NO_x would lead to ozone production. Savannah fires in the tropics during winter are a large source of ozone in the troposphere as they release large amounts of its precursor gases (NO_x and CO) in the boundary layer of the troposphere. These precursor gases are then photochemically converted to ozone by intense solar radiation found at these latitudes.[16] Ozone at surface level (lower troposphere) is environmentally considered a pollutant because of its detrimental effects (oxidative effect) on human health and plants.[16] While the stratospheric ozone layer is thinning, tropospheric ozone is increasing,[77,78] with much of the evidence of increased baseline levels of tropospheric ozone coming from Europe where monitoring of ozone was started in the 1800s.[15] The seasonal trends in southern Africa show that higher levels of ambient O_3 are present in non-urban locations during winter.[56] This can be attributed to the increased emissions of NO_x and CO from the combustion of biomass, which occurs with a higher frequency during this period. It can also be attributed to the somewhat hindered pollution removal processes in winter.[56] Long-term averages of O_3 concentrations in South Africa show higher O_3 concentrations in rural and remote regions than in urban sites, even if elevated O_3 concentrations in urban areas are largely due to photochemical processes, as is shown by short-term measurements.[61] This is due to the destruction of O_3 by NO_x, SO_2 and H_2S, which can be present in high concentrations in urban air. Although there are exceptions, relatively low levels, if any, of O_3 are present during the night in urban areas, since the NO_2 emissions are minimal.[63]

Tropospheric ozone, although present in trace amounts, plays a controlling role in the oxidation capacity of the atmosphere and controls the levels of reduced gases such as CO, hydrocarbons and most sulphur and reactive nitrogen compounds to prevent their accumulation.[16] Ozone represents almost the entire oxidative potential of the atmosphere and is directly or indirectly involved in most reactions of trace species in it. Ozone is highly reactive and therefore has a short residence time in the troposphere. In the stratosphere, its residence time can vary up to months, depending on the availability of compounds at the different altitudes to react with.[15] A lot of ozone's chemistry was already presented in the formation of it as a source, and more

will be discussed when NO_x's chemistry is considered in Paragraph 2.3.1.3. Only the chemical processes leading to its ultimate destruction, which mainly involve NO_x, O_x, HO_x and halogen cycles, will be presented in this section.[15] The first and most important reaction of ozone leading to its destruction in the stratosphere is the photo-dissociation of O_3 as was shown in Equation 2.5. The oxygen singlet atoms (^1D) that remain in the exited state after its production due to the dissociation of O_3 are able to combine with water and produce the very reactive hydroxyl radical (Equation 2.7).[15]

$$O(^1D) + H_2O \rightarrow 2HO^{\bullet} \qquad 2.7$$

$$O(^1D) + CH_4 \rightarrow HO^{\bullet} + CH_3 \qquad 2.8$$

Between 20 and 50 km from the earth's surface, the total $HO^{\bullet}$ produced is 90% in Equation 2.7 and only 10% in Equation 2.8.[15] The $HO^{\bullet}$ radical is responsible for *initiating* the removal of a vast number of trace gases from the atmosphere, is shown in the photochemical oxidant cycle in Figure 2.2. Gases that do not react with $HO^{\bullet}$ have long lifetimes and are transported into the stratosphere where they are chemically or photolytically destroyed.[56]

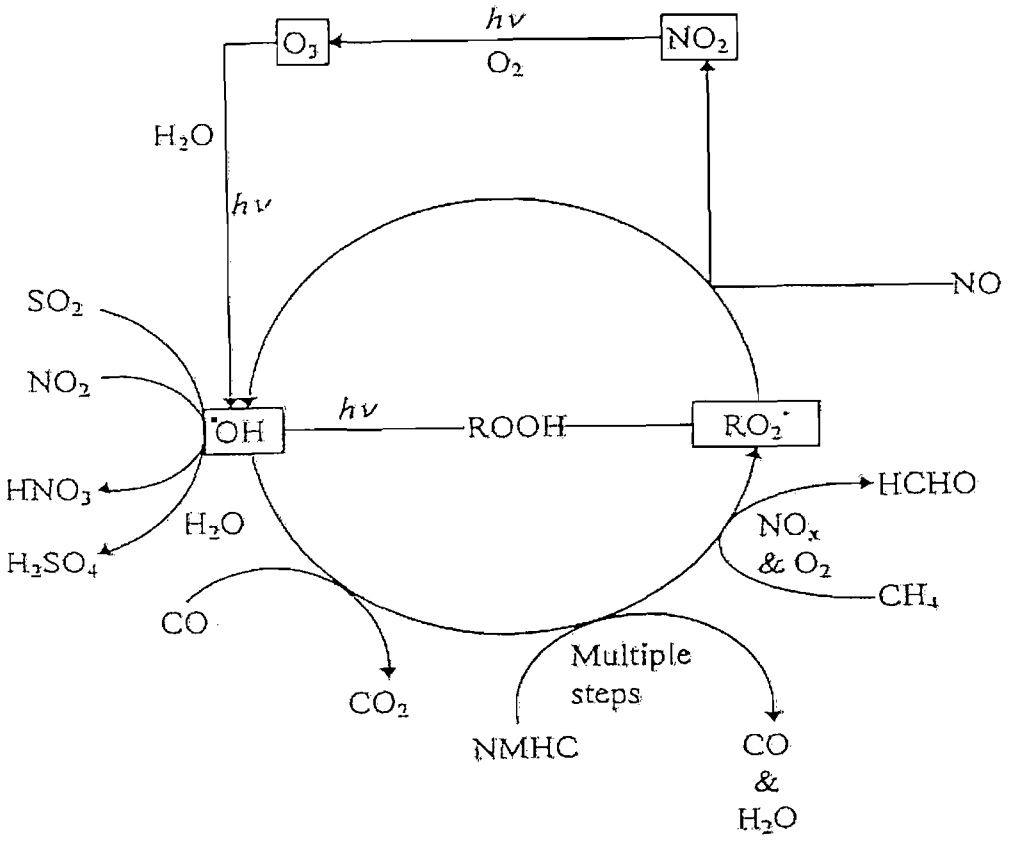


Figure 2.2: *The photochemical oxidant cycle (R represents a homologue in the alkane series)*[79]

The tropics are considered nature's "washing machine", as prevailing atmospheric conditions (high humidity and radiation intensity) are responsible for elevated concentrations of $HO^{\bullet}$, high production and destruction rates of CO and CH_4, as well as the lowest O_3 levels.[79] $HO^{\bullet}$ and HO_2 rapidly interconvert (Equations 2.9 and 2.10, respectively) to establish and continue in the HO_x chemical cycles. HO_x has two catalytic ozone-depletion cycles, which are as follow.[15]

Cycle 1:

$$HO^{\bullet} + O_3 \rightarrow HO_2 + O_2 \qquad 2.9$$

$$HO_2 + O \rightarrow HO^{\bullet} + O_2 \qquad 2.10$$

Cycle 2:

$$HO^{\bullet} + O_3 \rightarrow HO_2 + O_2$$

$$HO_2 + O_3 \rightarrow HO^{\bullet} + O_2 + O_2$$

In both cycles, O_3 is removed only if the HO_2 reacts with O or O_3, before it can react with NO. At an altitude of 15 km, 90% of total ozone destruction is due to HO_x Cycle 2. Below 20 km, HO_x Cycle 2 is dominant in ozone destruction, while the HO_x Cycle 1 dominates above 40 km.[15] Ozone is also destroyed by the ClO_x and BrO_x chemical cycles that can also couple with the HO_x cycles at lower altitudes, where the O-atom levels are lower. The ClO_x cycle is presented in Equation 2.11, followed by its coupled cycle with HO_x in Equation 2.12.[15]

ClO_x cycle:

$$Cl + O_3 \rightarrow ClO + O_2$$

$$ClO + O \rightarrow Cl + O_2 \qquad 2.11$$

HO_x/ClO_x cycle:

$$Cl + O_3 \rightarrow ClO + O_2$$

$$HO^{\bullet} + O_3 \rightarrow HO_2 + O_2$$

$$ClO + HO_2 \rightarrow HOCl + O_2 \qquad 2.12$$

Similar to the HO_x cycles presented in the previous paragraph, ClO and Cl must not react with NO_x, otherwise no net O_3 destruction will occur, as NO_2 will form, which leads to O_3 regeneration (Equation 2.6). It is estimated that 10% of ozone destruction occurs at an altitude of 30 km, due to the ClO_x cycle. Of all the halogen cycles, the most destructive one for ozone is the HO_x/ClO_x cycle in the lower stratosphere and the ClO_x cycle in the upper stratosphere.

Two main cycles exist for BrO_x destruction of ozone in the lower stratosphere. The first is the BrO_x/HO_x cycle presented in Equation 2.13 followed by its coupling with ClO_x in Equations 2.14-15.[15]

BrO_x/HO_x cycle:

$$Br + O_3 \rightarrow BrO + O_2$$
$$HO^{\bullet} + O_3 \rightarrow HO_2 + O_2$$
$$BrO + HO_2 \rightarrow HOBr + O_2 \qquad 2.13$$

BrO_x/ClO_x cycle 1:

$$Br + O_3 \rightarrow BrO + O_2$$
$$Cl + O_3 \rightarrow ClO + O_2$$
$$BrO + ClO \rightarrow BrCl + O_2 \qquad 2.14$$

BrO_x/ClO_x cycle 2:

$$Br + O_3 \rightarrow BrO + O_2$$
$$Cl + O_3 \rightarrow ClO + O_2$$
$$BrO + ClO \rightarrow ClOO + Br \qquad 2.15$$

Equations 2.13-15 are all important for ozone destruction at altitudes where the O-atom levels are significantly lower than in the lower stratosphere (~ 20 km). Although bromine is 150 times less abundant than chlorine in the atmosphere, it is as important as chlorine in overall ozone destruction processes.[15] At an altitude of 15 km, 10% of total ozone destruction is due to HO_x/BrO_x Cycle 1. At 20 km, BrO_x cycles are comparable to ClO_x cycles in ozone destruction, while ClO_x/BrO_x coupled cycles are responsible for ~25% of all the halogen-controlled loss in the lower troposphere.[15]

The formation and destruction of O_3 are largely determined by the ambient concentrations of NO_x.[75] NO_x plays an important role in coupling with all the ozone destruction cycles mentioned above and the rate of ozone consumption is largely determined by the concentrations of NO and NO_2 in the atmosphere.

2.3.1.3 Sources and atmospheric processes of nitrogen dioxide

Nitrogen (N_2) is the most abundant element in the earth's atmosphere representing up to 80% of the atmospheric content of the earth. In the absence of fertilisers, the biological fixation (by bacteria) of nitrogen to NO_x or any other nitrogen containing compound, is the ultimate source of nitrogen for living organisms.[16] Nitrogen dioxide

(NO_2) is also one of the most important molecules in the troposphere as it absorbs radiation over the entire visible and ultraviolet solar spectrum range.[15] This enables it to become a source of the odd O atom in the production of ozone and thus influences the oxidative capacity of the troposphere.

NO_2 only represents a small fraction of the total NO_x (NO + NO_2) emitted from anthropogenic and natural sources. The NO:NO_2 emission ratio varies significantly depending on the source.[56] Large amounts of NO_x are emitted mainly during combustion processes of industry, as well as automobiles and biomass burning,[16] but are also emitted by natural processes. Fossil fuel combustion can account for up to 50% of the total NO_x present in the atmosphere.[74] Another source for NO_x is combustion where NO_x is produced even if no nitrogen is present in the combustible biomass or fossil fuel. In such cases, the mere presence of both nitrogen and oxygen in the air at high combustion temperatures is enough to produce NO_x.[62] An important natural source of atmospheric nitrogen and a factor leading to the return of nitrogen from soil and water back to the atmosphere, is denitrification. Denitrification occurs mainly in stagnant fresh and in deep organically rich waters of the sea and under anaerobic conditions in soil.[62] Although denitrification is considered a natural process, it can be enhanced by human activities as we supply nitrate substrate in the form of fertilizers.[62] There is good evidence to show that the atmospheric NO_x concentrations have increased over the past 50 years.[80] In South Africa, diurnal trends in ambient concentrations of NO_2 in highly urban areas show a maximum in NO_2 concentrations during morning rush-hour traffic, while O_3 concentrations show a maximum around midday.[56] The seasonal variations of ambient NO_2 concentrations in South Africa also show higher concentrations during winter and this is associated with combustion products emitted by domestic fires that increase in frequency as the ambient temperature drops. The maximum ambient NO_2 concentrations are observed at around 21:00 during the winter in Soweto.[63] The reduced amount of radiation available for photo splitting of NO_2 during winter has a small effect contributing to its ambient concentrations.

Nitrogen oxides are produced in the troposphere primarily in the form of nitric oxide (NO). In conventional combustion, NO_x consists of approximately 95% NO, mainly due to the thermal stability of NO over NO_2.[81] The triple bond between two N atoms is a strong bond (ΔH = 945 kJ mol^{-1}) and temperatures in excess of 1000°C are necessary for atomisation of atmospheric N_2. NO reacts rapidly with ozone to form NO_2 (Equation

2.6). This can either lead to a continuous cycle of production and destruction of NO_2 with ozone, or a net destruction of O_3 in the troposphere, depending on the sequence in which the reactions presented in Equations 2.16-2.18 occur (e.g. if 2.17 immediately follows 2.16 it will be a sink of ozone and if 2.18 follows 2.16 net ozone destruction will take place).[15]

$$NO + O_3 \rightarrow NO_2 + O_2 \qquad 2.16$$

$$NO_2 + O \rightarrow NO + O_2 \qquad 2.17$$

$$NO_2 + h\nu\ (\lambda < 424) \rightarrow NO + O \qquad 2.18$$

NO_x is extremely reactive and thus has very short residence times in the lower troposphere, while it can have relatively long lifetimes in the upper troposphere.[16] The dominating role of NO_x in strong anthropogenic source regions, such as North America, is evident in the NO_x concentrations that shows three orders of magnitude differences between urban-suburban areas and remote locations.[15]

The atmospheric chemistry of nitrogen compounds is complicated and may be transformed by a number of different compounds before it is eventually deposited to the earth's surface.[66] There are three major pathways (gas, aqueous phase oxidation and aerosol formation) by which NO_2 can be converted to nitric acid and nitrate, before eventually being deposited. These pathways will be discussed in this section.

Gas phase oxidation:

First, both NO and NO_2 are oxidised to the nitrate radical ($NO^{\bullet}_3$) in a reaction with ozone (Equation 2.19-20).[15]

$$NO + O_3 \rightarrow NO_2 + O_2 \qquad 2.19$$

$$NO_2 + O_3 \rightarrow NO^{\bullet}_3 + O_2 \qquad 2.20$$

The subsequent nitrate formed in Equation 2.20 will rapidly photolyse back to NO_2 and NO in the presence of sunlight, but reacts further in the dark with NO_2 to form denitrogen pentoxide (N_2O_5).[15]

$$NO^{\bullet}_3 + NO \leftrightarrow N_2O_5 \qquad 2.21$$

Unreacted NO present in the atmosphere will rapidly remove $NO^{\bullet}_3$ to again produce NO_2. The reaction in Equation 2.21 is readily reversible resulting in an equilibrium in the atmosphere. Both NO and NO_2 can also be oxidised directly to gaseous nitrous

acid (HONO) and nitric acid (HNO_3), respectively, by reacting with an $HO^{\bullet}$ radical as presented in Equations 2.22 and 2.23.[10]

$$HO^{\bullet}_2 + NO \rightarrow HNO_2 \qquad 2.22$$

$$NO_2 + HO^{\bullet} \rightarrow HNO_3 \qquad 2.23$$

The reaction in Equation 2.23 is responsible for the removal of NO_2 during the day, while the reaction in Equation 2.20-21 is responsible for removal of O_3 and NO_2 during the night.

Aqueous phase oxidation:

The reaction of NO_2 and NO with water, or two molecules of NO_2 with water, produces gaseous HONO in surface catalysed reactions (Equations 2.24 and 2.25), if NO_2 and NO do not dissolve in and react with the cloud water. This is due to the fact that NO_2 and NO have a low solubility in pure water, unless solubility is catalysed in the presence of other solutes.[10]

$$NO_2 + NO + H_2O \rightarrow 2HONO \qquad 2.24$$

$$2NO_2 + H_2O \rightarrow HONO + HNO_3 \qquad 2.25$$

In solution, HONO and nitrite (NO_2^-) ions can be oxidised to nitrate (NO_3^-) ions in reactions with oxidants like peroxide (H_2O_2), as is shown in Equation 2.26.

$$NO_2^- + H_2O_2 \rightarrow NO_3^- + H_2O \qquad 2.26$$

The above-mentioned reactions are the most important aqueous phase pathways for the oxidation of nitrogen oxides to nitrates. Although other pathways have been suggested no evidence exists to assess their importance.[66] Hydrolysis and reactions of organic nitrates can occur, as well as aqueous phase reactions leading to organic nitrate production.

Nitrate aerosols:

The most important pathway for nitrogen oxides (NO_y = i.e., NO_x, nitric acid, nitrate particle) to form nitrates and be eventually deposited by either wet or dry deposition, is through its incorporation into an aerosol and subsequent reactions as cloud condensation nuclei (in the case of wet deposition).[66] There are various mechanisms by which NO_y can be converted into a nitrate aerosol. Firstly NO_2, as well as HNO_3

and N_2O_5, which are day and night time oxidation products of NO_x, respectively, can react on surfaces of sea salt aerosols to form nitrate aerosols (Equations 2.27-29).[66]

$$2NO_2 + NaCl \rightarrow ClNO + NaNO_3 \quad 2.27$$

$$HNO_3 + NaCl \rightarrow NaNO_3 + HCl \quad 2.28$$

$$N_2O_5 + NaCl \rightarrow ClNO_2 + NaNO_3 \quad 2.29$$

Lastly, nitric acid can react with soil-derived particles to produce soluble nitrate aerosols as is shown in Equation 2.30.

$$2HNO_3 + CaCO_3 \rightarrow Ca(NO_3)_2 + CO_2 + H_2O \quad 2.30$$

Nitric acid also reacts with ammonia to form ammonium nitrate and the reaction is given when nitric acid reactions are discussed in Paragraph 2.3.1.4.

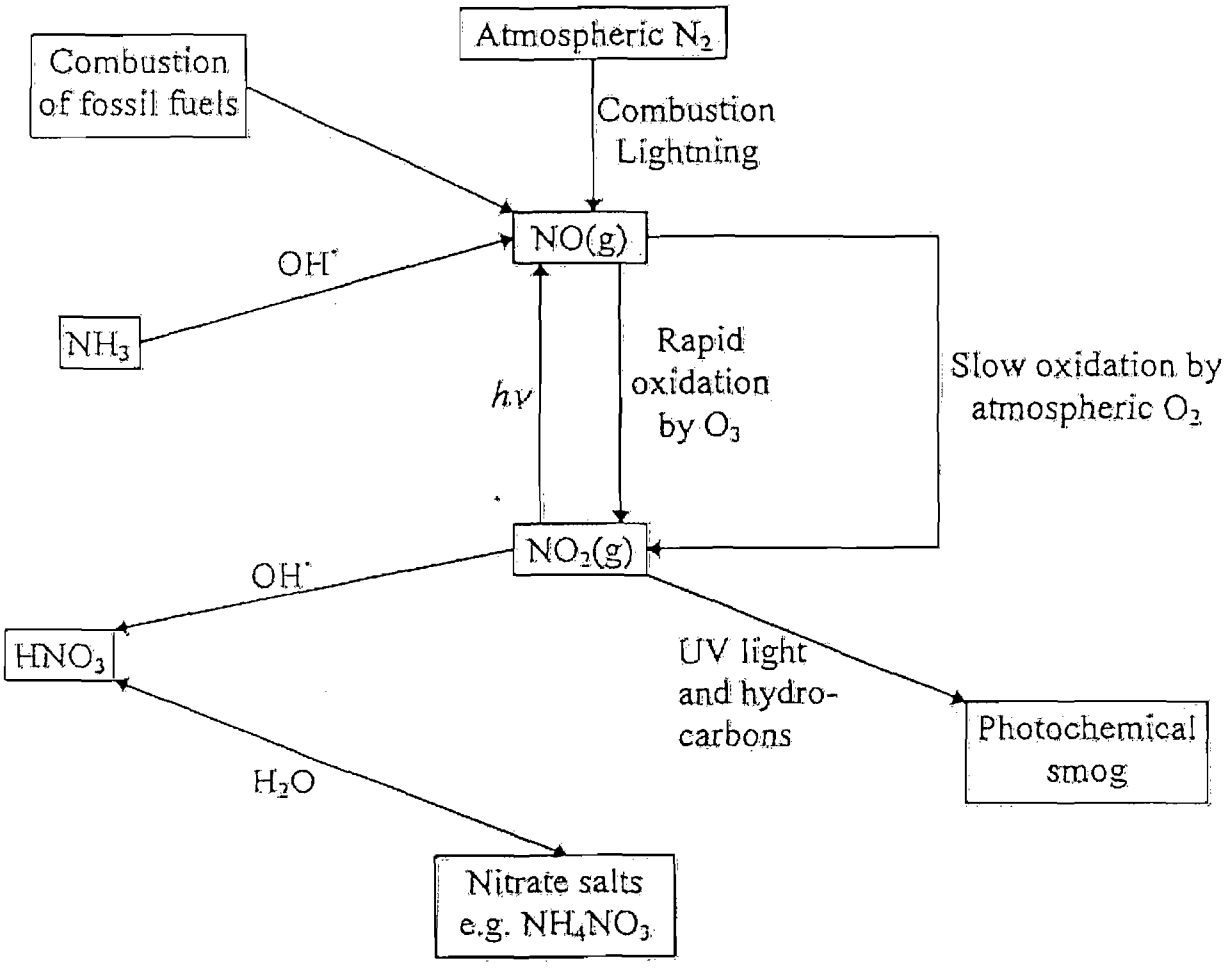


Figure 2.3: *Major processes involved in the NO_2 cycle*[67]

Figure 2.3 shows all the major processes involved in the NO_2 cycle from its formation (natural and anthropogenic) to its ultimate fate (e.g. dispersion and deposition).

2.3.1.4 Sources and atmospheric processes of nitric acid

Nitric acid (HNO_3) is the primary removal mechanism of NO_x from the atmosphere via wet and dry deposition.[15] Nitric acid dissolves quickly to the aqua faze (Equation 2.31) from which it dissociates readily to nitrate (Equation 2.32).

$$HNO_3(g) \leftrightarrow HNO_3(aq) \quad 2.31$$

$$HNO_3(aq) \leftrightarrow NO^-_3 + H^+ \quad 2.32$$

Nitrate is not only an important source of nitrogen for living organisms, but also important for denitrification of nitrogen species back into the atmosphere as part of the nitrogen cycle.

The only source of nitric acid (HNO_3) in the atmosphere is as an oxidation product of NO_x via its reaction with the $HO^\bullet$ radical or the heterogeneous conversion of N_2O_5.[16] Nitric acid is produced in different reaction mechanisms during the day and night:

During the day:

The principal reaction sequence contributing to the production of nitric acid during daytime begins with the oxidation of nitric oxide to nitrogen dioxide, due to nitric oxide emissions present in the atmosphere (Equation 2.33).[62] Nitric oxide are present in the atmosphere mainly due to high-temperature combustion processes. It is also present due to the combustion of organic nitrogen containing compounds such as wood, as well as biogenic activities (e.g. nitrification).[62]

$$NO^\bullet + O_3 \rightarrow NO^\bullet_2 + O_2 \quad 2.33$$

Nitric oxide is oxidised by O_2, O_3, or $ROO^\bullet$ (where R is an alkyl group). Nitrogen dioxide produced in this way (Equation 2.33) contributes to O_3 and $HO^\bullet$ production, which is in part responsible for the initiation of photochemical smog. Nitric acid is formed as the oxidation product of nitrogen dioxide with a hydroxyl radical during daytime and also constitutes the principal removal pathway of nitrogen dioxide from the atmosphere following Equation 2.34.[62]

$$NO^\bullet_2 + HO^\bullet + M \rightarrow HNO_3 + M \quad 2.34$$

(where M is a third body, mostly N_2 or O_2)

During the night:

During night time, nitric acid is produced via a different process, which involves the nitrate radical (Equation 2.35). It is formed during both day and night, but accumulates only at night time because of the absence of photolytic destruction at night and reactions with NO_x species.[62]

$$NO^{\bullet}_2 + O_3 \rightarrow NO^{\bullet}_3 + O_2 \qquad 2.35$$

The formation of a nitrite radical is followed by the rapid addition of oxygen. Similar to a hydroxyl, the nitrate radical also initiates sequences by first abstracting hydrogen and thus forming nitric acid as shown in Equations 2.36 and 2.37 with aldehydes and alkanes, respectively.[62]

$$NO^{\bullet}_3 + RCHO \rightarrow RCO^{\bullet} + HNO_3 \qquad 2.36$$

$$NO^{\bullet}_3 + RH \rightarrow {}^{\bullet}R + HNO_3 \qquad 2.37$$

(where R is an alkyl group)

Rapid reactions at night time involving the nitrate radical and the nitrogen dioxide result in the formation of dinitrogen pentoxide (N_2O_5), which is heterogeneously hydrolysed to produce nitric acid (Equations 2.38 and 2.39). This is one of the major pathways in removing NO_x from the atmosphere.[15]

$$NO^{\bullet}_3 + NO^{\bullet}_2 \leftrightarrow N_2O_5 \qquad 2.38$$

$$N_2O_5 + H_2O \rightarrow 2HNO_3 \qquad 2.39$$

According to Equations 2.35, 2.38 and 2.39, almost all NO_x is removed from the atmosphere during night time, resulting in the removal of smog precursors through the production of nitric acid.[62]

Nitric acid is one of the most water soluble atmospheric gases, with a Henry's law constant of 2.1×10^5 m atm^{-1} at 298 K.[15] Nitric acid is thus easily removed from the atmosphere by both wet and dry deposition. Nitric acid also produces NO_3 reservoirs in aerosols as ammonium or nitrate salts.[16] In the boundary layer and lower free troposphere, HNO_3 has very short lifetimes (<1 day), which is controlled more by physical or heterogeneous processes than gas phase reactions resulting in longer lifetimes in the middle and upper troposphere.[16]

Other reactions involving nitric acid include the heterogeneous reactions with water, during which it is produced (Equation 2.25), as well as with aerosols (Equations 2.27-

2.29), where it is destroyed as previously described in Paragraph 2.3.1.3. Nitric acid also reacts with ammonia (Equation 2.40) to form ammonium nitrate, which can act as a condensation nucleus for the formation of a water droplet or is deposited as part of the solid aerosol.[62]

$$NH_3 + HNO_3 \rightarrow NH_4NO_3 \qquad 2.40$$

Nitric acid can also be photolysed to form a hydroxyl radical (Equation 2.41), which can subsequently react with another nitric acid molecule (Equation 2.42) to produce water and nitrate and thus remove it from the gas phase.[16]

$$HNO_3 + hv \rightarrow OH^{\bullet} + NO_2 \qquad 2.41$$

$$HNO_3 + OH^{\bullet} \rightarrow H_2O + NO_3 \qquad 2.42$$

$$HNO_3 + H_2O(aq)/aerosol \rightarrow \text{removal from gas phase}$$

Nitric acid not only forms important species of NO_3 as secondary aerosols, but also converts much faster from NO_x than sulphur to sulphuric acids and subsequently deposits at far greater deposition velocities. Apart fom NO_x converting faster to its acids than sulphur other processes influencing deposition include gravitational settling, impaction and diffusion. These processes act simultaneously on the particle and are affected by other variables like wind speed, humidity, land/and sea roughness and ultimately the particles size. The species of NO_x and SO_x and its acids/salts are all of the submicron level in size as well as the particles produced through gas to particle conversion (GPC).[67] The particles of the submicron size range have lower deposition values than particles < 0.1 μm and > 1 μm.[15] Submicron particles are primarily subjected to Brownian movement which removes it from the nucleation mode through impaction and coagulation to the accumulation mode.[16] For particles > 1 μm sedimentation rates dominate deposition velocities. The rate at which particles increase in size therefore increases it's deposition except for the particles that are impacted directly on to surfaces. The rate at which particles grow depends on impaction and coagulation which are effected by particle concentrations and humidity.[15] The bigger acids/salts of NO_x and SO_x will have slightly higher deposition velocities due to its size and chemistry.

2.3.1.5 Sources and atmospheric processes of ammonia

Ammonia (NH_3) is the primary alkaline gas of the atmosphere[56] and the third most abundant nitrogen containing compound in the atmosphere after N_2 and N_2O. It has a

relatively short residence time of approximately 10 days.[16] NH_3 represents only a small fraction of the global nitrogen budget. Atmospheric NH_3 is easily removed from the atmosphere by both wet and dry deposition. Ammonia (NH_3) is essential in neutralising acidifying species in the atmosphere such as sulphates and nitrates. The deposition of NH_3 and NH_4^+ represents an important nutrient to the biosphere in some regions.[15]

Ammonia is a major component of surface nitrogen emissions[16] that are produced during nitrogen fixation reactions. This happens when a gaseous dinitrogen molecule is converted into fixed forms of nitrogen associated with aqueous or terrestrial environments as nitrate or ammonium ions.[62] This requires a large energy input result due to lightning discharges, cosmic rays or meteor trails and results in 5×10^6 $t.y^{-1}$ of nitrogen fixation. Other dominant biogenic (natural) sources include enzymatic decomposition of urea in animal urine and emanations from decomposing excrement, emissions from soils and also biomass burning.[16] Ammonia is also released during the application of fertilizers. Ammonium/ammonia can also be produced biogenically by dissimilatory denitrification by *Bacterium denitrificantis* in the absence of dissolved oxygen, as well as in ammonification processes where nitrogen containing organic matter decomposes in water and soil to produce nitrogen containing inorganic matter (mineralisation).[62] Major anthropogenic sources include the industrial Harber process as provided in Equation 2.43, which accounts for 6×10^7 $t.y^{-1}$ of nitrogen fixation during the production of NH_3 based fertilizers.[62]

$$N_2 + 3H_2 \rightarrow 2NH_3 \qquad 2.43$$

Other industrial activities that also release ammonia, include paper manufacture, waste water treatment, petroleum refining, cooking, and coal and oil combustion.[16]

NH_3 chemistry in the atmosphere is largely related to acid-base equilibriums in aerosols, as described in Paragraph 2.6, rather than gas-phase photochemistry[16] - the most common of which is the neutralisation of anthropogenic acidity by reactions such as Equation 2.44.

$$2NH_3 + H_2SO_4 \rightarrow (NH_4)_2SO_4 \qquad 2.44$$

NH_3 also reacts with $HO^{\bullet}$ radicals to form a range of amines as is illustrated in Equation 2.45. The amines can further react with gaseous nitric acid to produce corresponding nitrate salts.[15]

$$NH_3 + HO^{\bullet} \rightarrow H_2O + NH_2$$
$$CH_3NH_2 + HO^{\bullet} \rightarrow H_2O + CH_3HN^{\bullet}$$
$$(CH_3)_2NH + HO^{\bullet} \rightarrow H_2O + (CH_3)_2N^{\bullet}$$
$$\rightarrow H_2O + {}^{\bullet}CH_2NHCH_3 \qquad 2.45$$

NH_3 is highly soluble and reactive towards atmospheric acids and is removed in such reactions rather than reactions with $HO^{\bullet}$ radicals, which is relatively slow.[15] It is also known that NH_3 can be oxidised to NO_x, and that its reaction with nitric acid vapour is a major reaction pathway for producing particulate nitrate.

2.3.2 Health and environmental impacts of selected gaseous species

In 1952, a smog event in London, caused by emissions released during coal burning (with a high sulphur content), led to the death of over 4000 people.[19] This was mostly due to acute aggravation of respiratory problems, which ultimately led to legislation against coal burning.

The gaseous species selected to be monitored in this study, namely SO_2, O_3, NO_2, NH_3 and HNO_3, all have measurable impacts on health and the environment, and will be discussed now.

2.3.2.1 Impacts of sulphur dioxide

SO_2 on its own is not particularly harmful, but in combination with unburned coal (hydrocarbons) soot and high humidity, produces an overall reducing and acidic (H_2SO_4) atmosphere as carbon surfaces serve as nuclei for water condensation forming a visual impairing and irritating smog (aerosol).[62] Sulphur dioxide in the atmosphere is converted to sulphuric acid, which precipitates through rain, fogs and mist leading to forest decline, foliar damage[82,83] and soil acidification. This in return can result in the release of toxic metals such as aluminium into lakes and streams[84], root damage, and plant and nutrient leaching.[84,82] *Charlson et al.*[22] hypothesised that sulphuric acid aerosols affect the radiation balance in the troposphere on regional scale, by reflecting incoming radiation back to space. *Charlson et al.*[85] also hypothesised that dimethyl sulphide released by plankton is oxidised to H_2SO_4 aerosols, which may serve as cloud condensation nuclei in remote marine areas. Exposure over long time periods to low concentrations of sulphur dioxide leads to increased incidence of bronchitis, especially among smokers.[19] The WMO

recommends that short-term exposures of 24 h should not exceed 125 $\mu g.m^{-3}$ for both sulphur dioxide and black smoke, while annual long-term exposure should be less than 50 $\mu g.m^{-3}$.[19]

2.3.2.2 Impacts of ozone

Both ozone and its photochemically derived HO$^{\bullet}$ play a significant role in reactions leading to photochemical smog formation, which has become a major problem in the 20th and 21st centuries.[62] High levels of ozone at surface level have detrimental effects on human health and plants. Increased levels may lead to an increase in plant pests and pathogens.[86] High O_3 levels can enhance the corrosion of several materials. As ozone reflects harmful radiation from the sun in the stratosphere, a drop in the O_3 column (i.e. O_3 levels integrated vertically over the atmosphere) can result in up to 360,000 new skin carcinoma cases among the fair-skinned population of the world.[19] A decrement in pulmonary function in children may occur at O_3 concentrations as low as 220 $\mu g.m^{-3}$ (0.11 ppm). The WMO recommended that human exposures should not exceed 150-200 $\mu g.m^{-3}$ (0.076-0.1 ppm) in the 1 h range and an 8 h value of 100-120 $\mu g.m^{-3}$ (0.05-0.06 ppm).[19]

2.3.2.3 Impacts of nitrogen dioxide

Nitrogen dioxide, nitric oxide, together with unburned hydrocarbons, carbon monoxide, methane and HO$^{\bullet}$ radicals formed in subsequent photochemical reactions, all take part in photochemical smog formation,[16] which is a visible haze causing eye and skin irritation.[62] As nitrogen dioxide is the main source of ozone production, it is indirectly responsible for the greenhouse effects of ozone and the formation of HO$^{\bullet}$, which together with ozone, converts primarily pollutant species to secondary products that are more easily removed from the atmosphere.[16] Nitrogen dioxide is known to affect vegetation and cause corrosion in metals. Nitrogen dioxide in concentrations of the 1 ppm range, cause a whole range of reversible and irreversible effects, arising from structural changes in cells of the respiratory system. There are some indications that bacterial infection increases even at 0.5 ppm levels.[19] The recommended exposure to NO_2 has been difficult to set. The significant change in the pulmonary function of asthmatics when exposed to 0.3 ppm was used with other evidence to set the following guidelines: 0.21 ppm for 1 h and 0.08 ppm for 24 h.[19]

2.3.2.4 Impacts of nitric acid

Nitric acid is responsible for many environmental problems. This is as a result of chemical reactions with ammonia and NO_x such as acid precipitation formation and photochemical smog. Nitric acid is removed from the atmosphere by both wet and dry deposition and is one of the main contributors to acid precipitation leading to acidification of soil and surface water.

2.3.2.5 Impacts of ammonia

Ammonia is the only natural alkaline gas in the atmosphere making it an important neutraliser of anthropogenic acidity.[16] However, ammonia can upon deposition in soil or water lower its pH as result of nitrification of NH_4^+ (two hydronium ions for each ammonium molecule).[62] Forest shows a decline[87,88] and the pH of soil decreases as a result of nitrification of NH_4^+ in areas in close proximity down wind of a NH_3 source[86].

2.4 Aerosols

An aerosol is generally defined as a suspension of liquid or solid particles in a gas, with particle diameters in the range of 10^{-9}-10^{-4} m.[89-91,67] The most common examples of aerosols in the atmosphere are clouds consisting of primarily condensed water with diameters of approximately 10 μm. The term "aerosol" in atmospheric science refers to suspended particles that contain a large portion of condensed matter other than water.[92]

2.4.1 Sources and atmospheric processes of aerosols

Atmospheric aerosols originate from a wide variety of natural and anthropogenic sources.[93] All the natural and anthropogenic aerosols found in the atmosphere originate from two main sources into which both are classified, namely primary and secondary particulate material (PM) as shown in Figure 2.4. Primary particulate material is defined as particulate materials that are directly derived from the dispersal of solids from the earth's surface and are usually bigger in diameter size. Secondary particulate material forms due to physical and chemical reactions (Figure 2.5) in the atmosphere.[19] Secondary particulate materials are usually smaller in diameter, but can range to bigger sizes depending on the lifetime of the aerosol and the different physical and chemical transformations (Figure 2.4) they are exposed to within the

atmosphere before they get deposited onto the earth's surface. The primary and secondary particulate materials described above are also divided into a coarse and fine mode according to its particle diameter. The coarse mode describes particles larger than 2 μm in diameter, while the fine mode includes all particles between 0.01 and 2.0 μm[94] in diameter, which can also include particulate material of 10 μm in some air pollution control methods.[93]

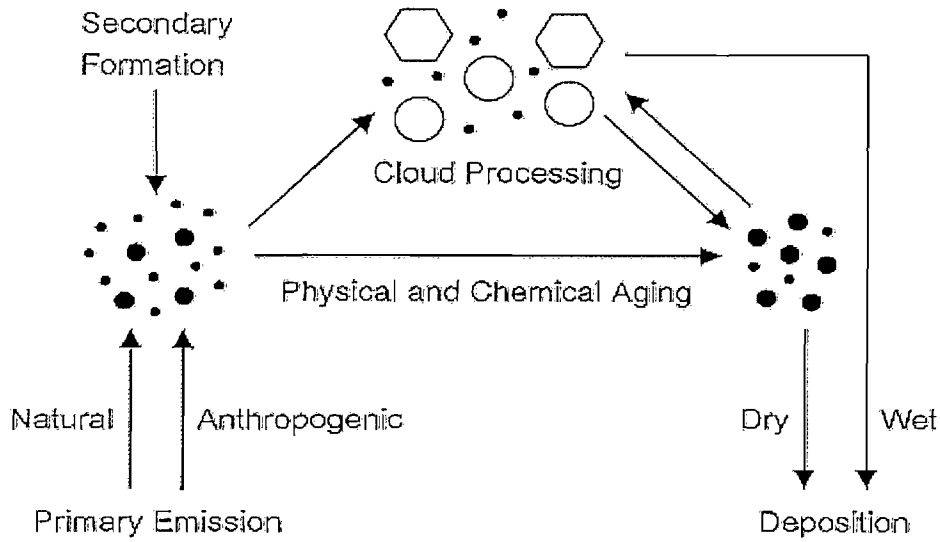


Figure 2.4: *Atmospheric cycling of aerosols*[88]

2.4.1.1 Primary particulate matter

Primary particulate material can either be emitted as liquids or solids from natural sources (biogenic materials (pollens, spores, micro-organisms, insects and needle-shaped particles), volcanic eruptions, biomass burning, sea salt, mineral dust and soil) or anthropogenic sources (incomplete combustion of fossil/biofuel, wind-driven or traffic-related suspension of roads).[93] Industry, especially those involving the mining of minerals, is responsible for anthropogenic aerosols emitted directly into the atmosphere[19] in the form of primary particulate material as large mineral dust aerosols (coarse mode).

2.4.1.2 Secondary particulate matter

Secondary particulate material, which forms as a result of gas to particle conversion in the atmosphere (Figure 2.5), includes new particle formation by nucleation and condensation of gaseous precursors, as well as atmospheric aging (transformation) of emitted airborne particles. These transformations include changes in particle size,

structure and composition through coagulation, restructuring, gas uptake,[93] as well as chemical reactions (e.g. nitrate-containing aerosols through oxidation of nitrogen oxides in the atmosphere, sulphate aerosols through oxidation of sulphur dioxide and ammonium bisulphate aerosol through the reaction of ammonia with sulphuric acid) in the atmosphere.[19] The main source of anthropogenic aerosols is its secondary formation (fine mode) through the oxidation of anthropogenically emitted gases caused by human activity. Soot is semi-volatile hydrocarbons and metals found in the fine particle mode and consists of black carbon primary emissions formed during the combustion processes of organic matter (naturally and anthropogenically).

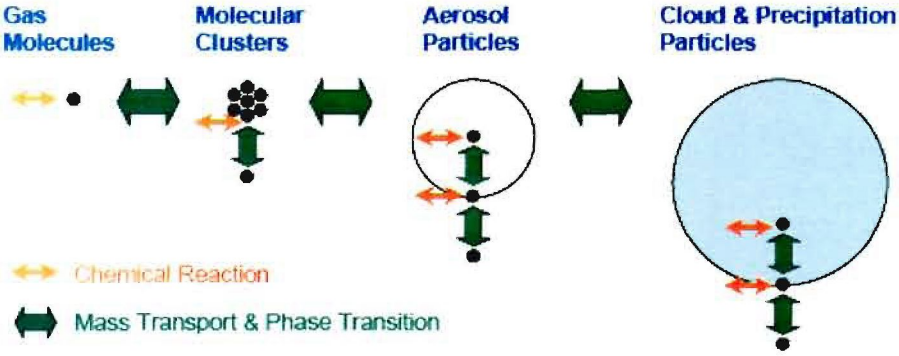


Figure 2.5: *Schematic illustration of the secondary formation of aerosols and the subsequent transformation of atmospheric aerosols and their components: mass transport and phase transitions in and between gas phase, clusters, aerosol, cloud and precipitation particles; chemical reactions in the gas phase, at the particle surface, and in the particle bulk*[93]

In this study, aerosols will be collected in two size fractions, namely PM<10 and PM<2.5. This is the most suited particle sizes for the study's objectives and also required for modelling purposes. These two sizes will be important when determining regional point sources as the PM_{10} together with its chemical composition can represent already-aged particles. The PM_{10} particles normally have a shorter atmospheric lifetime compared to $PM_{2.5}$ particles.

2.4.1.3 Formation and growth of atmospheric aerosols

The extent to which humans are affected by emissions from both natural and anthropogenic sources depends on the formation, growth, size, composition, motion, deposition, and electrical properties of the aerosol itself.[95] The size, composition and concentration of particles also determine the production, transport and ultimate fate of aerosols in the atmosphere. Increased aerosol concentrations are largely due to secondary aerosol production, i.e. homogeneous nucleation and subsequent growth of vapours.[96] The various size ranges and ultimate fate of atmospheric particulate material are largely determined by coagulation, nucleation, accumulation, condensation, evaporation and the chemical reaction processes thereof. All the preceding processes involving the aerosol's fate will now be briefly discussed.

Aerosols are divided into three groups according to its size, of which the size categories are: Aitken particles or nucleation mode (0.001-0.1 μm), large particles or accumulation mode (0.1-1 μm) and giant or coarse mode (> 1 μm).[67] Particles formed by the dispersal of surface materials generally have diameters larger than 0.1 μm and are already in the accumulation mode, while the Aitken particles must first be produced by the condensation of vapours, preceded in many cases by gaseous chemical reactions.[97] The large influence of the photochemical production of Aitken particles is visible in the difference in aerosol concentrations of 0.1 μm, which is less during winter than summer periods, as well as before and after sunrise. The amount of visible light, as well as UV-radiation, has been seen to correlate with the growth of particles. The particle formation and growth rate were also seen to correlate weakly with each other. The size distribution of aerosol particles also varies as a function of relative humidity due to the presence of water-soluble material in the particulate matter.[97]

The production as well as the elimination of different aerosol size pollutants are driven by the coagulation factors like Brownian motion (random motion that is a result of the fluctuations in the impact of gas molecules on particles), differential sedimentation and turbulence, which forces two particles or drops into contact and the particles stick to form a larger aggregate or drop.[67] Brownian motion of aerosol leads to collisions and coagulation of aerosols that ultimately lead to particle loss. Brownian motion is also a dominant driving force for the formation of sub-micron particles, due to coagulation processes, while turbulent flow would be a dominant driving force for particles ranging

from 1 to 10 micron. Due to Brownian movement, particles with diameters in the nm range coagulate very efficiently with larger particles and freshly-nucleated particles need to grow fairly rapidly past the 10 nm limit, otherwise it will be lost due to collision processes.[98] Agglomeration occurs in solid particles, while coalescence occurs in liquid particles. Sedimentation will be the dominant coagulation force for particles larger than 10 microns. The rate of coagulation depends not only on the forces driving the particles motion but also the hydrodynamic, van der Waals and electrostatic inter-particle interactions. The intensity of particle loss due to thermal coagulation is directly proportional to the square of the particle concentration, while coagulation efficiency increases with decreasing particle radius.[97] Aerosols only become climatically important if it grows to sizes of 50 nm and larger, while particles ranging between 1 and 10 micron meters in diameter pose the greatest threat to human health.[99]

Nucleation and accumulation account for the formation of most atmospheric aerosols and refer to mechanical and chemical processes by which aerosol particles in those particular sizes are usually produced. Nucleation is a spontaneous condensation process that occurs when a pure vapour or a gas mixture exceeds the saturation condition in an unconfined space.[100] Homogeneous nucleation is the spontaneous formation of liquid droplets directly from the gas phase, while heterogeneous nucleation occurs with aerosols with sufficient surface area.[101] Aerosols in the nucleation mode are mainly produced through gas to particle conversion (<0.1 μm). Aerosols in the accumulation mode (0.1-1 μm) are usually produced through the heterogeneous condensation of gas vapour into existing aerosol particles.[98] The residence time of aerosols depends on its size, chemistry and height in the atmosphere, which will also determine its impact on health and the environment. Aerosols between 0.1-1 μm remain in the atmosphere longer than the other two size ranges and are therefore more harmful to humans and have a larger impact range. Higher sedimentation rates for particles > 1 μm and the faster coagulation rates for nucleation mode particles of 0.001-0.1 μm force its faster removal rates from the atmosphere to limit both these size range impact compared to the 0.1-1 μm. The number of nucleation particles (< 0.1 μm) starts to increase several hours before sunrise indicating that homogeneous nucleation can proceed also at night, most likely as chemical reactions of atmospheric gases and water vapour.[97]

Condensation and evaporation involve particle growth at saturations higher than the saturation vapour pressure. The saturation equilibrium ratio, which is determined by

the droplets (surface tension, molecular weight, density, diameter of droplet in equilibrium, the equilibrium vapour pressure over the droplet surface and at the droplet surface) must be larger than the environment's saturation in order for particle growth to occur. If it is smaller, the droplet will evaporate.[102] Chemical formation proceeds through free radical species acting as nuclei upon which other molecules interact and react chemically. Chemical reactions between various gases also result in gas-to-particle conversions (GPC), which is mostly catalysed by ultraviolet radiation from the sun. All particles produced by GPC are hygroscopic and act as cloud condensation nuclei (CNN).[101]

A fraction of air molecules is electrically charged (ions) as a result of ionisation radiation.[97] Charged particles can exist as molecular clusters up to large aerosol particles.[103,104] If a cluster of ions grows to 1-2 nm, spontaneous nucleation occurs.[105,106] The cluster of ions behaves like kernels of condensation of nucleation vapours, converting it from the gas to particle phase.[107] Aerosol ions, just like ordinary aerosol particles above 1.6 nm, experience all the processes known from aerosol physics, growth and vapour condensation, coagulation, wet and dry deposition, and propagation in the atmosphere.[108,109] Charged particles with the added electrical properties can influence its motion and thus subsequent collision processes and removal.

2.4.1.4 Removal of aerosols from the atmosphere

The major processes for removing aerosols from the atmosphere are through dry deposition or sedimentation and wet deposition (rain, fog and snow).[101,110] In the presence of water vapour, aerosols act as condensation nuclei to form clouds, and are removed from the atmosphere during rain events (wet deposition).[101] The efficiency of collision between falling droplets and aerosol particles is largely influenced by the inertial impaction, Brownian diffusion, phoresis caused by thermal or concentration gradients, turbulent effects and electrical forces.[110] In the submicron range, particles are removed either by cloud processing, below-cloud scavenging or coagulation.[67] For particles smaller than 1 μm, however, Brownian diffusion is the main removal mechanism.[110] The rate of aerosol removal through sedimentation under gravity is determined by the basic parameters of fall velocity and diffusion coefficient. Removal of larger particles is easier, as gravitational impact results in fall-out. Smaller particles

are removed by coagulation, while particles with long residence times (e.g. r < 0.3 μm) appear to accumulate.[19]

The size of particles, the radiation and time of day, different natural and anthropogenic processes that determine physical and chemical characteristics of the particle, as well as the geographic location are all important factors that determine the formation, growth and removal of atmospheric aerosols, as is described in preceding paragraphs. It is therefore important to take all these factors into consideration when monitoring aerosols at a specific location and making conclusions with regard to the characteristics of it based on the analytical results.

2.4.2 Health and environmental impacts of selected aerosols

Aerosol sources determine its composition and together with its composition-dependant properties such as particle size, determine its impact on climate, atmospheric chemistry as well as health and the environment. These interdependent properties are illustrated in Figure 2.6.

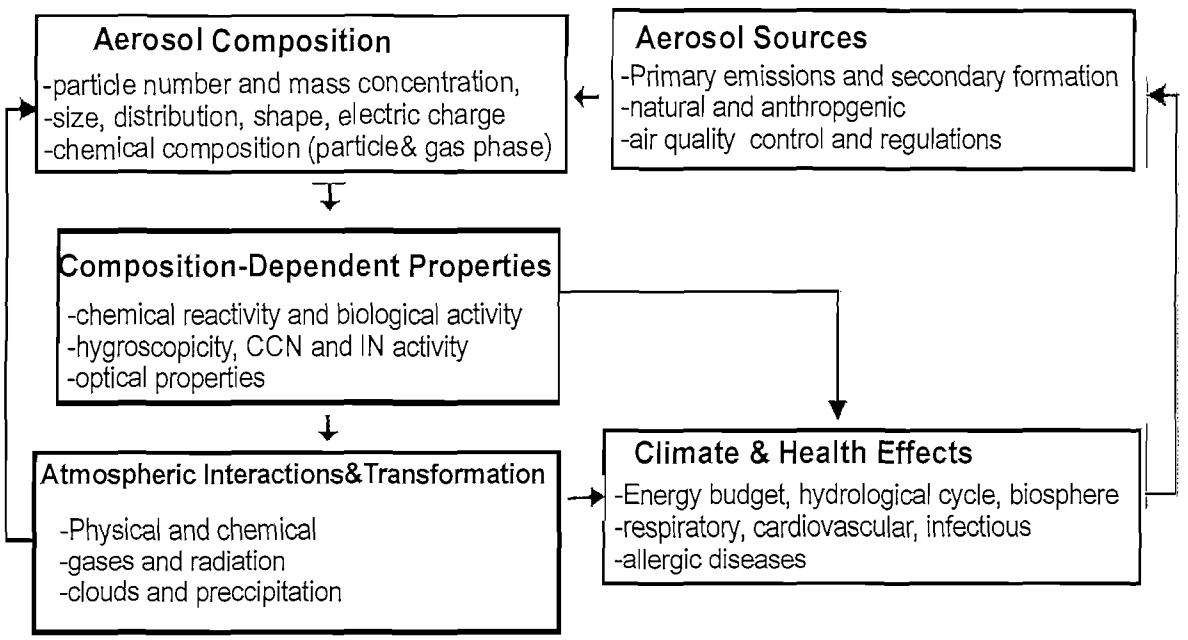


Figure 2.6: *Interdependence and feedback between atmospheric aerosol composition, properties, interactions and transformation, climate and health effects*[93]

Fine particulate matter can stay airborne for days up to weeks being transported over long distances and therefore has a larger effect on atmospheric chemistry, impact on

the environment and is more harmful to humans. The constituents in the smaller aerosol also tend to be more chemically active. The smaller size makes it possible to penetrate deep into the lungs, causing permanent damage.[111] Coarse mode particles on the other hand are classified as aerosols with a diameter of 10 μm and larger. These large particles do not stay in the air for too long and therefore do not travel long distances or have the same global health and environmental risks or impacts associated with their smaller counter parts.

2.4.2.1 Health impacts of aerosols

The World Health Organization (WHO) has identified particulate pollution as one of the most important contributors to ill health.[112] Health-effects reported to be associated with PM can be linked with increased daily and annual mortality rates in adults and include cardiopulmonary disorders, symptoms of respiratory dysfunction (e.g. wheeze, cough), asthma attacks, pneumonia, bronchitis, and chronic obstructive pulmonary disease.[113] Cardiovascular mortality is significantly associated with CO, NO_2, SO_2, $PM_{2.5}$ and $PM_{2.5-10}$, as well as elemental carbon. Combustion-related pollutants and secondary aerosols are also associated with cardiovascular mortality.[114] A number of potential harmful substances has been identified in fine mode aerosols especially the $PM_{2.5}$. These include nickel, lead and cadmium, which are all more concentrated in $PM_{2.5}$ than PM_{10}.[95] Heavy metals, such as nickel and chromium, have been defined by the International Agency for Research on Cancer (IARC) as potential cancer causing agents.[115] Organic aerosols are a complex mixture of many classes of compounds[116] of which certain fractions contain polycyclic aromatic hydrocarbons (PAHs). These PAHs have been shown to be carcinogenic in animals and mutagenic in *in vitro* bioassays.[15]

2.4.2.2 Climatic and other environmental impacts of aerosols

Airborne particles and their transformation products are removed from the atmosphere through wet and dry deposition processes. These removing processes lower the long-term build-up of lethal concentrations of these pollutants in air and moderate the potential for direct human health effects caused by inhalation. These deposition processes, however, transfer the PM pollutants to other environmental media where they can alter the structure, function, diversity and sustainability of complex ecosystems.[117] The species with the greatest impact on vegetation are in the following

order: SO_2, fluoride (where it still exists as a problem), particulate heavy metals, base cations, sulphates and nitrates. The precipitation of aerosols causes adverse environmental impacts and has the potential to alter ecosystem structure and function by altering the nutrient cycling and changing the biodiversity.[118] The majority of documented toxic effects of particles on vegetation reflects its chemical content (e.g. acid/base, trace metal, nutrient), surface properties or salinity.[117] Atmospheric PM may affect vegetation directly by deposition on foliar surfaces or indirectly by changing the soil chemistry or by changing the amount of radiation reaching the earth's surface. Indirect effects are most significant since they alter the nutrient cycle and inhibit nutrient uptake. Measurable responses have been observed as reductions in photosynthesis, changes in soil salinity, and foliar effects resulting from nitrate, sulphate, and acidic and heavy metal deposition. The SO_4^{2-} is about 30 times less phytotoxic than SO_2. Nitrate and sulphate associate with sea-salt particles and the sodium and chloride that constitute the bulk of the particles are known to cause foliar damage.[119] Available data from plant effect studies suggests that hydrogen and sulphate ions are more likely to cause damage than ions containing nitrogen.[120] Soil acidification is a result of deposition of NO_3^-, SO_4^{2-} and associated H^+, which causes the reduction of soil-exchangeable base cations.[121] The loss of K^+, Ca^{2+} and Mg^{2+} with nitrogen enrichment results in abnormal plant growth rates and altered competitive relationships. The integrated study of *Johnson and Lindberg*[122] provided extensive data showing particulate deposition contributing considerably to the total impact of base cations. This study showed particle deposition contributing 47% of total Ca^{2+} deposition, 49% of K^+ deposition, 41% of total Mg^{2+} deposition, 36% of total Na^+ deposition and 43% of the total cation deposition. This makes aerosol deposition an important source of base cations back to the environment.

Aerosols both absorb and scatter solar radiation affecting the amount of radiation reaching the earth's surface. By scattering and absorbing visible radiation, aerosols change the planetary albedo (reflectance of the planet) and by absorbing and re-radiation of infrared radiation, they enhance the greenhouse effect. Both the above-mentioned processes result in direct radiative forcing by aerosols causing climate change.[101] The chemical composition of aerosols determines its complex refractive index, which is an important parameter while determining its radiative effects. Each aerosol contains a real and imaginary part with the real part scattering radiation and

the imaginary part absorbing radiation. Aerosols originating from combustion processes usually have high absorption properties.[95]

A total direct aerosol radiative forcing combined across all aerosol types was reported for the first time as –0.5 ± 0.4 $W.m^{-2}$ with a medium to low level of understanding.[3] The direct radiation forcing for important individual aerosol species has been estimated from models with less uncertainty to be –0.4 ± 0.2 $W.m^{-2}$ for sulphate, –0.05 ± 0.05 $W.m^{-2}$ for fossil fuel organic carbon, +0.2 ± 0.15 $W.m^{-2}$ for fossil fuel black carbon, +0.03 ± 0.12 $W.m^{-2}$ for biomass burning, –0.1 ± 0.1 $W.m^{-2}$ for nitrate, and –0.1 ± 0.2 $W.m^{-2}$ for mineral dust.[3]

Indirect radiative-influenced aerosols can act as cloud condensation nuclei (CCN) for the formation of clouds. An increase in concentration of aerosols results in an increase in the concentration of cloud droplets, leading to an increase in the albedo (or reflectance) of clouds, which has negative radiative forcing (cooling effect) on the climate. The total indirect radiative effect of aerosols through the cloud albedo is estimated to be –0.7 $W.m^{-2}$, which is a low-level scientific understanding model estimate.[3] Black carbon aerosol deposited on snow reduced the surface albedo and is estimated to yield a radiative forcing of +0.1 ± 0.1 $W.m^{-2}$.

2.5 Dry deposition estimates of gaseous and aerosol species

Dry deposition involves the transport of gaseous and particulate species from the atmosphere onto any surfaces of the earth, in the absence of precipitation. The transport (deposition) of these gaseous species and particulates to the earth's surface is governed by three primary factors:

i) atmospheric turbulence;

ii) chemical properties of depositing species; and

iii) the nature of the surface itself.[15]

The complexity and variability of the physical, biological and chemical properties of these surfaces and the diversity of the chemical and physical properties of the substances make it difficult to parameterise the processes affecting dry deposition. The primary mean of conducting atmospheric budgets is using numerical models to simulate the meteorology, atmospheric chemistry and deposition.[123]

In routine monitoring programmes where data is readily available, the inferential model is most suited for calculating dry depositions rates.[16] The US Environmental Protection Agency's Clean Air Status and Trends Network (CASTNet, originally known as the National Dry Deposition Network) also focused on an inferential approach to continuously estimate dry deposition velocities at some of their sites.[124] The inferential technique for determining dry deposition rates is based on the direct application of Equation 2.46:

$$F = -V_d C \qquad 2.46$$

This is a universally used formulation for dry deposition, where it is assumed that the dry deposition flux (F) is directly proportional to the product of C (the local ambient concentration of the depositing species at some reference height above the surface) and the estimated deposition velocity V_d. For the inferential model to be effective, the detailed surface and meteorology conditions surrounding the concentration monitoring sites must be incorporated in determining V_d, as the derived dry deposition flux is strongly dependent on this value. The deposition velocity V_d is determined by a three-step resistance process called the 3-leaf resistance analogy as is shown in Figure 2.7[15]

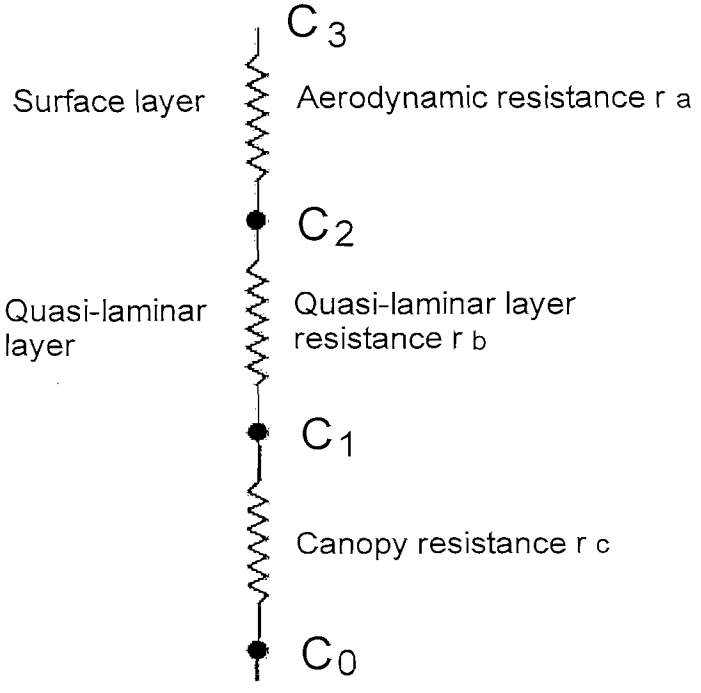


Figure 2.7: *Schematic presentation of the three-leaf resistance model for dry deposition*[15]

From Figure 2.7 the deposition velocity (V_d) is determined by the sum of three resistances in series. These resistances represent the three layers that gases and aerosols have to overcome before they can deposit on the final surfaces as presented in Equation 2.47.

$$V_d = r_a + r_b + r_c \qquad 2.47$$

(where r_a = aerodynamic resistance; r_b = quasi-laminar resistance; r_c = surface of canopy resistance)

Deposition of gas and aerosols is a three-step process, which occurs as follows:

i) gas or aerosol with concentration C_3 is aerodynamically transported down by turbulent diffusion through the atmospheric surface layer of resistance to the quasi-laminar layer adjacent to the earth surface where its concentration is now C_2;

ii) from here it is transported across the quasi-laminar layer of resistance through molecular diffusion (gases and aerosols) and sedimentation (aerosols) to the surface itself where its concentration is now C_1;

iii) surface uptake of gas and aerosol occurs where concentration of gas or aerosol is C_0.[15]

The concentration difference between C_1 and C_0 represents the resistance of the surface itself for the uptake of the gas and aerosol. Aerosols can also be removed in the quasi-laminar layer through interception and impaction directly to the earth's surface.

2.6 Heterogeneous reactions between gases and aerosols

The deposition/degradation of aerosols and gases in the atmosphere can be described by the aging/degradation/deposition of aerosols in the atmosphere via heterogeneous reactions with anthropogenic gas emissions into the atmosphere. The partitioning equilibrium between aerosol and gases in most heterogeneous reactions between them in the atmosphere is governed by the sulphate uptake process.[41] This uptake process is diffusion-limited and a rate-determining process, which involves volatile inorganic species that rapidly reach equilibrium on time scales shorter than the time step over which other changes occur.[125] Most studies use the pseudo-first-order irreversible uptake kinetic equation to describe the sulphate deposition process.[126-130] Non-sea-salt sulphate irreversibly deposits to both the coarse and fine modes of the

aerosol particles through the pseudo-first-order kinetic relationship, with rate coefficients from *Luria and Sievering's* work[127] as given in Equation 2.48.

$$dC_{sulphate}/dt = k_{SO_2.H_2SO_4}C_{SO_2.H_2SO_4} \qquad 2.48$$

(where: $k_{SO_2.H_2SO_4}$ = rate coefficient ($cm^3.s^{-1}$) and $C_{sulphate}$ and $C_{SO_2.H_2SO_4}$ are concentrations of SO_4^{2-} in the aerosol particles and SO_2 or H_2SO_4 in the gas phase, respectively. Particulate sulphate is produced via both SO_2/H_2SO_4 deposition from the gas phase and binary homogeneous nucleation of H_2SO_4 and H_2O)

In heterogeneous chemistry the initial volatile inorganic species distribution is determined by the initial mass (or mole) of the non-volatile cations (Na^+, Ca^{2+}, Mg^{2+} and K^+) and non-sea-salt sulphate in each aerosol mode.[41] The volatile inorganic species (NH_3, HNO_3 and HCl) partitioning in these equilibriums are also governed to charge-neutrality condition at each aerosol mode through thermodynamic relations. The major heterogeneous reactions of inorganic volatile gases and the two aerosol modes (particle sizes) of sea-salt (marine) and mineral (dust) aerosol, as predicted by *Song and Carmichael,*[41] with their model, will be discussed in the following paragraphs.

Marine aerosols:

The major heterogeneous reactions involving gases and the two marine aerosol modes (particle sizes) are represented in Figures 2.8-10. SO_2/H_2SO_4 deposition is an irreversible diffusion-limited process, thus available surface area is a critical factor in determining the deposition characteristics of sulphate. With a marine aerosol, SO_2/H_2SO_4 deposits to the fine mode (in the log-normal distribution of the sea-salt aerosol, the primary peak exists in the fine mode).[41]

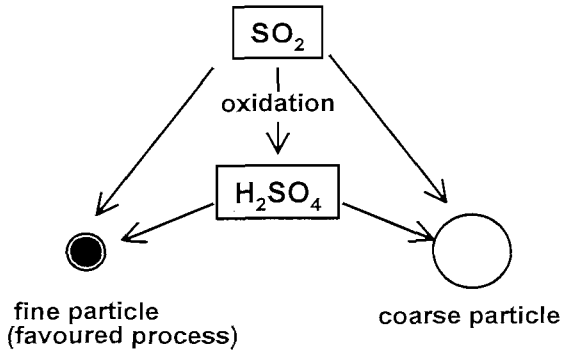


Figure 2.8: *Interaction between sulphur and the two marine aerosol modes*

Natural contributions to marine SO_2 are due to the oxidation of H_2S, COS and DMS from the sea environment. Almost all SO_2 is oxidised to H_2SO_4 in the form of aerosol, which rapidly incorporates into water droplets. Both homogeneous and heterogeneous oxidations take place, with heterogeneous oxidation dominating. H_2SO_4 and SO_2 both deposit to the coarse and fine modes. The deposition to the fine mode is much stronger than to the coarse mode due to the larger available surface area (diffusion limited process) of the fine mode of the marine particle.[41,131] The degree in which sulphate dominates aerosol chemistry is demonstrated by Equation 2.49.

$$R_{si} = [NH_4^+] + [Na^+] + [K^+] + 2 \times [Ca^{2+}] + [Mg^{2+}]/2 \times [SO_4^{2-}] \qquad 2.49$$

(where $[NH_4^+]$ = total concentration of the ammonia in this mode; R_{si} = initial sulphate richness)

The R_{si} ratio is used to explain changes in the composition of aerosols in the fine mode where R_s describes the sulphate richness and composition changes occur accordingly:

i) highly sulphate rich ($R_s < 0.5$);

ii) sulphate rich ($0.5 < R_s < 1$) and

iii) cation rich ($R_s > 1$)

If the aerosol is cation rich the sulphate deposition will take place to neutralise the non-volatile cations. When the fine mode becomes sulphate rich, as a result of deposition to the fine mode, it will take up ammonia (Figure 2.9) from the gas phase to neutralise the sulphate. If the fine mode becomes highly sulphate rich, the process of self neutralisation will take place by means of Equation 2.50.

$$H_2SO_4 \rightarrow HSO_4^- + H^+ \qquad 2.50$$

The sulphate deposition process controls the distribution of ammonium. Ammonium in the fine mode increases as the sulphate deposition in the fine mode proceeds (see Figure 2.9).[41]

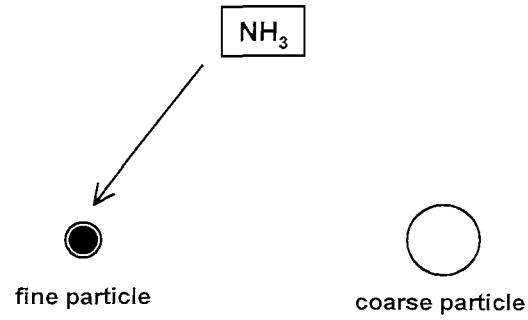


Figure 2.9: *Interaction between ammonia and two marine aerosol modes*

The slow sulphate deposition onto the coarse mode in comparison with its deposition to the fine mode also controls the distribution of ammonium, causing ammonium in the fine mode to increase as the sulphate deposition onto the fine mode proceeds.
Sulphate will preferentially substitute chloride rather than the less-volatile nitrate in the coarse mode and the chloride levels will continuously decrease in both modes as the particulate sulphate increases (see Figure 2.10).[41,132] In particular, the chloride in the fine mode is almost exhausted after one day. This is a well-known phenomenon and has been confirmed by an observational field study.[132]

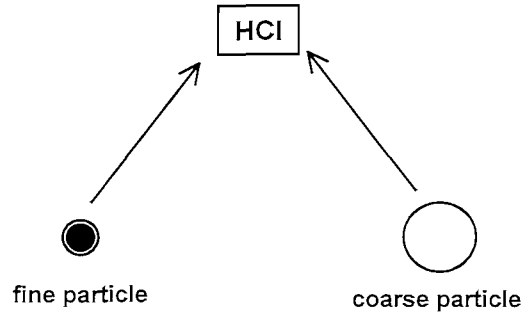


Figure 2.10: *Interaction between hydrochloric and two marine aerosol modes*

Nitric acid is continuously produced via gas phase reactions in simulations and this increase contributes to its increased concentration in the gas phase and thus the fine mode because of its less volatile nature as an inorganic gas in comparison with the other gases. However, it is quickly replaced by sulphate deposition in the fine mode.[41]

The sulphate deposition to the coarse mode being so slow in comparison to the fine mode causes a ratio of the total sulphate (sulphate + bisulphate) in the fine mode to total sulphate in aerosol mode to be 0.68 within 48 hours.[41] This compares well with the 0.73 found for the experimental size resolved composition in the same region by *Kim et al.*[131]

Mineral Aerosol:

The major heterogeneous reactions of inorganic volatile gases and the two mineral aerosols modes are given in Figures 2.11-14. For the mineral aerosol, the coarse mode has a larger available surface area causing a higher deposition of SO_2/H_2SO_4 to the coarse mode (see Figure 2.11).[41,133]

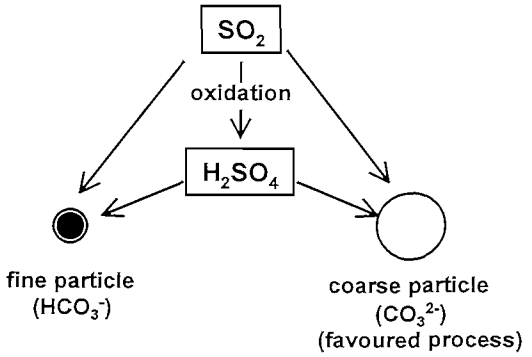


Figure 2.11: *Interactions between sulphur and the two mineral aerosol modes*

SO_2/H_2SO_4 is deposited to both modes continuously releasing carbonate in the coarse mode and bicarbonate in the fine mode (see Figure 2.12), which are initially associated with the cations Na^+, Ca^{2+}, Mg^{2+} and K^+. The H_2SO_4 and SO_2 deposited to the fine mode also continuously substitute nitric acid and hydrochloric acid, neutralising the non-volatile cations.[41,134,135]

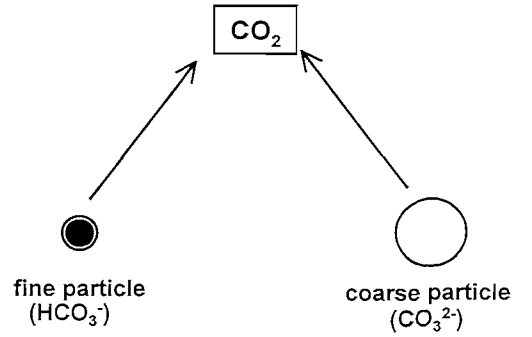


Figure 2.12: *Interactions between bicarbonate/carbonate/CO_2 and the two mineral aerosol modes*

This carbonate liberation process is very similar to the chlorine-release process in the sea-salt particles, and similar chemistry was also observed in rain.[134] Studies by *Hirai et al.,*[135] also suggested that $CaCO_3$ is in fact replaced with $CaSO_4$.

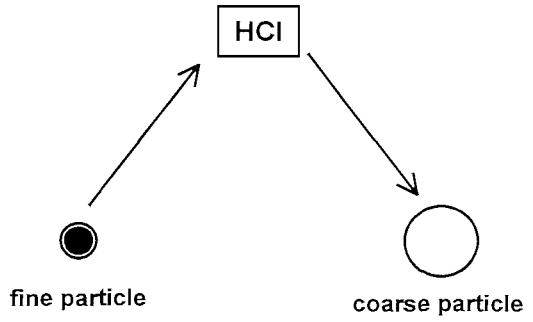


Figure 2.13: *Interaction between hydrochloric acid and the two mineral aerosol modes*

A large amount of chloride is initially present in the fine mode, which gets liberated through sulphate deposition and a comparable amount of it goes to the coarse mode (see Figure 2.13).

A large amount of nitric acid is also initially present in the fine mode, which is liberated through sulphate deposition and ends up in the coarse mode (see Figure 2.14).[41,35,36]

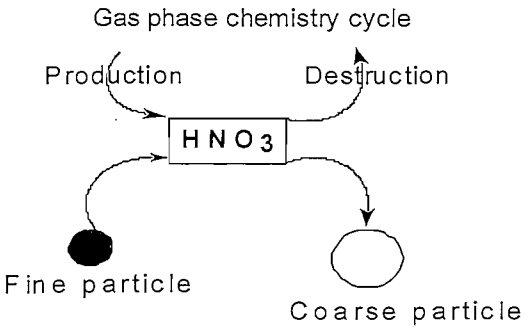


Figure 2.14: *Interactions between nitric acid and the two mineral aerosol modes*

Nitrate and chloride distribution is largely driven by the acidity (sulphate richness) of both aerosol modes. Both chloride and nitrate are attracted (volatile acids) from the more acidic fine mode to the less acidic coarse mode. In studies conducted by Song and Carmichael the release slopes of HCO_3, HCl^- and NO_3^- showed their difference in volatility through the decrease of the anions concentration with time.[41] This showed the order in which substitution will take place due to the volatility of species such as $HCO_3 > HCl^- > HNO_3^-$.

Another important heterogeneous reaction in the troposphere is the hydrolysis of N_2O_5 on aerosol particles. N_2O_5 exists in equilibrium with NO_3, according to Equation 2.51.

$$NO^{\bullet}_2 + NO^{\bullet}_3 \leftrightarrow N_2O_5 \qquad 2.51$$

This process is limited to night time since NO_3 production is very slow compared to the photolytic destruction of NO_2, which is needed for its formation. The impact of N_2O_5 hydrolysis at the surface of aerosol particles on the oxidising capacity of the troposphere (in terms of NO_x, ozone, and $HO^{\bullet}$ distributions in time and space) was demonstrated by *Deneter and Crutzen*[136] in a pioneering modelling study.

Heterogeneous interactions of NO_2 with aerosol particles are the likely night time source of HONO, as repeatedly detected by differential optical absorption spectrometry and denuder techniques in polluted urban atmospheres.[137-140] After sunrise, HONO is photolysed (photolysis frequency in bright sunshine ca.$1.3 \times 10^{-3}.s^{-1}$ [141,142]), producing $HO^{\bullet}$, which triggers degradation processes of environmental chemicals long before other radical sources (e.g. the photolysis of ozone, followed by the reaction of O (^1D) with water vapour) generate $HO^{\bullet}$ radicals at a significant rate.[143]

2.7 An overview of heterogeneous modelling

All equilibrium models are based on the assumption that volatile species in the gas and aerosol phases are in chemical equilibrium. Although this may be true in many cases, there are situations where it is not valid, for instance when the time needed for equilibrium is longer than the time local air is in contact with the particles. In these cases the equilibrium model is combined with a transport model.[144]

Many thermodynamic equilibrium models have been developed over the years, of which EQUIL was one of the first developed by *Bassett and Seinfeld.*[145] It was used to determine the composition of the ammonium-sulphate-nitrate-water aerosol system. It was improved to the KEQUIL model in 1984, to account for partial vapour pressure dependencies on the sphericity of particles (Kelvin effect).[146] In 1986, the MARS model was developed by *Saxena et al.*[147] The results from this model were in reasonable agreement with EQUIL and KEQUIL and took less computing time so that it could be incorporated into bigger aerosol models. This was done by reducing the number of equations by dividing aerosol species in sub-domains and it resulted in a four-hundred-times faster solution than KEQUIL. A major drawback was that it made use of equilibrium constants and activity coefficients that affected the partitioning between gas and particulate phases when calculations were made at different temperatures. The SEQUILIB model developed in 1987 by *Pilinis and Seinfeld*[125] was a huge improvement on the previous three models as it incorporated the sodium and

chloride species (marine aerosol). It also used an algorithm for calculating the distribution of volatile species among different particle sizes so that the thermodynamic equilibrium is achieved between all the particles and the gas phase.[144] One of the most recently developed thermodynamic equilibrium models was the SCAPE model by *Kim et al.,*[148,149] which implemented a domain-oriented solution algorithm similar to that of SEQUILIB, but with updated thermodynamic data for the components. It calculates the pH of the aerosol phase from the dissociation of all weak and strong acid/base components and includes the temperature dependence of single salt deliquescence points using the expressions derived by *Wexler and Seinfeld.*[150] SCAPE embodied the main correlations available for calculating multi-component solution activity coefficients, and could predict the presence of water at very low ambient humidities. Another improvement on the SCAPE and SEQUILIB models was the ISORROPIA model developed by *Nenes et al.,*[144] which incorporated an algorithm for mutual deliquescence regions of humidity or MDRH. MDRH is a region of relative humidity where the combined humidity of all salts is lower than the minimum humidity of each component individually, hence being the only humidity where the aqueous solution can co-exist with a precipitate composed of all the aerosol salts. Thus, ISORRPIA predicts water where the other models cannot, which can have a great influence in predicting dry aerosol estimates. This model is also 400 times faster in calculating solutions than SCAPE.[144]

The most recent development in equilibrium models, is the ORISAM model (organic and inorganic spectral aerosol module) developed by *Bessagnet and Rosset,*[151] which is a combination of models incorporated as one. In this model, aerosols are not assessed as independent tracers with no interaction with the gaseous environment, but simulates in some way gas-particle interactions and the chemical and size evolution of the resulting heterogeneous aerosols.[151] With this model, the sectional approach was retained for solving aerosol multi-component systems, while describing the microphysical processes. The model includes the aerosol size distribution of aerosols, as well as the organic part (organic and black carbon) of the aerosol, while taking into account the processes of nucleation, coagulation, condensation, absorption, chemical reaction and deposition.[20] All of the latter three processes are resolved in this model using different methods, such as nucleation as done according to *Kulmala et al.,*[152] coagulation as in *Gelbard et al.,*[153] nitrate heterogeneous chemistry as in *Jacob,*[154] gas to particle partitioning for inorganics by using

ISORROPIA of *Nenes et al.,*[144] and the empirical partitioning coefficients for organics of *Odum et al.*[155] After the original ORISAM model, a few other models were developed using the same base model, but adding a new parameter. The first of which was the ORISAM-0-D model developed by *Liousse et al.,*[50] which focused on the organic part of the aerosol to account for both types of primary carbonaceous particles (primary organic carbon and black carbon) and simulating the formation of secondary inorganic and organic aerosols.[50] In 2006, the ORISAM-RAD model was developed by *Mallet et al.,*[156] where the 3-D distribution of aerosol radiative properties (aerosol optical depth, single scattering albedo and asymmetry parameter) was added to the ORISAM model.

As described in the beginning of Paragraph 2.7, it is necessary to sometimes combine the models we have just mentioned with a transport model, to simulate transformation reactions where equilibriums are obtained long after aerosols were in contact with the regional air. These types of transport models were also improved through the years beginning with the STEM (sulphur transport eulerian model) type models that were first used in conjunction with the SCAPE model by *Song and Carmichael.*[41] The first STEM model consisted of gas-phase chemistry based on the chemical mechanisms of *Lurmann et al.,*[157] and aerosol physical processes such as nucleation and condensation/evaporation of water, processes modelled using empirical models as used by *Zang.*[34] Other aerosol physical processes also include absorption/dissolution of inorganic species and the empirical relations for condensation/evaporation processes suggested by *Hanel,*[158] used over three different ranges of relative humidity. The STEM model was improved to STEM-II by *Carmichael et al.,*[159] which simultaneously solves all processes that take place over an Eulerian grid covering the domain being studied by solving a mass balance for every chemical species considered in each phase (air and condensed water) within the different processes occurring in the pollutants (namely: physical dispersion, chemical gas reactions, absorption in condensed water and chemical aqueous reactions, dry deposition of pollutants by absorption at ground level and wet deposition of pollutants through falling of condensed water). Today transport models used in conjunction with the more evolved multidimensional equilibrium models like ORISAM resemble the TM type models. These models have evolved to the CHIMERE and TM-4 transport models used especially in Europe in conjunction with ORISAM. TM is a three-dimensional chemical transport model developed in collaboration with the KNMI (Royal

Netherlands Meteorological Institute), the Institute for Marine and Atmospheric Research Utrecht (IMAU) and the Institute for Environmental and Sustainability of the EU Joint Research Centre (EI-JRC) in Ispra. TM uses meteorological fields (weather data) of the European Meteorological Centre (ECMWF) off-line to calculate mass fluxes and various meteorological parameterisations, such as convective and turbulent transport to create pre-processed meteorology data. This data is then used in the model to calculate the temporal evolution of the three-dimensional distribution of various kinds of tracers, such as gases and aerosols.[160] The CHIMERE Eulerian chemistry transport model (CTM) was developed in 2001 by *Schmidt et al.*[161] based on the integration of the mass continuity equation for concentrations of several chemical species in each cell of a given grid (with the distance between horizontal grid points of 0.5°). Here the model area can be chosen with five vertical layers ranging from the boundary layer to the lower part of the free troposphere.[161] CHIMERE requires the emission input of 16 model species and the option of including different gas phase chemical mechanisms, of which the original scheme MELCHIOR as used by *Lattuati,* was used, which included 44 species and 116 reactions.[162] The original CHIMERE was later updated by *Vautard et al.*[163] Another model of the TM type was the TM4 global chemistry transport model developed by *Van Velthoven et al.,*[52] and upgraded by *Jeuken et al.*[53] It uses meteorological data reanalysed by ERA40 and pre-processed for use in TM4 by KNMI. The transport equations are solved for mass mixing ratios of 31 gaseous species using *Russel and Lerner's*[164] advection scheme at 3°x 2° horizontal resolution and 31 hybrid sigma-pressure vertical levels. A modified CBM-IV of *Howling et al.*[165] is used for tropospheric gas phase chemistry solved by an Euler-backward iterative method.[166] Cloud droplets bulk aqueous phase chemistry is treated according to *Jeuken et al.,*[53] while the dry deposition scheme is treated as in *Ganzeveld et al.*[167] The dry gas deposition used the resistance scheme of *Wesely and Hicks,*[123] applied to the vegetation types of *Olson et al.*[168] The sulphate to ammonia ratios in the TM4 particulate phase were computed using only bulk microphysics.[169]

2.8 Climatology of the sub-continent

The maintenance of a sustainable environment depends on the ability of wind and turbulence to disperse pollutants rapidly as it is emitted. Source characteristics (height of release, temperature and buoyancy of emissions), as well as meteorological factors (atmospheric stability, small-scale turbulence, local wind conditions) control the initial

mixing and transport of emitted material near either natural or anthropogenic emission sources.[10] Long-range material transport over distances of several hundred to a few thousand kilometres is primarily controlled by large atmospheric circulation patterns and the synoptic systems embedded within them.[170] Apart from the meteorological factors controlling the dispersion of the emissions, the composition of the emissions, its concentration and plume characteristics will play a significant role in its deposition and ultimate impact on the environment. The Savannah fires, industrial emissions, Indian and Atlantic Ocean, dry arid areas as well as the unique meteorological system on the southern African continent represent a complex system. It ultimately determines the regional atmospheric distribution of trace gas and aerosols, ecosystem functioning and biogeochemical cycling.[171] In the following paragraphs the meteorological conditions will be addressed followed by the major aerosol and gas species found in the southern African region.

The mean atmospheric circulation over southern Africa is anticyclonic during most parts throughout the year. The anticyclone is deep and stable, and stable substances associated with the semi-permanent subtropical anti-cyclone, produce the highly stable conditions.[172] This results in the stable conditions and stable discontinuities in the lower troposphere that control the development of the so-called African haze layer. The haze layer blankets southern Africa for most of the year on non-raining days to the level of the frequently occurring, sporadic ubiquitous ending stable layers observed at the 500 hPa level at an altitude of 5-6 km.[173] These thick aerosol layers covering most of southern Africa are visible from space during the dry season in September and can be attributed to the climate.[44] This southern African climate entails a dry season following a high rainfall season and prolific vegetative growth.[45] The biomass-burning emissions of the following dry season becomes the overwhelming atmospheric influence of the next dry season.[174]

Principle features influencing the climate in South Africa are the continental anticyclone, ridging anticyclone, westerly wave, cut-off low and tropical easterly disturbances.[175-177] The most important of these synoptic situations are the semi-permanent, subtropical continental anticyclones, which dominate 70% of the time during winter and 20% of the time in summer.[176] The northward and southward displacement of the Indian Ocean high pressure cell results in a significant seasonal variation of the boundary layer winds over the South African *Highveld region*. This is not only important for the study of deposition, but also for the impacts this will have on

the atmospheric chemistry of southern Africa. During winter, air flow in the lower boundary layer over the Highveld region is dominated by the Indian Ocean anticyclone circulation,[178] with an 800 hPa geo-potential height level, which occurs on average 500 m above the mean altitude of the interior plateau surface.[172] This results in dominant westerly and west-north-westerly winds over the northern regions of the subcontinent such as Gauteng and the industrial region of Mpumalanga.[178] Due to the southward migration of the high pressure belt during summer, circulation is characterised by weak northerly-component air flow over the same northern regions of the subcontinent. The winds change direction progressively towards north-north-east at the end of summer and tend to go back to a westerly direction at the onset of autumn, as the high pressure belt migrates northward.[178,179] A five-year backward and forward trajectory climatology of air transport from the industrial Highveld region of South Africa was compiled by Piketh and Prangley. It shows five major transport pathways for air moving from the Mpumalanga Highveld as seen in Figure 2.15.[180] The frequency of occurrence for these transport pathways are given as a percentage at an initiation level of 750 hPa. The most frequent pathway is over the Indian ocean (48%), followed by the recirculation pathway, which ends up again over the Indian ocean (32%), the southern African pathway over the Atlantic ocean (12%), the central African pathway back over Africa (6%) and the Cape pathway in Cape Town's direction (1%).

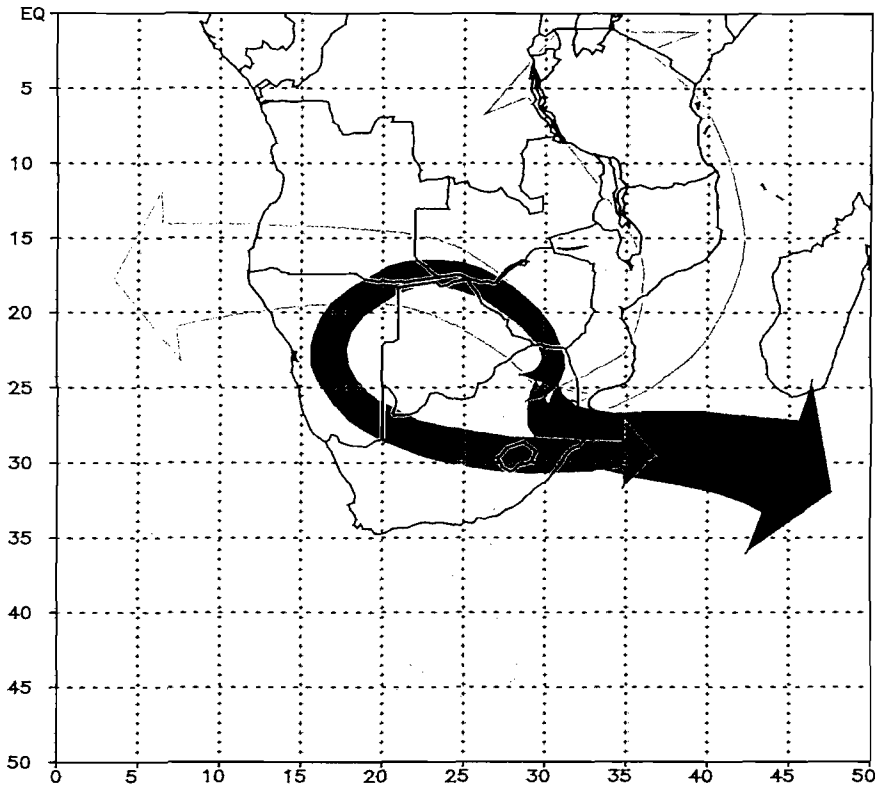


Figure 2.1 *Five transport pathways identified from the forward trajectory analysis for the five-year period 1990-1994. The shading represents the relative importance of the flow patterns*[180]

South Africa is part of the southern tropical Atlantic region consisting of the Amazon basin, the tropical South Atlantic, and southern Africa. Observation studies have shown elevated levels of O_3, CO, and other trace gases over vast regions from Africa to South America, the tropical Atlantic, the Indian Ocean, and the Pacific,[42] due to extensive biomass burning in these regions. During these fires a wide variety of species is emitted that influences global troposphere chemistry, including carbon monoxide (CO), nitrogen oxides (NO_X), hydrocarbons, halocarbons, oxygenated organic compounds and particles.[181] Recent estimates suggest that biomass burning may be the second largest source of anthropogenic aerosols, next to the production of sulphate from SO_2.[182,183,47] The regions of Africa covered by savannah grass are considered to experience the most extensive biomass burning in the world, contributing an estimated 49% of carbon lost from fires worldwide[184-186] and contributing about 30% of global biomass burning emissions of trace gases and aerosols.[187] An example of the influence of biomass burning on aerosol formation is the SAFARI 2000 campaign that found a two-fold increase in particle mass and

elevated concentrations of secondary species within 1-2 days from biomass emission into the haze layer. This is largely due to coagulation and condensation, which suggests large secondary aerosol transformations over the South African region during the winter.[47] Meteorological conditions in South Africa in spring favour the long-range transport of plumes of biomass combustion from central southern-Africa to South Africa.[46]

The highly industrialised region of the Mpumalanga Highveld and Gauteng (Johannesburg) accounts for 90% of South Africa's scheduled emissions[5] of SO_2, NO_x and particulates. The average annual emission density for sulphur in developing regions south of 18 S is estimated at 3 kg S ha^{-1} and ranges from zero in the desert and bushveld areas to as much as 200 kg S ha^{-1} on the South African Highveld region and parts of Zimbabwe.[188] The industrialised interior region of South Africa is responsible for 86% of particulate emissions.[5]

In summer, prevailing low pressure conditions over the South African interior cause unstable conditions promoting dispersal and removal of pollutants, while stable and dry conditions in the southern and western parts do not favour the removal of pollutants. The regular passage high-speed south-bound winds prevent pollutant build-up in these regions. In winter, stable conditions with low wind speeds prevail over most parts of South Africa and the dispersion and removal of pollutants are not favoured.[61] The intrinsically poor pollutant dispersion conditions assisted by anticyclonic flow patterns are exacerbated by the presence of semi-permanent, subsidence-induced absolutely stable layers at 700 and 500 hPa that extend over the subcontinent.[173] This means anticyclonic conditions and strong regional atmospheric recirculation[189-191] dominate the transport of aerosols and trace gases in the troposphere over southern Africa.[192] The different major sources of aerosols and gases and their emissions, transport and impacts have been the focus of many previous studies[193-196] Pollutants are trapped below the stable layers and their transport away from the source regions is largely controlled by the relative position of these anticyclones.[192]

2.9 Conclusion

In this study, the concentrations of trace gases and aerosol compositions are measured in order to estimate their depositions and assess their impact on the

environment and climate. The gas and aerosol data needed for this are accumulated by using the diffusive gas and active aerosol sampling techniques described in Chapter 3. This data is also used to simulate the aging process (chemical transformations) of natural and anthropogenic aerosols over specific representative regions in South Africa by using the ORISAM-TM4 model. The seasonal concentration data of the gases (Chapter 4) and the composition of the aerosols (Chapter 5) measured as well as the model simulation itself (Chapter 6) will help us to get a better understanding of transformation processes involved from the emission to removal of atmospheric species under southern African conditions. The continuous measurement of gases and aerosols as initiated in this study, will be continued as part of a long-term monitoring campaign of the DEBITS Africa project.

CHAPTER 3

Experimental Design

In this chapter the locations of the monitoring sites as well as the monitoring methods for both gas and aerosol monitoring are discussed. The instruments and setups required for analysing the samples of the chosen methods are also described. The introductory discussions are followed by detailed descriptions of each of the gas and aerosol monitoring methods and the details pertaining to the preparation of the samplers for sampling as well as analysing thereof. The quality assurance procedures of each method are also discussed.

3.1 Introduction and choice of sampling sites

The first consideration when selecting sampling sites is the availability of personnel with the required skills for managing the sampling process. Two of the selected four passive sampling sites were situated at two already fully functioning rain monitoring sites (Amersfoort and Louis Trichardt) managed by a research partner Eskom (a big electricity supplier in southern Africa). The GAW research station at Cape Point was selected as the third passive sampler site. The fourth and last site is located within a national park (Okaukuejo in Namibia), where nature conservation is a priority and park rangers act as site operators. A map of southern Africa with the four locations of the selected sites is given in red in Figure 3.1.



Figure 3.1: *Map of southern Africa depicting the locations of the sampling sites*

The Amersfoort site is located in the south-eastern part of the Mpumalanga Province of South Africa (see Figure 3.1). It is approximately 200 km south-east of Johannesburg and 50-100 km south-east to south-south-east of major industrial activities that include the main centre of electric power generation in the Mpumalanga Highveld area.[10] It represents a regional location, but one that lies within a global pollution hot-spot in terms of satellite observations of SO_2 and NO_2 concentrations.[197] Prevailing wind directions at the site anticipate the frequent transport of pollutants from the metropolitan and industrial regions (Gauteng and Mpumalanga) towards this site.[10] The site is situated 15 km from Amersfoort on a private farm at an altitude of 1608 m with a longitude at 29°52'0E and a latitude at 27°10'0S. This site is within a climatological transition region between the Highveld and the nearby escarpment, representing a semi-arid region with major anthropogenic influences.



Figure 3.2: *The sampling site at Amersfoort*

Figure 3.2 represents the actual site at Amersfoort, and depicts a predominantly grassland savannah region of vegetation present at Amersfoort and most of the surrounding Highveld region.

The Louis Trichardt site is located at an altitude of 1465 m, a longitude of 29°53'60E and a latitude of 23°30'0S on a private farm about 20 km outside the city in the Northern Province of South Africa. It is situated roughly 400 km to the north-north-east of Johannesburg (see Figure 3.1) with no major cities located within a 100 km radius of it. On the tip of the escarpment of the Highveld, it represents a tropical region belt near the South African border.



Figure 3.3: *The sampling site at Louis Trichardt*

Although it represents a sub-tropical region (see Figure 3.3), semi-arid regions are situated just a few kilometres away. This region represents no real direct influences of industry and is classified as a rural area. However, a common recirculation pathway from the Mpumalanga highveld[178] is known to influence air quality in this region.[198] This region is also affected by tropical air masses transported from the Mozambique Channel[199] and cross-border biomass burning activities[198,200] as it lies within the most common transverse recirculation pathway in southern Africa.[47]

The Cape Point sampling site is situated 260 m above sea level with a longitude of 18°50'0E and a latitude of 34°36'0S at a WMO-GAW site. The station is located at the southern tip of the Cape Peninsula within a national park, approximately 60 km south of Cape Town. It is a typical coastal site with conditions that include strong winds along with heavy bombardments of sea spray being exposed to clean southern hemisphere maritime air masses for most of the time.[201] Incorporating such a site into a sampling network with different natural source and meteorological parameters than most inland sites is important for comparison purposes. The South African Weather Bureau, together with the Fraunhofer Institute in Garmish, Germany, maintain a research laboratory at Cape Point.



Figure 3.4: *The sampling site at Cape Point*

The site is located within a region that is not influenced by any major industrial activities. However, except for only natural and marine time influences, it is still classified as a moderately urban site due to anthropogenic influences from the nearby

significantly urbanised Cape Town region. The site is also located in a region representing a very specific vegetation type called *fynbos*.

The ministry of Environment and Tourism based in Windhoek, Namibia, was instrumental in setting up the Okaukuejo site and arranged for an official from the Etosha Ecological Institute to act as site operator.[56] The site is located at 1000m above sea level with a longitude of 15°51'48E and latitude of 18°59'24S.



Figure 3.5: *The passive sampling site at Okaukuejo (Namibia)*

The site is situated 500 m west of the large Etosha saline pan and 1 km from the nearest tourist road. It therefore represents a rural background site not influenced by any real anthropogenic activities. It is, however, also situated within a common transverse recirculation pathway in southern Africa.[47] This site is situated within a semi-desert region, surrounded by small, vegetated sand hummocks as seen in Figure 3.5.

All of the above-mentioned sites are recognised within an international project called the IGAC-DEBITS-Africa (IDAF) project. Monitoring selected gases and aerosols species (paragraph 2.2.1-2) at the above-mentioned sites will enable the identification of regional background concentrations of these species. The further selection of sites with big anthropogenical influences compared to sites with no anthropogenical influences is important for determining point sources. Lastly, the sites were also selected within recirculation pathways in comparison with sites that are not, and this will not only improve the potential in determining regional sources, but also support the identification of the origin of trans-regional sources. The passive sampling of this

study was done over a period of ten years at all four of the above-mentioned sites. The aerosol sampling at the Amersfoort and Louis Trichardt sites was only done over the past three years in four separate campaigns.

3.2 Important considerations when monitoring air pollutants

In order to provide data, scientific assessments, and other information on changes in the chemical composition and related characteristics of the background atmosphere, sampling techniques are necessary to monitor atmospheric species.[202] Atmospheric species can be monitored by means of the following two basic methods:

i) offline sampling techniques that include active sampling techniques where species are sampled by dissolving them in liquids or with mechanical collection onto solid surfaces or passively (natural diffusion of species on solid surfaces, etc.).

ii) online sampling techniques that include high-tech instruments giving real-time measurements.

Both sampling techniques have its advantages and disadvantages. For example, the immediate availability of results in online sampling techniques is a huge advantage. All offline sampling techniques (passive and active) have analytical artefacts (e.g. evaporation, de- and absorption of trapped species, chemical reactions during storage as well as transport and preparation before chemical analysis), which is a huge disadvantage.[93] Online instruments do not have these problems, but require a certain level of analytical skill and are usually expensive to operate. Offline active sampling techniques also still require a certain amount of skill for deployment as well as costs and are generally not best suited for long-term measurement campaigns. Passive sampling techniques, on the other hand, are usually less expensive and require a low level of skill in operation. These techniques are most suited for long-term measuring campaigns, where non-specialists are used for maintaining the sampling sites. The analysis of the samples still requires high-tech equipment and skill, and the results are not immediately available. The best suited sampling methods were chosen for the selected gas and aerosol species of this study and are discussed in the following paragraphs.

3.3 Selection of monitoring methods

3.3.1 Selection of gas monitoring method

The most common active samplers used for monitoring gases today range from CO_2 - high precision non-dispersive infrared gas analysers[2], SO_2 -UV Fluorescence, O_3 -UV Absorption, NO_2 -Chemiluminescence[56] to annular denuder systems.[79,203,204] Gases like CO_2, CH_4 and N_2O are also actively trapped in canisters,[205] and acidic gases actively pumped through base-coated filter packs[206,207], all of which are later changed to remote sensing with FTIR Spectroscopy.[208] All of these techniques are, however, as previously mentioned, expensive and not suited for remote areas or long-term measuring campaigns at undeveloped remote sites. Passive samplers, on the other hand, are simple in design, small and require no electricity. They rely on the natural diffusion of pollutant species onto an impregnated filter. All the above-mentioned advantages of passive sampling were taken into consideration when a suitable sampling technique was considered for monitoring the selected inorganic gases of this study. The locations of three of the four sites were, in fact, on farms and nature reserves, where volunteers had to be used for sampling. There is also no electricity at three of the monitoring sites. This, together with the intended long-term scope for this study and the success of similar projects, contributed to the decision to use passive samplers in this study. The passive (diffusive) sampling technique will be described in detail in Paragraph 3.5.1.

3.3.2 Selection of aerosol monitoring method

Aerosols are sampled using mainly on- and offline sampling techniques, of which offline techniques involve both active and passive sampling. The offline technique is still presently favoured due to the lack of availability of online instruments such as aerosol mass spectrometers, fluorescence spectroscopy and aerodynamic sizing, although its technology is improving fast.[93] Offline active sampling of aerosols involves collection (mechanical) on solid substrates (membrane or quartz filters, inertial impaction plates, thermal or electrostatic precipitation plates) or in a liquid (wetted wall cyclone, impinger, or washing bottle).[93] Passive aerosol samplers have also recently been developed.[209] In this study, however, the offline active collection of aerosols on filters was used as monitoring method. Regional monitoring of aerosols in South Africa is still in its infant stage. Most of the sites in use are mostly rural and

remote; therefore a portable MiniVol sampler made by Air Metrics was selected as a suitable monitoring instrument and will be discussed in Paragraph 3.6.1.

3.4 Apparatus used in analysing samples

In this study, five different instruments were used to analyse the specific selected analytes in the gas and aerosol samples collected. The type of instruments used for each analysis was determined by the methodology of the sampling technique and the selected species. The different instruments and their setups will be discussed in the following sections.

3.4.1 Dionex 100 Ion Chromatograph

SO_2, O_3 and HNO_3 were all monitored by passive sampling techniques and analysed as sulphate and nitrate anions, respectively, using a Dionex 100 ion chromatograph.

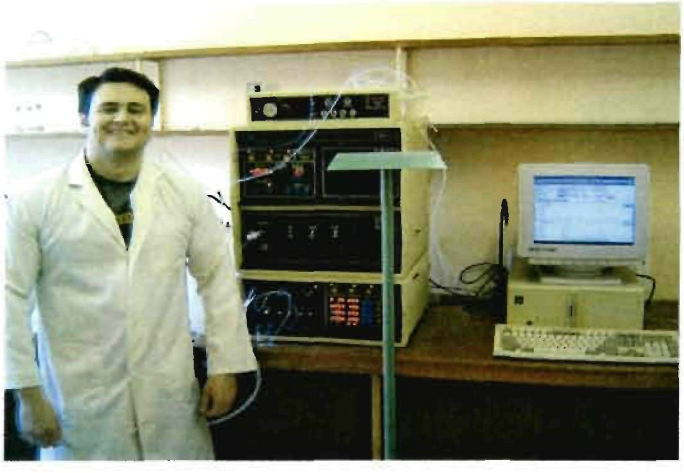


Figure 3.6: *The Dionex 100 Ion Chromatograph used for sulphate and nitrate analyses*

A Dionex Chromatography module/SP (Suppressed Ion Chromatography) system in isocratic mode fitted with an ion Pac AS4A-SC 4 mm analytical column, an ion Pac AG4A-SC guard column and conductivity detector was used on this instrument. It was also equipped with an electrochemical, anion-self-regenerating suppressor ASRS-1 (4 mm) to lower the background conductivity, and the system was operated at a flow rate of 2 cm^3 $min.^{-1}$. The eluent was a mixture of 1.7 $mmol.dm^{-3}$ $NaHCO_3$ and 1.8 $mmol.dm^{-3}$ $NaCO_3$. The CO_3^{2-} concentrations within samples were not negligible compared to that of the eluent, leading to slightly shorter retention times and differences in peak areas of 5-10%. For this reason, the standards used for calibration purposes were prepared with a $NaCO_3$ concentration of 2.5 $mmol.dm^{-3}$.

3.4.2 UV visible spectrophotometer

NH_3 and NO_2 were monitored by passive sampling techniques and analysed as ammonium cations and nitrite anions, respectively, using a UV-visible spectrophotometer.



Figure 3.7: *The UV visible spectrophotometer used for determining the NH_3 and NO_2 concentrations*

The Varian Cary 50 Conc. UV-Visible Spectrophotometer used for analysis was equipped with a temperature-controlled sample cell and connected to a compatible computer as shown in Figure 3.7. The sample solutions of NH_3 and NO_2 were introduced into the UV using a quartz cuvette.

3.4.3 The DX 100 Ion Chromatograph

All the water-soluble cations in the aerosol samples were analysed using the DX 100 Ion chromatograph as shown in Figure 3.8.



Figure 3.8: *The DX 100 Ion Chromatograph used for determining the water-soluble cations in the aerosol samples*

The DX 100 Ion Chromatograph (Figure.3.8) was fitted with a CG 12A + CS12 column and a Dionex CSRS ULTRA auto suppressor. It was also supplied with an auto-sampler. The instrument was operated in an isocratic mode using a 20mM CH_3SO_3H (MSA) solution diluted in de-ionised water as eluent with a flow rate of 1ml/min.

3.4.4 The DX 500 Ion Chromatograph

The water-soluble anions in the aerosol samples were analysed using the DX 500 Ion chromatograph as shown in Figure 3.9.

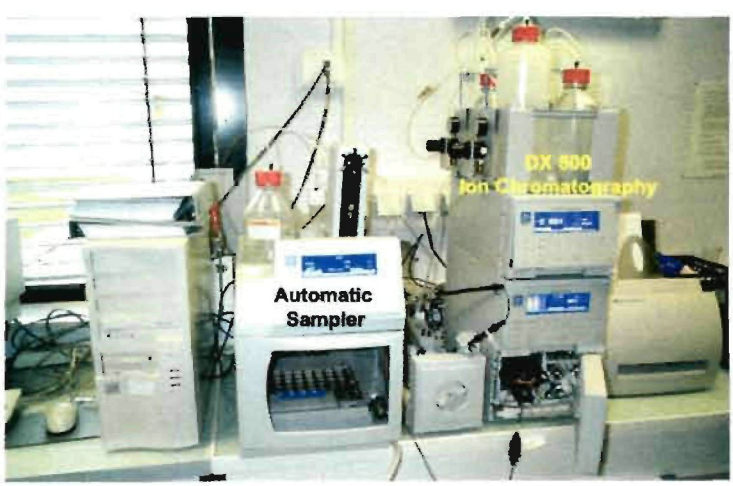


Figure 3.9: *The DX 500 Ion Chromatograph used for determining the water-soluble anions in the aerosol samples.*

The DX 500 Ion Chromatograph (Figure 3.9) was fitted with an AG11 + AS11 column and a Dionex ASRS ULTRA auto-suppressor. It was also supplied with an auto-

sampler. The instrument was used in a gradient mode and uses a 90% H_2O-10% NaOH (5 mM) and 80% H_2O-20% NaOH (100 mM) solution as eluent. A three-point calibration curve was used and the flow rate is 1ml/min.

3.4.5 The Thermal/Optical Carbon Analyser

The carbon-containing fractions of the aerosols, e.g. the organic carbon (OC) and black carbon (BC), were analysed using the Thermal/Optical Carbon Analyser from the Desert Research Institude (D.R.I.) shown in Figure 3.10.

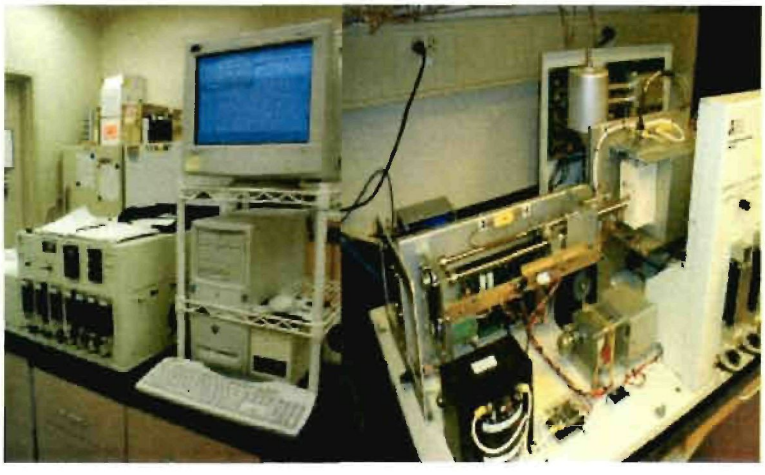


Figure 3.10: *The Thermal/Optical Carbon Analyser from D.R.I. used for determining the OC/BC content of aerosol samples*

This method is based on the preferential oxidation of organic carbon and elemental carbon compounds at different temperatures. Organic compounds are volatilised from the sample deposit in a helium (He) atmosphere at low temperatures, while elemental carbon is not oxidised and removed. The sample is a 5/16 inch diameter punch (0.512 cm^2) taken from a quartz fibre filter. These compounds are converted to carbon dioxide (CO_2) by passing the volatilised compounds through an oxidiser (heated manganese dioxide, MnO_2). The CO_2 is reduced to methane (CH_4) by passing the CO_2 gas through a methanator (hydrogen-enriched nickel catalyst). A flame ionisation detector (FID) is used to quantify the methane concentration. The optical component of the analyser is used to correct for pyrolysis of organic carbon compounds to elemental carbon in order to avoid the underestimation of OC (organic carbon) and overestimation of EC (elemental carbon). The sample reflectance and transmission are continuously monitored by means of a helium-neon laser and a photo-detector

throughout an analysis cycle. When pyrolysis takes place, there is an increase in light absorption resulting in a decrease in reflectance and transmission. Thus, by monitoring the reflectance/transmission, the portion of the elemental carbon peak corresponding to pyrolysed organic carbon can be correctly assigned to the organic fraction.[210]

3.5 The gas monitoring method

Diffusive sampling, as used internationally by scientists today, was pioneered by Martin Ferm at the Swedish Environment Research Institute (IVL) Sweden and began monitoring SO_2 in December of 1993. Since then, diffusive samplers for monitoring NO_2, O_3, NH_3 and non-methane hydrocarbons (NMHC) have been developed and tested against active sampling and have rendered very good results. In this study, the sampling method developed by *Dhammapala*[56] was used, which is based on the same principles as used by Martin Ferm at the IVL in Sweden. It is also exactly the same as the sampling protocol used by the IDAF programme in Africa, which forms part of the international DEBITS network.[51]

3.5.1 Theory and functioning of passive (diffusive) samplers

Pressures of cost and changing priorities make it difficult to maintain and expand long-term measurement programmes. Passive (or diffusive) samplers, one of the tools of modern atmospheric chemistry research,[211-213] present a means of addressing these types of measurements in that they provide a cost-effective way of monitoring many key pollutant species. The samplers are small, lightweight, silent, do not require electricity or field calibration, and can easily be deployed by non-specialists. As a result, they can be used to obtain long-term measurements at rural, regional and global scales.[211-213]

The passive sampler is a device that measures average gas concentrations (time weighted) at a rate controlled by molecular diffusion through an entrapped volume of air without any active movement (hence passive) of air through the device.[214] A filter impregnated with a chemical capable of very selectively reacting and quantitatively trapping the gas of interest, is placed at the one end of the sampler device. It also entraps a volume of air. This volume of air creates a transport resistance layer for target molecules to overcome, in order to reach the impregnated filter hence creating

a concentration gradient (Figure 3.13, C_{Amb}) within the sampler chamber, creating a net flux of the chemisorbed gas, which is proportional to the ambient gas concentration and is trapped on the impregnated filter.[214]

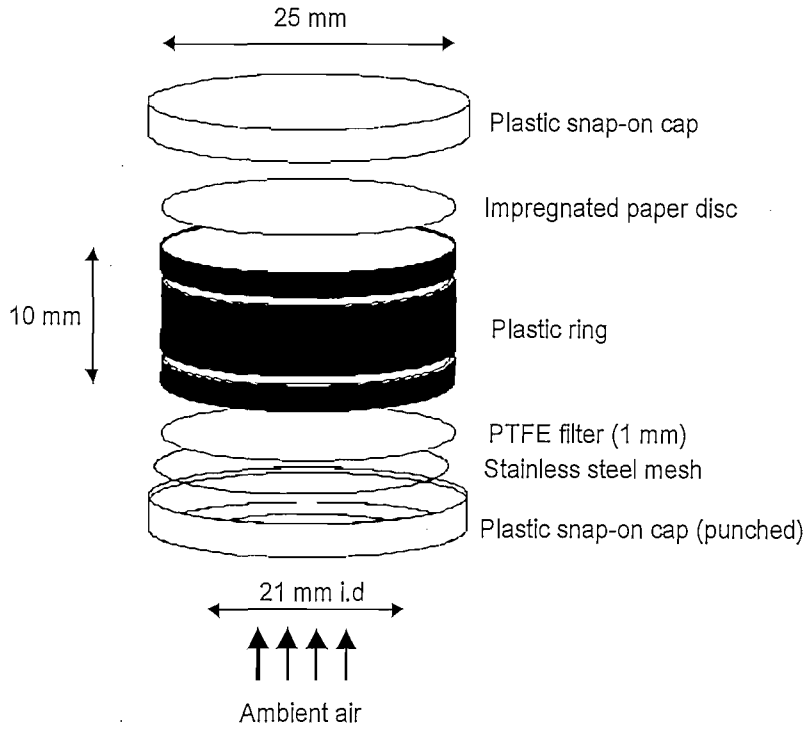


Figure 3.11: *Schematic representation of the diffusive sampler*[56]

Figure 3.11 shows the typical construction of a passive sampler containing a series of caps, rings and filters, each with a specific function within the sampler. The inlet of the sampler consists of a plastic (polypropylene) snap-on cap with an opening cut out. The snap-on cap is followed by a steel mesh (25 mm in diameter, 160 µm in thickness with a total porosity of 40%) to ensure no turbulence interference at the inlet of the sampler.[56] After the steel mesh, a PTFE filter (25 mm in diameter, with a 175 µm filter thickness and a 1µm pore size) is inserted, which further minimises internal turbulent diffusion in the sampler itself as well as excluding interferences of aerosols. The snap-on cap with both the steel mesh and PTFE filter is snapped onto a plastic ring that forms the sampling chamber in which the concentration gradient is created, as previously mentioned. Cellulose Whatman filter paper no. 40, 25 mm in diameter, was used as the impregnating and trapping surface of the gaseous pollutants (Figure 3.11). This filter was placed within another closed snap-on cap and snapped onto the other side of the sampling chamber ring. All the components of the sampler, except the filters and steel mesh, were carefully individually cut from polypropylene shells

supplied by the Adcock Ingram Company. They are also individually fitted together to ensure that no air can enter the inside of the sampler other than through the sampler inlet and reach the trapping surface. This, together with the fact that no pollutant species are lost due to sampler surfaces, ensures optimal sampler efficiency. As previously mentioned, extra care must be taken in order to prevent turbulence at the sampler inlet, which may present problems in this type of sampling. Typical interference due to low wind speeds (starving of pollutant in trapped air volume within sampler) in the environment surrounding the sampler[215] may lead to the increase of the diffusion path length. High wind speeds (perturbing the trapped air volume within the sampler), on the other hand, may lead to the shortening of the diffusion pathway. This will influence sampling efficiency, which needs a consistent air flow so that the sampling rate can remain constant.[56] Except for the PTFE filter and steel mesh placed within the sampler to curb wind effects, other meteorological conditions (e.g. direct sunlight and rain) are excluded by placing the sampler under a draft shield as shown in Figure 3.12. This shield is manufactured from aluminium at the North-West University.



Figure 3.12: *Aluminium stand, 1.5 m in height (left), used for the deployment of samplers at sites in aluminium rail under hood on top of stand (right)*

3.5.1.1 Concentration calculations of passive sampling method

The pathway of gas pollutants from the sampler inlet to the impregnated filter is demonstrated by Figure 3.13.

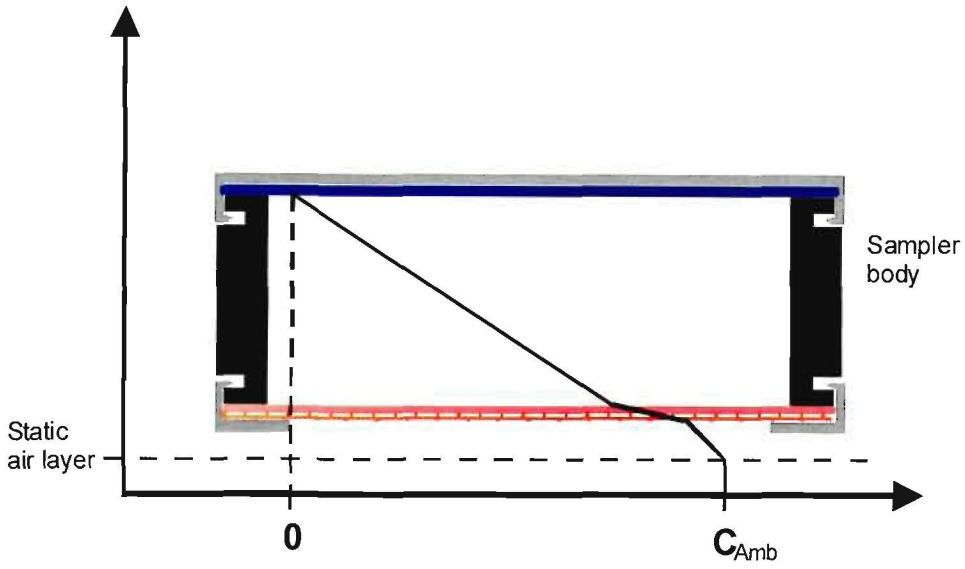


Figure 3.13: *Concentration profile of pollutant in and around sampler*[56]

The net flux of pollutant gas (ambient sampling rate), which is proportional to the concentration gradient created within the sampler, can be calculated using *Fick's* first law of diffusion.[216] The diffusion coefficient representing the proportional constant is summarised in Equation 3.1.

$$\emptyset = -D\,(dC/dL) \qquad 3.1$$

(where: $\emptyset$ = Flux of gas in direction of concentration gradient ($\mu g.m^{-2}s^{-1}$); D = diffusion coefficient of gas (m^2s^{-1}); C = concentration of pollutant ($\mu g\ m^{-3}$); L = diffusion path length (corrected for the Teflon filter, steel mesh and static air layer (m)) and -dC/dL = instantaneous concentration gradient of pollutant in direction of air flow).

Passive sampling is time integrated (Equation 3.2)[56]:

$$(dX/dt) = \emptyset.A \qquad 3.2$$

(where: X = amount of pollutant trapped on paper disk corrected for the blank (μg); A = cross-sectional area of diffusion path (m^2) and t = sampling time (s)).

Combining Equation 3.1 and 3.2 produces Equation 3.3, which includes all the parameters needed to calculate the ambient gas concentrations.

$$C_{Avg} = (X/D.t).(L/A) \qquad 3.3$$

(where: $L/A = [(L_R/A_R) + (L_F/A_F) + (L_N/A_N) + (L_S/A_R)]$ and L_R and A_R are the thickness and area of the plastic ring, respectively; L_F is the thickness of the

Teflon filter and A_F is the total area of the pores through which diffusion takes place; L_N and A_N are the same parameters for the steel net and L_S is the length of the static layer).

Additional important parameters used in the calculation of pollutant concentrations include the 21 mm diameter section through which the actual diffusion takes place and not the total 25 mm diameter as specified for the Teflon filter and steel mesh. The thickness of the static air layer for non-indoor sampling locations is 1.5 mm on average,[217] and the L/A ratio according to this particular sampler specification is 35 m^{-1}.[56]

The results are expressed as mixing ratios[218] or ppb units i.e. mm^3 pollutant gas per m^3 moist air under sampling conditions to eliminate pressure dependence (NB: mm^3 is the SI Unit for what is more commonly known as µl). The concentration is then expressed as inversely proportional to the square root of the absolute temperature and will fluctuate by less than 0.2 % per 1°C at ambient temperatures.[56] The ideal gas law is applied for this purpose and the mixing ratio is provided in Equation 3.4.

$$C_{Avg}\ (ppb) = (1000\ X.R.T/\ Mr.D.t) \times (L/A) \qquad 3.4$$

(where: T = average temperature during the sampling period; Mr = relative molecular mass of the gas in question; R = (gas constant) = 8.31 J K^{-1} mol^{-1}).

The amount of gas pollutant trapped on the filter (X) can be calculated as the product of the analytical result (analyte of interest in the sample (µg.dm^{-3})) and volume of the sample (dm^3), minus the analytical result of the corresponding blank.

The diffusion coefficients for the gas species of interest used in this study are the same as those used by *Dhammapala*[56] and the IDAF (DEBITS-AFRICA Initiative[51]) network and are as follows:

NO_2	1.52×10^{10} m^2s^{-1}
SO_2	1.30×10^{10} m^2s^{-1}
NH_3	2.51×10^{10} m^2s^{-1}
$O_3 + HNO_3$	1.48×10^{10} m^2s^{-1}

3.5.2 Species specific preparation of samplers prior to exposure

One of the most important factors when monitoring trace elements in the atmosphere, is the level of cleanliness associated with preparing and analysing the samplers, which includes the surrounding conditions in the laboratory when preparation for sampling or analysis is carried out. A contamination of only 20 nmol can amount to a 50% error in the sample.[56] The use of high-purity reagents is therefore a necessity. In this study, only analytical grade products from MERCK (South Africa Pty. Ltd.) were used in the preparation of absorbing solutions and calibration standards. Deionised water (resistance of 18.2 MΩ cm) was used for all activities, including rinsing of glassware, sample preparations, analytical procedures and preparation of solutions for both. Sterile surgical gloves were used when handling sampler components and tweezers with plastic tips to handle the filters and steel meshes. All reagents were prepared immediately prior to use as described by *Dhammapala*[56] who developed the methods used in this study at the North-West University (Potchefstroom Campus) in South Africa.

Prior to any sampler preparation, the polypropylene components of the sampler, as well as the reusable PTFE filter, were treated in the following way to ensure no contamination was present from the previous sampling period:

i) soaked in analytical grade 0.2 % (v/v) phosphoric acid for 3 to 4 hours;

ii) soaked overnight in 3% (v/v) EXTRAN MA O2 neutral solution; and

iii) thoroughly rinsed and sonicated in deionised water and completely dried before use in any of the sampling procedures.

The cellulose Whatman filters that were only used once were also pre-treated after they were received from the manufacturer to remove debris and ensure maximum sampling efficiency. This was done in the following way:

i) firstly, the filters were soaked in deionised water and sonicated (with ultrasonic bath) at least 4 times after which they were rinsed with deionised water; and

ii) they were then soaked in methanol and sonicated (with ultrasonic bath) at least 4 times after which they were rinsed with methanol and dried in a vacuum before being used in the preparation of samplers.

3.5.2.1 Preparation of sulphur dioxide samplers

The reaction that makes it possible to quantitatively trap SO_2 in order to monitor it with a passive sampling method is shown in Equation 3.5. This is based on the same sampling method developed by the IVL in Sweden.

$$2SO_2\,(g) + 4OH^- + O_2 \rightarrow 2H_2O + 2SO_4^{2-} \qquad 3.5$$

NaOH solution was used for filter impregnation and prepared by dissolving 1 g NaOH in 15 cm^3 deionised water and diluting it to 100 cm^3 with methanol. When the SO_2 is absorbed on the NaOH surface it produces an unstable SO_3^{2-} species, which undergoes further oxidation with oxygen and a variety of other catalysts present in trace quantities in the atmosphere, to form stable SO_4^{2-} species. If incomplete oxidation is suspected, the filters are leached with a 5 cm^3 0.03% (v/v) H_2O_2 solution. A total volume of 50 mm^3 of the absorbing solution is evenly pipetted over the surface area of the cellulose Whatman filter using a Gilson Pipetman micro-pipette and loaded against the snap-on cap casing at the end of the sampler.

3.5.2.2 Preparation of ozone samplers

The reaction that makes it possible to monitor O_3 with a passive sampling method is shown in Equation 3.6. This is an indirect method to monitor O_3, as the quantity of nitrite oxidised to nitrate is directly proportional to the amount of O_3 present. This is based on the same sampling method as developed by *Koutrakis et al.*[219]

$$O_3\,(g) + NO_2^- \rightarrow NO_3^- + O_2 \qquad 3.6$$

The solution used for filter impregnation consists of 1% (w/v) $NaNO_2$, 1% (w/v) K_2CO_3 and 2 cm^3 glycerol made up to 100 cm^3 with a 70:30 water: methanol mixture. K_2CO_3 is used to keep the medium alkaline (pH ≈ 12), as the rate constant of the reaction increases with pH up to a maximum at pH = 12. The hygroscopicy (potential for presence of water) of sorbent (nitrite) crystals enhances its oxidation potential with ozone and thus the collection efficiency. This can be manipulated by adding glycerol (increase hygroscopicy) and using nitrite and carbonate of different salts to form sorbent crystals (increase hygroscopicy). It is speculated that the trapping process is a homogeneous phase reaction that takes place in microscopic water droplets at the filter surface.[219] H_2O_2 also oxidises NO_2^-, but at low pH with no interferences for levels up to 76 ppb. HNO_3 also reacts with K_2CO_3 to form NO_3^-, but ambient concentrations

of HNO_3 are negligible in comparison to O_3 and accounts for less than 5% of NO_3^- accumulated. Peroxyacetyl nitrate (PAN) is also a strong atmospheric oxidant, but its low ambient concentrations and diffusion coefficient make it negligible. A total volume of 50 mm^3 of the absorbing solution is evenly pipetted over the surface area of the cellulose Whatman filter using a Gilson Pipetman micro-pipette and loaded against the snap-on cap casing at the end of the sampler.

3.5.2.3 Preparation of nitrogen dioxide samplers

The reaction that makes it possible to quantitatively trap NO_2 in order to monitor it with a passive sampling method, is shown in Equation 3.7. This is based on the same passive sampling method developed by the IVL in Sweden, which also recommends a mixture of iodide salts as impregnating solution.

$$2NO_2\,(g) + 3I^- \rightarrow 2NO_2^- + I_3^- \qquad 3.7$$

The solution for filter impregnation was prepared by dissolving 0.88 g NaOH and 7.9 g NaI in 15 cm^3 deionised water and diluting it to 100 cm^3 with methanol. The function of the NaOH is to maintain a pH of 13 or higher in order to stabilise the NO_2^- species, which can be oxidised to NO_3^- by O_3 if the pH drops to or below 12. I^- is added in excess so that atmospheric oxidants which oxidise this species to I_2, may be removed as they diffuse into the sampler. A total volume of 50 mm^3 of the absorbing solution is evenly pipette over the surface area of the cellulose Whatman filter using a Gilson Pipetman micro-pipette and loaded against the snap-on cap casing at the end of the sampler.

3.5.2.4 Preparation of nitric acid samplers

The reaction that makes it possible to monitor HNO_3 with a passive sampling method, is shown in Equation 3.8. This is based on the same passive sampling method as described by the IDAF-DEBITS project, which is based on work done by *Ferm*.[217]

$$HNO_3\,(g) + OH^- \rightarrow NO_3^- + H_2O \qquad 3.8$$

Nitric acid is reduced to nitrate on the filter surface by NaOH, and the amount of nitrate produced determines the amount of HNO_3 present. Therefore, NaOH was used as solution for filter impregnation and prepared by dissolving 1 g NaOH in 15 cm^3 deionised water and diluting it to 100 cm^3 with methanol. A total volume of 50 mm^3 of

the absorbing solution is evenly pipette over the surface area of the cellulose Whatman filter using a Gilson Pipetman micro-pipette and loaded against the snap-on cap casing at the end of the sampler.

3.5.2.5 Preparation of ammonia samplers

The reaction that makes it possible to quantitatively trap NH_3 in order to monitor it with a passive sampling method, is shown in Equation 3.9. This is based on the same passive sampling method as developed and tested by *Ferm and Rodhe.*[220]

$$NH_3\,(g) + H^+ \rightarrow NH_4^+ \qquad 3.9$$

Citric acid was used as solution for filter impregnation and prepared by dissolving 2 g citric acid in 15 cm^3 deionised water made up to 100 cm^3 with methanol. NH_3 reacts with acids even when they are in solid form and citric acid is preferably used due to its high molecular mass and thus low volatility. Although any pollutant with alkaline properties will be trapped by this sorbent, only NH_3 is present in significant quantities in ambient air. A total volume of 50 mm^3 of the absorbing solution is evenly pipetted over the surface area of the cellulose Whatman filter using a Gilson Pipetman micro-pipette and loaded against the snap-on cap casing at the end of the sampler.

3.5.3 Quality control procedures

Samplers were sealed in air-tight plastic containers to ensure that sampling only begins when it is intended, and not before it reaches its destination or after the intended sampling period expired. Passive samplers were exposed between one and four weeks (optimum exposure time), where after they were returned to the lab for analysis with the appropriate analytical methods and the concentration of the gas species determined. Each sampler was marked with the date of preparation, site for exposure and pollutant impregnated for, and sealed within a plastic container for transport to each sampling site. Samplers were exposed in pairs to ensure the reproducibility and accuracy of the results and to reduce data loss due to interferences or lost samplers.[56] A laboratory blank is prepared for every two samplers assembled to compensate for any matrix effects, systematic errors and contaminants present in the reagents, containers, filters and laboratory when samplers are prepared. It is assembled and analysed in exactly the same way and time interval as field samples, but it is kept in its container in the laboratory. Samplers are transported to all the sites

by mail. A data sheet that needs to be completed at each site for each sampler batch, contains not only the information necessary for processing each gas species concentration results, but also events (e.g. fires, rain), which may affect the results and interpretation thereof.

Once the samplers were received back from the sites, they were identified, prepared and analysed according to their specific analytical procedure, which will be described in the following paragraphs.

3.5.4 Preparing and analysing samples and standards

Calibration standards, covering the range of expected sample concentrations, were prepared in order to calculate the analyte concentrations in the exposed samples. All the reagents used for the preparation of the standards were first dried in an oven at 105°C (with the exception of $NaNO_2$ used for the preparation of standards for the analysis of NO_2, which was dried in a vacuum desiccator) before being used.[56] A calibration blank was prepared in exactly the same manner as the standards, but without the analyte of interest to compensate for any contributions from the reagents and apparatus. The analytical signal of the analyte of interest within the samples, standards and blanks was measured by each of the respective instruments (only the gases, Paragraph 3.4) as specified by the species and specific analytical procedure that will be described in the following paragraphs. The signal of the calibration blank was subtracted from the signal of the standards. A straight line was fitted to a plot of concentration versus signal for all standards, using the least squares regression programme. The intercept and gradient of this line were then used to calculate the concentration of the analyte in the sample. The concentration of the sample blank which was kept in the lab to compensate for any variances in preparation conditions were calculated using the same gradient line as for analytes and subtracted from the concentration of the analyte. Equation 3.4 was used to calculate the corresponding concentration of the pollutant in question in ambient air.[56]

3.5.4.1 Preparing and analysing sulphur dioxide

Before any analysis of samples, a series of standards for calibration purposes was prepared. First, by dissolving 0.331 g of $NaCO_3$ in 50.0 cm^3 deionised water, a 62.5 $mmol.dm^{-3}$ $NaCO_3$ stock solution is prepared. A 1.0 $mmol.dm^{-3}$ $NaSO_4$ stock solution is then prepared by dissolving 0.142 g $NaSO_4$ in 1.0 dm^3 deionised water and used to

prepare standards of 0.0, 1.0, 5.0, 10.0 and 25.0 $\mu mol.dm^{-3}$ $NaSO_4$ by adding 0.0, 25.0, 125.0, 250.0 and 625.0 mm^3 of $NaSO_4$ stock solution to the 1.0 cm^3 of 62.5 $mmol.dm^{-3}$ $NaCO_3$. The standards are filled up to 25.0 cm^3 with deionised water.

After the five calibration standards were prepared, injected and analysed on the IC, a calibration curve is plotted, and if compliant with lab procedure, the analysis of the samples may begin. The cellulose Whatmann filters are removed from each sampler casing and leached in 5 cm^3 deionised water and sonicated for 15 minutes after which the solution is injected into the Dionex 100 ion chromatograph. The sulphate, which is the analyte of interest, has a retention time of around 7.0 minutes on this particular instrument setup. The measuring range for this method is approximately 0.1-80 ppb for a sampling period of one month under southern African conditions.[221]

3.5.4.2 Preparing and analysing ozone

Before any analysis of samples took place, a series of standards for calibration purposes was prepared. By dissolving 0.085 g $NaNO_3$ in 1.0 dm^3 deionised water, a 1.0 $mmol.dm^{-3}$ $NaNO_3$ stock solution is prepared. This stock solution is used to prepare standards of 0.0, 1.0, 10.0, 25.0 and 50.0 $\mu mol.dm^{-3}$ $NaNO_3$ by adding 0.0, 25.0, 250.0, 625.0 and 1250.0 mm^3 of $NaNO_3$ stock solution and diluting it to a volume of 25.0 cm^3 with deionised water.

After the five calibration standards were prepared, injected and analysed on the IC, a calibration curve is plotted, and if compliant with lab procedure, analysis of the samples may begin. The cellulose Whatmann filters are removed from each sampler casing and leached in 25.0 cm^3 deionised water (ozone concentration is much higher than other pollutants measured and needs to be diluted) and sonicated for 15 minutes, after which it is injected into the Dionex 100 ion chromatograph. The nitrate, which is the analyte of interest, has a retention time of 3.5 minutes for this particular instrument setup. The measuring range for this method is approximately 0.6-110 ppb for a sampling period of one month under southern African conditions.[221]

3.5.4.3 Preparing and analysing nitrogen dioxide

A spectrophotometrical analytical procedure was used for the analysis of nitrite. The nitrite in the samples and standards was hence treated with a colour dye and analysed spectrophotometrically. The colour dye used was a diazotising agent and

consisted of 2.0 g sulphanilamide, 0.05 g N-1-Naphthylethylenediamine dihydrochloride (NEDA) and 2.0 cm^3 H_3PO_4 dissolved into 250.0 cm^3 of deionised water. Before any analysis of samples took place, a series of standards for calibration purposes were prepared. By dissolving 0.069 g $NaNO_2$ in 1.0 dm^3 deionised water, a 1.0 $mmol.dm^{-3}$ $NaNO_2$ stock solution is prepared. Standards of 0.0, 1.0, 2.5, 5.0 and 12.5 $\mu mol.dm^{-3}$ $NaNO_2$ are prepared by adding 0.0, 10.0, 25.0, 50.0 and 125.0 mm^3 of the $NaNO_2$ stock solution to the 5.0 cm^3 diazotising, as well as a 1.0 cm^3 of 0.79 $g.dm^{-3}$ NaI (0.198 g NaI dissolved in 50.0 cm^3 deionised water) solution and diluting it to a final volume of 10.0 cm^3 with deionised water. The NaI is added to maintain the same I^- concentration in both standards and samples.

After the five calibration standards were prepared, introduced and analysed at 540 nm on the Varian Cary 50 Conc. UV, a calibration curve is plotted and, if compliant with lab procedure, the analysis of the samples may begin. The cellulose Whatmann filters are removed from each sampler casing and leached in 5.0 cm^3 of the diazotising agent and left for 15 minutes for colour development before they are introduced into the Varian Cary 50 Conc. UV within a quartz cuvette and scanned at 540 nm. This method has a measuring range of approximately 0.05-40 ppb for a sampling period of one month under southern African conditions.[221]

3.5.4.4 Preparing and analysing nitric acid

Before any analysis of samples, a series of standards for calibration purposes was prepared. By dissolving 0.085 g $NaNO_3$ in 1.0 dm^3 deionised water, a 1.0 $mmol.dm^{-3}$ $NaNO_3$ stock solution is prepared. Standards of 0.0, 1.0, 10.0, 25.0 and 50.0 $\mu mol.dm^{-3}$ $NaNO_3$ are prepared by adding 0.0, 25.0, 250.0, 625.0 and 1250.0 mm^3 of $NaNO_3$ stock solution and diluting it to a volume of 25.0 cm^3 with deionised water.

After the five calibration standards were prepared, injected and analysed on the IC, a calibration curve is plotted and, if compliant with lab procedure, analysis of the samples may begin. The same sample preparation solution as prepared for the SO_2 sampler was used for the analysis of HNO_3 and injected into the Dionex 100 ion chromatograph. The nitrate, which was the analyte of interest, had a retention time of 3.5 minutes for this particular instrument setup. The measuring range for this method was approximately 0.1-50 ppb for a sampling period of one month under southern African conditions.[221]

3.5.4.5 Preparing and analysing ammonia

The analysis of NH_3 gas was done by a spectrophotometrical analysis method. The ammonium in the samples and standards was hence treated with a colour dye and analysed spectrophotometrically. This was done by using the Indophenol-Blue method.[222] In this method the colouring dye consists of a combination of two solutions:

i) a hypochlorite solution (by adding 0.25 g NaOH and 20.0 cm^3 commercially-available Javel with 3.5% OCl^- content and diluting it to 500.0 cm^3 with deionised water); and

ii) a phenol-nitroprusside solution (adding 5.0 g phenol to 25.0 mg sodium nitroprusside and diluting to 500.0 cm^3 with deionised water).

Before any analysis of samples took place, a series of standards for calibration purposes were prepared. By dissolving 0.113 g di-ammonium hydrogen citrate ($C_6H_{14}N_2O_7$) in 1 dm^3 deionised water, a 1.0 $mmol.dm^{-3}$ $C_6H_{14}N_2O_7$ stock solution is prepared. Standards of 0.0, 2.0, 5.0, 10.0 and 20.0 $\mu mol.dm^{-3}$ $C_6H_{14}N_2O_7$ are prepared by adding 0.0, 50.0, 125.0, 250.0 and 500.0 mm^3 of $C_6H_{14}N_2O_7$ stock solution to 10.0 cm^3 of both the phenol-nitroprusside and hypochlorite solution and diluting it to a final volume of 25.0 cm^3 with deionised water. The standard solutions were left for 30 minutes for colour development.

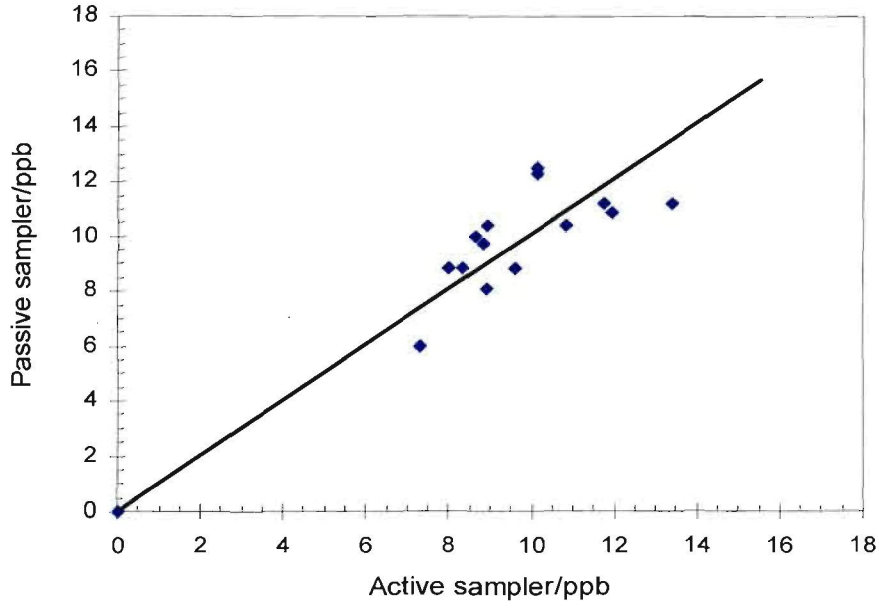
After the five calibration standards were prepared, introduced and analysed at 633 nm on the Varian Cary 50 Conc. UV, a calibration curve is plotted and, if compliant with lab procedure, analysis of the samples may begin. The cellulose Whatmann filters are removed from each sampler casing and leached in both the phenol-nitroprusside and hypochlorite solution with the phenol-nitroprusside solution preceding the hypochlorite solution with about 15 minutes. The sample solutions were left for 30 minutes for colour development. The sample solutions were then introduced into the Varian Cary 50 Conc. UV within a quartz cuvette and scanned at 633 nm. This method has a measuring range of approximately 0.2-40 ppb for a sampling period of one month under southern African conditions.[221]

3.5.5 Inter-comparison and quality control for passive samplers

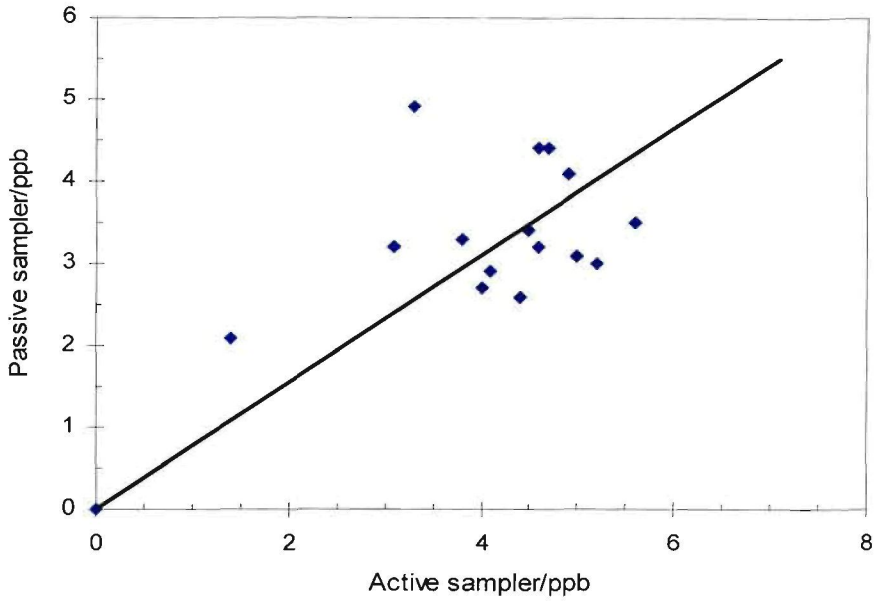
The passive samplers used in this project were developed and tested within the IGAC-DEBITS programme, as well as various international studies.[211, 223] More recent inter-comparison studies between the passive samplers at the North-West University

(Potchefstroom Campus), South Africa, included the NH_3 sampler compared to a calibrated active sampler in the Vaal Triangle.[224]. There were also comparisons between calibrated active samplers at the Elandsfontein site (for SO_2, NO_2 and O_3) and the GAW-operated Cape Point station (for SO_2 and O_3), which all yielded good comparative results.[225] However, a correction factor for O_3 and NO_2 is needed to compensate for sampled species lost due to the sampler itself and the South African climatic conditions; the NH_3 samplers also had to be analysed within a month after exposure. The last inter-comparison studies for the 2004 to 2005 period were done to ensure the continued validation of the method for the gases of O_3, NO_2 and SO_2 at the Elandsfontein site. The Elandsfontein research station is situated in the Mpumalanga Highveld of South Africa within a 50 km radius of seven power stations, ranging between 1200 and 3700 MW and equipped with a commercial UV Fluorescence SO_2, a UV Absorption O_3 and a chemiluminescence's NO_2 active monitor. All the gases again showed good reproducibility and comparability, which were well within the acceptable ranges. The results are shown in Figure 3.14 and briefly discussed.

SO_2



NO_2



O_3

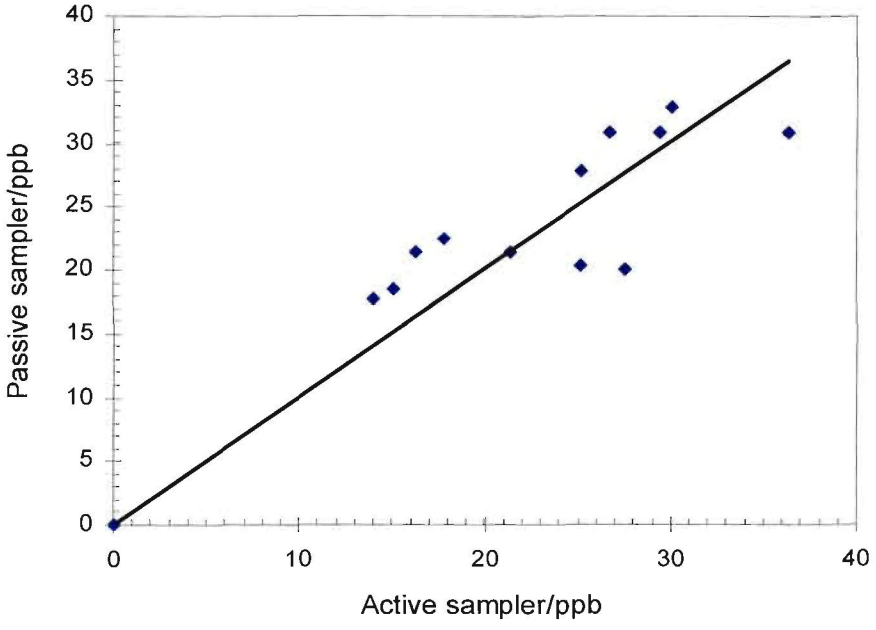


Figure 3.14: *Comparison of active and passive SO_2, NO_2 and O_3 samplers at Elandsfontein for the May 2004 to May 2005 period*

SO_2 had an average comparative concentration ratio of 1:0.9 between the passive and active sampling methods (as seen in Figure 3.14). This is very close to the 1:1 ratio observed (reported) by *Dhammapala.*[56]

NO_2 had an average comparative concentration ratio of 1:0.7 between the active and diffusive sampling methods (as seen in Figure 3.14). This is very close to the 1:0.6

ratio observed in previous comparisons by *Dhammapala.*[56] This rather low ratio can be explained by a number of factors of which the chemistry involved in the sorbent is considered to be a major factor. A number of decomposition and reverse processes for NO_2^- are known, resulting in the under-prediction of the NO_2 diffusive sampler and care should be taken to have a sufficient number of blanks for each sample as well as continuous comparison data with calibrated active samplers.

O_3 had an averaged comparative concentration ratio of 1:0.8 between the active and diffusive sampling methods (as seen in Figure 3.14). This is the same ratio as was observed in a number of previous comparisons done by *Dhammapala.*[56] The lower ratio can be explained by the fact that ozone is not measured (or collected) directly in the passive sampler, but rather the overall oxidation potential of the atmosphere as well as losses due to wall effects. From this information we expect the ratios to slightly differ from site to site and this is also our experience. The comparative concentration ratios between active and passive sampling determined for SO_2, NO_2, and O_3 were used to correct all the concentration data obtained from passive sampling.

In August 2007, an international inter-comparison study by all countries involved with the RAPIDC programme compared NO_2 and SO_2 passive samplers used by the CAD, APINA and DEBITS projects. This study was initiated by the University of Singapore. Although no published report was made yet the first leg of this study showed good comparisons for the passive SO_2 and NO_2 samplers of the North-West University with those of the other institutions as well as the active samplers used.

A field blank is included with each set of samplers deployed. Detection limits for each trace gas were calculated from field blanks and found to be 0.1 parts per billion (ppb) for SO_2, 0.05 ppb for NO_2, 0.2 ppb for NH_3, 0.6 ppb for O_3 and 0.1 ppb for HNO_3.[221] Only data above detection limits were used in reports. All the samples were collected in duplicate and their average was used in all computations, except when contamination of one of the samples was suspected (this was evident in less than 5% of all data). The covariances compare well with those reported by the IDAF laboratory at the Laboratoire d´Aérology in Toulouse, France, for the same pollutants (17,4%, 28,9%, 7,9%, 14,6% and 3,7%, for SO_2, HNO_3, O_3, NH_3 and NO_2, respectively).[51] The outcome of the above-mentioned validation and inter-comparison studies of passive sampling assures the quality and control of its sampling and analytical protocols to

make it a viable means of obtaining credible atmospheric data at remote sites on a long-term basis.

3.6 Aerosol monitoring method

3.6.1 Theory and functioning of the Air metric MiniVol sampler

Aerosols were measured in this study by using the Air metric MiniVol samplers. This sampler was jointly developed by the U.S E.P.A and the Lane Regional Air Pollution Authority. It is accurate and precise, requires no field calibration, is both AC (electricity outlet) and DC (battery) operated and the fact that it is so light makes it ideal for sampling at remote sites without power. The relatively low cost of the sampler allows the deployment of it as a network at a fraction of the cost compared to similar networks.[226]

The monitoring of aerosols by using Airmetrics MiniVol samplers fulfilled all the requirements needed for this study. The samplers are also affordable and can be deployed at the remote sites where aerosols needed to be sampled without permanent electricity. A performance evaluation of the MiniVol portable sampler was conducted by *Baldauf et al.*,[227] who concluded it to be reliable and producing similar results if deployed in pairs. The characterisation of spatial distributions of $PM_{2.5}$ and PM_{10} mass concentrations can also be accomplished with a high level of confidence. The MiniVol also produced statistically reliable results when co-located with a Versatile Air Pollutant Sampler (VAPS) and a Tapered Element Oscillating Microbalance (TEOM).[227] The entire sampler assembly is made out of all-weather PVC and is extremely durable. These factors all contributed in making the decision to use the Airmetric MiniVol sampler in this study.



Figure 3.15: *The portable Air metric MiniVol sampler*[228]

The mini-volume sampler mainly consists of three physical and detachable pieces containing all parts for sampler operation and consists of a main sampler body (middle), battery pack (bottom) and grey, specially-designed inlet (on top) as seen in Figure 3.15. The battery pack on the bottom of the sampler enables the sampler to either operate from the battery pack in the DC mode (lasting up to 24 hours) or operating connected to a 240 V power source by using the charging cable of the battery pack. The battery pack (two battery packs, one for operating and one for charging) is connected to the main sampler body as seen in Figure 3.15 by means of banana pins and secured with latches on the side. The sampler body itself contains a twin cylinder diaphragm pump, which draws air through the designed inlet and forces it through a standard flow meter located within the sampler body where it is exhausted to the atmosphere. A valve system on top of the sampler body connects the specially-designed inlet to the sampler body (see Figure 3.15).

The MiniVol sampler is a pumping system controlled by a timer that starts or stops sampling either automatically through programming or manually with display buttons on the console, as seen in Figure 3.16 next to the flow meter. It has a seven-day programmable timer and can make up to six runs within 24 hours or throughout a week.



Figure 3.16: *Sampler controls and adjustments*[228]

The sampler has a standard flow meter located next to the programmable timer, which together forms the controlling unit of the sampler and are located within the main sampler body (Figure 3.16). The flow system can be set manually to deliver a constant flow rate. The sampler shuts down automatically as it is equipped with two fault circuits that shut the sampler down if the battery fails to supply sufficient voltage (need to be charged) or the flow rate falls below a specified rate due to accumulation of particulate matter or restriction in tubing.[226] If the sampler stops due to one of the above-mentioned faults, it needs to be reset before it can be started, by pressing a reset button located on the right side edge of the control unit in line with the bottom part of the flow meter in Figure 3.16. An elapsed time totaliser, linked in parallel with the pump, records the total time in hours of the pump operation, enabling the volume of air sampled to be calculated.

Sampling principal

In this sampling technique, aerosols are collected on filters within filter holder assemblies (see Figure 3.17) mounted in the specially-designed inlet (see Figure 3.18) of the sampler through which air is actively sucked. The sampled filters with the trapped aerosols are sealed within Petri slides and transported to the analytical lab where they are analysed for the analytes of interest, as described in Paragraph 3.4. The MiniVol sampler collects aerosols for particle sizes of 2.5 and 10 µm as well as TSP. Particle size separation is achieved by impaction within impactors designed to separate particles below 2.5 and 10 µm (see Figure 3.18).



Figure 3.17: *Filter holder assembly of air metrics mini-volume sampler*[228]

The particle size discrimination characteristics of both the inlet and the impactors depend critically on specified air velocities through the sampling system. For this reason, it is imperative that the flow rate through the sampler be maintained at a constant value that is as close as possible to the design flow rates. The design flow rate for the MiniVol is 5.0 L/min. The sampler flow rate should be within ±10% of 5 L/min to ensure optimal collection of selected size fraction.[226]



Figure 3.18: *Specially-designed inlets with impactors*[228]

Only aerosols with sizes of 2.5 μm and smaller and 10 μm and smaller were sampled with impactors as shown in Figure 3.18. The impactors are made of aluminium and positioned inside the designed inlets just above the filter holder assemblies. The specially-designed inlets are presented in Figure 3.18, each with an impactor beside it (silver coloured 10 μm and bronze coloured 2.5 μm impactors).[228] For collecting 2.5 μm aerosols, both impactors are inserted within the designed inlets with the 10 μm impactor preceding the 2.5 μm impactor. For collecting 10 μm aerosols, only the 10

μm impactor is inserted. The opening to the designed inlet futures a protective cap that fits on top of the inlet and protects it from adverse weather conditions.

3.6.2 Filter selection

The WMO and GAW guidelines and recommendations for aerosol measurements were used to select the filters to be used.[229] Teflon and quartz filters were selected as they had been and still are used with great success on routine bases for long-term programmes of international networks such as the IDAF-DEBITS network.[229] This study is focussed on the major ionic and carbonaceous species of an aerosol for which the WMO and GAW, within their guidelines, also recommend the use of Teflon and quartz filters in order to determine the major ionic and carbonaceous species of an aerosol, respectively.[229] It is also recommended that when these samplings occur, they should be simultaneously with both types of filters and at least two particle sizes - preferably those of fine < 2.5 or 1 μm and coarse < 10 μm.

3.6.2.1 Carbonaceous aerosol collection

It is recommended that the total aerosol carbon mass (TC), organic carbon (OC) and elemental carbon (EC) be measured in the GAW programme, leaving out the relatively minor and difficult inorganic carbon component and more complicated issues of organic carbon speciation.[229] For the sampling of carbonaceous materials, it is recommended to use quartz filters pre-fired at 350-400°C for two hours with no particular filter size suggested. A temperature-controlled thermal evolution technique coupled with optical reflectance/transmittance correction for charring is recommended for the GAW programme for OC/EC measurement.[229] Quartz filters of 47 mm in diameter supplied by Whatmann were used to sample for carbonaceous aerosol collection and pre-fired at 400°C for two hours. A Thermal/Optical Carbon Analyser from D.R.I was used to measure the OC/EC content of each sample collected.

3.6.2.2 Ionic aerosol collection

The WMO and GAW guidelines recommend filtration with Teflon filters to collect aerosol for various chemical analyses, except organic carbon and mass measurements and the reasons for this choice include:

i) the extensive use of it in various existing measurement networks;

ii) commercial availability;

iii) efficiency of aerosol collection (99% of particles ≥ 5 nm are trapped on filters with pore size <1 μm);
iv) chemical inertness (suitable for many kinds of chemical analyses); and
v) low chemical content (lower atmospheric detection limit).[229]

Teflon filters, 47 mm in diameter, are recommended, as a standard size facilitates inter-comparison of data and adaptation of common QA/QC procedures. An ion chromatography (IC) is recommended for the analyses of ionic species in aerosols as they are the most cost effective. Teflon filters, 47 mm in diameter and 0.45 μm pore size supplied by G.I.C. scientific, were used and analysed on the IC instruments mentioned in Paragraphs 3.4.3-4.

3.6.3 Quality control procedures

Teflon and Quartz filters were sealed in air-tight Petri slides to ensure no contamination takes place before or after sampler exposure. The Petri slides were kept under 4°C after exposure to minimise sample loss during transport. Minimising filter handling, loading filter holders in as clean as possible environments as well as the use of surgical gloves when handling the filters all contribute to minimising contamination and filter loss.

Aerosol samples were taken daily (24-hour samples) as recommended by WMO and GAW and for both quartz and Teflon filters for the two particle sizes of 2.5 and 10 μm simultaneously, as prescribed. The guidelines recommend sampling times for up to 48 hours in pristine locations to ensure sufficient sample volume for analysis.[229] A laboratory blank was prepared for every ten sampler filters prepared (within the recommended 5-10% range set by WMO/GAW) to compensate for any matrix effects, systematic errors and contaminants in Petri dishes, filters and laborator when samplers were prepared and analysed. Blanks filters were prepared and sent to the field along with the other filters and analysed in exactly the same way and time as field samples. Detailed log sheets containing records of each sampled filter (including the particle size, type of filter, sampling date, exposure time, volume sampled, as well as weather conditions and anomalies like fires) always accompany the referenced filters to and from the field.

Once the sampled filters were received from the sites, they were identified, prepared and analysed according to the prescribed analytical procedures, which will be described in the following paragraphs.

3.6.4 Preparation of samples for analysis

The Teflon and quartz filters were kept under 4°C until they could be transported to the Laboratoire d'Aérologie, Université Paul Sabatier, Toulouse, France, where they were analysed. Both types of the sampled filters had their own analytical methods and preparation before analysis, which will be discussed now, as well as matters pertaining to the analytical technique.

3.6.4.1 Preparing and analysing samples and standards

Calibration standards, covering the range of expected sample concentrations, were prepared for both the DIONEX instruments used in the analysis of the ionic content of aerosol in this study. A three-point calibration curve is used for calibration. Standards are made from mono-element stock solutions supplied by Dionex, each containing 1 g/L of the element. The standards are diluted with deionised water to the required concentrations. The calibration curve is fitted for the three points with 5% precision or better, after which the analysis of ionic sample filters may begin.

Desert Research Institute (DRI) Thermal/Optical Carbon Analyser is calibrated twice a year or when new calibration gas cylinders are started, to establish the calibration slope used to convert the counts to µg of carbon. Calibration is done using a series of KHP or sucrose solutions injected onto clean blank punches as well as various volumes of the calibration gases of CO_2 and CH_4.[210] Calibration curves are plotted as actual µg carbon vs. the ratio of the integrated sample peak counts to the calibration peak counts. The calibration slope is compared to previous calibration results and values should not differ more than 10%. Now the analysis of carbonaceous sample filters may proceed.[210]

3.6.4.2 Preparation and analysis of carbonaceous sample filters

The carbon analyser was calibrated as described in Paragraph 3.6.4.1 before the analysis of the carbonaceous sample filters began. Each sample filter's information is entered into the instrument computer before each analysing run, which only initiates

the run once certain information that serves as identification of the filters results is supplied. After the quartz filter is removed from the Petri slide, a 0.512 cm^2 punch is taken from it and placed with tweezers in the boat of a movable slot of the carbon analyser. The boat transports the filter into a pre-oven chamber region of the analyser for 90 seconds before it is transferred into the oven for analysis. The analytical run takes ±30 minutes plus another 10 minutes for the previous sample filter to be ejected within the movable slot, as the analyser keeps the boat within the pre-oven chamber to cool down to a safe enough temperature (50°C). After each run is completed, the computer automatically sends the results to a printer, which gives a tabular print out of the total, elemental and black carbon concentrations of each sampled filter in $\mu g.cm^{-2}$. A thermogram (a graphic diagram of carbon peaks at the different temperatures corresponding to the different carbon detected, as well as a reference calibration peak at the end of the analysis) is also included within the report print out.

3.6.4.3 Preparation and analysis of ionic sample filters

Both the DX 500 and DX 100 Ion Chromatographs were calibrated using standard solutions as described in Paragraph 3.6.4.1 before any analysis was done. Teflon filters were taken out of the Petri slides and leached in 10 cm^{-3} deionised water and sonicated for 30 minutes. The content of these vials is split into two to accommodate both cation and anion analysis and inserted into appropriated auto-sampler vials and analysed on the DX 500 and DX 100 IC (see Paragraphs 3.4.3-4), respectively. Each sampler filter is referenced with a number specified on the computer, which correlates with its position within the auto-sampler. The computer initiates each sample analysing run according to its reference number specified on the computer. The analysing time depends on the retention time of each of the species, and varied from 15 minutes for anions to 20 minutes for the cations. The analysed results are determined by linear regression in conjunction with the calibration curve of the standards and given in µg/L.

3.6.4.4 Quality control for aerosol sampling

All of the analysers used for analysing aerosol sample filters at the Laboratoire d'Aérologie in Toulouse, France are located in clean rooms with positive air pressure and dedicated to air quality analysis only within the DEBITS project. Ionic chromatography measurements made in the Laboratoire d'Aérologie are all evaluated

by WMO inter-comparisons. Every year, three unknown samples are received for analysis. These results from the laboratory are compared to referenced WMO values. The results presented in Figure 3.19 below were done for 2007 and allow us to estimate the analytical precision of Laboratoire d'Aérologie for measurements of mineral ions to be within 5% or better.

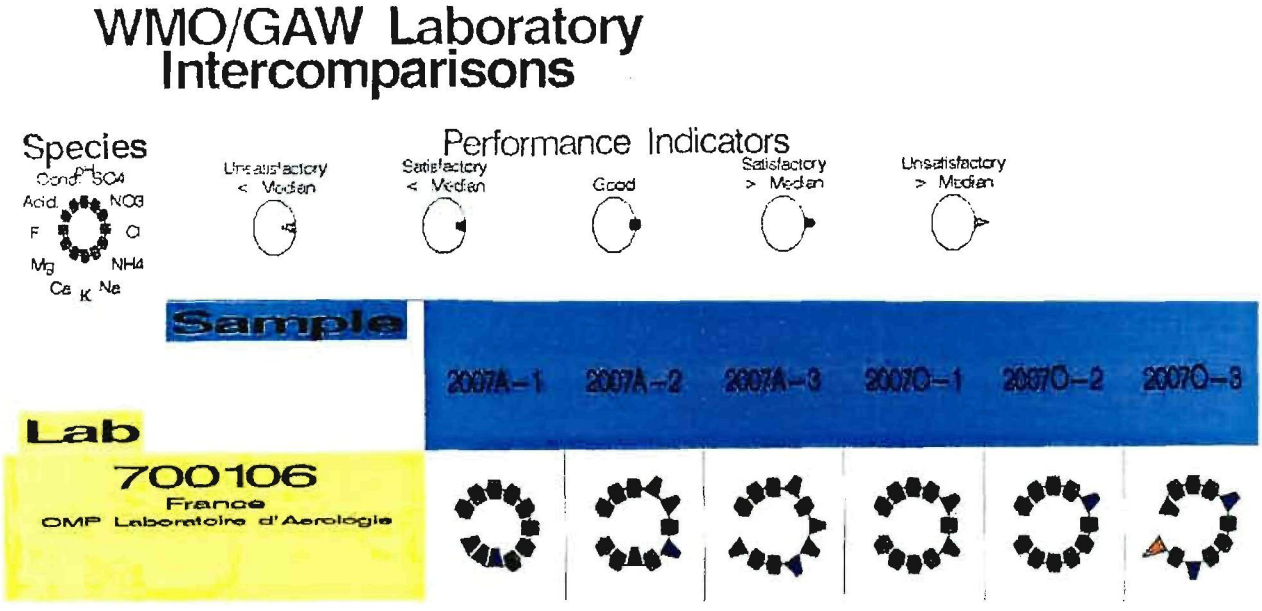


Figure 3.19: *The 2007 WMO Inter-comparison results of the Laboratoire d'Aérologie for mineral ions*

CHAPTER 4

Results of gaseous measurements

In this chapter, the data from the 10-year passive sampling initiative is provided and discussed. The monthly and annual fluctuations in the concentrations of the selected species are also interpreted and the dry deposition estimations of the species are made.

4.1 Introduction

The passive sampling initiative was initiated in 1995 and still continues today. This study deals with the data collected between 1995 and 2005 (e.g. the first ten years of the initiative). It consists of all the selected gas species mentioned in Chapter 2 and was measured at all the four sites mentioned in Chapter 3. After applying the quality control procedures mentioned in Paragraph 3.5.6, 1620 of the data points obtained were approved as sound. The distribution of these approved results between the sites and species is given in Table 4.1.

Table 4.1 The distribution and number of approved results at each of the four regional sites.

Station	SO_2	NO_2	*HNO_3	O_3	NH_3
Amersfoort	70	71	27	72	65
Louis Trichardt	10	105	26	89	85
Cape Point	106	114	29	114	120
Okaukuejo	125	121	25	122	124

** Monitoring of HNO_3 only started in 2003*

Less than 10% of all the samplers deployed at the four sites during this time period produced results below the detection limit. Only the HNO_3 sampler at the Okaukuejo site produced a 36% loss of results due to low detection limits. In this chapter, the results from each of these regional sites (both urban and rural) in southern Africa are

presented and discussed. The collected data is provided in table format in Appendix A.

4.2 Results

Table 4.2 represents a summary of all the gas data collected for this study and contains the average concentration for all the species monitored at the four sites for the time period 1995 to 2005, calculated using only the approved data points given in Table 4.1. It is regarded as the best representative values available for these sites.

Table 4.2 Total average mean gas concentrations (ppb) at each site for the period 1995-2005

Station	SO_2	NO_2	O_3	NH_3	HNO_3
Amersfoort	2.8±1.1	2.5±1.0	27±8	1.2±0.7	0.9±0.5
Louis Trichardt	0.8±0.7	0.7±0.4	35±9	1.2±0.7	0.2±0.1
Cape Point	0.7±0.4	1.2±0.6	27±7	1.5±0.7	0.5±0.2
Okaukuejo	0.4±0.2	0.3±0.2	23±6	1.5±0.7	0.3±0.2

The high NO_2 and SO_2 average concentrations at Amersfoort in comparison with the other sites confirms the fact that this region has to be regarded as a global industrial hotspot, because it is downwind of nearby industrial sources for most of the time.[178] The high ozone concentrations observed at Louis Trichardt have been confirmed by several modelling studies[198,230] and are most probably due to a large inter-continental mixing zone of ozone precursor gases (namely volatile organic compounds from biomass burning from Zambia and Zimbabwe and NO_2 from the industrial activities in South Africa). The important role of NH_3 and SO_2 in atmospheric aerosol formation is widely recognised.[231,211] NH_3/SO_2 ratios of 3.49, 1.46, and 2.73 were observed at Okaukuejo, Louis Trichardt and Cape Point, respectively, while a ratio of 0.43 is observed at Amersfoort. Differences in these ratios are mostly SO_2 -driven and in this case, the ten-year average ratios are relatively close to values reported by *Carmichael et.al.*[211] for Cape Point (ratio 3.3) and Elandsfontein (0.3) for the 1999-2000 period. *Carmichael et.al.*[211] reported higher NH_3/SO_2 ratios for several other background sites in Africa, but the differences stem mainly from lower SO_2 concentrations. The higher background SO_2 levels in southern Africa are a consequence of increased industrial activities and coal-fired plants in South Africa compared to other regions in Africa.

4.3 Monthly averages

A summary of the monthly mean, median, minimum and maximum concentrations for the selected pollutant species at the four sites over the sampling period is shown in Figures 4.1-5 for SO_2, NO_2, O_3, NH_3 and HNO_3, respectively. The maximum-minimum and mean-median values show larger differences than on the annual plots, due to the large inter-annual monthly variations of these species. Annual meteorological variations for a given month may be large and the presence or absence of rain for instance result in these large differences.

4.3.1 Sulphur dioxide

The monthly mean SO_2 concentrations for the 1995-2005 time period at the four sites are is graphically displayed in Figure 4.1. The monthly mean concentrations show a maximum for Amersfoort, Louis Trichardt and to a lesser extent the Okuakuejo sites during the dry winter and early spring months of June to October. The reverse is observed at the Cape Point site where the maximum SO_2 concentrations are recorded from January to April (see Figure 4.1). These observations clearly indicate the important role of meteorological conditions on atmospheric concentrations of chemical species. The higher values during winter are linked to both increased emissions during the winter months (resulting in increased energy use) as well as the stable atmospheric conditions experienced during the winter months in the interior of southern Africa. The Cape Point station is situated within a winter rainfall region and the SO_2 minimum observed during the winter period may be ascribed to both meteorological conditions as well as removal processes by rain.

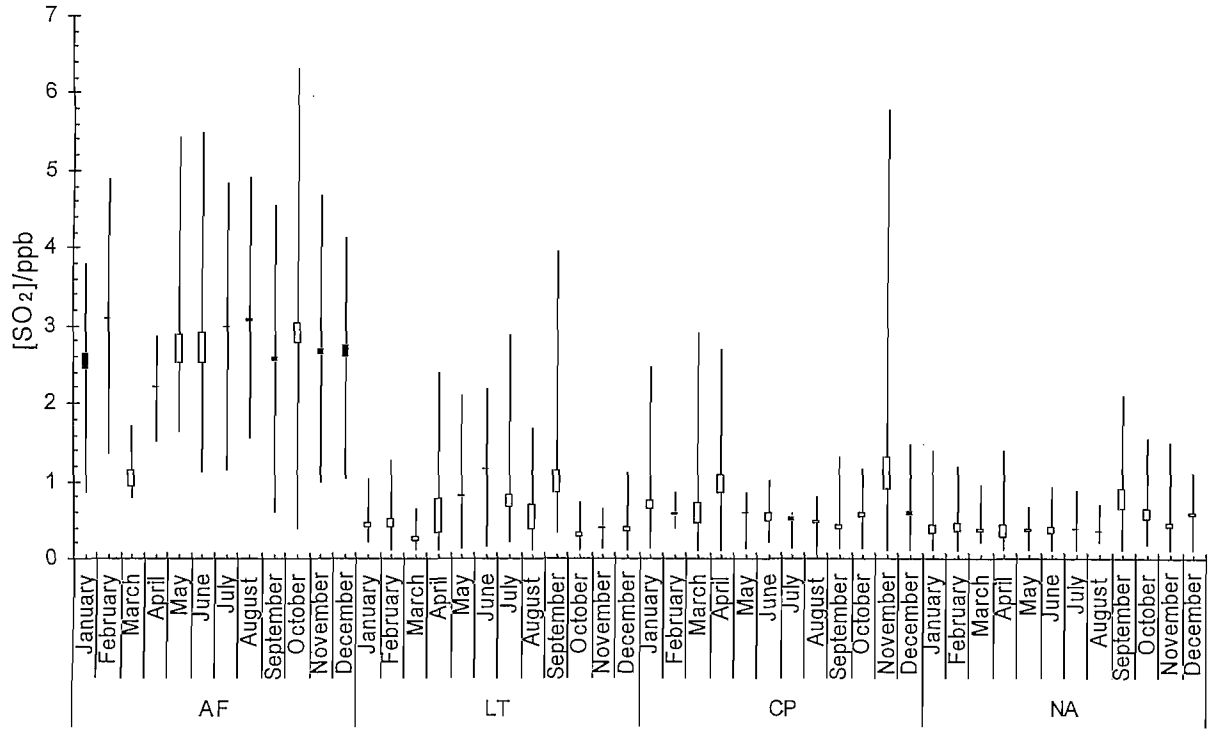


Figure 4.1 *Monthly SO_2 concentrations at Amersfoort (AF), Louis Trichardt (LT), Cape Point (CP) and Okaukuejo (NA). In this box-and-whisker plot, each whisker indicates the range of the respective maximum and minimum values. An open box indicates that the corresponding mean value (presented by the top of the box) is greater than the median value (represented by the lower limit of the box). A filled black box is used when the corresponding median value (represented by the top of the box) is greater than the mean value (represented by the lower limit of the box).*

4.3.2 Nitrogen dioxide

The monthly mean NO_2 concentrations for the 1995-2005 time period at the four sites are graphically displayed in Figure 4.2. The monthly mean concentrations show a very clear seasonal signal at all the South African sites (see Figure 4.2). The Okaukuejo site (Namibia) seems to be the exception, where more constant NO_2 values throughout the year are observed. The early spring maximum in NO_2 concentrations at the South African sites is linked to bio-geogenic activity as it marks the start of the growing season. The NO_2 concentration at CP starts to increase a bit earlier than in the inland sites due to differences in the biogeochemistry cycles of this winter rainfall

region. The high NO_2 values at Amersfoort are indicative of the anthropogenic contribution (power generation) from the Mpumalanga Highveld.

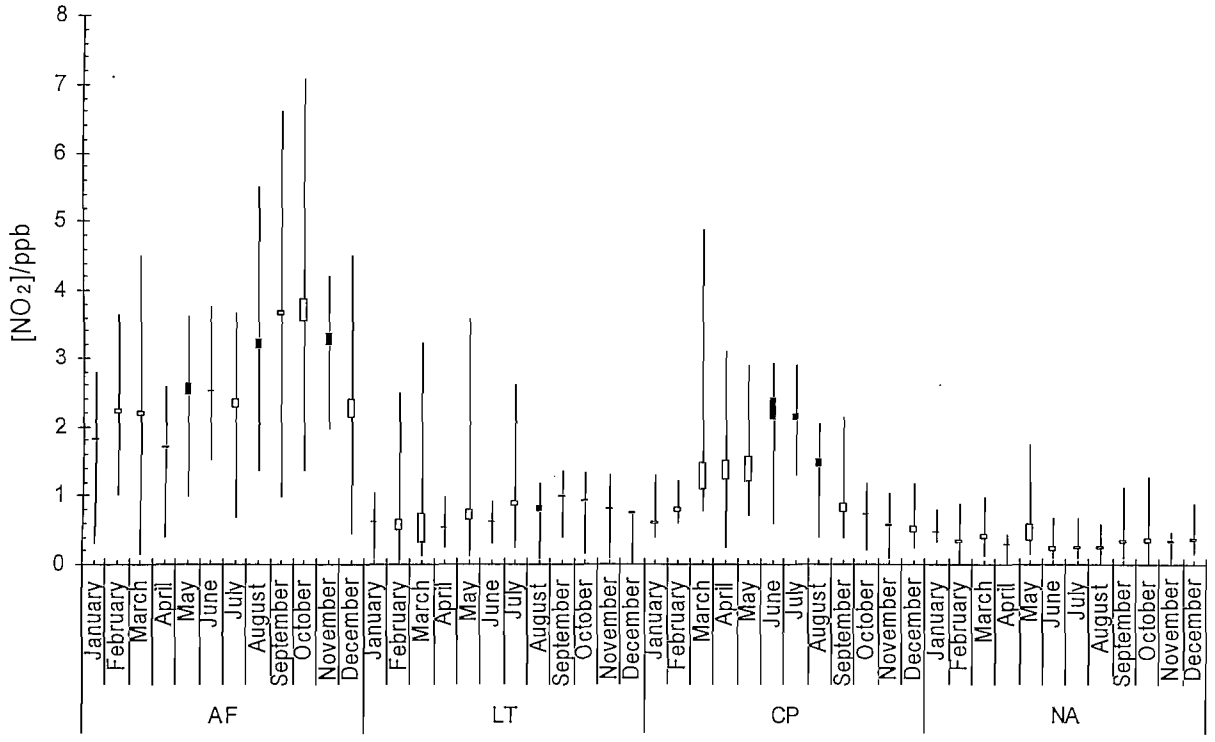


Figure 4.2 *Monthly NO_2 concentrations at Amersfoort (AF), Louis Trichardt (LT), Cape Point (CP) and Okaukuejo (NA). See Figure 4.1 for explanation of the box-and-whisker plots.*

4.3.3 Ozone

The monthly mean O_3 concentrations for the 1995-2005 time period at the four sites are graphically displayed in Figure 4.3. A clear spring and early summer maximum is observed at Amersfoort, Louis Trichardt and Cape Point, while it seems that the maximum O_3 concentration is observed from January to December at the Okaukuejo site. The O_3 maximum shows, as is expected, a direct relation with the NO_2 maximum (see Figure 4.2) and is one of the precursors for the photochemical production of ozone.

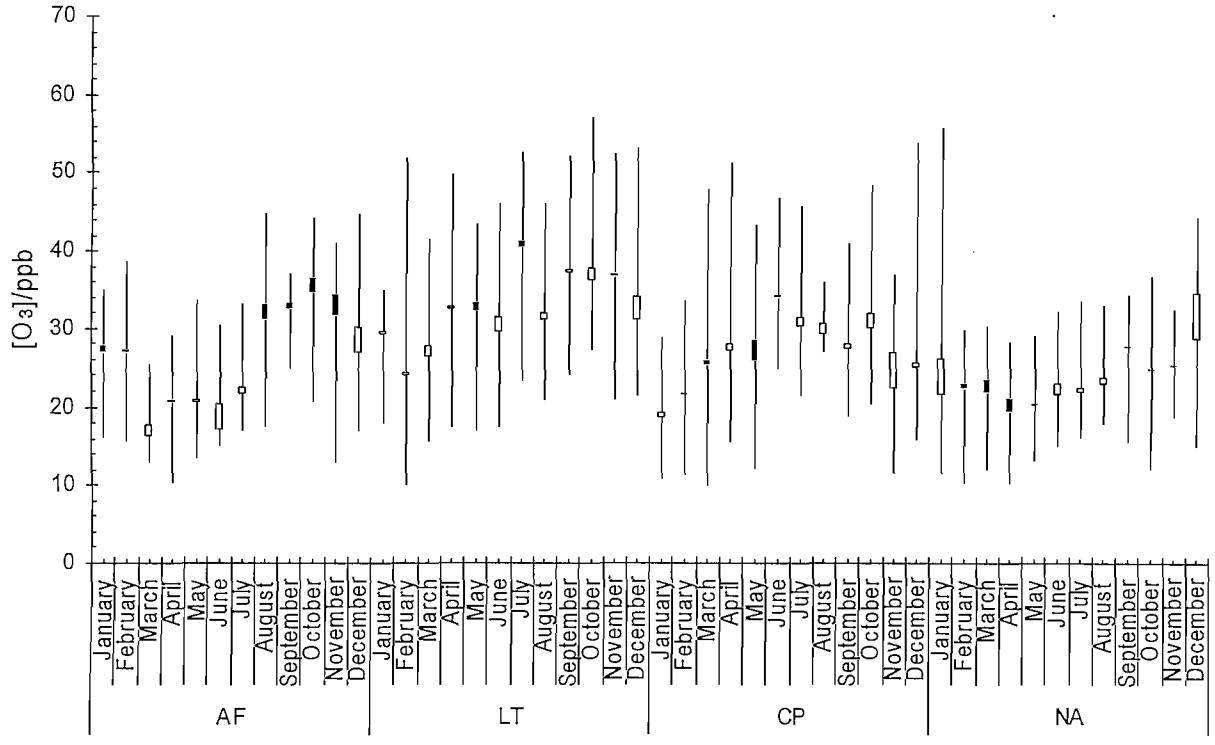


Figure 4.3 *Monthly O_3 concentrations at Amersfoort (AF), Louis Trichardt (LT), Cape Point (CP) and Okaukuejo (NA). See Figure 4.1 for explanation of the box-and-whisker plots.*

4.3.4 Ammonia

The monthly mean NH_3 concentrations for the 1995-2005 time period at the four sites are graphically displayed in Figure 4.4. The monthly mean NH_3 concentration increased during the stable winter months at Amersfoort. These slightly elevated levels are probably linked to a less effective removal process during this time of the year. It is known that NH_3 is one of the pollutants emitted by industry in this region. The relatively high NH_3 values observed at Cape Point are linked to the high density of nesting birds around this site. The monthly mean NH_3 concentration at Okaukuejo site remains relatively constant throughout the year.

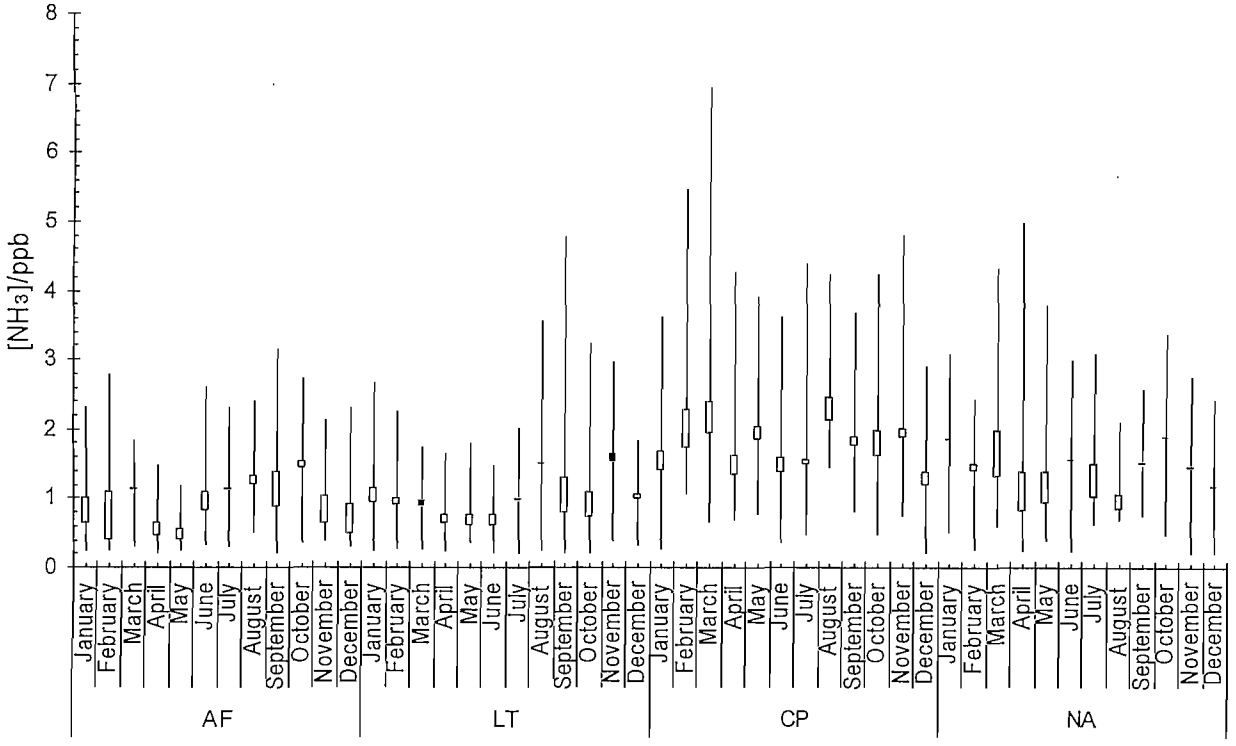


Figure 4.4 *Monthly NH_3 concentrations at Amersfoort (AF), Louis Trichardt (LT), Cape Point (CP) and Okaukuejo (NA). See Figure 4.1 for explanation of the box-and-whisker plots.*

4.3.5 Nitric acid

The monthly mean HNO_3 concentrations for the 2003-2005 time period at the four sites are graphically displayed in Figure 4.5. Although no real long-term data for HNO_3 is available, it is clear from the data in Figure 4.5 that the maximum monthly mean HNO_3 concentrations are observed during the spring months of August to November (end of winter) at all the sites, following the same accumulation trend during the stable winter period as NH_3. Most of the sites have elevated HNO_3 concentrations at the same time as the NO_2 concentrations are elevated and thus may indicate a direct link between these two pollutants in the atmospheric NO_x cycle. The lack of long-term data prevents any conclusive conclusions to be made. A maximum for HNO_3 is observed at exactly the same time as for NH_3.

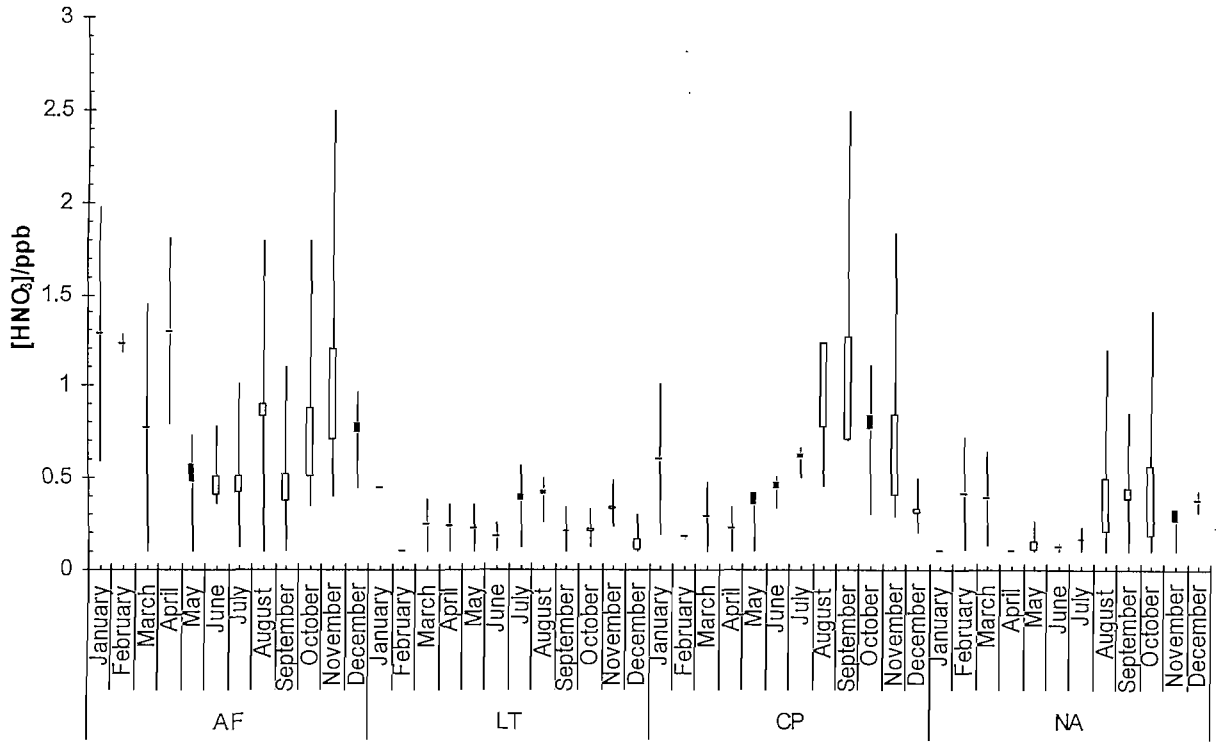


Figure 4.5 *Monthly HNO_3 concentrations at Amersfoort (AF), Louis Trichardt (LT), Cape Point (CP) and Okaukuejo (NA). See Figure 4.1 for explanation of the box-and-whisker plots.*

4.4 Annual averages

Summaries of all the annual mean, median, maximum and minimum concentrations for all the species at all the sites over the time period are presented in Figures 4.6-10. The difference between the maximum and minimum levels of each pollutant gives an indication of the large differences in pollutant concentrations during the different seasons of the year. The difference between the mean and median values is rarely more than 0.2 ppb and shows the consistency of the measured values on an annual basis.

4.4.1 Sulphur dioxide

The annual mean SO_2 concentrations for the 1995-2005 time period at the four sites are graphically displayed in Figure 4.6. Annual mean concentrations show that on the long term, the concentration at the Amersfoort site decreased from 3.6 ppb in 1997 to 1.7 ppb in 2004, where after an increase is observed; except for 2002 where the SO_2 concentration was higher than the norm. For the Cape Point site, the SO_2 mean

annual concentration (<1 ppb) showed little variation between 1995 and 2005, except in 2002 with a higher value of 1.3 and 2005 with a value of 1.1 where the SO_2 concentrations seem to increase again. The Okuakuejo and Louis Trichardt sites show a slight constant decline for the SO_2 mean annual concentration and are all below 1 ppb for the period 1995-2003, except for 1998 for Louis Trichardt, when the value was 1.8 ppb. The SO_2 concentrations for Louis Trichardt and Okuakuejo increase again slightly from 2003.

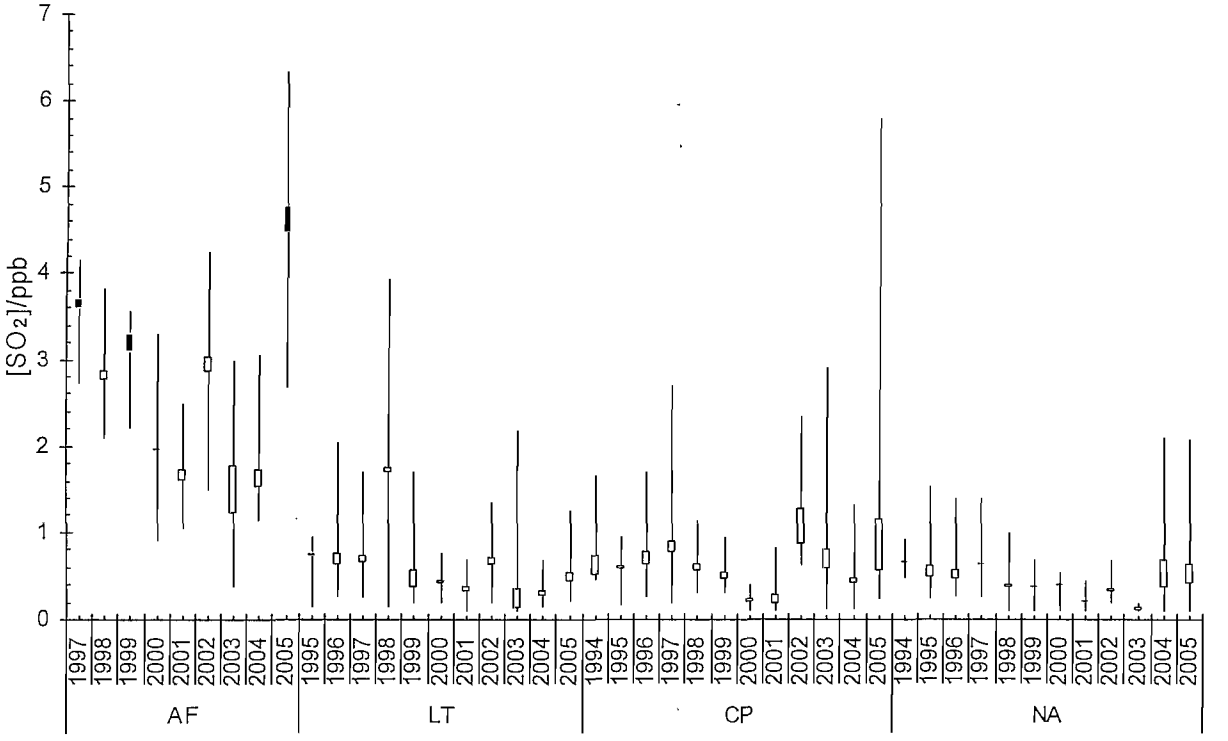


Figure 4.6 *Annual SO_2 concentrations at Amersfoort (AF), Louis Trichardt (LT), Cape Point (CP) and Okaukuejo (NA). See Figure 4.1 for explanation of the box-and-whisker plots.*

4.4.2 Nitrogen dioxide

The annual mean NO_2 concentrations for the 1995-2005 time period at the four sites are graphically displayed in Figure 4.7. Annual mean concentrations at Amersfoort decreased from 3.8 ppb in 1997 to 1.2 ppb in 2002, and increased again to 3.8 ppb in 2005. The concentrations at the Cape Point site decreased from 2.1 ppb in 1996 to 0.5 ppb in 2002 and then increased again to 0.8 ppb in 2005. The concentrations at Louis Trichardt decreased from 1.2 ppb in 1996 to 0.3 ppb in 2002 and then increased

to 0.8 ppb in 2005. The concentrations at Okaukuejo were constant and below 0.6 ppb for the entire 1995-2005 period.

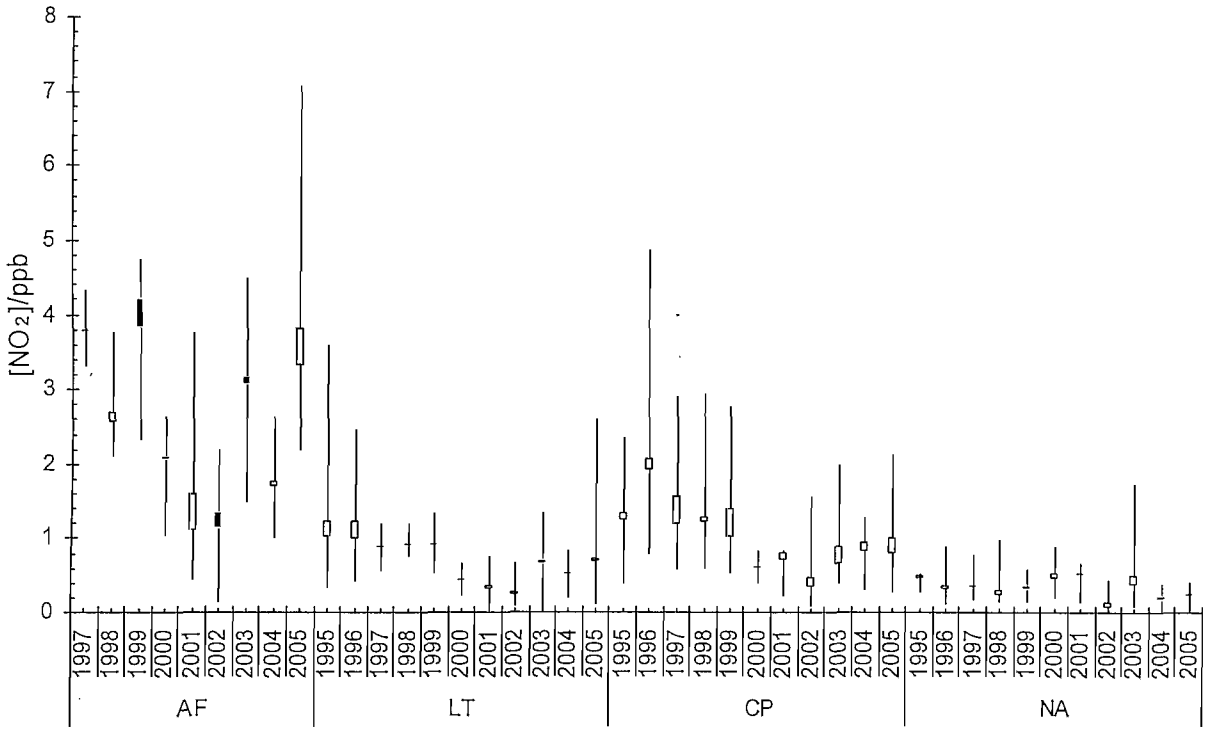


Figure 4.7 *Annual NO_2 concentrations at Amersfoort (AF), Louis Trichardt (LT), Cape Point (CP) and Okaukuejo (NA). See Figure 4.1 for explanation of the box-and-whisker plots.*

4.4.3 Ozone

The annual mean O_3 concentrations for the 1995-2005 time period at the four sites are graphically displayed in Figure 4.8. Annual mean concentrations for all the sites steadily decrease from 1994 to 2001, after which they increase again. This tendency is especially evident in the data obtained at Cape Point and Louis Trichardt. A very similar profile over this period was observed for these two and (to a lesser extent) the Amersfoort and Okuakuejo sites.

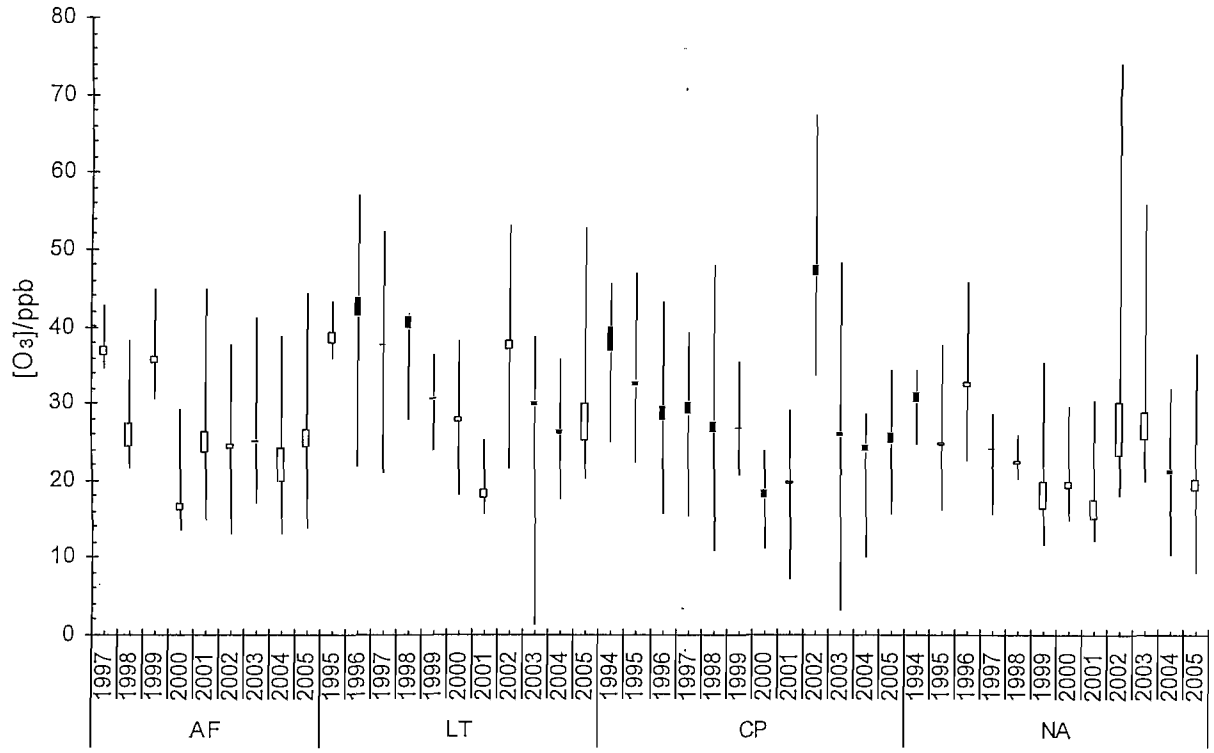


Figure 4.8 *Annual O_3 concentrations at Amersfoort (AF), Louis Trichardt (LT), Cape Point (CP) and Okaukuejo (NA). See Figure 4.1 for explanation of the box-and-whisker plots.*

4.4.4 Ammonia

The annual mean NH_3 concentrations for the 1995-2005 time period at the four sites are graphically displayed in Figure 4.9. Annual mean concentrations at Cape Point, Louis Trichardt and Okuakuejo increased during the first four years (1995-98) and then decreased until 2005 for all three sites, except for 1999 and 2000 at Cape Point. At the Amersfoort site, the annual mean concentration decreased from 2.0 ppb in 1999 to 0.5 ppb in 2005.

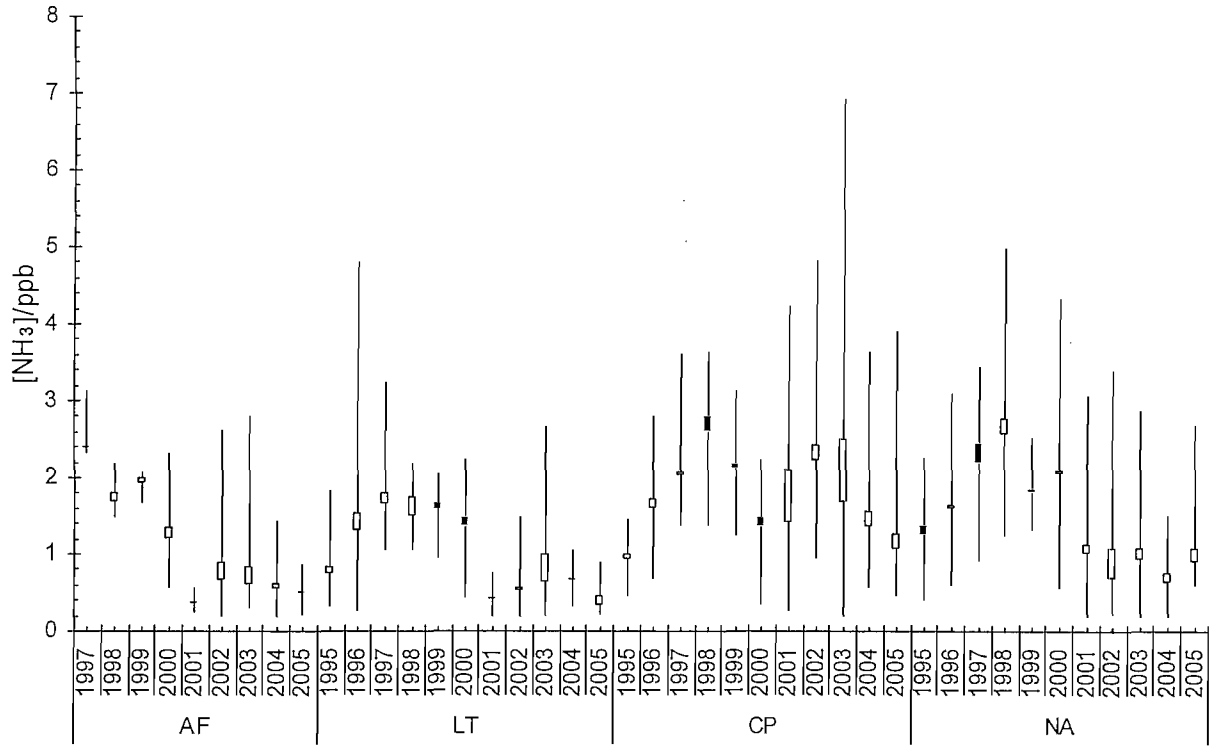


Figure 4.9 *Annual NH_3 concentrations at Amersfoort (AF), Louis Trichardt (LT), Cape Point (CP) and Okaukuejo (NA). See Figure 4.1 for explanation of the box-and-whisker plots.*

4.4.5 Nitric acid

The annual mean HNO_3 concentrations for the 1995-2005 time period at the four sites are graphically displayed in Figure 4.10. Annual mean concentrations of HNO_3 at Amersfoort increased since 2003, while it increased slightly at the Louis Trichardt site and stayed relatively constant at the Okuakuejo site. The annual mean HNO_3 concentration at the Cape Point site remained constant at 0.5 ppb for the last two years.

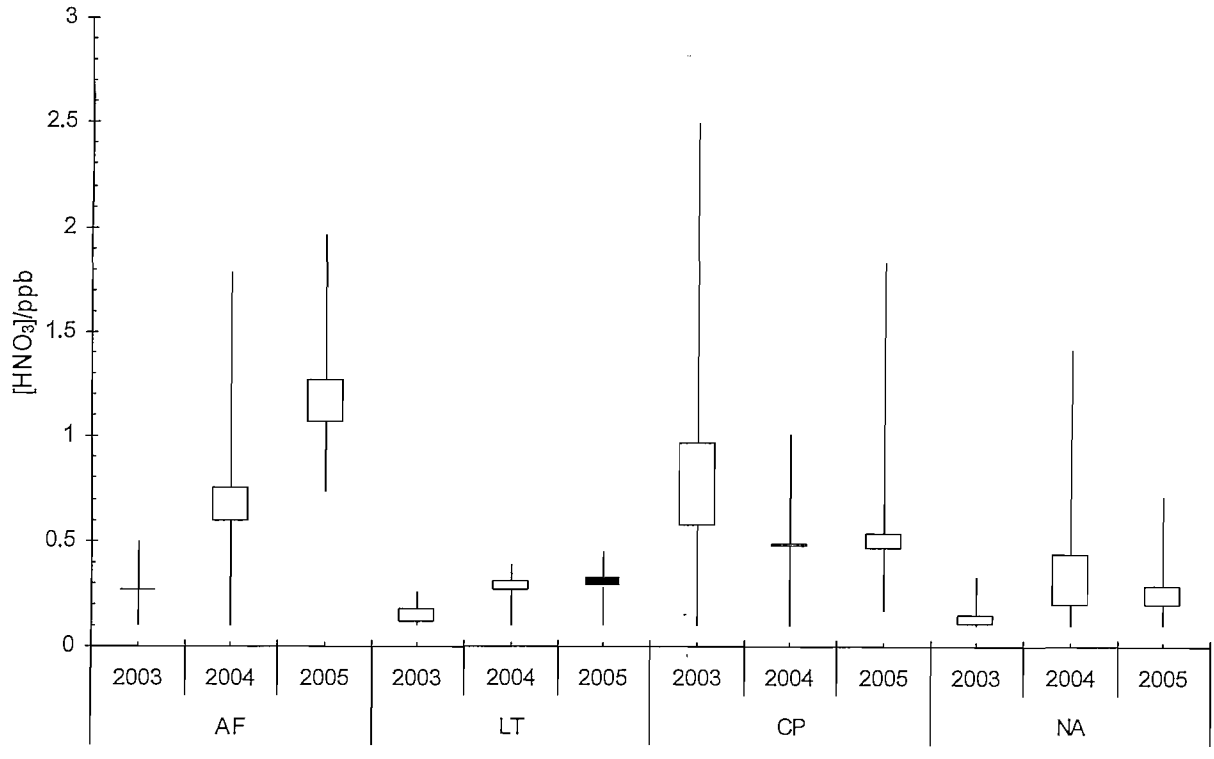


Figure 4.10 *Annual HNO_3 concentrations at Amersfoort (AF), Louis Trichardt (LT), Cape Point (CP) and Okaukuejo (NA). See Figure 4.1 for explanation of the box-and-whisker plots.*

4.5 Dependences and linkages

The gaseous concentrations of SO_2, NO_2, HNO_3, NH_3, and O_3 were measured on a monthly basis at four regional sites in southern Africa over several years. The monthly mean SO_2 concentrations ranged from a minimum of 0.2 ppb (at rural sites of Louis Trichardt and Okaukuejo) to a maximum of 6.3 ppb (industrial site of Amersfoort). The total mean SO_2 concentration over the period 1994-2005 was below 1.0 ppb (Table 4.2) for all sites except at Amersfoort, which had an average concentration of 2.8 ppb. The emission of SO_2 by large industries in close proximity of the Amersfoort site is responsible for the constant elevated SO_2 concentrations. The fact that the maximum of 6.3 ppb occurred during October (see Figure 4.1) supports the theory of the accumulation of SO_2 during winter/spring[61]. The SO_2 concentration at the Louis Trichardt site is about three times lower than at Amersfoort (Table 4.2), but seems to follow the same monthly trend. This confirms the transport of the SO_2 from the interior region of South Africa to the Louis Trichardt region as previously reported by *Mphepya.*[10] The SO_2 values at Cape Point are of the same magnitude as at Louis

Trichardt and are mainly influenced by the industrial and informal settlements found in and around Cape Town, as was described in Paragraph 3.1. Recirculation of air from the Mpumalanga area over Namibia represents 32% of the total air exported from the Mpumalanga Highveld (see Paragraph 2.8). Louis Trichardt and Okaukuejo are located within this recirculation path. The SO_2 concentration at the Okaukuejo site is exactly half of the SO_2 concentration at Louis Trichardt (Table 4.2) and may be indicative of the possible transport of SO_2 between the sites.

Monthly mean NO_2 concentrations ranged from a minimum of 0.2 ppb (Louis Trichardt and Okaukuejo) to a maximum of 7.1 ppb (Amersfoort). The total mean NO_2 concentration over the period 1994-2005 was below 1.5 ppb (Table 4.2) for all the sites except Amersfoort, where a concentration of 2.5 ppb was observed. The large industries located in close proximity to the Amersfoort site are again responsible for constant higher NO_2 concentrations present at this site. The maximum of 7.1 ppb for NO_2 was found during the same period as the maximum for SO_2, which was during October (see Figure 4.2). This is within the same season and indicates the same accumulation effect found for SO_2. There is however one discrepancy for SO_2 and NO_2 data which does not follow the same trend. For SO_2 there is an increment in 2002 and for NO_2 the increment follows in 2003. The same increment for O_3 exists in 2002 but is only visible at LT and CP. From this data a possible explanation could be large biomass burning activities in the AF region during 2002 when SO_2 concentrations were also elevated at all the sites in southern Africa. This does not explain NO_2 concentrations not increasing at all the other sites but possibly explains why LT and CP has an O_3 concentration increment in the same year. These sites are all within the re-circulation pathway of AF as described in Paragraph 2.8. Due to transport and production of ozone within transported plumes containing NO_2 and CO from biomass burning, as described in Paragraphs 2.3.1.2 and 3.1 will give this O_3 concentration increment. The increment of NO_2 during the next year could be a result of many things including a good wet season resulting in vegetation growth and increased bio-geogenic activity, soil-particle rain produced NO_2 emissions as well as NO_2 produced through electric storms which is frequent during a wet season. It is clear that both these gases are emitted in large quantities and constant relative ratio from large industries close to this site. The NO_2 concentration at the Louis Trichardt site is about three times lower than at Amersfoort (Table 4.2), but seems to follow the same monthly trend. The NO_2 concentrations at Cape Point are the second highest after

Amersfoort. The industrial and informal settlements found in the Cape Town region can account for these concentrations. The amount of vehicles in close proximity of the Cape Point site may also be responsible for the higher concentrations of NO_2, as it is a popular tourist destination. None of the other sites has a high density of vehicles in close proximity to be considered as an influence.

The mean monthly O_3 concentrations ranged from a minimum of 10 ppb at Amersfoort to a maximum of 57 ppb at Louis Trichardt. The total mean O_3 concentration over the period 1994-2005 was relatively constant and below 30 ppb (Table 4.2) for all the sites except Louis Trichardt, where a concentration of 35 ppb was observed. It is well known that ozone and nitrogen dioxide concentration ratio is dependant on each other. It follows from Figure 4.2 and Figure 4.3 that high NO_2 levels coincide with higher O_3 levels. At Louis Trichardt the O_3 concentrations are higher than at Amersfoort due to less direct plume effects. At Louis Trichardt, the high O_3 could be a result of both transport and production of ozone within transported plumes containing large amounts of NO_2 and CO from biomass burning, as described in Paragraphs 2.3.1.2 and 3.1. The large industries located in close proximity to the Amersfoort site are responsible for the lower O_3 concentrations at this site as NO_2 removes O_3 during both the day and night (Paragraph 2.3.1.4) as well as chemical reactions with SO_2 and H_2S (Paragraph 2.3.1.2) all of which are produced in large quantities in this region, as previously mentioned.

Mean monthly NH_3 concentrations ranged from a minimum of 0.4 ppb (Amersfoort) to a maximum of 7.2 ppb at Cape Point (Figure 4.4). The total mean NH_3 concentration over the period 1994-2005 was relatively constant and below 1.5 ppb (Table 4.2) for all the sites. The sites at Cape Point and Okaukuejo had slightly higher NH_3 concentrations that can only be explained by bird droppings, which is a known source of NH_3. Large quantities of bird colonies are found along the coastline where the Cape Point site is located. The same reason can be given for Okaukuejo, but here the site is located next to a large salt lake where large colonies of flamingos nest each year as well as the nearby coastline, which may also have an effect on the concentrations.

The mean annual HNO_3 concentrations were below 1.0 ppb (Table 4.2) for all the sites during the study period, and ranged from a mean monthly minimum concentration of 0.1 ppb at Louis Trichardt and Okaukuejo to a maximum of 2.5 ppb at Amersfoort and Cape Point (Figure 4.5). Paragraph 2.3.1.4 describes how nitric acid

is produced by NO_x and Table 4.2 shows how the HNO_3 is correlated to the NO_2 concentrations

The relatively large fluctuations in the Amersfoort data set (Appendix A) are probably due to the direct influence of industrial pollution plumes at this site. The relatively large concentration differences clearly indicate the large anthropogenic effect at this site.

4.6 Gaseous deposition estimates

The gaseous deposition rate (flux) is a product of ambient gas concentration and deposition velocity, which is specific for each gas and the region of deposition. In this study, a total of five different gas species were monitored at four different sites (regions). The dry deposition velocities at the four sites were calculated using a revised parameterisation model for gaseous dry deposition developed by *Zhang et al.*[232] The three-leaf resistance model is improved in this model to include non-stomatal resistance.

For the Amersfoort and Louis Trichardt sites, the SO_2 dry deposition velocities calculated by *Zunckel*[13] for the sites of Elandsfontein and Blyde were used as they are situated within a hundred kilometres radius of Amersfoort and Louis Trichardt, respectively. Zunckel used the SO_2 concentration collected data and incorporated the micro-meteorological conditions of each of the regions within an inferential model, as described in Paragraph 2.5, to calculate SO_2 deposition velocities. The dry deposition velocities of SO_2, as calculated by *Zunckel,*[13] were used and extended to the other gas species of interest using the revised model of *Zhang et al.,*[232] which is based on vegetation cover and applied to the different regions of the sites.

No deposition velocities could be found for the Cape Point and Okaukuejo sites. The same SO_2 deposition velocity values as calculated by *Zunckel*[13] for the Elandsfontein site were used as the deposition velocities for the Cape Point site. The summer and winter velocities were switched to compensate for more turbulent and active vegetation conditions prevailing during winter at this site. For Okaukuejo, which is situated within a desert region, the same deposition values used by *Zang et al,*[232] were used, as Zang provided deposition velocities for desert regions. Meteorological conditions may result in a difference of 15 to 35% in deposition rates of species between winter and summer days, with higher summer values mostly due to increased solar radiation,[13] isolation, and greater turbulence and photosynthetically

active vegetation. It was therefore important to adjust these values accordingly, which was done for all the selected sites to include separate velocities for both winter and summer periods. The estimated summer and winter deposition velocities for the monitored trace gases at the four sites are presented in Table 4.3.

Table 4.3: The deposition velocities ($cm.s^{-1}$) for winter and summer for SO_2 at AF, LT and CP after *Zunckel,*[13] NA after *Zang et al.,*[232] and the rest of the gaseous species after a combination of both authors for all the different sites.

	LT	AF	CP	NA
SO_2 (W)	0.39	0.18	0.27	0.13
SO_2 (S)	0.45	0.27	0.18	0.20
NO_2 (W)	0.34	0.11	0.21	0.13
NO_2 (S)	0.40	0.16	0.14	0.20
O_3 (W)	0.39	0.11	0.23	0.13
O_3 (S)	0.45	0.16	0.15	0.20
HNO_3 (W)	1.84	0.45	0.77	0.13
HNO_3 (S)	2.15	0.68	0.51	0.20
NH_3 (W)	0.47	0.19	0.35	0.07
NH_3 (S)	0.55	0.29	0.23	0.10

W = Winter; S = Summer; AF = Amersfoort; LT = Louis Trichardt; CP = Cape Point; NA = Okaukuejo

Using average mean monthly concentrations of each gas species during the time period 1995-2005, the mean average deposition flux for each month of the year was calculated using summer deposition velocities for the months November to April and winter deposition velocities for the months May to October. The monthly deposition results for SO_2; NO_2; O_3; NH_3 and HNO_3 are given in Tables 4.4-8.

Table 4.4: Total estimated monthly dry deposition values ($kg.ha^{-1}$) of S in SO_2 at the selected sites for 1995 to 2005

Month	AF	LT	CP	NA
January	0.232±0.073	0.074±0.037	0.048±0.037	0.031±0.021
February	0.269±0.103	0.077±0.044	0.032±0.009	0.030±0.016
March	0.109±0.036	0.045±0.019	0.045±0.038	0.028±0.012
April	0.204±0.034	0.122±0.095	0.066±0.044	0.027±0.021
May	0.183±0.055	0.110±0.045	0.055±0.018	0.018±0.007
June	0.180±0.069	0.157±0.080	0.056±0.028	0.018±0.011
July	0.189±0.063	0.103±0.070	0.044±0.014	0.017±0.009
August	0.197±0.060	0.094±0.076	0.047±0.018	0.017±0.005
September	0.155±0.072	0.136±0.101	0.041±0.022	0.042±0.027
October	0.193±0.085	0.042±0.022	0.056±0.032	0.031±0.016
November	0.242±0.109	0.062±0.024	0.081±0.064	0.032±0.017
December	0.247±0.110	0.067±0.040	0.035±0.019	0.042±0.016

It follows from Table 4.4 that the Amersfoort and Okaukuejo sites have higher SO_2 deposition values during the warmer months of the year that can be ascribed to the higher deposition velocities (Table 4.3), as a direct result of higher summer solar radiation.[12] The deposition of SO_2 is higher during the winter months only for the Louis Trichardt site. This is probably due to the fact that the difference between the actual deposition velocities for the summer and winter months at the Louis Trichardt site is small. The high SO_2 concentrations during winter counter-balance the lower deposition velocities. The higher deposition values at Cape Point during the winter months, on the other hand, are due to the higher deposition velocities during winter. Dry deposition of SO_2 is mainly determined by its deposition velocity as is evident from the monthly data in Table 4.4. This deposition velocity trend remains the same

for the gases of NO_2, O_3, NH_3 and HNO_3 as discussed in the following paragraphs. The deposition velocities of each month are assigned according to season and the concentration differences between months are too small to have a visible effect on the gases monthly deposition rates. There are exceptions were concentrations are high enough to effect deposition rates which is discussed.

Table 4.5: Estimated monthly dry deposition values ($kg.ha^{-1}$) of N in NO_2 at the selected sites for 1995 to 2005

Month	AF	LT	CP	NA
January	0.046±0.021	0.036±0.019	0.012±0.004	0.015±0.003
February	0.052±0.018	0.037±0.029	0.016±0.003	0.010±0.005
March	0.057±0.029	0.046±0.044	0.031±0.018	0.014±0.006
April	0.041±0.015	0.031±0.012	0.030±0.015	0.008±0.003
May	0.041±0.012	0.043±0.029	0.050±0.023	0.012±0.009
June	0.041±0.009	0.032±0.010	0.064±0.024	0.005±0.002
July	0.041±0.011	0.050±0.024	0.066±0.015	0.005±0.002
August	0.053±0.023	0.039±0.018	0.045±0.015	0.006±0.003
September	0.045±0.019	0.050±0.012	0.028±0.011	0.007±0.003
October	0.066±0.022	0.047±0.017	0.022±0.006	0.008±0.005
November	0.080±0.021	0.046±0.018	0.011±0.004	0.009±0.003
December	0.062±0.027	0.047±0.012	0.012±0.005	0.012±0.005

The estimated dry deposition values of NO_2 for the Amersfoort and Okaukuejo sites follow a similar monthly pattern as SO_2 with higher depositions values during the warmer months, as shown in Table 4.5. Only Cape Point has higher NO_2 deposition values during the winter months and this is due to the higher deposition velocities. No

real trend between the different months of the year at the Louis Trichardt site is observed due to the same reasons given for SO_2 at this site.

Table 4.6: Estimated monthly dry deposition values ($kg.ha^{-1}$) of O_3 at the selected sites for 1995 to 2005.

Month	AF	LT	CP	NA
January	2.38±0.48	7.16±1.21	1.56±0.43	2.83±1.13
February	2.18±0.62	5.33±2.03	1.56±0.39	2.16±0.43
March	1.58±0.36	6.70±2.10	2.02±0.81	2.34±0.56
April	1.76±0.56	7.70±2.19	2.18±0.72	2.02±0.60
May	1.22±0.32	6.62±1.43	3.15±1.04	1.43±0.29
June	1.15±0.27	6.29±1.91	4.03±0.85	1.57±0.37
July	1.31±0.24	8.34±1.53	3.85±0.70	1.57±0.35
August	1.81±0.56	6.65±1.32	3.75±0.39	1.67±0.30
September	1.83±0.21	7.51±1.45	3.32±0.53	1.87±0.41
October	2.62±0.41	7.81±1.68	3.93±0.85	1.75±0.48
November	2.72±0.67	8.51±2.22	2.10±0.84	2.61±0.48
December	2.68±0.82	8.23±2.02	2.08±0.83	3.71±1.37

Table 4.6 shows the similar higher O_3 deposition values during the warmer months at Amersfoort and Okaukuejo that are mainly due to the higher deposition velocities and slightly higher O_3 concentrations found during the summer months. The Cape Point site shows higher deposition values during the winter months that can be ascribed to the higher deposition velocities given to this site during winter months. The higher deposition values during the warmer months at the Louis Trichardt site are not as obvious as for the other sites although they do exist. This is also due to the high O_3

concentrations at this site with a dominant influence over the deposition velocities when it comes to the estimated deposition values.

Table 4.7: Estimated monthly dry deposition values ($kg.ha^{-1}$) of N in NH_3 at the selected sites for 1995 to 2005.

Month	AF	LT	CP	NA
January	0.045±0.033	0.100±0.065	0.060±0.033	0.029±0.010
February	0.045±0.036	0.079±0.042	0.073±0.037	0.021±0.010
March	0.050±0.025	0.075±0.038	0.086±0.042	0.031±0.019
April	0.029±0.019	0.064±0.035	0.056±0.031	0.021±0.017
May	0.017±0.010	0.058±0.030	0.112±0.040	0.014±0.010
June	0.031±0.017	0.055±0.027	0.084±0.031	0.015±0.009
July	0.033±0.016	0.069±0.034	0.086±0.038	0.015±0.009
August	0.040±0.016	0.109±0.059	0.135±0.039	0.011±0.004
September	0.040±0.026	0.094±0.074	0.101±0.042	0.015±0.003
October	0.046±0.026	0.081±0.058	0.109±0.052	0.019±0.007
November	0.046±0.025	0.126±0.066	0.069±0.033	0.022±0.009
December	0.042±0.032	0.092±0.038	0.049±0.024	0.018±0.008

The estimated dry deposition values for NH_3 in Table 4.7 show higher values during the warmer summer months for all the sites except the Cape Point site. The higher summer deposition is directly related to the higher deposition velocity values during the summer months at all the sites, as the concentrations during the different months do not vary much. The reason for the higher deposition estimates at the Cape Point site during winter is due to the higher deposition velocity at this site during the winter months as well as the fact that the NH_3 concentration remains more or less the same throughout the year.

Table 4.8: Estimated monthly dry deposition values ($kg.ha^{-1}$) of N in HNO_3 at the selected sites for 1995 to 2005.

Month	AF	LT	CP	NA
January	0.137±0.135	0.151±0.150	0.047±0.047	0.003±0.003
February	0.118±0.117	0.030±0.030	0.013±0.013	0.012±0.011
March	0.083±0.081	0.081±0.081	0.023±0.023	0.012±0.012
April	0.134±0.132	0.075±0.074	0.017±0.017	0.003±0.003
May	0.033±0.033	0.065±0.065	0.041±0.041	0.003±0.003
June	0.035±0.034	0.050±0.049	0.050±0.050	0.002±0.002
July	0.036±0.036	0.105±0.105	0.072±0.072	0.003±0.003
August	0.064±0.063	0.115±0.115	0.148±0.148	0.010±0.010
September	0.035±0.035	0.060±0.059	0.147±0.147	0.009±0.008
October	0.062±0.061	0.062±0.062	0.090±0.090	0.012±0.011
November	0.124±0.122	0.112±0.111	0.064±0.064	0.008±0.007
December	0.079±0.078	0.055±0.055	0.026±0.026	0.012±0.011

The estimated dry deposition values for HNO_3 in Table 4.8 show higher values during the warmer summer months for the sites of Amersfoort and Okaukuejo. The higher summer deposition values are largely due to the higher deposition velocities during the summer months. The reason for the higher deposition values at the Cape Point site during the winter months is due to the higher deposition velocities during the winter months. The deposition estimates for the Louis Trichardt site show no clear trend as is the case with other gases.

The average mean monthly depositions for the period 1995-2005 were added together to estimate the average annual deposition for all the gaseous species at all four sites and are provided in Table 4.9. The strong influence of the concentration on the mean

annual deposition values when calculated using the inferential method is again evident in Table 4.9, when compared with the initial concentrations in Table 4.2.

Table 4.9: Total estimated annual dry deposition values of N from NO_2, NH_3 and HNO_3 and S from SO_2 and O_3 in $kg.ha^{-1}.y^{-1}$.

	SO_2	NO_2	O_3	NH_3	HNO_3
AF	2.4±0.9	0.6±0.2	23±5	0.5±0.3	0.9±0.5
LT	1.1±0.7	0.5±0.2	87±21	1.0±0.6	1.0±0.3
CP	0.6±0.3	0.4±0.2	33±8	1.0±0.4	0.7±0.4
NA	0.3±0.2	0.1±0.1	25±7	0.2±0.1	0.1±0.1

Amersfoort has the highest deposition value of sulphur from SO_2 of 2.4 $kg.ha^{-1}.y^{-1}$ followed by Louis Trichardt, Cape Point and Okaukuejo and decreasing in deposition values as the concentration decreases for the sites in that order. Only the deposition value at Louis Trichardt seems to be high in comparison with its ambient concentration and this is due to the higher deposition velocities used for this site.[13] The deposition values for NO_2 follow the same trend, with the higher deposition values found at the sites with the higher concentrations with Amersfoort having the highest deposition of nitrogen from NO_2 of 0.62 $kg.ha^{-1}.y^{-1}$ followed by Louis Trichardt, Cape Point and Okaukuejo. A clear concentration gradient is therefore observed according to the distance from large point sources as described by *Zunckel et al.*[13,192] The deposition estimates found for nitrogen from NO_2 in comparison to the actual concentration gradient found between the sites are not as pronounced as for SO_2. This is mainly due to the fact that the deposition velocities used here are a combination of the values of *Zunckel*[13] and *Zang et al.*[232] (Table 4.3). In this model, vegetation (e.g. non-stomatal resistance parameterisation) plays a more important role resulting in higher deposition velocities.

The deposition of O_3 shows a very high deposition value of 87 $kg.ha^{-1}.y^{-1}$ for Louis Trichardt. No strong seasonal trend is observed at Amersfoort and Cape Point, which has the same ambient O_3 concentrations. The high deposition value at Cape Point is directly related to the higher deposition velocities (Table 4.3). This is also the reason for the higher deposition value found at Okaukuejo. The accumulation of average deviation also factor into the higher annual deposition rate, as higher deviations lead to higher annual depositions, as can be seen in Table 4.9 for O_3, as well as all the

other gaseous species. From the deposition results thus far it is clear that the precision used (incorporating meteorological and vegetation parameters) when calculating deposition velocities is of great importance when the ambient concentrations are not very high (far from point sources). The deposition estimates of nitrogen from NH_3 in Table 4.9 are largely determined by the deposition velocities rather than the actual concentrations of ambient NH_3 concentrations. This is evident as both Cape Point and Okaukuejo have the same NH_3 concentrations, but with Cape Point having a much higher nitrogen deposition value, which is mainly determined by its higher deposition velocity. The deposition value of 1.02 $kg.ha^{-1}.y^{-1}$ for Cape Point is very close to the 0.99 $kg.ha^{-1}.y^{-1}$ of Louis Trichardt, with a lower NH_3 concentration, and is ascribed to higher deposition velocities (Table 4.3) as well as larger cumulative averaged deviations.

From Table 4.9, the highest deposition of nitrogen from HNO_3 is found at Louis Trichardt, which has the lowest HNO_3 ambient concentration. This shows the dominant influence of higher deposition velocities on the deposition of HNO_3 as derived from *Zang et al.*[232] and enhanced by the meteorological parameters of the region by *Zunckel.*[13] This results in the highest deposition of nitrogen from HNO_3 at Louis Trichardt followed by Amersfoort, where the deposition is largely determined by the much higher HNO_3 concentration. Cape Point and Okaukuejo have lower deposition values due to a combination of lower concentrations and deposition velocities. From Table 4.9 it is evident that the final deposition estimates are dominated by the concentration of the species if it is in an excess (close to a source) e.g. SO_2 and NO_2 at the Amersfoort site, which is located within the region of several point sources. When the concentration is not in excess, as the sites are further removed from point sources, the deposition velocities themselves become the dominating factors in estimating depositions. Parameters determining the deposition velocities also become more important and factors like higher annual solar radiation, a convective boundary layer as well as more consistent active vegetation throughout the year,[13] result in higher deposition velocities, especially in the case of Louis Trichardt (Table 4.3).

Average dry deposition values of 10.9 and 3.36 $kg.ha^{-1}.y^{-1}$ for sulphur from SO_2 were determined by *Zunckel*[13] at Elandsfontein and Blyde, respectively. Average dry deposition values of 2.40 $kg.ha^{-1}.y^{-1}$ and 1.09 $kg.ha^{-1}.y^{-1}$ for sulphur from SO_2 were determined in this study for Amersfoort and Louis Trichardt, respectively. As the same

deposition velocities for Elandsfontein and Blyde were used for Amersfoort and Louis Trichardt, respectively (as previously described in Paragraph 4.5), the only difference in deposition values can be attributed to the species concentrations. This is also true for this study where the SO_2 concentration as measured at Elandsfontein for comparison purposes as mentioned in Paragraph 3.5.6 by *Dhammapala*[56] and *Martins et al.,*[221] was approximately four times higher at Elandsfontein than the Amersfoort site for the same sampling period. This then also results in an almost four times higher deposition value for sulphur from SO_2. The deposition value of sulphur from SO_2 at Blyde compared to Louis Trichardt is 3.36 $kg.ha^{-1}.y^{-1}$ and 1.09 $kg.ha^{-1}.y^{-1}$, respectively. The difference can be explained by the concentration difference of SO_2 between the two sites with Blyde having an average annual concentration of 1.5 ppb[13] and Louis Trichardt having an annual concentration of 0.8 ppb (Table 4.2). This results in the SO_2 concentrations almost being halved between the sites and directly relates to the annual deposition between the sites being more than halved. In addition, *Zunckel*[13] reported that with increasing distance from the point source (e.g. decreasing SO_2 concentration), the SO_2 deposition flux will decrease by 65% in winter and 75% in summer from Elandsfontein to Palmer situated 150 km apart. The Louis Trichardt site is situated an additional 100 km away from the effective point sources.

The reported annual dry deposition rates for sulphur at Palmer and Blyde (*Zunckel*[13]) are similar to those reported for the CASTNet sites by *Clarke et al.,*[124] which are regionally representative and well removed from major cities and point sources in the United States. At these sites, deposition is determined by the US Environmental Protection Agency (EPA) Clean Air Status and Trends Network (CASTNet) by also using the inferential technique.[124] The average total sulphur dry depositions (contribution of SO_4^{2-} included) ranged between 8.5 and 1 $kg.ha^{-1}.y^{-1}$ at the CASTNet monitoring sites located within regions that are considered free from influence of nearby sources in the United States. The SO_4^{2-} contribution to sulphur deposition, as determined by *Zunckel,*[13] contributes only 20% at Elandsfontein and 21% at Blyde of the total sulphur deposition (also determined for Amersfoort and Louis Trichardt in Chapter 5). This is relatively low compared to the CASTNet monitoring sites in the United States. More recently, *Peters et al.*[233] reported on the wet and dry deposition of sulphur and nitrogen at the Panola Mountain Research Watershed (PMRW), a forest research site 25 km southeast of Atlanta, Georgia and within 120 km of several major point sources. The inferential model estimates of annual dry sulphur and nitrogen

deposition from 1986-97 averaged 2.1 $kg.ha^{-1}$ after Phase I of Title IV of the 1990 Clean Air Act Amendments were implemented to reduce S emissions and thus decrease S depositions resulting in an annual decrease of 2.4-4.0 $kg.ha^{-1}$ for some stations.[234] The 2.4 $kg.ha^{-1}.y^{-1}$ sulphur deposition at Amersfoort minus the SO_4^{2-} contribution, and the 0.62 $kg.ha^{-1}.y^{-1}$ nitrogen deposition minus the NO_3^- contribution are still relatively low compared to these data for a site located within much closer proximity to large point sources.

CHAPTER 5

Results of aerosol measurements

In this chapter the aerosol results are given for a total of four sampling campaigns. The aerosol composition of each region is also discussed and possible sources identified. The major aerosol components are then correlated between the different sites and conclusions made about possible sources within each region. Aerosol composition is also correlated to wind trajectories and conclusions made about trans-regional aerosol transport and its influences on each region. Lastly, the dry deposition estimations of the aerosol species are made.

5.1 Introduction

The monitoring of aerosols in this study was done over a three-year period (2005-2007). A total of four campaigns were launched, including three winter campaigns and one summer campaign. The main focus was to determine the ionic- and organic content of aerosols at the selected sites. The chemical composition of the aerosols measured is used to identify potential sources within the region. The two selected sites represent two different regions in South Africa, each region with its own influences as described in the site selection in Chapter 3, Paragraph 3.1. At each site, both the ionic and carbon contents of aerosols were determined for $PM_{2.5}$ and PM_{10} as described in Chapter 2, Paragraph 2.2.2 and recommended by WMO/GAW (Chapter 3, Paragraph 3.6.2).

In this chapter, the results of all four monitoring campaigns are presented and discussed, where after deposition estimates for the ionic content of the aerosols are made.

5.2 Average aerosol composition ($PM_{2.5}$ and PM_{10}) and possible regional sources

In order to compare regions and also determine regional sources, several campaigns (mean that sampling was performed at both sites at the same time) were launched. This was done on four separate occasions (campaigns) over a three-year period, once in the summer and three times during winter. The campaigns were done at approximately the same time of the year for the winter periods in order to confirm a trend in aerosol composition and seasonal contributors. One campaign was launched during summer to compare the aerosol content between seasons and thus help to verify potential contributing sources that are season specific. The exact dates of the campaigns were 30 August to 12 September 2005 (winter); 24 July to 6 August 2006 (winter); 9 to 22 April 2007 (summer) and 5 July to 11 July 2007 (winter). A campaign duration ranged between one- and two-week periods during which samples were taken for 24 hours per sample. Four different MiniVol samplers were simultaneously operated at each site to collect filter samples to determine the $PM_{2.5}$ and PM_{10} organic and water-soluble composition. The raw data of these campaigns are given in Appendix B. The average relative carbon and water-soluble composition (determined from Appendix B) for each campaign is presented in Figure 5.1-8, followed by identifications of possible regional and trans-regional sources.

5.2.1 Identification of possible regional sources contributing to the carbonaceous aerosol composition

Aerosols that were measured within aged haze layers during the SAFARI 2000 campaign over southern African consisted of an 80% carbonaceous content (organic and elemental) and the remaining 15% consisted of sulphate and nitrogen species.[47] This, however, was done within haze layers of biomass burning plumes during the dry season and does not fully represent the typical southern Africa aerosol content. For this to happen, all the major sources contributing to aerosols must be taken into account, especially those originating from fossil fuel and other biofuel combustion processes. These combustion processes emit large quantities of carbonaceous and other trace species that play a significant role in aerosol chemistry.

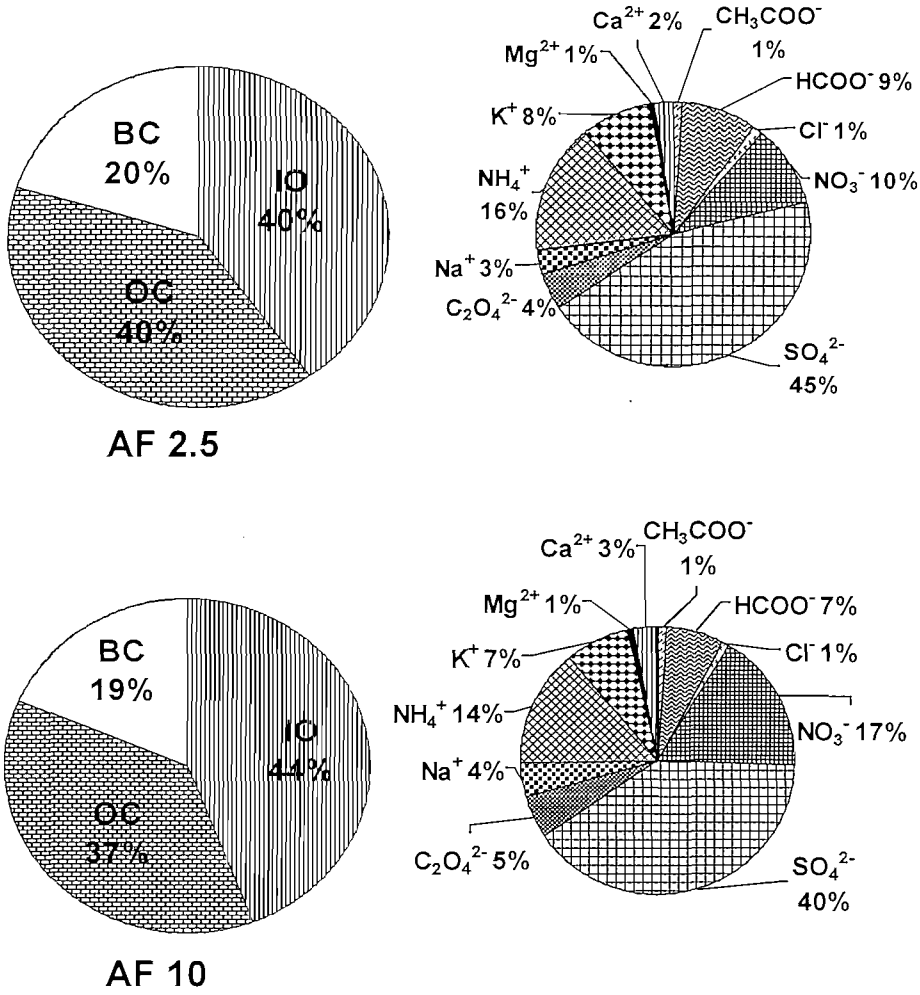


Figure 5.1 *Average relative BC, OC and IO aerosol composition for $PM_{2.5}$ and PM_{10} at Amersfoort (AF) for 30 August to 12 September 2005 (IO = inorganic + organic water-soluble; BC = elemental carbon; OC = organic carbon)*

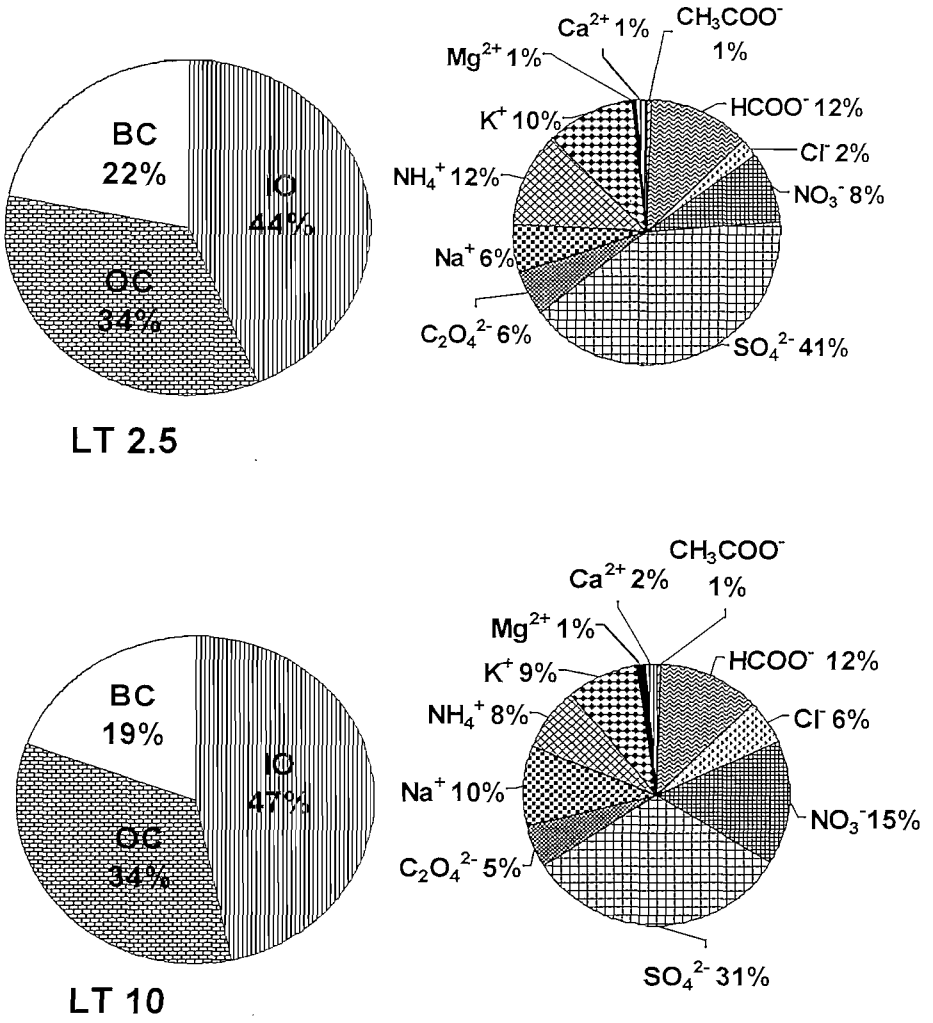


Figure 5.2 *Average relative BC, OC and IO aerosol composition for $PM_{2.5}$ and PM_{10} at Louis Trichardt (LT) for 30 August to 12 September 2005 (see Fig. 5.1 for abbreviations)*

In Figures 5.1-8 the carbonaceous content of the aerosol at the two representative sites ranges between 43% and 65% in the dry season and 27% and 36% for the summer season. All the ambient measurements were taken at ground level (± 1.5 meter above the surface). The relative percentage of the main species appears to be fairly similar within the same season. This could indicate possible similar source influences and will be discussed in more detail later in this chapter. The ratio of organic carbon (OC) to elemental carbon (BC) is slightly different between sites per season as well as even smaller differences for the two particle sizes at each site. This is most probably due to the carbon content of the aerosol that depends on the regional

source influences. In this study we attempted to validate this statement by using methods similar to the ones used by *Guazzotti et al.*[235] Guazzotti used aerosol measurements to obtain its content in order to discriminate between the possible sources contributing to the carbonaceous content of aerosols. This mainly involves the major sources of carbon emissions, such as biofuel (industrial processes and biomass burning with incomplete combustion) and fossil fuel (complete combustion processes such as energy production with coal) combustion. The method is based on the assumption that K^+ is a tracer of biomass burning in the particulate phase where it is released during the combustion of plant matter. This is used together with BC, which is a good tracer for incomplete combustion processes of bio- and fossil fuel in the particle phase.[236] Hence, the application of the nss K^+/BC ratios will theoretically indicate the type of combustion responsible for the carbon content of the aerosol.

The nss K^+/BC ratio was also applied to the four sampling campaigns of this study and the results are provided in Table 5.1.

Table 5.1 The nss K^+/BC ratio of the average aerosol composition of each campaign

Campaign	AF $PM_{2.5}$	AF PM_{10}	LT $PM_{2.5}$	LT PM_{10}
30 August - 12 September 2005	0.16	0.18	0.21	0.21
24 July - 6 August 2006	0.21	0.31	0.34	0.42
9 April - 22 April 2007	0.08	0.08	0.04	0.09
5 July - 11 July 2007	0.07	0.13	0.11	0.09

The nss K^+/BC ratio of Amersfoort compares well to the 0.18 ratio found at the Arabian Peninsula site during the INDOEX experiment. The Peninsula site, like Amersfoort, is a site primarily influenced by fossil fuel combustion within its proximity. This is a good result for the region of Amersfoort where fossil fuel combustion processes (complete combustion) dominate, as Amersfoort lies within a coal energy producing region, as described in Chapter 3, Paragraph 3.1. In most of the other nss K^+/BC ratios, Louis Trichardt has higher values than Amersfoort during the dry winter season. The differences in these ratios are also greater in the smaller particle sizes ($PM_{2.5} < PM_{10}$).[236] This all indicates that the sources contributing to the carbon content at Louis Trichardt are of a more incomplete biomass, biofuel combusting nature during winter. The higher ratios for Louis Trichardt are also a good result, as biomass burning (incomplete combustion) is more frequent during the dry season within and around

this region. The Louis Trichardt region is also influenced by across-border biomass burning activities to the north as described in Chapter 3, Paragraph 3.1.[198,200] The different source contributions are further justified by this ratio through the summer campaign, which shows the ratio at the Louis Trichardt site to be equal to that of Amersfoort. This could possibly suggest the absence of the biomass burning contribution during summer periods in Louis Trichardt and neighbouring regions. The large differences between the ratios for the winter and summer campaigns show the important role biomass burning plays in aerosol formation during the dry season in Africa. The ratios show an actual higher value for the $PM_{2.5}$ at Amersfoort than Louis Trichardt during the summer campaign. This could possibly be the result of carbonaceous aerosols transported from neighbouring urban regions with large petrochemical industries (incomplete coal combustion). This is not noticeable during winter periods when it is overwhelmed by the excessive biomass/biofuel contribution. The ratios also shows a huge difference between summer and winter for Amersfoort and this is due to Soweto one of the biggest informal settlements in the world where large amounts of incomplete combustion during cold winter months take place directly upwind of Amersfoort.

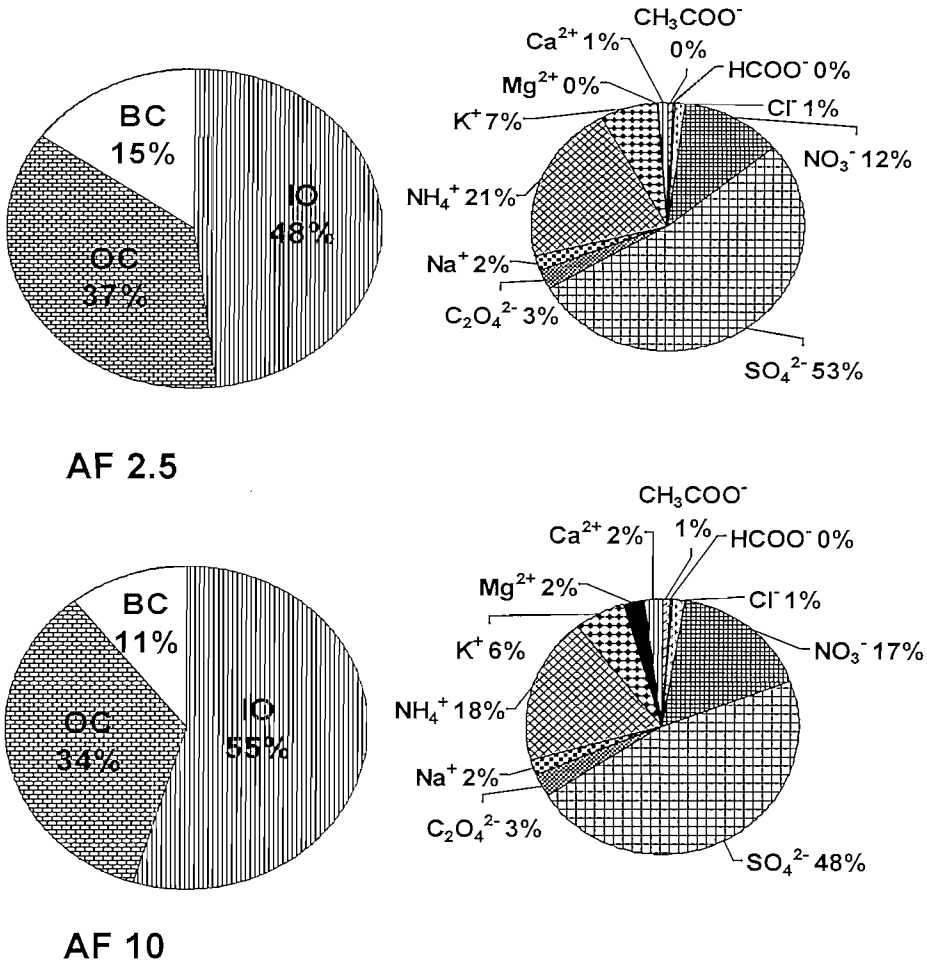


Figure 5.3 *Average relative BC, OC and IO aerosol composition for $PM_{2.5}$ and PM_{10} at Amersfoort (AF) for 24 July - 6 August 2006 (see Fig. 5.1 for abbreviations)*

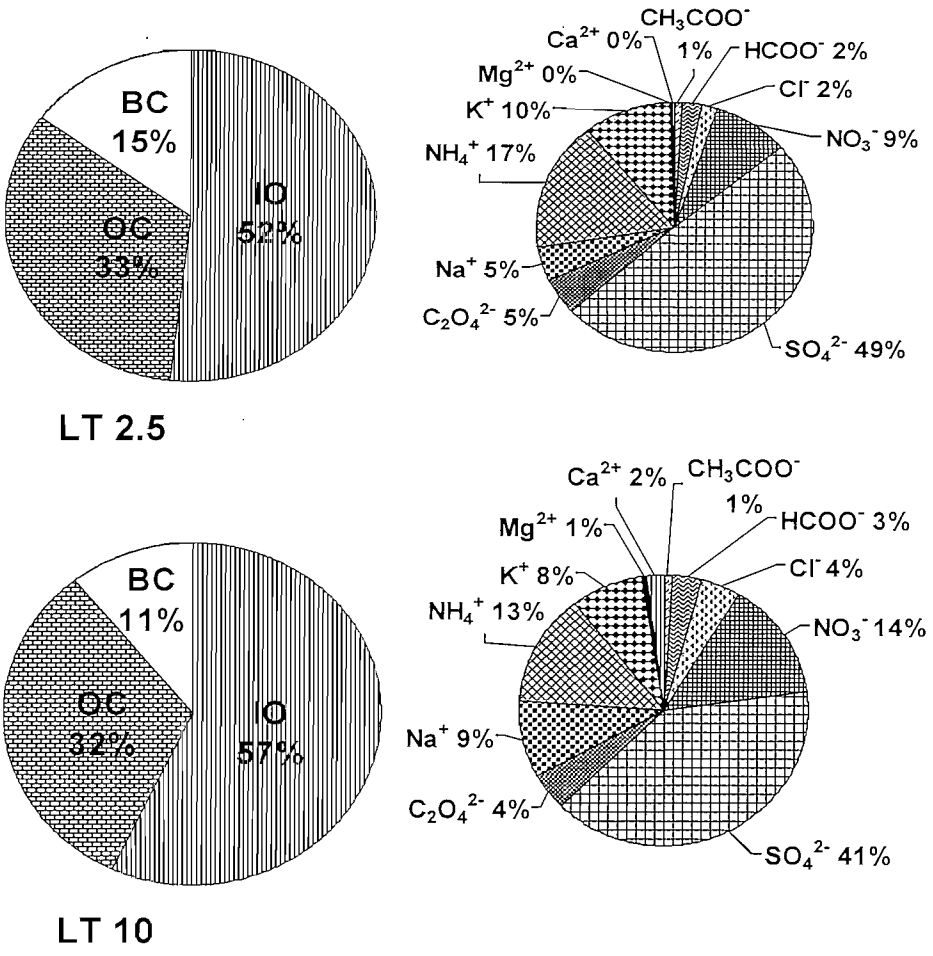


Figure 5.4 *Average relative BC, OC and IO aerosol composition for $PM_{2.5}$ and PM_{10} at Louis Trichardt (LT) for 24 July - 6 August 2006 (see Fig. 5.1 for abbreviations)*

The possible sources contributing to the carbonaceous aerosol composition of a region can be further identified by the BC/OC ratio which is characteristic of the aerosol measured. Reddy and Venkatarama found BC/OC ratios to range between 0.18-0.27 for fossil fuel and 0.08-0.22 for biomass/biofuel combustion processes, by using the emission data inventory from India.[237] If this BC/OC ratios are calculated for the four sampling campaigns of this study, the results provided in Table 5.2 were obtained.

Table 5.2 The BC/OC ratio of the average aerosol composition of each of the sampling campaigns

Campaign	AF $PM_{2.5}$	AF PM_{10}	LT $PM_{2.5}$	LT PM_{10}
30 August - 12 September 2005	0.50	0.49	0.64	0.57
24 July - 6 August 2006	0.42	0.32	0.45	0.33
9 April - 22 April 2007	0.51	0.50	0.42	0.37
5 July - 11 July 2007	0.54	0.57	0.49	0.56

For the dry seasons of 2005 – 2007, the BC/OC ratios in this study ranged between 0.32-0.64. This is rather high compared to the same ratios determined by *Andreae and Merlet*[42], which ranged between 0.07-0.3 for various types of biomass and biofuel combustion processes. However, *Guazzotti et al.*[235] determined these ratios to be between 0.22-1.61 during the INDOEX experiment. They ascribed these high values to elemental carbon from incomplete fossil fuel combustion processes in rural regions.[238] In this study, the highest ratios are present at the Louis Trichardt site, and for $PM_{2.5}$ specifically. The ratio differences between the sites are also steadily decreasing from 2005 up to 2007, at which point a higher ratio is present at the Amersfoort site during both the winter and summer campaigns. This high ratio of 0.32-0.57 at the Amersfoort site can also be ascribed to higher elemental carbon concentrations of incomplete combustion processes of biofuels/fossil fuels from petroleum industries/coal. These sources are located in and around Johannesburg and the Vaal Triangle, which are both located upwind from this site. The higher values at the Louis Trichardt site during 2005-2006 are possibly the BC being transported over this Amersfoort region along a circulation pathway to the Louis Trichardt region (these circulation pathways will be discussed later in this Chapter). Once the aerosol reaches the Louis Trichardt region, it gets supplemented with added BC from the increased biomass burning activities in this region. The higher values during the dry season of 2007 at the Amersfoort site are most probably due to the changing circulation pattern of aerosol transport between the sites. During August, meteorological conditions favour transport over the continent, while the aerosol gets transported over the ocean in July. This will be discussed in more detail later in this chapter.

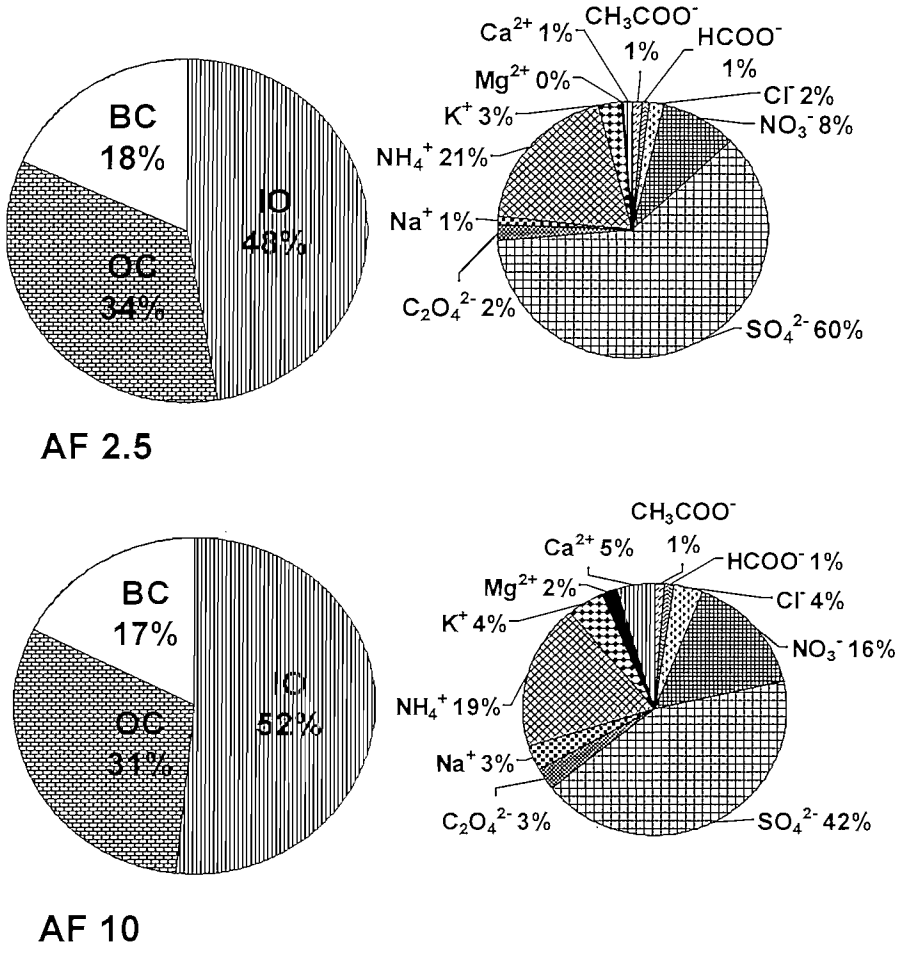


Figure 5.5 *Average relative BC, OC and IO aerosol composition for $PM_{2.5}$ and PM_{10} at Amersfoort (AF) for 5-11 July 2007 (see Fig. 5.1 for abbreviations)*

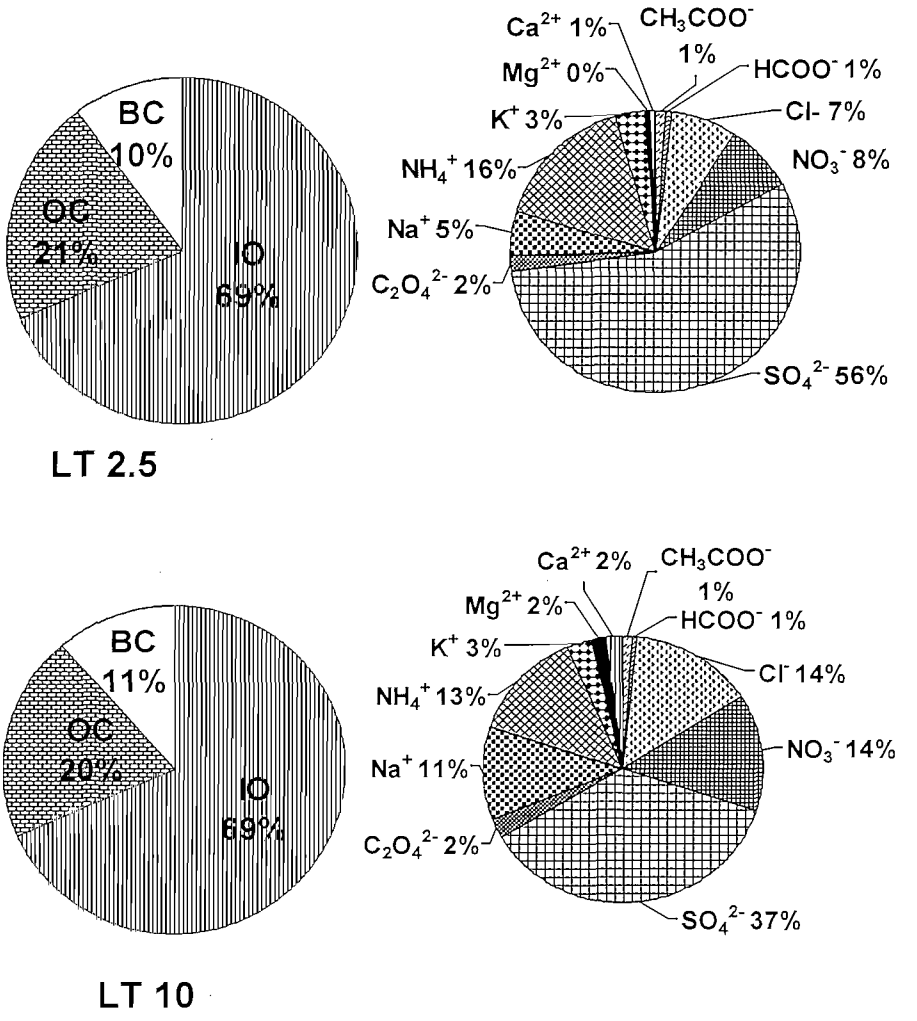


Figure 5.6 *Average relative BC, OC and IO aerosol composition for $PM_{2.5}$ and PM_{10} at Louis Trichardt (LT) for 5-11 July 2007 (see Fig. 5.1 for abbreviations)*

Another method where the aerosol content can be used to identify possible sources contributing to the carbonaceous content of the aerosol, is with the nss SO_4^{2-}/BC ratio.[235] With this method, the sulphate concentration was used as a tracer for fossil fuel combustion, as only a very small amount of it is emitted during biofuel/biomass burning.[181, 238] These ratios were calculated for the four sampling campaigns of this study and the results are provided in Table 5.3.

Table 5.3 The nss SO_4^{2-}/BC ratio of the average aerosol composition of each of the sampling campaigns

Campaign	AF $PM_{2.5}$	AF PM_{10}	LT $PM_{2.5}$	LT PM_{10}
30 August - 12 September 2005	0.88	0.97	0.80	0.76
24 July - 6 August 2006	1.64	2.32	1.69	2.10
9 April - 22 April 2007	4.15	3.45	5.43	1.23
5 July - 11 July 2007	1.55	1.25	1.99	1.26

The sulphate species in the particulate form are not only a tracer for fossil fuel combustion, but also an indicator of direct SO_2 emissions. It can also be an indication of an aerosol age.[235] The aging effect was also evident in this study and will be discussed using the above ratios. For the 2005-2006 dry seasons, a higher SO_4^{2-} content at the Amersfoort site is present and this is a direct result of the high amount of fossil fuel combustion of this region. However, the PM_{10} ratio was higher than the $PM_{2.5}$ at the Amersfoort site itself suggesting that this aerosol was possibly already an aged aerosol. These aerosols possibly came from other combustion point sources in nearby surrounding regions transported to the Amersfoort region. This can be confirmed by the fact that Amersfoort is mostly down wind from the industrial activities of the Mpumalanga Highveld, which is densely populated by power generation plants. The PM_{10} aerosol at Louis Trichardt did not show the same aging effect; in fact the smaller ratios show no fossil fuel influences of nearby regions. It is interesting to note that the values of the $PM_{2.5}$, which is the aerosol size that travels the furthest, are similar for each site within the same sampling periods. This could possibly be regarded as partial proof of the cross-regional transport theory as this represents average values for this period. The higher ratios for $PM_{2.5}$ compared to PM_{10} at the Amersfoort site during summer, could indicate that the sources contributing to the major aerosol load in this region are local. The lower ratio for PM_{10} compared to $PM_{2.5}$ during summer also suggests that unstable meteorological conditions during this season prevent aging. The ratio for $PM_{2.5}$ at Louis Trichardt is slightly higher than that found at Amersfoort. This is due to the transported aerosols being supplemented in this region with alternative sources of incomplete biofuel combustion. This was proven seeing as biofuel burning was found to be a dominant contributor to regional SO_2 emissions in developing countries.[239]

5.2.2 Possible regional sources contributing to the ionic aerosol composition

The inorganic and organic water-soluble species (IO = ionic content) in Figures 5.1-8 range between 40 % and 67%, and 44% and 69% for the $PM_{2.5}$ aerosol of Amersfoort and Louis Trichardt, respectively; while they range between 44% and 64%, and 47% and 77% for the PM_{10} aerosol of Amersfoort and Louis Trichardt, respectively. There is a definitive difference in the IO content of the $PM_{2.5}$ and PM_{10} aerosols at each site and between sites. This difference in IO content is most probably due to aerosol aging processes as more volatile carbon species are being replaced by certain less volatile inorganic species. This is also evident from the aerosol composition reaching Louis Trichardt as it is transported over regions with high anthropogenic activities. Despite the aging effect, which is also evident at the Amersfoort site, SO_4^{2-} and NH_4^+ dominate the IO content in the $PM_{2.5}$ aerosol. These species are characteristic of anthropogenic sources within the region, which will be discussed in more detail later, since it is a characteristic of this region. The theory of aerosol aging during transport is validated by the NO_3^- concentrations that are consistently higher for PM_{10} than $PM_{2.5}$ aerosols at each site. This is due to the fact that NO_3^-, within the bigger and probably older aerosol, is attracted to the less acidic coarse mode of the aerosol during heterogeneous transformation processes (Chapter 2, Paragraph 2.6). The high SO_4^{2-} composition of these aerosols also elevates the acidity within these aerosols and thus encourages heterogeneous processes like the preceding one during long-range transport.

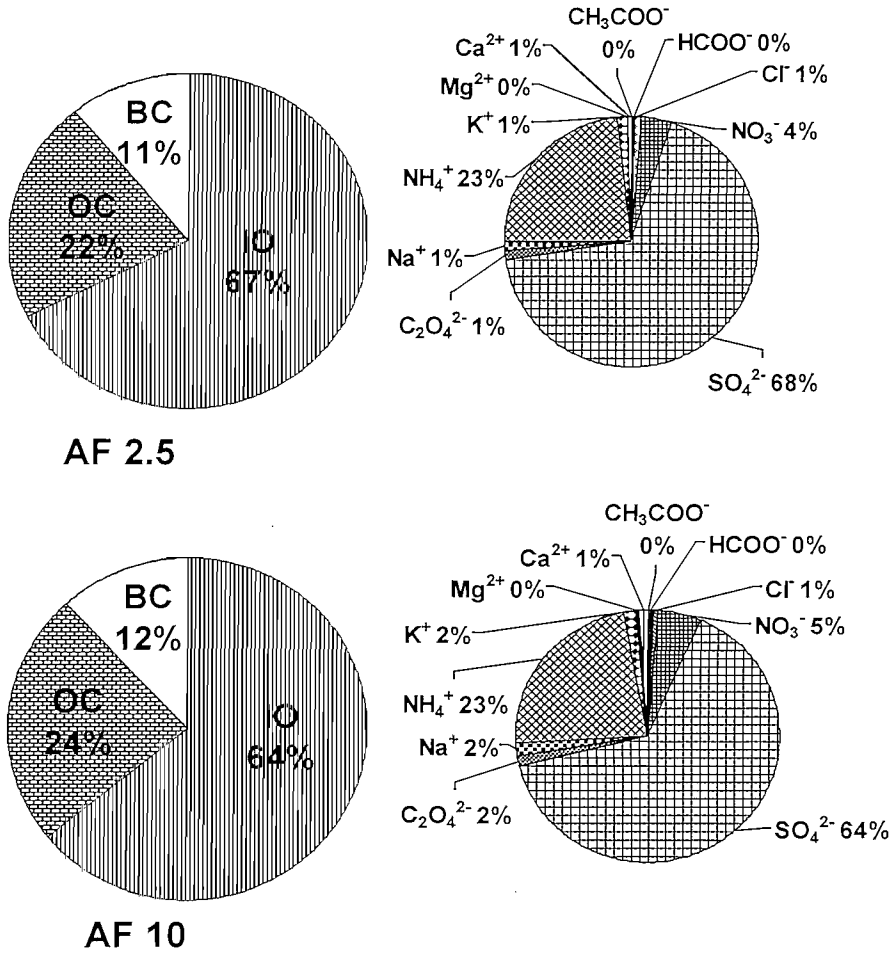


Figure 5.7 *Average relative BC, OC and IO aerosol composition for $PM_{2.5}$ and PM_{10} at Amersfoort (AF) for 9-15 April 2007 (see Fig. 5.1 for abbreviations)*

It follows from Figures 5.1-8 that the IO composition of the aerosols is dominated by three major inorganic species, namely SO_4^{2-}, NH_4^+ and NO_3^-, which are characteristic of anthropogenic source influences, especially in $PM_{2.5}$ aerosols. Anthropogenic activity is usually associated with emissions of precursor gases contributing to the direct emission of the finer size aerosols during combustion processes. The average ionic aerosol contents of all four of the sampling campaigns of this study were totally dominated by sulphate, which was on average three times the amount of the next abundant ion species, namely NH_4^+, followed by NO_3^-. The remaining ionic species, on average, only made up the remaining 10-15% of the total ionic aerosol composition. All the aerosols were predominantly acidic over both of the two representative regions due to the high sulphate content. Most of these aerosols also recirculate within air masses over the southern African subcontinent during anticyclonic conditions.[200,240,241] The aerosol composition was found to be dominated

by OC, BC, SO_4^{2-}, NH_4^+ and NO_3^- in the $PM_{2.5}$ aerosol of each site, which is the same as was found by *Formenti et al.*[47] within haze layers during the SAFARI 2000 project. This possibly indicates that the sources responsible for the aerosol content during the SAFARI project could be the same as those found in this study, especially those relating to the carbonaceous content.

The ER values (enhancement ratios of specific trace gases due to the contribution of a specific source) found for the trace gases (O_3, NO_x, methanol, acetonitrile, acetone and SO_2) measured during SAFARI 2000 within haze layers, are consistent with the predominant influence of biomass emissions.[242] The ER value of O_3 relative to CO (ER value of CO is an important indicator of biomass burning), as determined by *Formenti et al.*[47] during the SAFARI campaign, indicates a significant photochemical production of ozone within these haze layers. The aerosols measured at Louis Trichardt were also measured during the biomass burning period (winter). We can therefore assume the same transformation patterns of aerosols due to biomass burning influences exist, especially pertaining to O_3 production. This explains the higher O_3 concentrations in the Louis Trichardt region (Chapter 4, Table 4.2). This also explains the relatively high NO_3^- concentrations in the Louis Trichardt aerosols. The high NO_3^- concentrations at Louis Trichardt, in the absence of NO_2 producing industries in the proximity, if compared to Amersfoort, are therefore explained as the removal process of NO_2 by ozone from the atmosphere. We know NO_2 is removed from the atmosphere during the day due to the production of HNO_3. During night time it reacts with ozone to form NO_3^-. Considering the actual low concentration of NO_2 present in the Louis Trichardt samples (Chapter 4, Table 4.2) compared to the high O_3 concentration (Chapter 4, Table 4.2), this preceding transformation process is the only plausible explanation. This also happens with the Louis Trichardt aerosols during the transport of NO_2 to this site from the Amersfoort region.

Strong correlations exist between the dominant three ionic species from each size fraction between the sites during all the campaigns. This indicates possible trans-regional aerosol transport of fine aerosol as well as the aging of fine aerosol during transport to coarser aerosols.

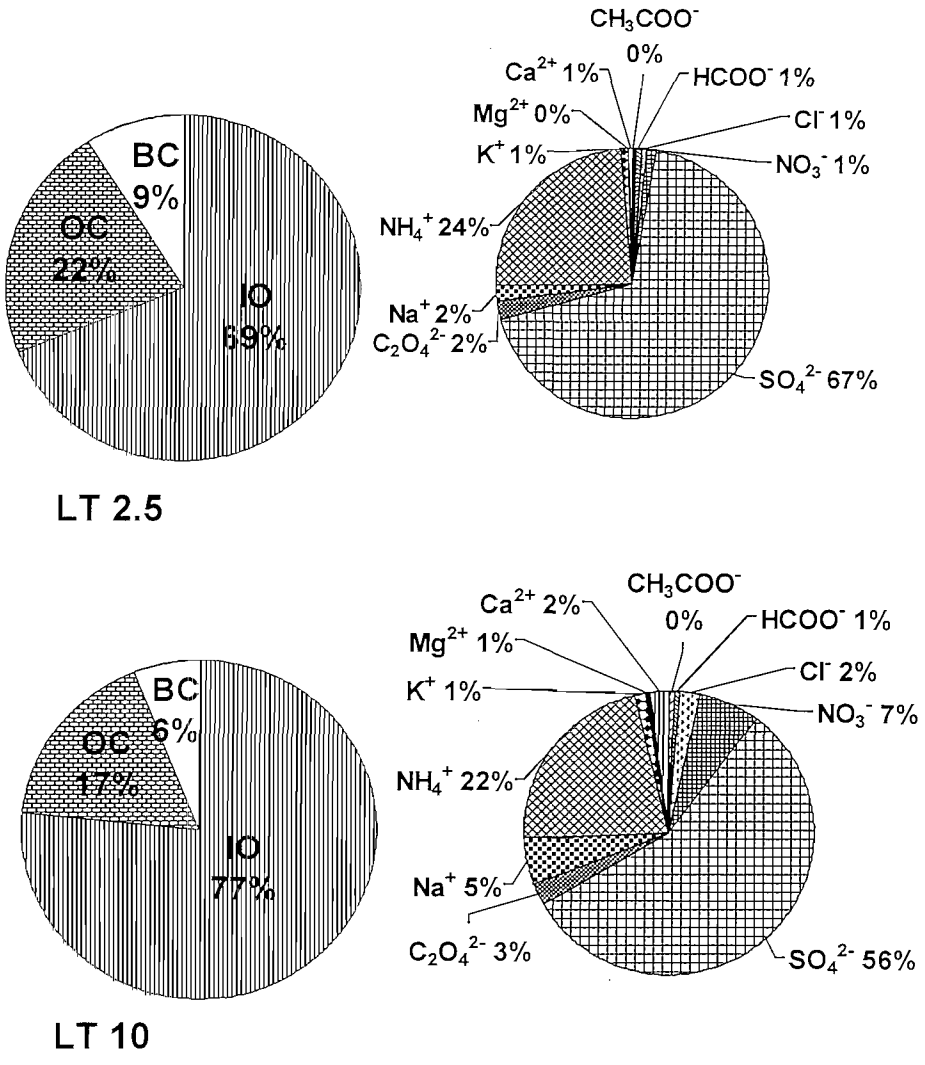


Figure 5.8 *Average relative BC, OC and IO aerosol composition for $PM_{2.5}$ and PM_{10} at Louis Trichardt (LT) for 9-15 April 2007 (see Fig. 5.1 for abbreviations)*

The Ca^{2+}, Mg^{2+} and K^+ content of these aerosols over both regions is fairly similar to slightly higher concentrations of Ca^{2+} at the Amersfoort site, which is attributed to fly ash produced during the combustion of coal within this region.[10] It is difficult to discriminate between mineral dust originating from soil erosion and dust being emitted by coal combustion. *Maenhaut et al.*[240] indicated that the mineral dust at Palmer (180 km east of Pretoria) is mainly soil derived. *Picketh et al.*[172] also found that soil-dust is a major constituent of regional aerosols in South Africa. The higher concentrations of species originating from mineral dust, e.g. Ca^{2+}, Mg^{2+}, K^+, in both $PM_{2.5}$ and PM_{10} at the Amersfoort site, depict the semi-arid region it is situated in. At Louis Trichardt, where more sub-tropical vegetation prevails, the organic acids of CH_3COO^-, $HCOO^-$ and $C_2O_4^{2-}$ are consistently higher than at Amersfoort and especially for $PM_{2.5}$. This

indicates increased biogenic activities and biomass burning of the more lush vegetation in this region. Lastly, the concentrations of Na^{2+} and Cl^- ions are the highest at the Louis Trichardt site, especially for PM_{10}. This is a direct result of air masses being transported over the ocean to this site (Chapter 3, Paragraph 3.1), which will be shown later in this chapter using the HYPSPLIT wind trajectories model.

5.3 Source-related regional aerosol composition correlations

Correlations between dominating inorganic and organic species within all the aerosols measured in this study were made. Principal component analyses (PCA) were used to make the correlations. This is a sub-program of the XLSTAT 4.4 data analysis program, which is a Windows TM product and can be customised into the Microsoft Excel toolbar. By using the correlation between species, the likely sources of the species transported within the same air mass or originating from the same sources can be identified.[10] Factor analysis with PCA has previously been used by many researchers on acid rain chemistry.[243-246] The results obtained from PCA in this study are presented in Tables 5.1-2.

The highest correlation, which remains the same throughout Tables 5.1-2 for both $PM_{2.5}$ and PM_{10} at both sites and all the sampling periods, is that between SO_4^{2-} and NH_4^+ (0.96-0.99). It is most probably linked to $(NH_4)_x(SO_4)_y$ compounds according to aerosol equilibrium considerations.[125] The correlation also remains the same at both sites, meaning it comes from sources situated in the same region. Another typical secondary aerosol that will form and compete for NH_4^+, is NH_4NO_3 through neutralisation reactions.[67] Both NH_4^+ and NO_3^- are present in relatively high quantities, as can be seen in the aerosol composition at the Amersfoort site. An excess of NH_4^+ is most probably the reason for the high correlations for both $PM_{2.5}$ and PM_{10}, as $(NH_4)_x(SO_4)$ is the preferred process. The same correlations are not present at the Louis Trichardt site (Tables 2.1-2) possibly due to lower NH_4^+ concentrations. The high occurrences of both NH_4^+ and NO_3^- are due to the presence of their precursor gases (NO_2 and NH_3) in high enough quantities within the Amersfoort region. The correlations are better for PM_{10}, the bigger aged particle where the transformation processes have taken place over a longer time period. The SO_4^{2-} also correlates well with Na^+ and K^+ for both $PM_{2.5}$ and PM_{10} at the Amersfoort site. This is probably due to the neutralisation of SO_4^{2-} and liberation of Cl^- as a gas over this region leading to

low Cl^- concentrations in the aerosol phase. The same correlations are not found at the Louis Trichardt site, leaving slightly higher Cl^- concentrations in the aerosol phase of this region. Surprisingly, higher correlations between NH_4^+ and K^+ exist for both $PM_{2.5}$ and PM_{10} at the Amersfoort site, which is a strong indicator of either biomass or biofuel burning,[247] and could indicate strong biomass/fuel influences within this region. As stated in Paragraph 5.2.1 Amersfoort are downwind of the informal settlement of Soweto which will generate large amounts of biomass/fuel emissions during winter.

Table 5.1 Average ratios of the dominating aerosol species for both sites and particle size during the 2005-2006 winter campaigns

Species	Winter 2005				Winter 2006			
	LT2.5	LT10	AF2.5	AF10	LT2.5	LT10	AF2.5	AF10
OC/OA	0.54	0.83	0.07	0.33	0.42	0.78	0.75	0.68
OC/M	0.62	0.88	0.11	0.39	0.11	0.75	0.69	0.67
OC/SO_4^{2-}	0.30	0.41	-0.35	0.17	-0.53	0.44	0.59	0.41
OC/NH_4^+	0.30	0.37	-0.37	0.12	-0.51	0.38	0.40	0.41
OC/NO_3^-	0.06	0.60	-0.04	0.27	-0.02	0.74	0.57	0.44
SO_4^{2-}/NH_4^+	0.98	0.96	0.98	0.97	0.99	0.99	0.88	0.99
SO_4^{2-}/NO_3^-	0.27	0.14	0.72	0.81	0.21	0.30	0.84	0.83
SO_4^{2-}/OA	0.45	0.56	0.62	0.79	0.75	0.69	0.85	0.89
SO_4^{2-}/M	0.54	0.54	0.74	0.86	0.62	0.56	0.77	0.95
NH_4^+/NO_3^-	0.23	0.13	0.77	0.85	0.16	0.24	0.81	0.88
NH_4^+/OA	0.39	0.56	0.54	0.78	0.68	0.61	0.81	0.90
NH_4^+/M	0.49	0.51	0.66	0.83	0.56	0.47	0.82	0.96
NO_3^-/M	0.69	0.74	0.71	0.90	0.93	0.76	0.83	0.92
NO_3^-/OA	0.38	0.74	0.60	0.74	0.72	0.67	0.86	0.87
Na^+/Cl^-	0.63	0.90	0.83	0.29	0.47	0.86	0.17	0.80
Na^+/ SO_4^{2-}	0.27	0.29	0.72	0.75	0.52	0.08	0.03	0.83
Na+/ NH_4^+	0.22	0.09	0.65	0.64	0.47	0.15	0.45	0.84
Na^+/ NO_3^-	0.86	0.04	0.67	0.70	0.89	0.68	0.06	0.83

(OA = Organic acids; M = Mineral species)

Consistent high correlations between Na^+ and Cl^- were found for the coarse mode (PM_{10}) at the Louis Trichardt site (0.86-0.96), indicating the marine influence of the nearby Mozambique Channel, as previously described (see Chapter 3, Paragraph 3.1). The Na^+/Cl^- ratio weakly correlates to the sea-salt ratio of 1.8, with values between 0.44 and 1.23. This is probably due to the Cl^- depletion of sea-salt particles at the Louis Trichardt site. This is evident in the good correlations found for Na^+ and NO_3^- in both $PM_{2.5}$ and PM_{10} at the Louis Trichardt site (0.66-0.98). This happens as HNO_3 deposits onto sea-salt particles to form a secondary aerosol of $NaNO_3$ due to the heterogeneous transformation processes as described by *Seinfeld et al.*[67] Good correlations were also found between NO_3^- and mineral species (Ca^{2+}, Mg^{2+} and K^+) for both $PM_{2.5}$ and PM_{10} at both the Amersfoort and Louis Trichardt sites. This indicates that these mineral species (soil/anthropogenic) are transported over each of these regions and incorporated as part of its aerosol. Good correlations were also found between OC and organic acids for both $PM_{2.5}$ and PM_{10} at each site. This could indicate anthropogenic[248] as well as biomass influences[1,2,5] as part of the carbonaceous content of the aerosol being transported over and from each region.

The good correlation between organic acids with both SO_4^{2-} and NH_4^+ at the Amersfoort site for $PM_{2.5}$ and PM_{10} indicates that there are significant biomass/biofuel influences situated near the Amersfoort site. The fact that the correlation is even better for the PM_{10}, suggests that the aerosol is already aged when it reaches Amersfoort. The NO_3^- correlates very poorly to SO_4^{2-} and NH_4^+ at Louis Trichardt for both $PM_{2.5}$ and PM_{10}, but correlates very well with mineral species (Ca^{2+}, Mg^{2+} and K^+) and organic acids. This provides possible evidence that NO_3^- most probably originates from the same biomass sources as the organic acids and that they are transported together to this region. The poor correlations of NO_3^- with SO_4^{2-} and NH_4^+, suggest that the SO_4^{2-} and NH_4^+ are transported from sources other than the biomass activity in the Louis Trichardt region. These sources are most probably situated in the Amersfoort region from where it gets transported within the aerosols to the Louis Trichardt region.

Table 5.2 Average ratios of the dominating aerosol species for both sites and particle size for the 2007 winter and summer campaigns

Species	Winter 2007				Summer 2007			
	$LT_{2.5}$	LT_{10}	$AF_{2.5}$	AF_{10}	$LT_{2.5}$	LT_{10}	$AF_{2.5}$	AF_{10}
OC/OA	0.72	1.0	0.97	0.96	0.89	0.41	0,49	0.01
OC/M	0.84	0.99	0.98	0.97	0.96	0.13	0.02	0.48
OC/SO_4^{2-}	0.77	0.89	0.89	0.39	0.79	0.66	-0.32	0.01
OC/NH_4^+	0.38	0.93	0.52	0.07	0.84	0.77	-0.29	0.01
OC/NO_3^-	0.06	-0.93	0.93	0.99	0.16	0.08	-0.04	0.11
SO_4^{2-}/NH_4^+	0.45	0.99	0.83	0.79	0.96	0.96	0.99	0.98
SO_4^{2-}/NO_3^-	-0.44	-0.67	0.98	0.41	-0.33	0.13	0.66	0.08
SO_4^{2-}/OA	0.16	0.89	0.95	0.68	0.71	0.46	0.16	0.07
SO_4^{2-}/M	0.32	0.98	0.80	0.78	0.85	0.54	0.42	0.28
NH_4^+/NO_3^-	-0.72	-0.74	0.79	0.72	-0.10	0.10	0.72	0.15
NH_4^+/OA	0.91	0.93	0.64	0.17	0.72	0.47	0.13	0.08
NH_4^+/M	0.07	0.96	0.40	0.31	0.88	0.40	0.47	0.25
NO_3^-/M	0.93	0.96	0.87	0.97	0.75	0.78	0.83	0.71
NO_3^-/OA	0.54	0.73	0.95	0.97	0.67	0.79	0.38	0.76
Na^+/Cl^-	0.04	0.96	-0.69	0.90	-0.73	0.56	0.33	0.48
Na^+/SO_4^{2-}	-0.65	-0.54	0.83	0.37	0.81	0.47	0.03	0.33
Na^+/NH_4^+	-0.54	-0.62	0.45	0.10	0.86	0.32	0.05	0.30
Na^+/NO_3^-	0.94	0.98	0.89	0.99	0.11	0.66	0.40	0.63

(OA = Organic acids; M = Mineral species)

During the summer campaign, the highest correlations between SO_4^{2-} and both organic acids and minerals were found at Louis Trichardt for both $PM_{2.5}$ and PM_{10}. This could be an important change from the same species correlations during winter where it was higher at the Amersfoort site. It is possibly due to the biomass activity and the role it plays in dominating the aerosol chemistry in the Louis Trichardt region. The good correlations at Louis Trichardt during the summer campaign between NH_4^+ and minerals species (Ca^{2+}, Mg^{2+} and K^+) may suggest that they originate from the same source and the similar correlation ratios suggest it to be from the Amersfoort region. The good correlations of NH_4^+, OA and OC at the Louis Trichardt site during

summer suggest the same source influences within this region and can be attributed to biogenic activities. Noticeable high correlations were found especially for Ca^{2+} and Mg^{2+} and the anthropogenic species (NH_4^+ and SO_4^{2-}) with an average of 0.66 at Louis Trichardt and 0.96 at Amersfoort. This positive relationship suggests the importance of the particles eroded from semi-arid regions to the chemical content of the precipitation. Soil-dust is a major constituent to regional aerosol loading in South Africa.[179] The relatively higher correlations for coarse (PM_{10}) aerosol particles at the Amersfoort site depict the semi-arid region it is situated in compared to Louis Trichardt where a more sub-tropical region prevails.

5.4 Tracking characteristic species within plumes from possible source regions

The measured aerosols during the four sampling campaigns showed certain species concentrations to be above the average on several days. The days where these species concentrations were notably higher (events) were found at both sites within the same sampling campaign, following each other in a time sequence. These events were first noticeable at the Amersfoort site and then a few days later at the Louis Trichardt site. Two types of these events occurred during each sampling campaign. The first type of event, which we called Event 1, was where the concentrations of the main three anthropogenically influenced species of SO_4^{2-}, NH_4^+ and NO_3^- were present in higher than average concentrations. The second type of event, which we called Event 2, was where the concentrations of the marine influenced species of Na^+ and Cl^- were present in higher than average concentrations. Only Event 1 occurred at both sites, while Event 2 only occurred at the Louis Trichardt site. Event 1 usually occurred first at the Amersfoort site and then showed up within days at the Louis Trichardt site. By using wind trajectory models, the air masses transporting these elevated concentrations between the sites could be tracked. The trajectories were made with the HYPSPLIT model with a database supplied by the NOAA website.[249] Tables 5.3-6 present the actual ionic and organic carbon concentrations of the aerosols measured on individual days. These are the data which were used in the HYPSPLIT wind trajectory model and represent each event. The last two rows give the actual day where the species-specific content was at its highest.

Table 5.3 Elevated concentrations ($\mu g.m^{-3}$) of species during the 2005 winter campaign

Species	Event 1				Event 2	
	$AF_{2.5}$	AF_{10}	$LT_{2.5}$	LT_{10}	$LT_{2.5}$	LT_{10}
Na+	0.63	0.65	0.45	0.35	0.68	1.56
NH_4+	2.03	2.20	1.25	1.59	0.64	0.68
K^+	1.46	1.51	0.98	1.09	0.19	0.22
Mg^{2+}	0.04	0.08	0.03	0.06	0.04	0.11
Ca^{2+}	0.17	0.32	0.08	0.15	0.05	0.12
CH_3COO^-	0.16	0.20	0.06	0.07		0.01
$HCOO^-$	0.54	0.85	0.44	0.84	0.38	0.40
Cl^-	0.23	0.07	0.03	0.02	0.50	1.66
NO_3^-	1.39	1.77	0.44	0.73	0.66	1.31
SO_4^{2-}	6.31	6.80	4.54	4.83	2.11	2.35
$C_2O_4^{2-}$	0.85	0.93	0.57	0.68	0.12	0.14
Higest OC	18.50	12.84	8.43	12.84		0.82
Event IO	1 Sep.	2 Sep.	6 Sep.	6 Sep.	10 Sep.	10 Sep.
Higest OC	2 Sep.	2 Sep.	2 Sep.	2 Sep.	10 Sep.	10 Sep.

(IO = inorganic and organic water soluble species, OC = organic carbon, Sep. = September)

From Table 5.3, Event 1 represents the elevated presence of SO_4^{2-}, NO_3^- and NH_4^+ in aerosols at both LT and AF. The concentrations of these species are higher for PM_{10} at the site and present a day after they are first noticed for $PM_{2.5}$ at the Amersfoort site. This suggests a possible aging as well as secondary aerosol formation effect within this region. These elevated concentrations at both sites occur within a timeframe of five days (1-6 September) during the same sampling campaign. The day the event is observed at Louis Trichardt is the same day for both $PM_{2.5}$ and PM_{10}, which supports the transportation of the aerosol within the same plume between sites. Almost all of the transported species get supplemented and aged during transport from the Amersfoort to the Louis Trichardt region within the plume, as seen in the PM_{10} and $PM_{2.5}$ concentration differences at Louis Trichardt. Theoretically, the $PM_{2.5}$ concentrations should always be less than the PM_{10} at each site, since the PM_{10}

includes $PM_{2.5}$. This was not always found to be the case in Table 5.3, and is obviously not practically possible and must be due to experimental errors. Wind trajectories for the five-day period between the event occurrences at both sites were made and are given in Figure 5.9.

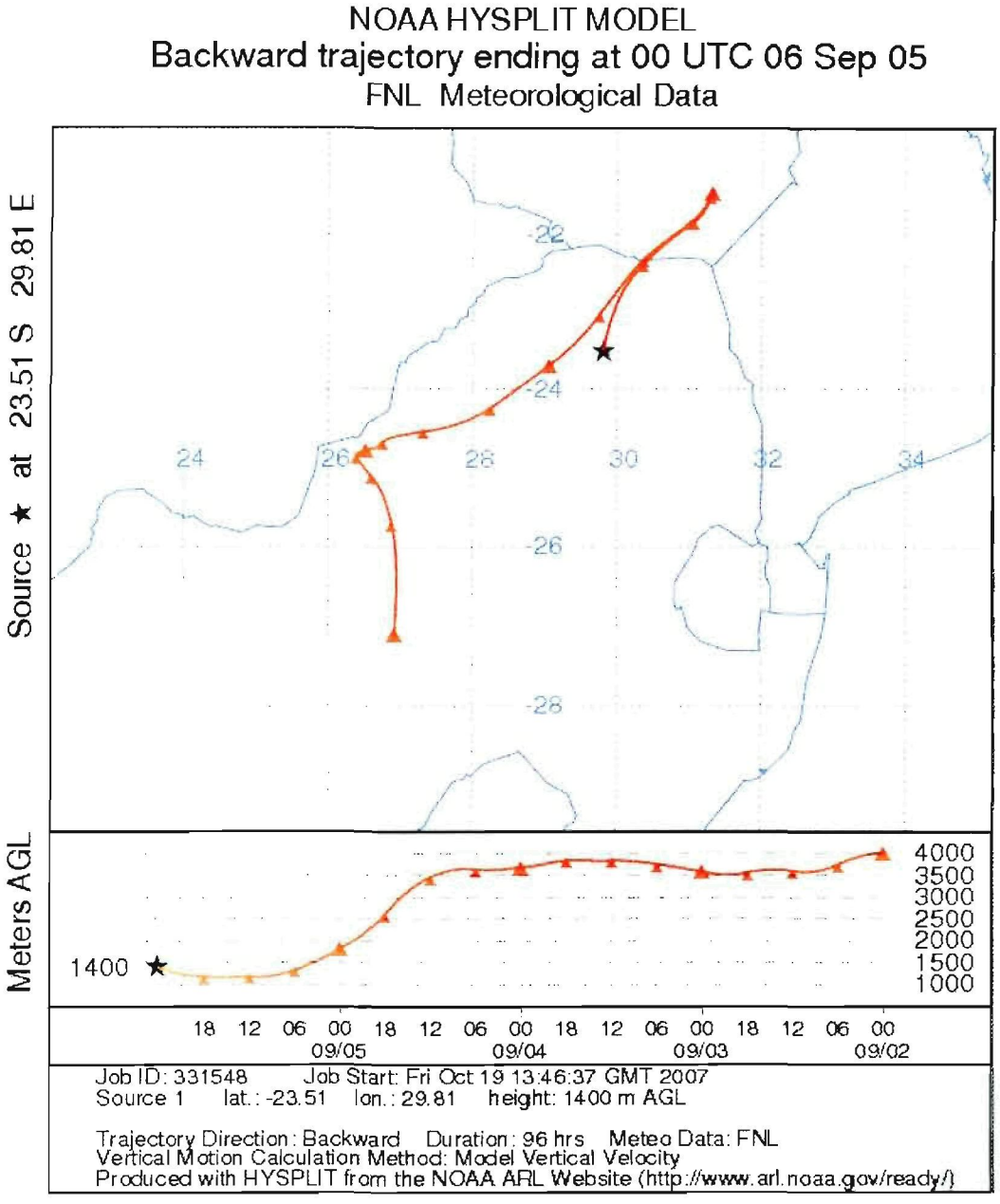


Figure 5.9 *Wind trajectories for the period 2-6 September 2005*

The wind trajectory model in Figure 5.9 indicates a backward wind trajectory of five days for an air mass to circulate between these regions. This trajectory coincides perfectly with this particular event, where elevated concentrations of the aerosol

species are present at Louis Trichardt precisely within five days from when the event was first observed at Amersfoort.

By using the ratios of the species concentrations for the two aerosol sizes and comparing it between the sites, we can get an idea of the type of source responsible for the aerosol and possibly the region of origin. The ratio of $PM_{2.5}/PM_{10}$ is above 0.92 for SO_4^{2-} at both sites, indicating the same source of origin. This suggests, with a certain level of confidence, that all the SO_4^{2-} measured at Louis Trichardt during this period originates from the same source and although the trajectory does not include Amersfoort, it is transported over Ellisras, which contains similar point sources to Amersfoort (Lephalale power station). The $PM_{2.5}/PM_{10}$ ratio of NH_4^+ during this event indicates a 90% agreement with each other attributing all the NH_4^+ present at Louis Trichardt originating from the same sources found in Ellisras and thus the Amersfoort region (Lephalale power station) with only 10% coming from an alternative source in the Louis Trichardt region. These sources (10%) are most probably biogenic as it is situated within a sub-tropical region. The $PM_{2.5}/PM_{10}$ ratio of NO_3^-, however, shows the largest difference of about 20% in the ratios between the sites, indicating alternative NO_3^- sources of about 20% originating in the Louis Trichardt region or during transport. Approximately 80% of NO_3^- is still transported to the Louis Trichardt region. This, however, correlates well with the high ozone formation phenomenon within a plume, as previously described (Paragraph 5.2.2), which reacts with large amounts of NO_2 gases transported in the same plume (Paragraph 2.3.1.3) to produce NO_3^- as an alternative source. The cations K^+, Mg^{2+}, Ca^{2+} and the organic anion $C_2O_4^{2-}$ are also elevated during these events. The ratio of K^+ in $PM_{2.5}/PM_{10}$ at the Amersfoort site (same point sources as Ellisras) is 0.96 and is within a 10% agreement with corresponding ratios at Louis Trichardt. This difference is most probably due to the higher biomass burning contribution to K^+ at the Louis Trichardt region as previously described (Chapter 3, Paragraph 3.1). The Mg^{2+} and Ca^{2+} ratios in $PM_{2.5}/PM_{10}$ are very low and around 0.50 and 0.53, respectively. This ratio also stayed the same for the Amersfoort site and indicates that these species are transported to Louis Trichardt from the same sources as found in the Amersfoort region.

The ratio of $PM_{2.5}/PM_{10}$ for OC shows no correlation between the sites or aerosol sizes. In fact, more OC is present in $PM_{2.5}$ at Amersfoort, while more OC is present for PM_{10} at Louis Trichardt. As the organic fraction was not identified, nothing can be

concluded about its transport between regions. However, the much larger OC concentrations at the Louis Trichardt site for the PM_{10} aerosol, indicate that it could have originated from another source origin and transported to the Louis Trichardt region. These event concentrations are a good indicator of the sources influencing the ionic and organic content of each of these regions. This is mostly due to the very low natural background concentrations of these specific species, which will have very little effect on the total composition of an average aerosol at each of these sites compared to those present within the plume events.

In Table 5.3, Event 2 is the presence of above-average elevated concentrations of the marine species of Na^+ and Cl^- and especially for PM_{10} at the Louis Trichardt site. This event was tracked by wind trajectories from the nearby Mozambique Channel through incoming air masses to the Louis Trichardt region. These event concentrations are present on the same day for both $PM_{2.5}$ and PM_{10} at the Louis Trichardt site. It was transported from 8-10 September 2005 from the coast line to Louis Trichardt as seen in Figure 5.10.

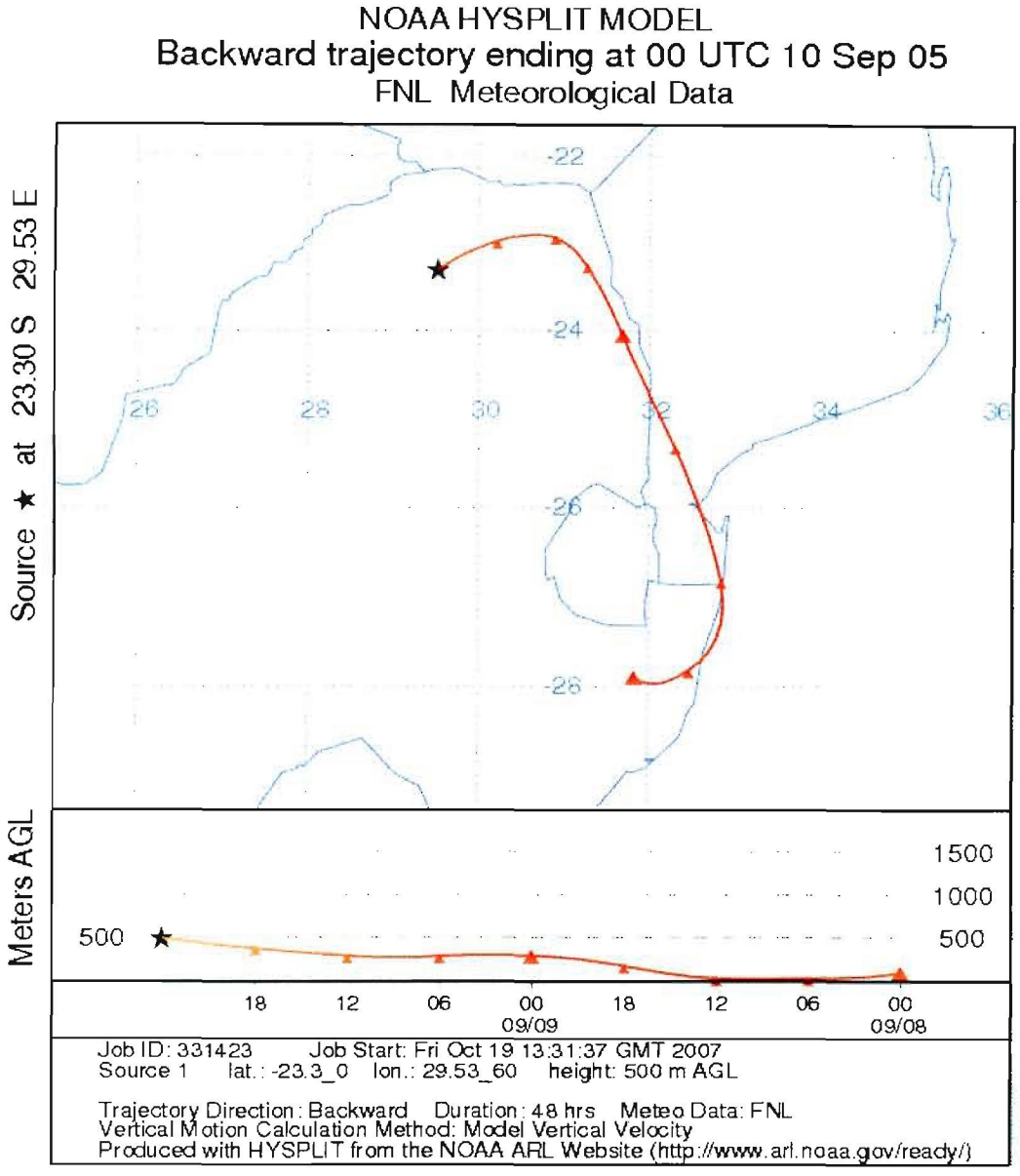


Figure 5.10 *Wind trajectories for the period 8-10 September 2005*

It is of particular interest that the highest OC concentrations were found on the same day as the highest ionic species at Amersfoort, while the actual OC values present on the day of marine events at the Louis Trichardt site are very low in comparison. This is explained by the air masses being transported from the ocean before they reach Louis Trichardt on these days. The air masses are expected to be relatively clean of all the other species being washed out by rain over the ocean. The low concentrations of all the other species within the aerosol during these days, except NO_3^-, support this condition. The NO_3^- concentrations are most probably high only due to the fact that they are deposited on the fresh marine aerosol, as an excess of it is already present in this region, as previously discussed. The organic acids (formic, oxalic and acetic) at

both sites have $PM_{2.5}/PM_{10}$ ratios within 10% of each other, indicating a large number of these acids being transported from the same sources. The higher concentrations of acids present in PM_{10} aerosol suggest most of these acids are already aged when they reach both regions. The difference of 10% in the ratios suggests incomplete combustion activities coming from different regions and sources to each of the sites. There are larger contributions of oxalic and formic acid to the PM_{10} aerosol at Louis Trichardt, while larger acetic acid contributions exist for PM_{10} at the Amersfoort site.

For the 2006 winter sampling campaign, the elevated concentrations during events are presented in Table 5.4. During this campaign, the same events as in 2005 were identified and of the same nature. Wind trajectories for a five-day period for Event 1, which were present at both sites, were made and are provided in Figure 5.11. Event 1 again showed the same above-average elevated SO_4^{2-}, NO_3^- and NH_4^+ concentrations on specific days for both $PM_{2.5}$ and PM_{10} at both sites. Event 1 took place on 24-28 July 2006 of the sampling campaign. As in 2005, Event 1 was first seen for aerosol species of $PM_{2.5}$ at Amersfoort and then even higher in concentration for PM_{10} the next day. Aging of the aerosol also seems to be present and the origin of sources begins to form a trend during the winter. The ratios of $PM_{2.5}/PM_{10}$ concentration for SO_4^{2-} were found to be within 10% between the sites and the 2005 results. This not only indicates a 90% agreement of the same SO_4^{2-} aerosols being transported between sites, but also that it agrees for different years of the same calendar period. There is 10% of SO_4^{2-} coming from an alternative source around the Louis Trichardt region during 2006.

Table 5.4 Elevated concentrations ($\mu g.m^{-3}$) of species during the 2006 winter campaign

Species	Event 1				Event 2	
	$AF_{2.5}$	AF_{10}	$LT_{2.5}$	LT_{10}	$LT_{2.5}$	LT_{10}
Na+	0.12	0.17	0.14	0.51	0.24	0.69
NH_4+	2.32	2.48	1.15	1.40	0.19	0.22
K^+	0.93	0.99	0.31	0.37	0.25	
Mg^{2+}	0.01	0.03	0.01	0.03	0.01	0.07
Ca^{2+}	0.10	0.19	0.04	0.09	0.01	0.07
CH_3COO^-	0.05	0.07	0.03	0.04	0.04	0.02
$HCOO^-$	0.04	0.07	0.09	0.19	0.12	0.85
Cl^-	0.07	0.05	0.09	0.15	0.13	0.86
NO_3^-	1.85	2.25	0.52	1.15	0.30	0.38
SO_4^{2-}	5.88	6.83	3.28	4.11	0.51	0.70
$C_2O_4^{2-}$	0.35	0.43	0.18	0.26		
Highest OC	9.65	7.64	3.44	5.08	2.20	1.45
event IO	24 July	25 July	28 July	28 July	30 July	30 July
Highest OC	25 July	25 July	25 July	25 July	30 July	30 July

(IO = inorganic and organic water soluble species, OC = organic carbon)

The $PM_{2.5}/PM_{10}$ ratios of NH_4^+, K^+, Ca^{2+}, Mg^{2+}, formic acid and acetic acid were found to be the same as the 2005 results, leading to the same conclusions of these species being transported from the same sources and this time the Amersfoort region. These species are transported within the event plume over both the Amersfoort and Louis Trichardt regions where they are supplemented with similar sources. The $PM_{2.5}/PM_{10}$ ratios for NO_3^-, which had a 20% difference in regional aerosol composition in the 2005 campaign, now have a 40% difference in the 2006 campaign. This follows the OC concentrations during events (see Appendix B) that have reduced extensively for PM_{10} from the 2005 to the 2006 campaigns at both sites. This again points to the fact that biomass influences promote O_3 formation in plumes that transform the NO_2 in plumes to produce NO_3^- (alternative source), as previously described (Paragraph 5.2.2). The $PM_{2.5}/PM_{10}$ ratio differences in NO_3^- between the two campaigns could

only follow this trend if the aerosol source composition remained the same during both campaigns. It can therefore be said that the larger differences in NO_3^- ratios are mainly due to the OC (biomass contribution) content of the aerosol being transported from the different regions to Louis Trichardt where higher OC compositions equals higher NO_3^- compositions given in the data of Appendix B.

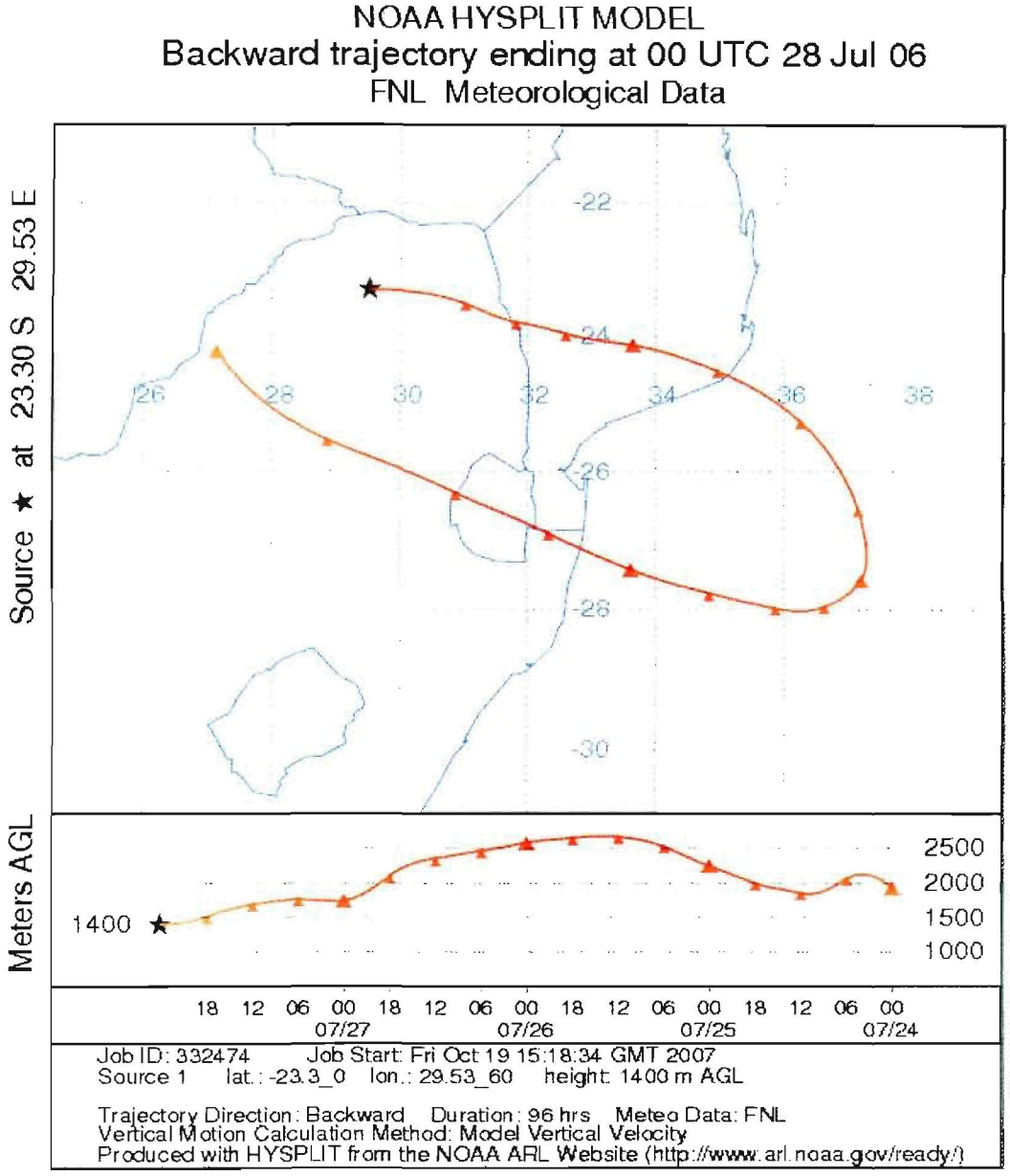


Figure 5.11 *Wind trajectories for the period 24-28 July 2006*

The wind trajectories model in Figure 5.11 indicates a backward trajectory of five days, which coincides with the time period in which the elevated event concentrations are observed at both sites. It starts over the Amersfoort region on 24 July, where the event is first seen, and ends on 28 July, when it reaches the Louis Trichardt region. It

also indicates the path of the event plume over the Indian Ocean to reach the Louis Trichardt region. There are slight differences in concentrations for most of the species reaching Louis Trichardt from Amersfoort during the 2006 campaign compared to the 2005 campaign. The path of the plume over the Indian Ocean in theory should have an effect, however, the differences seem a bit small and dry deposition could also be responsible.

In Table 5.4, Event 2 is the same elevated concentrations of the marine species of Na^+ and Cl^- as found in the 2005 campaign at Louis Trichardt. This event was tracked by wind trajectories from the nearby Mozambique coast line from 30-31 July 2006 and can be seen in Figure 5.12.

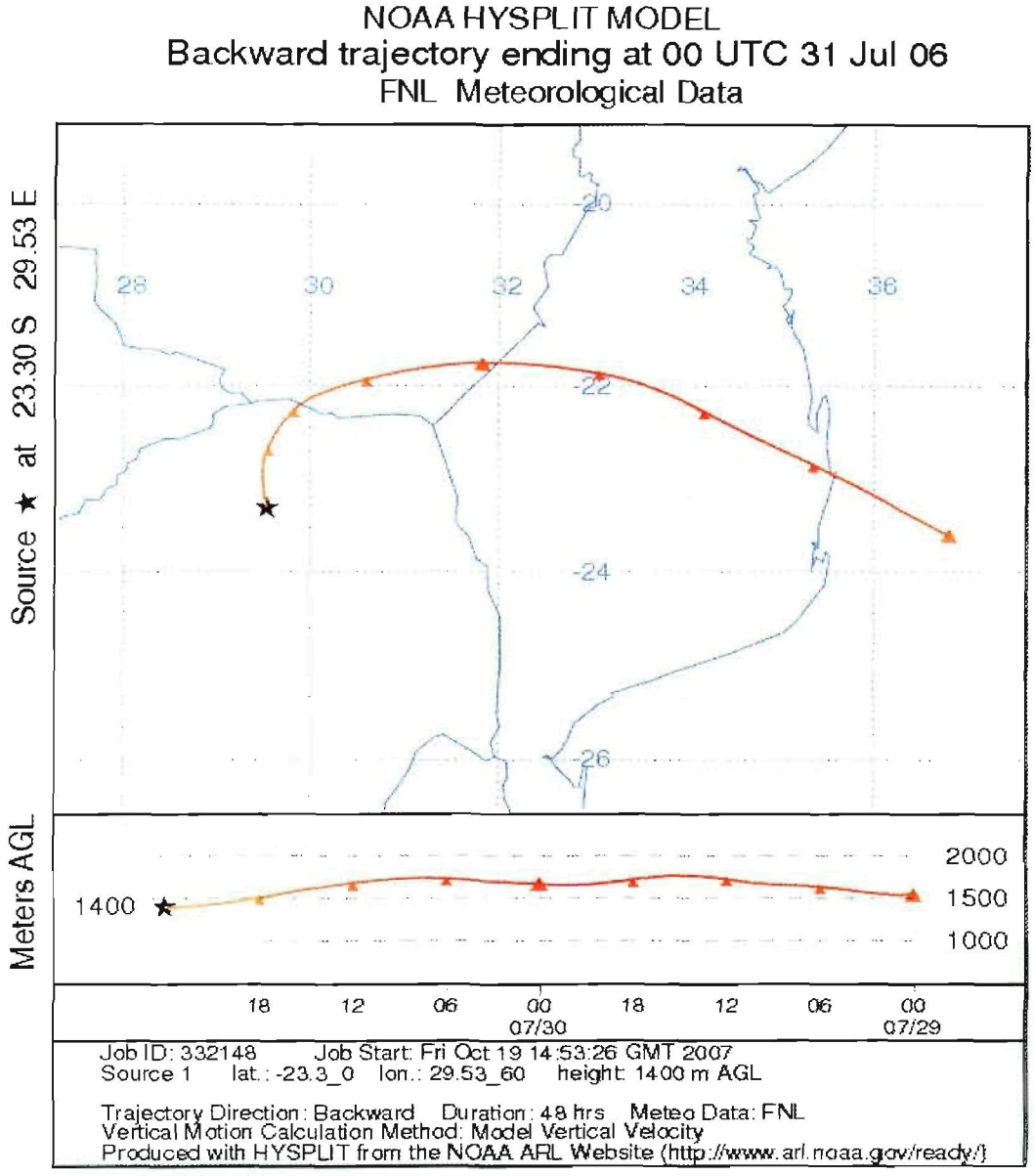


Figure 5.12 *Wind trajectories for the period 29-31 July 2006*

The concentrations of the typical marine species during the event are again present on the same day for both $PM_{2.5}$ and PM_{10} at the Louis Trichardt site. Event 2 indicates the same marine influence as in 2005. The OC concentrations for the marine event are of similar magnitude as for the 2005 results, resulting in the same conclusions regarding the air masses coming from the ocean.

Table 5.5 Elevated concentrations ($\mu g.m^{-3}$) of species during the 2007 winter campaign

Species	Event 1				Event 2	
	$AF_{2.5}$	AF_{10}	$LT_{2.5}$	LT_{10}	$LT_{2.5}$	LT_{10}
Na+	0.03	0.06	0.21	0.04	0.41	1.20
NH_4+	1.60	1.65	0.87	0.95	0.46	0.47
K^+	0.09	0.10	0.14	0.19	0.14	0.16
Mg^{2+}	0.01	0.01	0.01	0.02	0.04	0.19
Ca^{2+}	0.11	0.18	0.03	0.06	0.04	0.13
CH_3COO^-	0.03	0.04	0.03	0.03	0.04	0.05
$HCOO^-$	0.02	0.03	0.02	0.04	0.04	0.04
Cl^-	0.04	0.10	0.33	0.02	0.37	1.46
NO_3^-	0.46	0.61	0.47	0.84	0.47	1.09
SO_4^{2-}	3.28	3.30	2.36	2.51	1.30	1.51
$C_2O_4^{2-}$	0.08	0.09	0.10	0.14	0.10	0.12
Highest OC	6.11	9.08	4.37	5.72	1.35	1.59
Event IO	6 July	6 July	8 July	8 July	9 July	9 July
Highest OC	9 July	9 July	8 July	8 July	9 July	9 July

(IO = inorganic and organic water soluble species, OC = organic carbon)

The final two sampling campaigns were both performed during 2007. The first one was during the summer period in South Africa and the second one during the winter. The winter campaign results are presented in Table 5.5 and have more or less the same patterns as the winter campaigns of 2005 and 2006. The same conclusion are made with regard to the sources contributing to SO_4^{2-}, NO_3^-, NH_4^+, Mg^{2+} and formic acid at both sites. The above-mentioned species have the exact same $PM_{2.5}/PM_{10}$

ratios as was found in the 2005 campaign. The only differences in ratios are for K^+, Ca^{2+}, acetic and oxalic acid. The higher concentrations of K^+, Ca^{2+}, acetic and oxalic acid for PM_{10} again point to aerosol aging upwind from the Amersfoort region, most probably by incomplete biofuel/fossil fuel combustion influences. The $PM_{2.5}/PM_{10}$ ratios for OC once again show no correlations between either sites or aerosol sizes. The marine event for this campaign appears to be the same as the previous two years' campaigns with the same marine influences. Wind trajectories over a three-day period between the event occurrences of Event 1 at both sites were made and are provided in Figure 5.13.

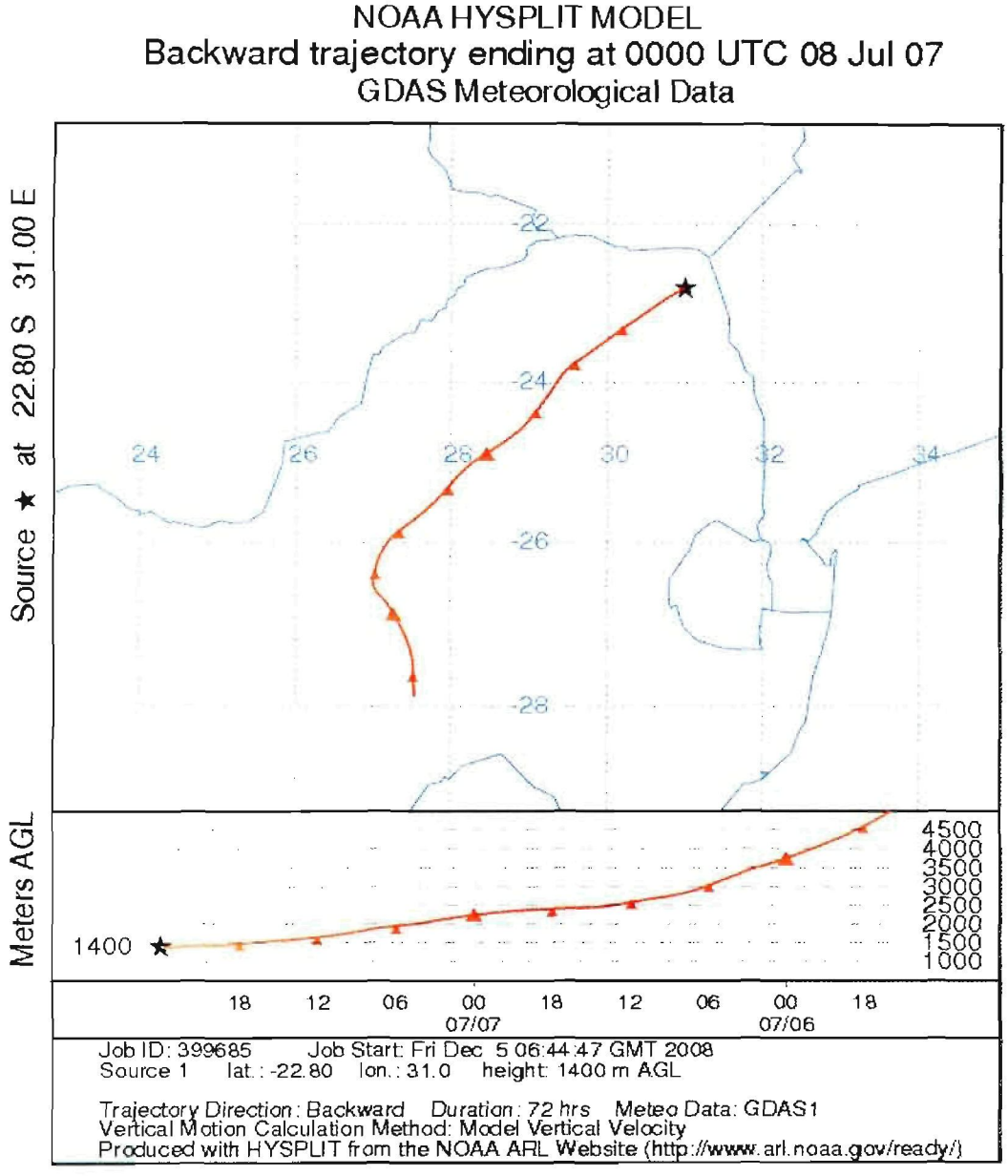


Figure 5.13 *Wind trajectories for the period 6-8 July 2007*

The wind trajectory model in Figure 5.13 indicates a backward wind trajectory of three days for an air mass to circulate from sources similar to Amersfoort (Ellisras-Lephalale power station) over the Louis Trichardt region. This trajectory coincides perfectly with this particular event and elevated concentrations of the aerosol species are present at Louis Trichardt precisely within three days from when the same species concentrations were first observed at Amersfoort. In Table 5.5, Event 2 is the same elevated concentrations of the marine species of Na^+ and Cl^- as found in both the 2005 and 2006 winter campaigns at Louis Trichardt. This event was tracked by wind trajectories from the nearby Mozambique coast line from 9 July 2007 and can be seen in Figure 5.14.

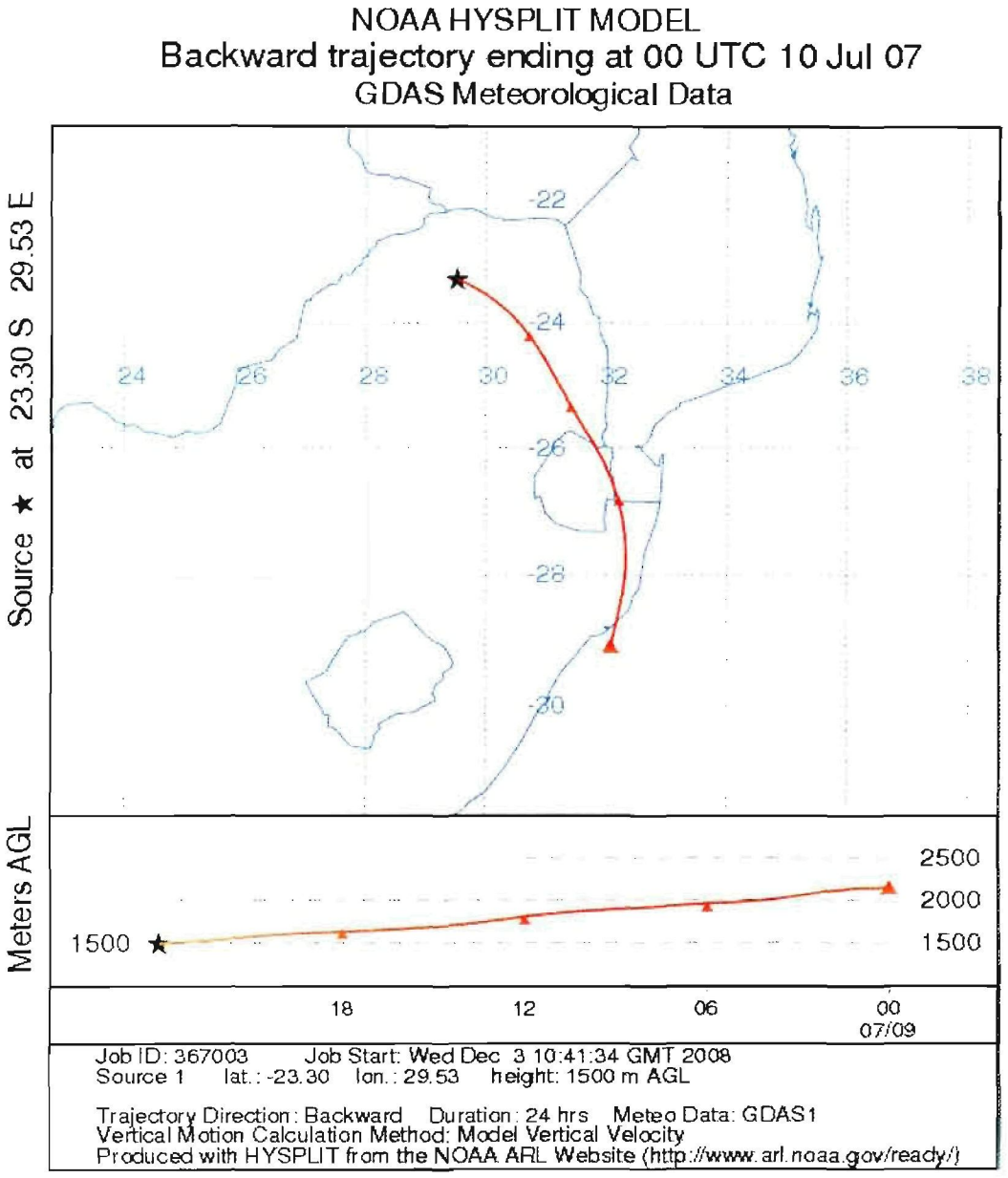


Figure 5.14 *Wind trajectories for the period 9-10 July 2007*

The concentrations of the typical marine species during the event are again present on the same day for both $PM_{2.5}$ and PM_{10} at the Louis Trichardt site. Event 2 indicates the same marine influence as in 2005 and 2006. The OC concentrations for the marine event are of similar magnitude as for the 2005 and 2006 results, resulting in the same conclusions regarding the air masses coming from the ocean.

Table 5.6 Elevated concentration ($\mu g.m^{-3}$) of species during the 2007 summer campaign

Species	Event 1				Event 2	
	$AF_{2.5}$	AF_{10}	$LT_{2.5}$	LT_{10}	$LT_{2.5}$	LT_{10}
Na+	0.04	0.07	0.16	0.35	0.14	0.59
NH_4+	2.21	1.90	1.68	1.76	1.33	1.15
K^+	0.05	0.06	0.04	0.07	0.01	0.05
Mg^{2+}	0.01	0.03	0.01	0.05	0.01	0.06
Ca^{2+}	0.04	0.09	0.02	0.06	0.11	0.15
CH_3COO^-	0.01	0.02	0.02	0.05		0.02
$HCOO^-$	0.01	0.02	0.04	0.11	0.03	0.05
Cl^-	0.04	0.05	0.01	0.06	0.13	0.81
NO_3^-	0.17	0.22	0.08	0.17	0.10	0.26
SO_4^{2-}	5.88	5.68	6.57	5.64	4.32	4.03
$C_2O_4^{2-}$	0.08	0.10	0.15	0.26	0.03	0.05
Highest OC	4.74	4.38	3.33	3.28	1.40	1.85
Event IO	14 April	14 April	16 April	16 April	9 April	9 April
Highest OC	11 April	11 April	12 April	12 April	9 April	9 April

(IO = inorganic and organic water soluble species, OC = organic carbon)

The elevated concentrations of species measured during the events in the summer campaign of 2007 are given in Table 5.6. During the summer period of 2007 there was one event of the Event 1 type and one of the Event 2 type at both sites during the summer campaign, listed in Table 5.6. Wind trajectories over a four-day period between the event occurrences of Event 1 at both sites were made and are provided in Figure 5.15.

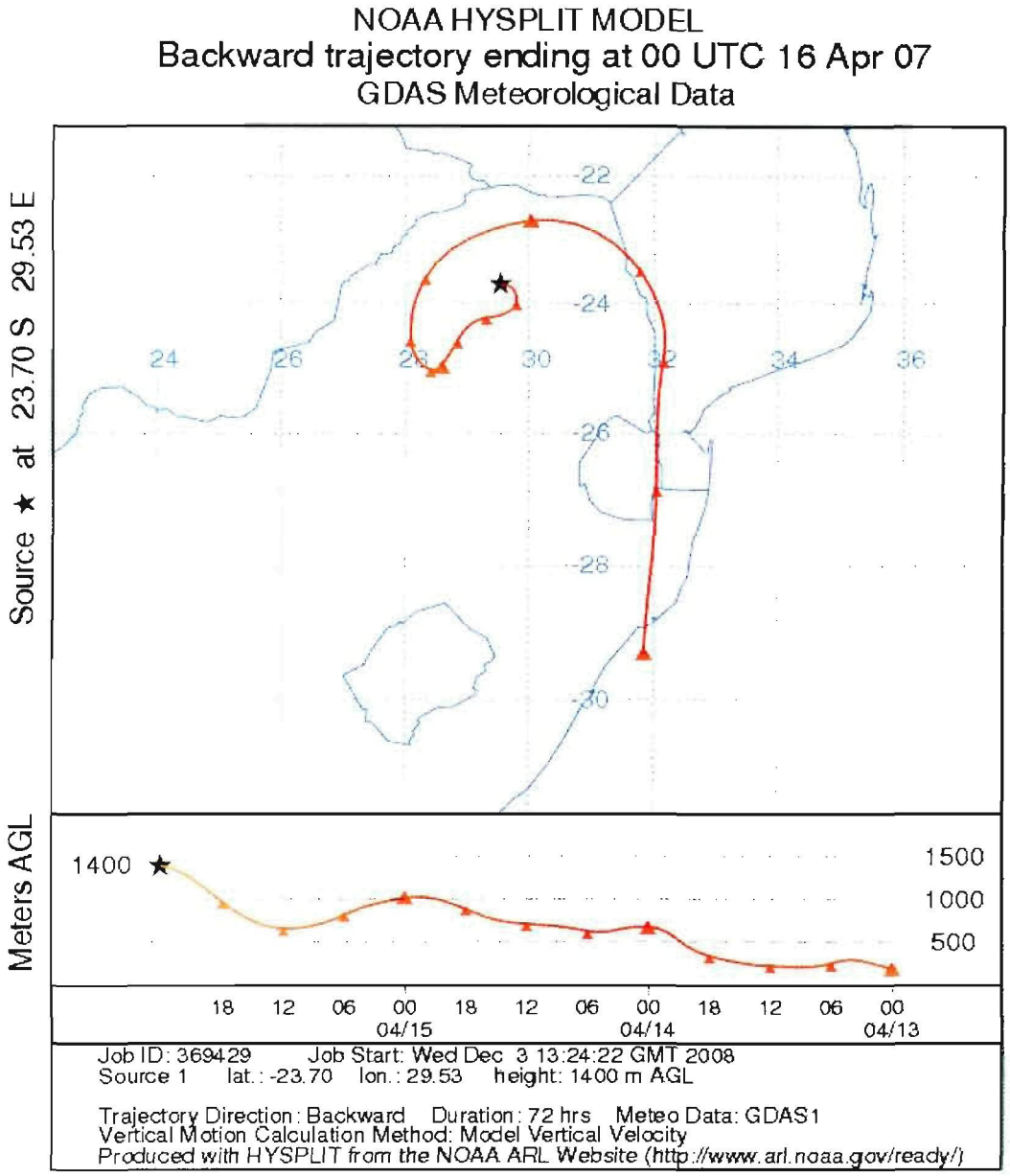


Figure 5.15 *Wind trajectories for the period 13-16 April 2007*

The wind trajectories model in Figure 5.15 indicates a backward trajectory of four days, which coincides with the time period in which the elevated event concentrations are observed at both sites. It starts over the Amersfoort region between 13 and 14 April where the event is first seen and ends on 16 April when it reaches the Louis Trichardt region.

The sources contributing to the aerosol species during these events are similar to the ones in the winter events of 2005-2007. The $PM_{2.5}/PM_{10}$ concentration ratios of SO_4^{2-}, and NH_4^+ also indicate the sources to be mostly of the same origin, transported from the Amersfoort region to the Louis Trichardt region. The $PM_{2.5}/PM_{10}$ concentration

ratios of NO_3^-, Mg^{2+}, K^+, Ca^{2+}, acetic, formic and oxalic acid during these events show a considerable alternative source other than the one transported from the Amersfoort region during summer. The alternative sources may be linked to sources from regions closer and across the border from the Louis Trichardt region. The highest concentration of OC is present for PM_{10} at Amersfoort and indicates the large amount of biofuels being used by informal settlements upwind from this region. It is important and clearly evident that NO_3^- aerosols do not have elevated concentrations during these events in the summer. This shows once again the large OC effect of biomass burning on the formation of ozone and subsequent NO_3^- during the event, which is absent during the summer. The cations are all elevated at both sites during these events, while the organic acids are elevated at the Louis Trichardt site. The organic acids can be attributed to biomass activities of the Louis Trichardt region, with its lush vegetation, during summer. The concentrations of SO_4^{2-} and NH_4^+ are higher for $PM_{2.5}$ than PM_{10} at both sites and relate to the unstable meteorological conditions during summer. This prevents aged aerosols from reaching the sites from other regions through long-range transport.

In Table 5.6, Event 2 is the same elevated concentrations of the marine species of Na^+ and Cl^- as found in both the 2005, 2006 and 2007 winter campaigns at Louis Trichardt. This event was tracked by means of wind trajectories from the nearby coastline from 8-9 April 2007 and can be seen in Figure 5.16.

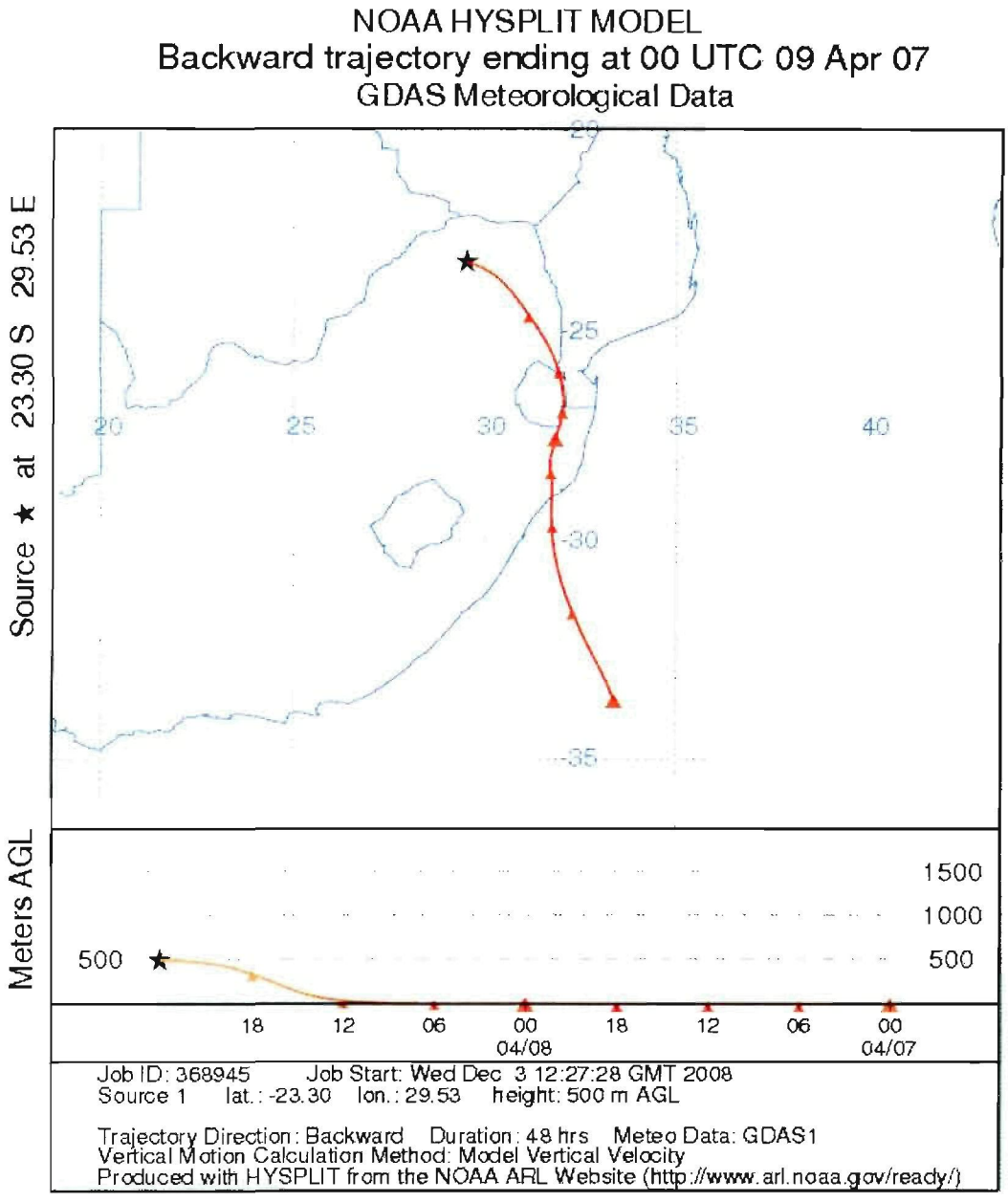


Figure 5.16 *Wind trajectories for the period 8-9 April 2007*

The concentrations of the typical marine species during the event are again present on the same day for both $PM_{2.5}$ and PM_{10} at the Louis Trichardt site. Event 2 shows the same marine influence as in the 2005, 2006 and 2007 winter campaigns. The OC concentrations for the marine event are of similar magnitude as for the 2005-2007 winter campaign results, resulting in the same conclusions regarding the air masses coming from the ocean.

5.5 Source group estimations based on the ionic content of $PM_{2.5}$ and PM_{10} aerosols of the sampling campaigns

Paragraph 2.6 describes how the marine or terrigenous content of aerosols have different preferred surface areas for sulphate deposition which ultimately effects the concentration of gases in its vicinity. It is therefore important to determine the marine and continental content of the aerosol, which will give a better insight into the transformation chemistry. First the sea salt (ss) and non sea salt (nss) content of each ionic aerosol species is calculated. These calculated values are used to separate the content of the ionic species of natural origin into marine and terrigenous sources. Sulphate is grouped individually into natural and anthropogenic sources. The natural sulphate is further divided into marine and terrigenous sources. The other ionic species are labelled as Other sources. These groups represent the total aerosol content. All the source group estimations made at each site and the particle size measurements were characterised according to these groups and the calculations of the different groups are described in the following paragraphs.

Marine and Terrigenous contributions

In order to determine the contribution of sea salt to each ionic aerosol species concentration, the Cl^-/Na^{2+} ratio of the aerosol were compared to that of a sea aerosol where the influence of both ions were at its highest. The aerosol ratio constants that was used for determining the marine (ss) aerosol contributions were values used by the Laboratoire d'Aérologie in Toulouse, France. The constants were 1.8; 0.12; 0.04; 0.037 and 0.25 for Cl^-; Mg^{2+}; Ca^{2+}, K^+ and SO_4^{2-} respectively.

First the Cl^- ratio constant was used in Equation 5.1 to calculate the ss-Na^{2+} contribution to the aerosol in $\mu g.m^{-3}$.

$$[Na^{2+}]ss = [Na^{2+}]_{measured} - ([Cl^-]_{measured}/[\ Cl^-]_{ratio}) \qquad 5.1$$

(where: $[Na^{2+}]ss$ is the marine contribution of Na^{2+} in $\mu g.m^{-3}$; $[Na^+]_{measured}$ is the concentration of sodium ions per sample ($\mu g.m^{-3}$); $([Cl^-]_{measured}$ is the concentration of clorine ions per sample ($\mu g.m^{-3}$) and $[\ Cl^-]_{ratio}$ is the ratio constant given to Cl^- of a sea salt aerosol.

After the ss-Na^{2+} contribution of the aerosol was determined the marine contribution of each of the aerosols species was determined by multiplying the $[Na^{2+}]ss$ with the ratio constant of each of the species as indicated in previuos paragraphs. This product was

subtracted from the concentration of the species of interest measured per sample to give the terrigenous contribution shown in Equation 5.2.

$$[X]nss = [X]_{measured} - ([Na^{2+}]ss \times [X]_{ratio}) \quad 5.2$$

(where: [X]nss is the terrigenous contribution for the element X in $\mu g.m^{-3}$; $[X]_{measured}$ is the concentration of species X per sample ($\mu g.m^{-3}$) ; $[Na^{2+}]ss$ is the marine contribution of Na^{2+} in $\mu g.m^{-3}$ and $[X]_{ratio}$ is the ratio constant given to species X of a sea salt aerosol.

The contribution of marine sources to the total ionic content of the aerosol for both $PM_{2.5}$ and PM_{10} at each site were calculated as the sum of Mg^{2+}, Ca^{2+}, Cl^-, Na^+, SO_4^{2-} and K^+ ions individual marine contributions as calculated in Equation 5.1-2 and are given as source estimations in Figure 5.17-20.

The contribution of terrigenous sources to the total ionic content of the aerosol for both $PM_{2.5}$ and PM_{10} at each site are the sum of Mg^{2+}, Ca^{2+}, Na^+, SO_4^{2-} and K^+ ions individual terrigenous contributions as calculated in Equation 5.1-2. The source group estimations are given in Figure 5.17-20.

Sulphate contribution

The excess SO_4^{2-} can be attributed to either terrigenous sources or anthropogenic pollution. Assuming that the SO_4^{2-} contribution from terrigenous sources is the concentration in excess of that supplied by gypsum the anthropogenic SO_4^{2-} can be determined by using Equation 5.3.

$$[SO_4^{2-}]_{anthropogenic} = [SO_4^{2-}]nss - 0.47\,[Ca^{2+}]_{measured} \quad 5.3$$

(where: $[SO_4^{2-}]_{anthropogenic}$ is the anthropogenic contribution of sulphate ions per sample ($\mu g.m^{-3}$); $[SO_4^{2-}]nss$ is the terrigenous contribution of sulphate ions per sample ($\mu g.m^{-3}$); $[Ca^{2+}]_{measured}$ is the concentration of calcium ions per sample ($\mu g.m^{-3}$) and 0.47 a ratio constant.

Other contributions

The additional species are grouped as Other sources and consists of the ionic species NO_3^-, NH_4^+, CH_3COO^-, $CHOO^-$ and $C_2H_4^{2-}$, which was all added together without any adjustments.

Since all the winter sampling campaigns show the same trends and source group estimations, only the results for 2007 will be shown, after which the only summer sampling campaign source group estimations will be given. All the source group estimations were calculated according to the preceding paragraphs. It compares well to the individual anthropogenic and marine species reported in Figures 5.1-5.8. The source group estimations are given in Figure 5.17-5.20.

5-11 July 2007 (winter)

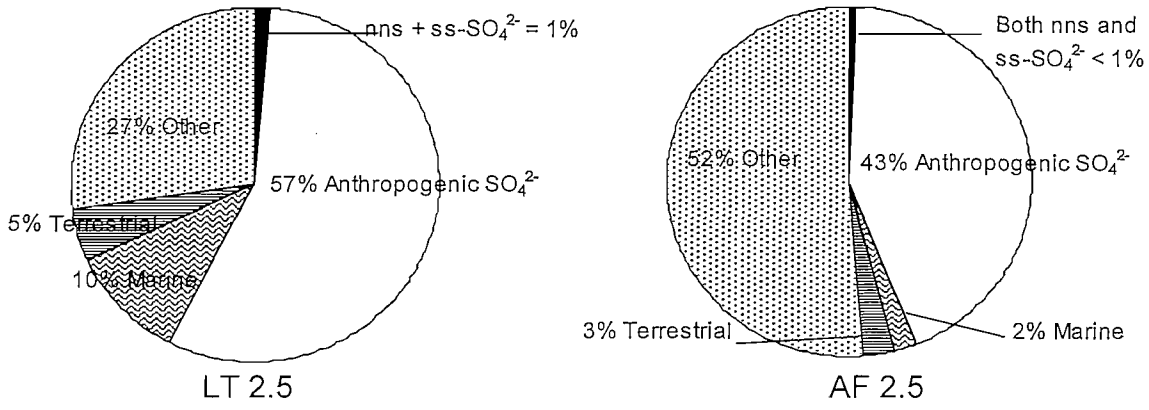


Figure 5.17 *Source group estimations at AF and LT for $PM_{2.5}$ during winter*

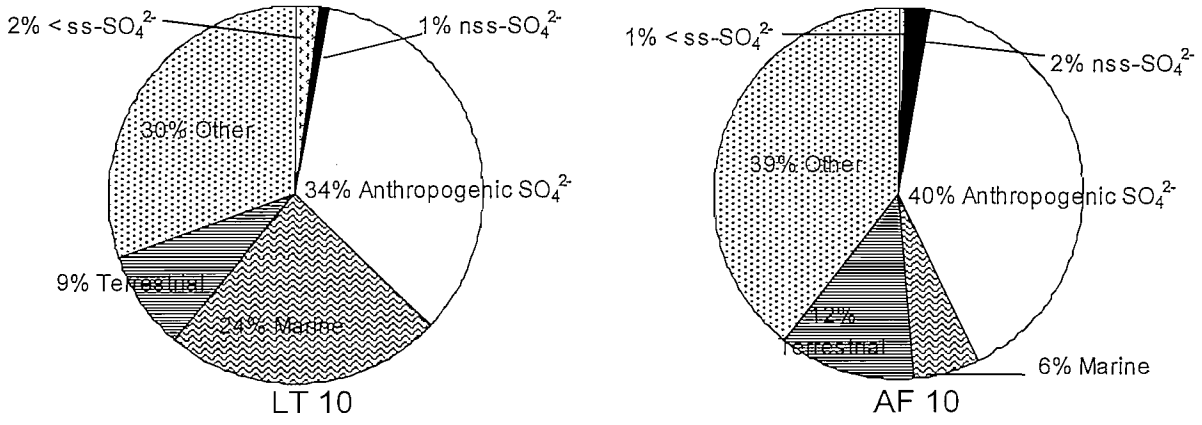


Figure 5.18 *Source group estimations at AF and LT for PM_{10} during winter*

For $PM_{2.5}$ the nns and ss-SO_4^{2-} influence is less than 1% during winter, while the nns-SO_4^{2-} for PM_{10} at AF reaches 2%, which is double the amount found at LT. This is indicative of the arid AF conditions. The ss-SO_4^{2-} at LT reaches 2%, which is twice the amount ss-SO_4^{2-} found at AF indicative of the sea influence as mentioned in preceding paragraphs. The anthropogenic-SO_4^{2-} source estimation is prevalent for PM_{10} at AF but not for $PM_{2.5}$ that has a higher estimation. The marine source contribution is constant for $PM_{2.5}$ and PM_{10} and is prevalent at the LT site. Terrestrial

sources prevail at AF with the exception of $PM_{2.5}$ at LT that shows a higher contribution. Additional (other) source contributions, which include NH_4^+ and NO_3^-, are constantly higher for $PM_{2.5}$ and PM_{10} at the AF site and is also indicative of anthropogenic sources.

9 April to 22 April 2007 (summer)

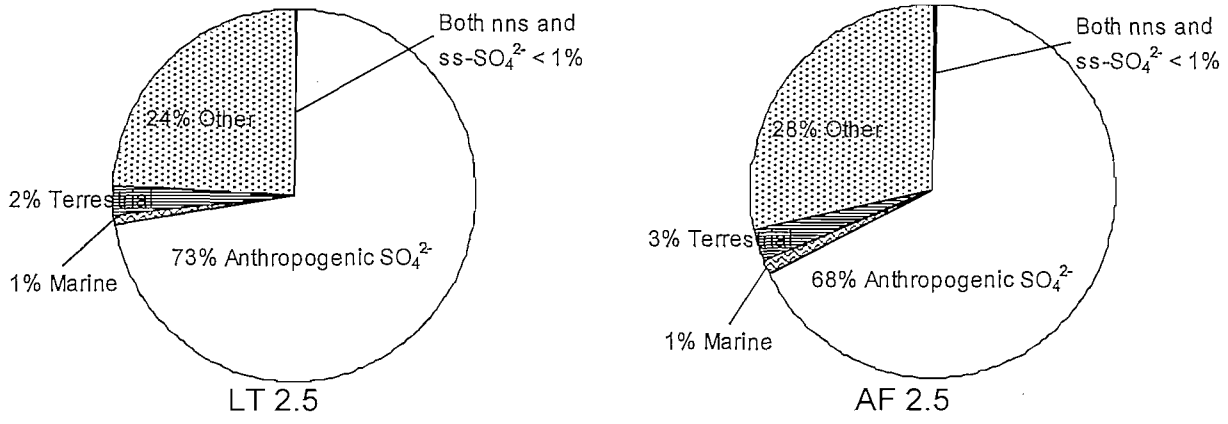


Figure 5.19 *Source group estimations at AF and LT for $PM_{2.5}$ during summer*

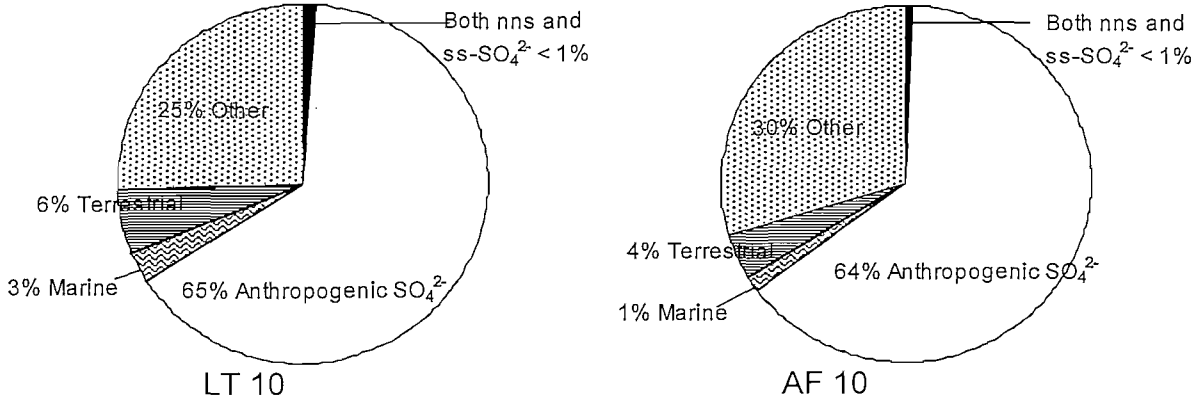


Figure 5.20 *Source group estimations at AF and LT for PM_{10} during summer*

During summer the source contribution of nns and ss-SO_4^{2-} for $PM_{2.5}$ and PM_{10} remained less than 1%. The anthropogenic-SO_4^{2-} source estimations are almost the same for $PM_{2.5}$ and PM_{10} at both sites, with a larger contribution to the $PM_{2.5}$ aerosol. The anthropogenic-SO_4^{2-} estimations seems higher during summer than winter, which is due to much lower contributions of other sources like terrestrial and marine that is associated to the seasonal differences (wind direction) and foliage. The terrestrial source estimations are relatively the same for $PM_{2.5}$ and PM_{10} at both sites with larger contributions to the PM_{10} aerosol. The marine influence on the LT site can only be seen from the PM_{10} aerosol during summer. Additional contributions (NH_4^+ and NO_3^-)

are also constantly higher during summer for $PM_{2.5}$ and PM_{10} at AF and indicative of anthropogenic sources.

5.6 Comparison of aerosol concentration data with similar work done in South Africa

The average aerosol species concentration for the winter period was calculated and the concentrations are given in Table 5.7. The data obtained from similar work done in South Africa by *Formenti*[47] as well *Puxbaum*[250] are compared with this study's data in Table 5.7.

Table 5.7 The comparison of aerosol concentration ($\mu g.m^{-3}$) data of different studies done in South Africa

	AF & LT winter				AF & LT summer				Formenti		P
	$AF_{2.5}$	AF_{10}	$LT_{2.5}$	LT_{10}	$AF_{2.5}$	AF_{10}	$LT_{2.5}$	LT_{10}	Fine	CRS	CRS
Na^+	0.12	0.23	0.23	0.55	0.07	0.10	0.10	0.28	0.19	0.15	0.33
NH_4^+	1.01	1.24	0.63	0.60	1.38	1.43	1.31	1.19	0.90	0.50	2.85
K^+	0.35	0.46	0.37	0.39	0.08	0.10	0.03	0.05	0.60	0.31	0.28
Mg^{2+}	0.03	0.13	0.02	0.06	0.01	0.02	0.01	0.03	0.01	0.05	0.08
Ca^{2+}	0.08	0.22	0.04	0.09	0.03	0.08	0.03	0.12	0.05	0.15	0.26
Acet.	0.05	0.08	0.03	0.04	0.01	0.02	0.02	0.02			
Form.	0.20	0.21	0.29	0.37	0.01	0.01	0.04	0.04			
Cl^-	0.07	0.13	0.15	0.41	0.05	0.05	0.03	0.12		0.10	0.12
NO_3^-	0.58	1.21	0.37	0.81	0.24	0.32	0.06	0.38	1.09	1.18	0.40
SO_4^{2-}	2.79	3.17	2.08	1.97	4.07	4.08	4.64	4.60	1.90	1.15	11.8
$C_2O_4^{2-}$	0.19	0.27	0.21	0.24	0.07	0.10	0.12	0.15	0.79	0.90	0.18
OC	4.67	5.09	3.04	3.40	1.93	2.34	2.03	1.55	6.15		
BC	2.26	2.32	1.70	1.71	0.98	1.18	0.85	0.57			0.85

AF & LT winter = averaged winter concentrations at LT and AF (2005-2007); AF & LT summer = averaged summer concentrations at LT and AF (2007); Formenti = concentrations over Namibia at the end of winter 2000; P = concentrations over Nylsvley in the summer of 1997; CRS = particles > 1 and 10, Fine = aerosols < 1; Acet. = CH_3COO^- and Form. = $HCOO^-$; OC = organic carbon; BC = elemental carbon.

The data collected using the UK meteorology office C130 during SAFARI 2000, was only over the Namibian coast line, which is the main region of the anti-cyclone outflow of air masses transported more or less from the northern part of southern Africa.[47] The aerosols were measured for smaller than 1 μm and larger than 1 μm. Despite the difference in position and aerosol size measured, the data collected during the SAFARI experiment compare rather well with the concentrations and species distribution measured at the Louis Trichardt site. This comparison is necessary, as it supports some of the preceding conclusions made pertaining to the composition of the aerosols measured and their influences on atmospheric chemistry over southern Africa, especially the Louis Trichardt region.

Puxbaum[250] also reported chemical data on aerosols collected at Nylsvley in 1997. The data reported by Puxbaum for 4-10 May can be compared to that of the summer campaign of this study and the results are given in Table 5.7. When comparing the PM_{10} data of Louis Trichardt to the PM_{30} measured at Nylsvley, it compares very well. The chemical composition is almost the same at both sites, especially for NO_3^-, organic acid and BC. Regional sources of biomass origin were determined for contributions to the carbon content of the aerosol at the Nylsvley during non-burning days. Only the SO_4^{2-}, NH_4^+ and Ca^{2+} content, which can be directly related to anthropogenic activities, is relatively higher during these sampling periods. This can be directly linked to the vicinity of the Nylsvley site located exactly halfway between Amersfoort and Louis Trichardt. This supports the circular transportation theory of wind masses over southern Africa.

5.7 Dependences and linkages

During the dry season (winter) of the SAFARI 2000 campaign, the aerosol measured within haze layers in the lower troposphere consists of an 80% carbonaceous fraction (organic and elemental) and a total of 15% of sulphate and nitrogen species accounting for the rest.[47] In this study, the average ambient aerosols measured at ground level consisted of carbonaceous fractions ranging between 43% and 65% in the dry winter season and between 27% and 36% for the summer season. During winter, the inorganic species of sulphate, ammonia and nitrate made up on average 25%, 10% and 5%, respectively, with the remaining 5% made up out of different cations and organic acids. During summer, the carbonaceous fraction only represents 30% of the aerosol composition resulting in sulphate, ammonia and nitrate making up

36%, 14% and 10%, respectively, with the remaining 10% made up out of the different cations and organic acids. These aerosols are therefore predominantly acidic over these regions and recirculates during anti-cyclonic conditions.[200,240,241] The large OC fractions observed at both sites can only be ascribed to increased biomass/biofuel/fossil fuel burning (incomplete combustion processes) from different sources in these regions. These possible sources include petrochemical industries, vehicles and informal settlements and are amplified due to the stable winter meteorological conditions and the increased need for heating. In this chapter, the most probable sources contributing to the carbonaceous content of the aerosol were identified for both regions. It is concluded that the carbonaceous content of the aerosol is strongly influenced by incomplete combustion processes of biofuel/fossil fuel and biomass burning from different sources and regions to both sites. The carbonaceous content over the Amersfoort region is mainly influenced by incomplete biofuel and fossil fuel combustion processes. The carbonaceous content over the Louis Trichardt region is mainly influenced by incomplete biofuel combustion processes, of which biomass burning is the main contributor. It can be concluded that complete combustion processes of fossil fuels (mainly coal) dominate the ionic content of aerosols at both sites. This is a direct result of the transport of the ionic content between the industrialised regions near the Amersfoort and Louis Trichardt regions. There are also transformation reactions during transport responsible for the ionic content measured, especially for the formation of nitrate at the Louis Trichardt region.

During summer, the carbonaceous content of the aerosols at both sites decreased with 10-15% and 5-10% at Amersfoort and Louis Trichardt, respectively. This is a clear indication of the impact of biomass burning during winter in southern Africa.

5.8 Aerosol deposition estimates

Deposition values of the ionic component of aerosols were estimated using results from previous inferential method calculations[13] and making use of the concentration data of the aerosol sampling campaigns and the deposition velocities given in Table 5.8. Deposition velocities are specific for the aerosol size and the region it is depositing in. In this study, the two aerosol sizes of $PM_{2.5}$ and PM_{10} were monitored at the two sites (regions) of Amersfoort and Louis Trichardt. The dry deposition velocities of SO_4^{2-}, with an 8 µm diameter as calculated by *Zunckel*[13,12] for Elandsfontein and

Blyde, were used respectively for the PM_{10} monitored at Amersfoort and Louis Trichardt sites. These velocities can be used as they are very close to the PM_{10} size measured for Amersfoort and Louis Trichardt and situated within a 100 km radius of sites where they were calculated by Zunckel, eliminating meteorological conditions as a factor in the deposition calculations (the same reasons as stated in Chapter 4 for gas deposition velocities). Deposition velocities of SO_4^{2-} for $PM_{2.5}$ for forest and grassland of *Lorenz and Murphy*[251] and *Allen et al.*[252] were used, respectively for Louis Trichardt and Amersfoort as they represented the same aerosol size and vegetation. These values were in good agreement with the general deposition velocities calculated for these species.[253,254] *Zunckel 1996 and 1999* show differences of a 1.5 factor between winter and summer deposition velocity rates, which are mostly due to solar radiation. The deposition velocities used in this study for both the aerosol sizes of $PM_{2.5}$ and PM_{10} were adjusted accordingly and all the values used in calculations are presented in Table 5.8.

Table 5.8 Deposition velocities ($cm.s^{-1}$) of the aerosols of $PM_{2.5}$ and PM_{10} at AF and LT derived from *Zunckel's*[13] SO_4^{2-} calculation as well as *Lorenz and Murphy*[251] and *Allen et al.*[252]

Aerosol size	AF Winter	AF Summer	LT Winter	LT Summer
$PM_{2.5}$	0.90	0.57	1.17	0.78
PM_{10}	0.49	0.33	0.36	0.21

**Note that $PM_{2.5}$ velocities are higher than PM_{10} and is due to the combination of the different authors velocities being used.*

Using the average concentration of the aerosol species during the winter and summer campaigns as determined in Table 5.7, the average deposition flux for each aerosol species can be determined. For this study, the deposition fluxes for the summer (November to April) as well as winter (May to October) periods (both 6 months) were determined and the results are provided in Table 5.9. Once the deposition value of each species is determined, its total deposition flux per annum can be calculated and is presented in Table 5.10.

It is clear from Table 5.9 that the deposition flux of all the aerosol species is significantly higher during the winter than the summer periods at both sites. Only the

deposition fluxes of the SO_4^{2-} and NH_4^+ species at both sites do not seem to differ as much as the other species. The reason for this is that the SO_4^{2-} and NH_4^+ concentrations were actually found to be higher during the summer than the winter for both the species, partially eliminating the higher winter deposition velocity. The higher deposition of both species can also be ascribed to their origin, which is anthropogenic and much more consistent and with high concentrations throughout the year than most other naturally occurring species within the aerosol. High OC and BC deposition differences between winter and summer are evident and relate directly to the increased biomass burning and subsequent atmospheric aerosol concentrations during winter. For the rest of the table, higher deposition velocities during winter mean higher winter deposition fluxes. Higher deposition velocities during winter seem to dominate the outcome of deposition fluxes at both these sites when using the inferential model as seen in Table 5.9 compared to data from both Tables 5.7 and 5.8.

Table 5.9 Average winter and summer deposition values ($kg.ha^{-1}$) of aerosol species at AF and LT sites during 2005-2007

	AF & LT winter				AF & LT summer			
	$AF_{2.5}$	AF_{10}	$LT_{2.5}$	LT_{10}	$AF_{2.5}$	AF_{10}	$LT_{2.5}$	LT_{10}
Na^+	0.17	0.18	0.43	0.32	0.06	0.05	0.13	0.09
NH_4^+	1.44	0.96	1.17	0.34	1.23	0.74	1.60	0.39
K^+	0.51	0.36	0.70	0.22	0.07	0.05	0.04	0.02
Mg^{2+}	0.04	0.10	0.04	0.03	0.01	0.01	0.01	0.01
Ca^{2+}	0.12	0.17	0.07	0.05	0.03	0.04	0.03	0.04
CH_3COO^-	0.07	0.06	0.06	0.02	0.01	0.01	0.02	0.01
$HCOO^-$	0.29	0.17	0.54	0.21	0.01	0.01	0.05	0.01
Cl^-	0.10	0.10	0.29	0.23	0.04	0.03	0.04	0.04
NO_3^-	0.83	0.94	0.69	0.46	0.22	0.17	0.07	0.12
SO_4^{2-}	4.00	2.47	3.87	1.13	3.43	2.00	4.52	1.01
$C_2O_4^{2-}$	0.27	0.21	0.38	0.14	0.06	0.05	0.14	0.05
OC	6.69	3.96	5.65	1.95	1.72	1.21	2.47	0.51
BC	3.24	1.81	3.16	0.98	0.87	0.61	1.04	0.19

The deposition flux data for both gas and aerosol species as calculated from measured ambient concentrations are given in Table 5.10. Both the ambient gas and

aerosol concentrations (indicator of sources) are converted to $kg.ha^{-1}.y^{-1}$ to be comparable to their deposition flux units (indicator of sinks) and are given in Table 5.10. The total gas and aerosol dry deposition fluxes of species containing N and S were then calculated.

Table 5.10 Annual total dry deposition fluxes and ambient concentrations of gases and aerosols at AF and LT

	Ambient	Flux	Total N	Total S	T Dry Flux	T Dry amb
Acet.	0.29 (0.20)	0.07 (0.09)			0.07 (0.09)	0.29 (0.20)
Form.	0.71 (1.29)	0.29 (0.58)			0.29 (0.58)	0.71 (1.29)
$C_2O_4^{2-}$	1.17 (1.23)	0.33 (0.53)			0.33 (0.53)	1.17 (1.23)
Ca^{2+}	0.94 (0.69)	0.21 (0.10)			0.21 (0.10)	0.94 (0.69)
Mg^{2+}	0.47 (0.28)	0.11 (0.05)			0.11 (0.05)	0.47 (0.28)
K^+	1.75 (1.39)	0.58 (0.74)			0.58 (0.74)	1.75 (1.39)
$O_{3(g)}$	165.7 (209)	13.9 (46.5)			13.9 (46.5)	165.7 (209)
Na^+	1.05 (2.64)	0.23 (0.55)			0.23 (0.55)	1.05 (2.64)
Cl^-	0.57 (1.65)	0.14 (0.32)			0.14 (0.32)	0.57 (1.65)
SO_4^{2-}	22.3 (18.3)	7.42 (8.40)		9.82	9.82 (9.49)	33.3 (21.1)
$SO_{2(g)}$	11.0 (2.75)	2.40 (1.09)		(9.49)		
$NO_{2(g)}$	4.80 (1.37)	0.63 (0.50)				
NH_4^+	8.42 (6.12)	2.67 (2.77)	5.8			
$NH_{3(g)}$	1.97 (1.96)	0.47 (1.00)	(6.0)		5.8 (6.0)	21.6 (13.7)
$HNO_{3(g)}$	1.57 (0.48)	0.93 (0.96)				
NO_3^-	4.84 (3.74)	1.11 (0.76)				
CO	23.4 (16.0)	8.41 (8.13)				
BC	11.0 (8.0)	4.11 (4.20)				

g = gas; Ambient = ambient concentrations converted to $kg.ha^{-1}.y^{-1}$; Flux = deposition flux of species in $kg.ha^{-1}.y^{-1}$; Total N = Total dry deposition flux of nitrogen in $kg.ha^{-1}.y^{-1}$; Total S = Total dry deposition flux of sulphur in $kg.ha^{-1}.y^{-1}$; T Dry Flux = Total dry deposition flux of aerosol species in $kg.ha^{-1}.y^{-1}$; T Dry amb. = Total dry ambient concentrations of species converted to $kg.ha^{-1}.y^{-1}$; (values) = Louis Trichardt values; Acet. = CH_3COO^- and Form. = $HCOO^-$; OC = organic carbon; BC = elemental carbon.

Table 5.10 indicates the comparison of the amount deposition per species taking place at the Amersfoort and Louis Trichardt sites (regions) within a year and the ambient concentration of the deposited species available for deposition per hectare per year. According to this out of all the potentially depositionable species per hectare per year on average only between 25 to 50 % gets deposited at each site. For HNO_3 at the Louis Trichardt site all the the potentially depositionable HNO_3 per hectare per year gets deposited at the site. The deposition totals indicate organic acid deposition to dominate at the Louis Trichardt site, while deposition of the mineral cations Ca^{2+} and Mg^{2+} will dominate at Amersfoort and both is characteristic of aerosol loadings in each region considering their major emission sources. As suspected, the deposition of K^+ (indicator of biomass burning) and the marine species Na^+ and Cl^- dominate at the Louis Trichardt site. The large difference in concentration between the ambient SO_2 of the sites, with the SO_4^{2-} concentrations almost the same, indicates sulphate sources to be significantly closer to the Amersfoort site.

Nitrogen and sulphur are some of the key elements that influence productivity in the biosphere[187] and the study of the deposition of their compounds is important in atmospheric studies. In total, 30% of all dry S (sulphur) emissions in the Amersfoort region is deposited, while 45% is deposited at Louis Trichardt. For total dry N (nitrogen) emissions, only 27% is deposited in the Amersfoort region and 44% of it in Louis Trichardt region. Therefore, one can conclude that most of the anthropogenic S and N emissions from the Highveld region are transported and deposited in the Louis Trichardt region, far away from the actual sources. The anthropogenic trace gases add to this problem, as their concentrations near the source are high enough to result in excess concentrations (not deposited) that are readily incorporated into aerosols and transported elsewhere to be deposited.

CHAPTER 6

Modelling heterogeneous atmospheric processes

In this chapter, a short introduction to the reason why modelling is important is provided. The basic principles of the model used in this study are briefly discussed, as well as the parameters used in this particular model. The modelling results obtained are provided and discussed in comparison to the measured aerosol concentrations. The formation of SOA (Secondary Organic Aerosols) is briefly discussed and the validation of the model results is done by means of comparison to similar studies.

6.1 Introduction

Heterogeneous reactions of trace gases on particulate matter in the atmosphere must be considered in the troposphere as aerosol particles are most abundant in the polluted boundary layer.[255] Most atmospheric compounds tend to partition between the gas and suspended particulate matter (PM) present in the atmosphere. Knowledge of the physical state and composition of particles is therefore of great importance, as they play key roles in atmospheric processes.[144] The main goal is to develop or choose an atmospheric model that accurately depicts the air quality of a region. To do that, the measured concentration of gases and aerosols (anthropogenic emissions and natural) and meteorological parameters must be incorporated within one model. This model must be able to simulate the aging process (deposition/degradation and transformation processes) of aerosols due to heterogeneous reactions, transport, nucleation and emissions. This has been accomplished by using the combined ORISAM-0-D (Organic and Inorganic Spectral Aerosol Model[48,49,20,50]) and Global CTM TM4 chemistry transport model[52,53] called the ORISAM-TM4 model. This model is able to accommodate size-differentiated chemistry in a selectable number particle sizes and optional gas phase chemistry schemes to model the formation of secondary inorganic and organic aerosols with the focus on the formation of secondary organic aerosols (SOA).

6.2 Modelling Results

In Figure 6.1, the basic principles for the ORISAM-TM4 are presented. The graphical presentation is followed by the initial parameters and conditions set for the simulations in this particular study. The initial emission concentrations for aerosols and gases are the ones measured during the 2005-2007 winter and summer aerosol campaigns, as well as gas data from the same time period measured at the Amersfoort and Louis Trichardt sites.

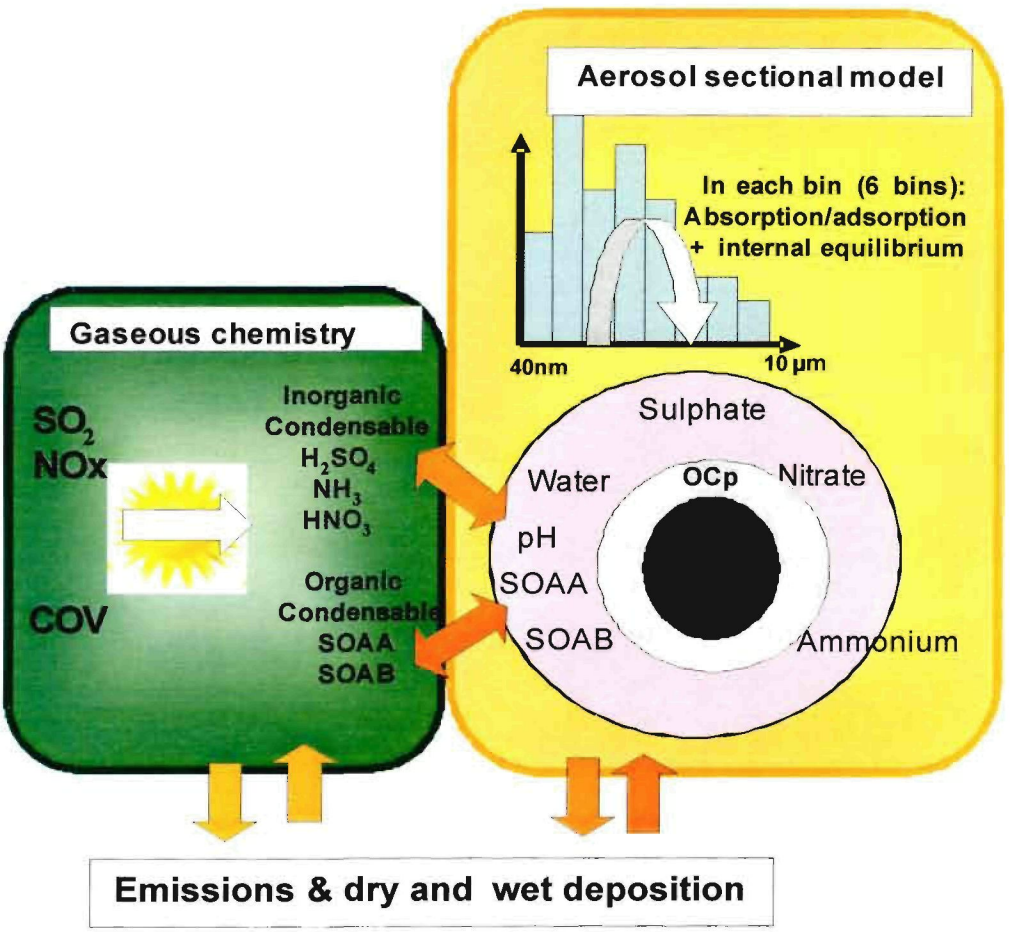


Figure 6.1 *A graphical representation of the ORISAM-TM4 model*[50]

The following initial set of parameters was used to simulate the conditions during the study period:

A 3°x2° horizontal grid at 31 vertical levels (10hPa) was used together with ECMWF wind and precipitation data of every six hours from January 2005 to March 2007. It included dry and wet deposition, the gaseous chemistry of *Houweling et al.,*[165] while utilising an ORISAM model with six bins ranging from 0.04 to 40µm. The

heterogeneous chemistry on dust and sea-salt was included with gas emission data from POET (COV) and EDGAR3 (other gases) as well as combustion emissions from Liousse *et al.*,[256] the daily biomass burning emission data from January 2005 to March 2007 and the fossil fuel emissions for the year 2000. The dust scheme of *Zakey et al.*[257] and the sea-salt scheme of *Gong et al.*[258] were used in the model.

From Figure 6.1 it is clear that the initial content of BC, sea-salt and OC of aerosol and gases, as well as the humidity for aerosol formation within the ORISAM-TM4 model are very important. The particle sizes, however, have no effect on the secondary aerosol formation within this model[50] and will not be discussed further. The modelling results gained with the ORISAM-TM4 model were compared to the experimental results measured at the sites of both regions and of each campaign. The results are plotted against the experimental values in Figures 6.2-5.

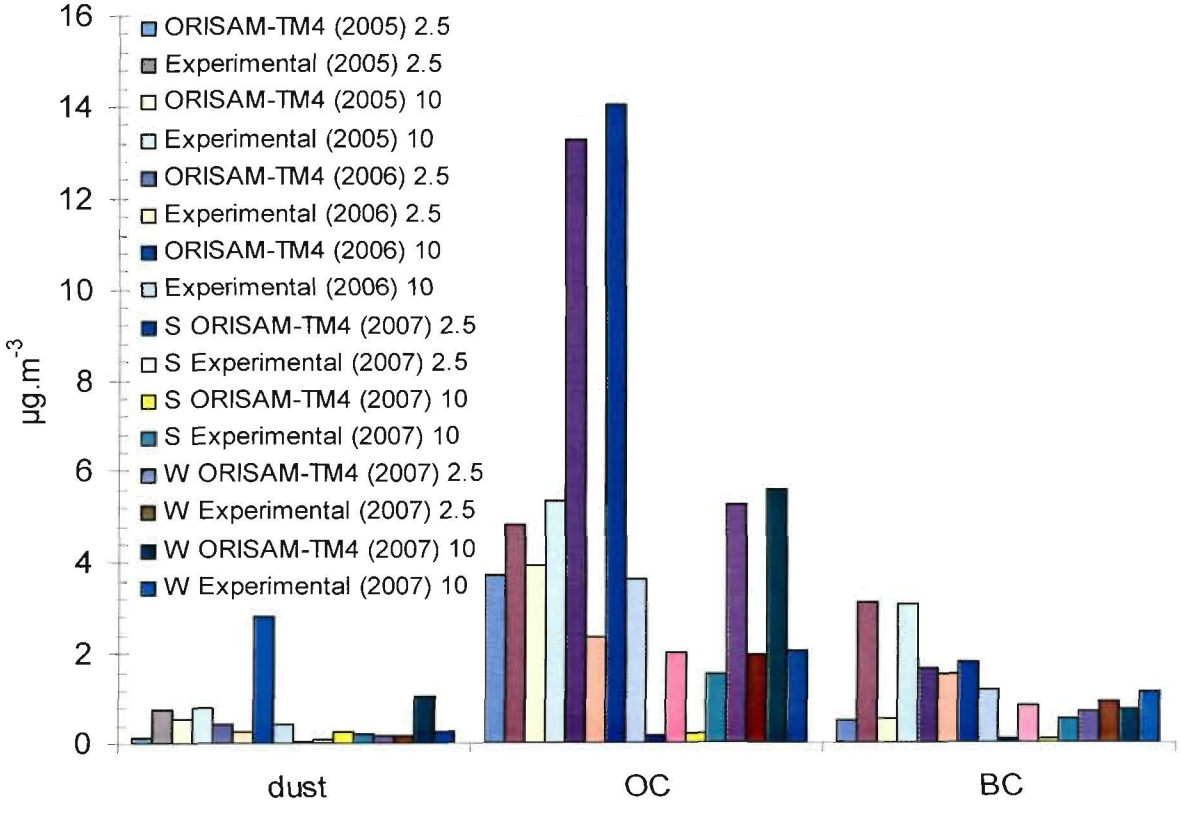


Figure 6.2 *Modelled aerosol concentrations compared to experimental results of dust (K^+, Mg^{2+}, Ca^{2+}), OC and BC at Louis Trichardt for the 2005-2007 monitoring campaigns*

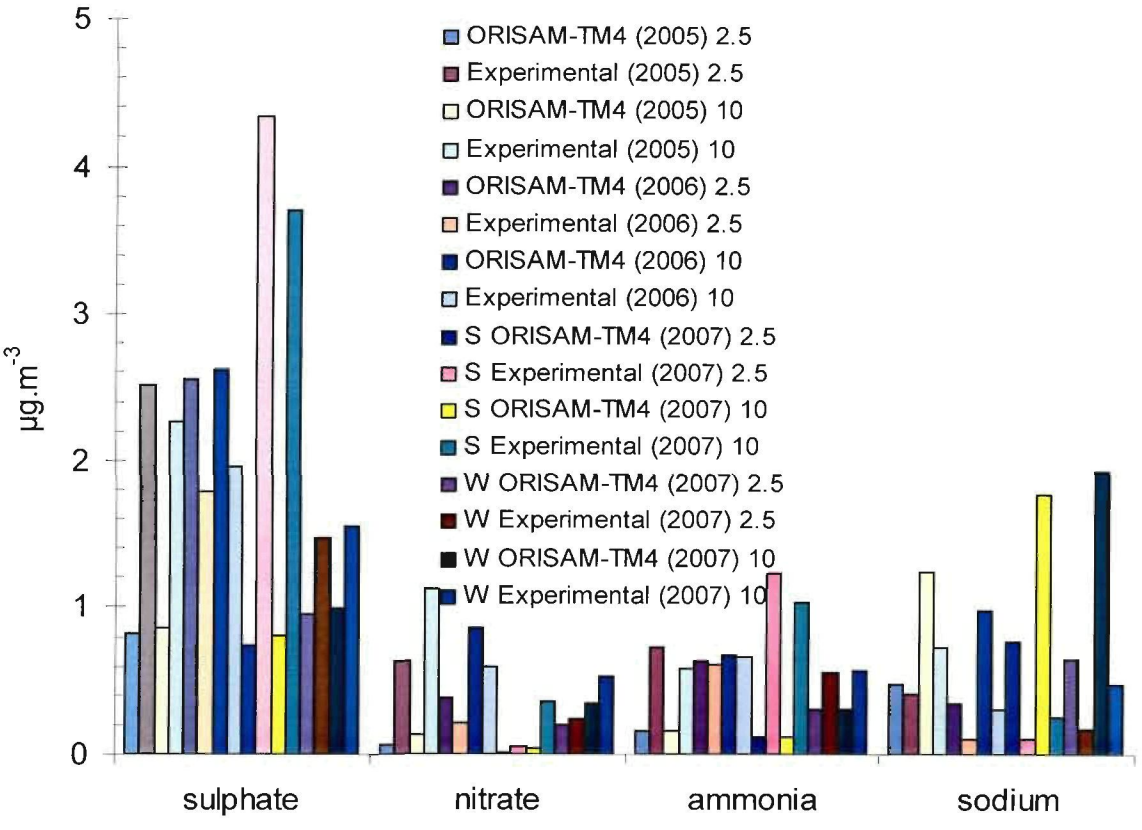


Figure 6.3 *Modelled aerosol concentrations compared to experimental results of sulphate, nitrate, ammonia and sodium at Louis Trichardt for the 2005-2007 monitoring campaigns*

The modelling results for the 2006 winter campaign (Figure 6.2-5) compared best with the experimental results. Percentage accuracies of experimental/modelling ratio for SO_4^{2-} of 71-87%, for NO_3^- of 84-88%, for NH_4^+ of 66-59% and for BC of 66-92% were found at Amersfoort for $PM_{2.5}$-PM_{10}, respectively. Also, percentage accuracies for SO_4^{2-} of 70-75%, for NO_3^- of 53-69%, for NH_4^+ of 96-98% and for BC of 67-92% were found at Louis Trichardt for $PM_{2.5}$-PM_{10}, respectively.

The OC compares the best for the 2005 and 2007 winter campaigns, with accuracy ratios at Louis Trichardt for 2005 of 73-77%, Amersfoort for 2005 of 70-74% and Amersfoort for 2007 of 76-87% as seen in Figures 6.2-5. The OC winter/summer concentration ratios of the model and experimental results for 2007 are poor for both sites. They show large differences for both sites, especially at Louis Trichardt. It is suspected to be due to temperature (high average temperature of 23°C) effects at Louis Trichardt that cause all the VOC precursors to be in the gas phase and thus inhibiting SOA formation. This is a similar but even larger difference than previously

found by *Liousse et al. 2005.*[50] The model simulation between winter and summer for OC is poor, especially at Louis Trichardt and is probably due to the complex chemistry of different OC sources contributing during winter and summer. At Amersfoort, the simulation indicates a 2.5 times difference with the experimental values (that are within an expectable range) and a much better correlation due to more similar sources for both winter and summer periods. The model predicts both OC and BC concentrations at Amersfoort that are double in difference from the other aerosol species simulations. This difference in predictions doubles again to the Louis Trichardt region for OC and BC, respectively, where the model predictions are as far off as 20 times for OC.

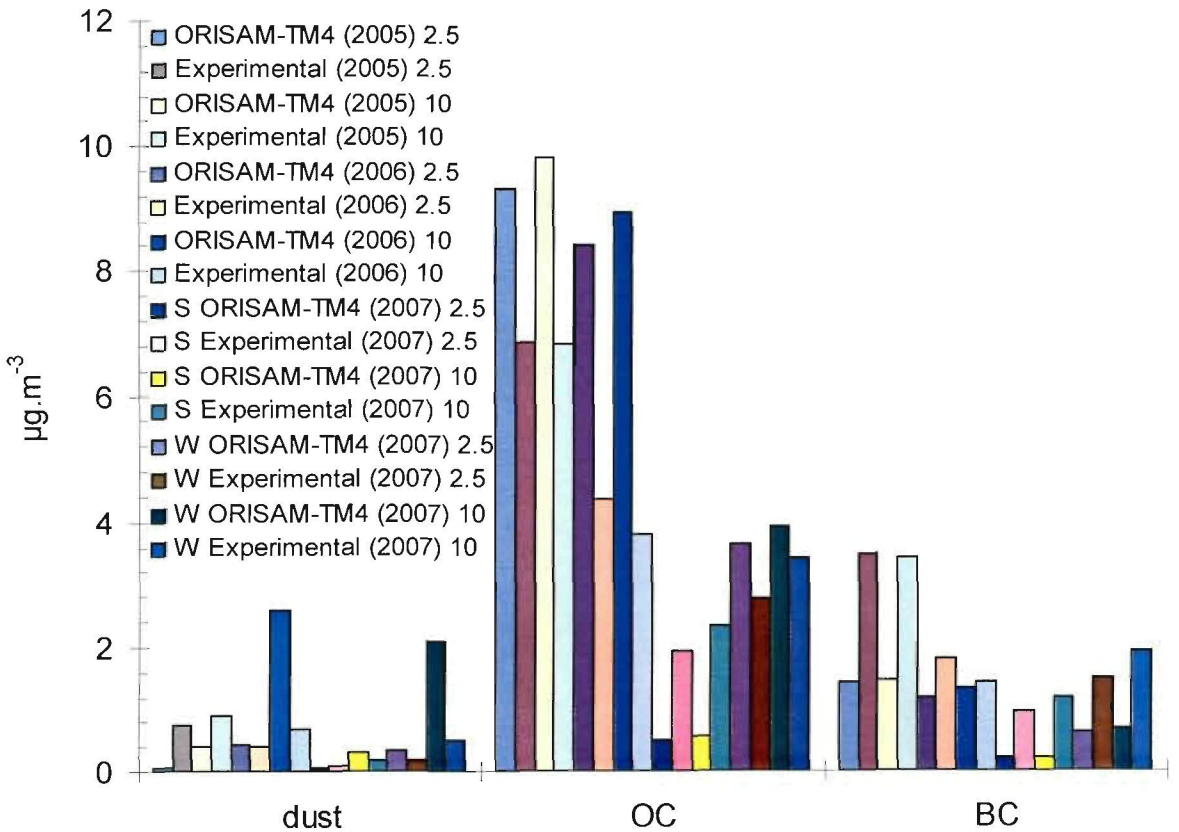


Figure 6.4 *Modelled aerosol concentrations compared to experimental results of dust (K^+, Mg^{2+}, Ca^{2+}), OC and BC at Amersfoort for the 2005-2007 monitoring campaigns*

For both winter periods of 2005 and 2007 at Amersfoort (with low humidity and temperature) the SO_4^{2-}, NO_3^-, NH_4^+, BC and OC experimental/model percentage accuracy ratios are within 90% of each other for both the winter campaigns. This indicates good accuracy and reproducibility of the model to simulate results during

winter periods, when no real interferences of humidity, temperature and variable gas concentrations are present. The same is not true for the winter period of 2005 at the Louis Trichardt site where the percentage ranges of the experimental/model ratios are not consistent. This is largely due to the higher temperatures (above the 20°C threshold) and slight differences in emission data concentrations. This results in a significant under-prediction of the model concentrations as aerosol formation with this model is very sensitive to the above-mentioned parameters. The effect of high temperature can be deduced from Figures 6.2-5 as the poorest comparison between the model and experimental results exists for both sites during the summer campaign in 2007.

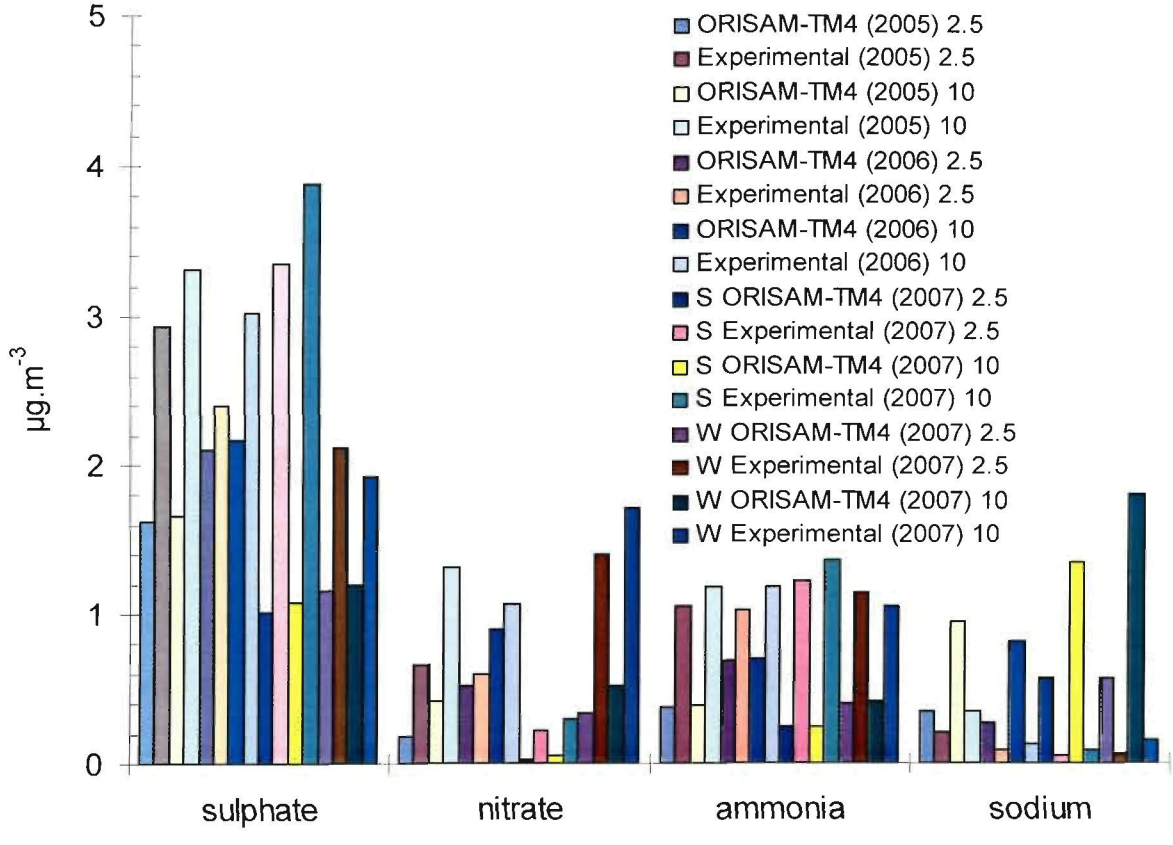


Figure 6.5 *Modelled aerosol concentrations compared to experimental results of sulphate, nitrate, ammonia and sodium at Amersfoort for the 2005-2007 monitoring campaigns*

The inorganic species of SO_4^{2-}, NH_4^+ and Na^+ at both the Amersfoort and Louis Trichardt sites, indicate that the winter/summer concentration ratios of the model are consistent 1 to 2.5 times less than the experimental values for the 2007 campaigns.

This, together with the percentage accuracy for winter, suggests that the winter predictions for these species with this model will be consistent and reproducible. This also means that the winter to summer predictions are consistent to one another for these species. This also compares well with the model-to-experimental results found for data from the ESQUIF experiment by *Liousse et al.*[50]. The summer experimental/model percentage accuracy ratios range between 10-21% and although consistent, will under-predict every time. The 1 to 2.5 times difference in the winter/summer concentration ratio for the aerosol species of BC and dust also exists at Amersfoort. The accuracy ratio thereof, however, means consistent under-predictions of the model. The model is able to predict the NO_3^- concentrations within the 1 to 2.5 times winter/summer ratio of the model-to-experimental results at Amersfoort. The winter/summer concentration ratio of OC of Amersfoort and the OC, BC and NO_3^- at Louis Trichardt, however, are not within the same 1 to 2.5 times difference and far exceeds this consistency of the model to predict from winter to summer periods. The difficulty for the model to predict NO_3^- at Louis Trichardt is due to its complex chemistry (mixed anthropogenic and biogenic) within the region. The model and the experimental results both indicated more aerosols present during winter at both sites for all aerosol species. This is due to winter conditions, which are more favourable for aerosol formation, as low temperatures persist in respect to the summer of less favourable conditions for aerosol formation due to high temperatures. The concentrations of SO_4^{2-} were higher during the summer at both sites as well as for NH_4^+ at the Louis Trichardt site. This most probably has to do with the season and the chemistry with gases associated with it.

Except for the 2005 winter period, the model's predictions overall compare better at the Louis Trichardt site for the SO_4^{2-}, NO_3^-, NH_4^+, BC and OC aerosol species. The only campaign that has a very good comparison is the winter of 2006. This is most probably caused by different sets of model simulation results incorporated as one to accommodate the time period of the experimental campaign. This could also have been caused by the almost perfect parameter conditions for secondary aerosol formation during this campaign. It is also important to note that when the BC comparison of the model is good, the other simulated species comparison is also good. This shows the importance of the initial BC concentration data incorporated into the model as can be seen in Figure 6.1. The model-to-experimental comparisons of dust and Na^{2+} (sea-salt) seem to have no correlation between winter campaigns at the

same site. There does, however, seem to be a slight correlation between the sites themselves within the same sampling periods and this may indicate its relation to initial emission concentrations of aerosol and gas data used in the model.

6.3 Secondary aerosol formation and its validation

Seeing as BC is an inert species, it can be used to determine SOA formation, as any decrease in BC/OC_{tot} ((OC_{tot} = OC_p + OC_{sec}), with OC_{sec} = SOA and OC_p = experimental)), may be interpreted as an indicator of SOA production.

Table 6.1 The BC/OC_{tot} % ratios for $PM_{2.5}$ and PM_{10} at both sites for 2005-2007

Campaign	Simulated BC/OC_{tot} ratio (%)				Measured BC/OC_{tot} ratio (%)			
	$AF_{2.5}$	AF_{10}	$LT_{2.5}$	LT_{10}	$AF_{2.5}$	AF_{10}	$LT_{2.5}$	LT_{10}
2005	8.9	8.8	6.0	5.8	21.5	20.5	36.3	32.9
2006	9.3	10.5	10.7	10.1	14.2	11.3	9.9	6.8
2007 (W)	8.5	7.6	3.9	5.4	40.2	40.8	38.4	42.4
2007 (S)	9.8	9.4	10.3	10.1	23.2	26.5	13.3	15.2

It is clear from Table 6.1 that there is a decrease in the BC/OC_{tot} ratio from the summer to the winter periods in the modelling results. This shows an increase in SOA formation during summer compared to winter as can be seen in Table 6.1; this was also found in similar studies.[50] SOA formation depends on photochemistry, precursor gas and aerosol concentrations, as well as temperature. This is still insignificant compared to the BC influence on the model simulation thereof, especially during summer under southern African conditions. The low and unpredictability of BC makes it impossible for the model to accurately predict SOA production between the two seasons at both sites. The experimental BC/OC_{tot} ratios range between 32.9-42.4% and 13.3-15.2% in winter and summer, respectively for the Louis Trichardt site. While 20.5-40.8% and 23.2-26.5% experimental BC/OC_{tot} ratios exist for winter and summer, respectively at the Amersfoort site. This compares well with experimental data found for urban areas by *Castro et al.*[248] for Coimbra in Portugal in the summer of 1993 (33%) and winter of 1992-1993 (48%). This in turn compares well with the ORISAM model data found by *Liousse et al.*[50] during the ESQUIF experiment. These results can still be compared without using the poor BC simulations by using the

$OC_P/OC_P + OC_{sec}$ ratios and comparing them to BC/OC_{tot} ratios from the experimental concentrations. This will provide a good idea of SOA production in the two seasons, which resulted in ratios of 27-88% and 43-81% from winter to summer at Louis Trichardt and Amersfoort, respectively. This favours SOA formation during winter in contrast to the experimental ones favouring summer. This indicates that the OC simulations of the model in the southern African conditions are not as good.

6.4 Dependences and linkages

Simulations of the ORISAM-TM4 model seem to give a good representation for the winter periods at both sites (although slightly better for Louis Trichardt) and sizes for most aerosol species when no humidity, temperature or precursor gas influences are present. The simulations are especially good when the optimum of the above parameters is present, as in the winter of 2006. The model predictions for most of the aerosol species during summer seem to be poor. The model is unable to accurately simulate OC, BC and dust at both sites during summer and also NO_3^- at Louis Trichardt during summer. The OC simulations are also very poor during summer, especially at Louis Trichardt and are mainly influenced by temperature as well as the vast range of different sources contributing to the atmospheric chemistry at this site during the winter and summer seasons. The different sources of the carbonaceous aerosols during the winter and summer periods are described in Chapter 5 and may be the origin of the large under-predictions in summer, especially at the Louis Trichardt site. This was the first attempt at comparing modelling and experimental results on the chemical composition of an aerosol with the ORISAM-TM4 model in southern Africa. The ORISAM-TM4 contains a model (Organic and Inorganic spectral aerosol model) that makes it possible to get an all-gridded point chemical composition for the primary aerosol (BC, OC_p and dust) as well as the secondary aerosol (sulphates, nitrates, ammonium and OC_{sec}). Comparisons are globally good, as was found during the winter campaigns in this study. There is, however, a problem with the inorganic component in the model leading to larger under-predictions of especially sulphates and nitrates as seen in this study at both the Amersfoort and Louis Trichardt sites.

CHAPTER 7

Critical evaluations

In this chapter, the study will be evaluated by means of its success in achieving the study objectives.

7.1 Evaluation of study objectives reached

The success of this study will be evaluated according to the extent the objectives set in Chapter 1 were reached, as well as the contribution it makes to the current knowledge within this field of study. The initial objectives are presented in Paragraph 1.2 and their critical evaluation given in the same order.

Objective 1:

The first objective was to determine ambient concentrations of inorganic gases and the ionic fraction of aerosols at selected sites. This was successfully done with a long-term data set of over 10 years of credible inorganic gas concentration data measured on a monthly basis for SO_2, NO_2, O_3, NH_3, and two years of HNO_3 data. This was measured at the four remote sites — Louis Trichardt (South Africa), Cape Point (South Africa), Amersfoort (South Africa) and Okaukuejo (Namibia) — in southern Africa. The ionic content of the aerosol was determined in three winter campaigns and one summer campaign. A total of 96 samples were collected at the Amersfoort and Louis Trichardt sites on a daily basis over a 49-day period between 2005 and 2007 for $PM_{2.5}$ and PM_{10}. All the samples collected were successfully analysed for their ionic composition by an international laboratory operating within the WMO framework. By determining the ionic composition of the aerosol, protocols were developed for future use in sampling and analysing for the ionic composition of aerosols in South African conditions.

Objective 2:

The validation of all analytical results was successfully done according to protocols set by international programmes. The gas pollutants measured in this study were chosen based upon the US EPA. The credibility of all the diffusive gas data was established through inter-comparison studies with the diffusive samplers of IVL, CSIRO (laboratories operating within the WMO framework) and active sampling methods of Elandsfontein, Cape Point (GAW) and the Vaal Triangle research stations. This was done for SO_2, NO_2, O_3 and NH_3, on more than one occasion and is an ongoing process. The most recent project of this kind the laboratory was involved in, is the participation in the development and quality control procedures for diffusive samplers for SO_2 and NO_2 in collaboration with the University of Singapore (September 2007 campaign). The results correlated well with most of the institutions that participated, especially with the IVL. The standard methods for diffusive sampling were also compared to those used internationally as published by GAW (no.122), which is internationally acknowledged. The diffusive sampling methods of this study compare well to quality checks like detection limits and covariances of the IDAF Laboratoire d' Aérologie, Toulouse, France. This also ensures the quality of the data. All aerosol analytical procedures were performed at the IDAF Laboratoire d' Aérologie, Toulouse, France, which is part of the quality control of the DEBITS network and a lab recognised within the WMO network itself.

Objective 3:

The total organic composition of aerosols, organic carbon (OC) as well as elemental carbon (BC) was determined with great success during three winter campaigns and one summer campaign. A total of 96 samples were collected at the Amersfoort and Louis Trichardt sites on a daily basis over a 49-day period between 2005 and 2007 for $PM_{2.5}$ and PM_{10}. All the samples collected were successfully analysed for their carbonaceous composition by an international laboratory operating within the WMO framework. By successfully determining the carbonaceous composition of the aerosol, protocols were developed for future use in sampling and analysing for the carbonaceous composition of aerosols in South African conditions.

Objective 4:

All the accumulated and accredited ambient gas and aerosols data measured during the sampling campaigns at both sites were successfully used and compared with the ORISAM-TM4 model. The model simulations compared well to the experimental results and indicate their success in modelling the fate of gases and aerosols in South African conditions.

Objective 5:

Possible sources contributing to the organic (aerosol) and ionic (aerosol and gases) composition of these atmospheric constituents over the selected regions could be successfully identified. Concentration trends for aerosol and gas species were successfully scrutinised and a seasonal and annual profile established. The seasonal and annual trends of the inorganic gases performed in this study have resonantly been published in *Martins et al.*[221]

7.2 Disappointments of study

The only real disappointment of the study was the unavailability of deposition velocity values for both inorganic gas and aerosol species in selected regions of this study, especially the Cape Point region. This may have a notable effect on accuracy when calculating the deposition fluxes. In order to improve on this aspect, flux measurements needs to be undertaken which were beyond the scope of this study. The availability of only one summer aerosol campaign to establish the aerosol composition trend during summer is also viewed as a real short-coming, since no good correlations between measured and modelled values was found.

7.3 Future research opportunities

It is necessary to continue and expand the gas and aerosol experimental data set in order to provide data for improved model simulations for all meteorological conditions and time periods of the year. This will improve the model simulations of all secondary aerosol formations under southern African conditions. Also, there needs to be wet deposition data for the same periods as dry deposition data and both need to be used to determine the total deposition fluxes. There is a need to develop a surface model (with adapted conditions for southern African ecosystems) for comprehensive models

like ORISAM-TM4 to simulate realistic dry deposition velocities for gases and aerosols. It is also necessary to find ways to analyse the organic part of the aerosol in more detail in order to assist in source quantification and the transportation thereof.

REFERENCES

1. Lehmann B.M.C., Bowersox Van C., Larson S.L. and Larson S.M., 2007. Monitoring Long-term trends in sulfate and ammonium in US Precipitation: Results from the National Atmospheric Deposition Program Trends Network. Water Air Soil *Polut: Focus*, **7**, 55-66.

2. Flower D., Rognvald S., Muller J., Cape J.N., Sutton M., Erisman J.W. and Fagerli., 2007. Long term trends in sulphur and nitrogen deposition in Europe and the cause of Non-linearities. *Water Air Soil Pollut: Focus*, **7**, 41-47.

3. Soloman S., Qin D., Manning M., Chen Z., Marquis M., Averyt K.B., Tignor M. and Miller H.L., IPCC. 2007. *Climate change 2007*: The Physical Science Basis. Contribution of Working Group I to the Fourth Assessment Report of the Intergovernmental Panel on Climate Change, Cambridge University Press, Cambridge, United Kingdom and New York, NY, USA, summary, 2pp.

4. Ravishankara A., Liu S., Platt U., Bates T., Bey I., Carslaw K., Chipperfield M., Douglass A., Fahey D. and Feingold G. 2003. Climate chemistry interactions, A report from the joint SPARC/IGAC workshop, International Global Atmospheric Chemistry Project, *IGACtivities Newslet.*, Issue No. 30, 2, June 2004.

5. Wells R.B., Lloyd S.M. and Turner C.R., 1996. National air pollution source inventory. Chapter 1 in Held G., Gore B.J., Surridge A.D., Tosen G.R., Turner C.R. and Walmsley R. (eds.), *Air pollution and its impacts on the South African Highveld*. Environmental Scientific Association, Cleveland, 3-9.

6. Turner C.R., 1993. A seven year study of rain chemistry in South Africa. Proceedings of the 24th *National Association for Clean Air Conference, Clean Air Challenges in a Changing South Africa, Paper No.5*, Dikhololo Game Lodge, Brits, 11-12 November, 7pp.

7. Turner C.R., Wells R.B. and Olbrich K.A., 1996. Deposition chemistry in South Africa. Chapter 12 in: Held G., Gore B.J., Surridge A.D., Tosen G.R., Turner

C.R. and Walmsley R. (Eds.), *Air pollution and its impacts on the South African Highveld*. Environmental Scientific Association, Cleveland, 80-85.

8. Held G., De Beer G. and Mphepya J.N., 1999a. *The Kiepersol Project: A national Network for Acid Rain Research (July 1998-1996)*. TRR/T99/056, Eskom, Johannesburg, 76pp.

9. Held G. and Mphepya J.N., 2000. Wet and Dry deposition in South Africa. *Proceedings, XI Congresso Brasiliero de Metoerologia* (CD ROM), SBMET, Rio de Janeiro, 16-20 October, 2824-2833.

10. Mphepya J.N., 2002. *Atmospheric Deposition characteristics of sulphur and nitrogen compounds in south Africa*, Ph.D thesis, North West University. Potchefstroom.

11. Turner C.R., Wells R.B. and Zunckel M., 1995. Dry deposition monitoring methodologies for the highveld region. *Proceedings of the 26th Annual Clean Air Conference of NACA, Durban, 22-24 November*, 17pp.

12. Zunckel M., Turner C.R. and Wells R.B., 1996. Dry deposition of sulphur on the Mpumalanga highveld: In a pilot study using the inferential method. *SA J. Sci.*, **92**, 485-491.

13. Zunckel M., 1999. Deposition of sulphur over eastern South Africa. *Atmos. Environ.*, **33**, 3515-3529.

14. Mphepya J.N. and Held G., 1999. Dry deposition of sulphur on the Mpumalanga highveld 1996-1998. *Proceedings of the 1999 Annual Conference of NACA, Cape Town, 7-8 October*, 10pp.

15. Seinfeld J.H. and Pandis S.N., 2006. *Atmospheric Chemistry and Physics*. Wiley&Sons, Inc., New Jersey, 1203pp.

16. Brasseur G.P., Orlando J.J. and Tyndall G.S. 1999. *Atmospheric chemistry and Global change.* Oxford University Press, 1007 pp.

17. Seinfeld J. H., 1985. *Atmospheric Chemistry and Physics of Air Pollution*, John Wiley & Sons, 5-8pp.

18. Gao W. and Wesely M.L., 1995. Modelling gaseous dry deposition over regional scales with satellite observations-1. Model development. *Atmos. Environ.* **29**, 6, 727-737.

19. Brimblecombe P., Air composition and chemistry, 2nd ed., 1996. Cambridge *Environmental Chemistry series 6*, 253pp.

20. Cousin F., Liousse C., Cachier H., Bessagnet B., Guillaume B. and Rosset R. 2005. Aerosol modelling and validation during ESCOMPTE 2001. *Atmos. Environ.* **39**, 1539-1550.

21. Ravishankara A.R. 1997. Heterogeneous and multiphase chemistry in the troposphere. *Science*, **276**, 1058-1065.

22. Charlson R.J., Swhartz S.E., Hales J.M., Cess R.D., Coakley Jr. J.A., Hansen J.M. and Hofmann D.J., 1992. Climate forcing by Anthropogenic aerosols. *Science* **255**, 423-430.

23. Penner J.E., Chaung C.C. and Liousse C., 1996. The contribution of Carbonaceous Aerosols to climate change. In Kulmala M., Wagner P.E. (Eds), *Nucleation and Atmospheric Aerosols*. Elsevier Science (Ltd), Amsterdam, 759-769pp.

24. Adams P.J., Seinfeld J.H., Koch D., Mickley L. and Jacob D., 2001. General circulation model assessment of direct radiative forcing by the sulphate-nitrate-ammonium-water inorganic aerosol system. *J. Geophys. Res.*, **106**, 1097-1111.

25. Houghton J.T., Meira Filho L.G., Callendar B.A., Haris N., Katenberg A. and Maskell K. (eds), 1995. Cambridge University Press. IPCC Climate Changes, The Science of Climate Change. In O'Dowd C., Kulmala M. and Hoffmann T., (eds), *IGACtivities Newsl.*, **18**, September 1999, 2pp.

26. Dentener F.J., Carmichael G.R., Zang Y., Lelieveld J. and Crutzen P.J., 1996. Role of mineral aerosol as a reactive surface in the global troposphere. *J. Geophys. Res.*, **101**, 22, 869-889.

27. International Panel on Climate Change (IPPC), 2001. *Climate Change 2001*, Cambridge Univ. Press, New York, 944pp.

28. Ramanathan V., Crutzen P.J., Holben B. and Priestley I., 2001. Indian Ocean Experiment: An integrated analysis of the climate forcing and effects of the great Indo-Asian haze. *J. Geophys. Res.*, **106**, 28, 371-398.

29. Andrea M.O., Artaxo P., Brandao C., Carswell F.E., Ciccioli P., da Costa A.L., Culf A.D., Esteves J.L., Gash J.H.C., Grace J., Kabat P., Lelieveld J., Malhi Y., Manzi A.O., Meixner F.X., Nobre A.D., Ruivo M.D.L.P., Silva-Dias M.A., Stefani P., Valentini R., von Jouanne J. and Waterloo M.J., 2002. Biogeochemical cycling of carbon, water, energy, trace gases and aerosols in Amazonia: The LBA-EUSTACH Experiment. *J. Geophys. Res.*, **107**(D20), 8066.

30. O'Dowd C., Kulmala M. and Hoffmann T., 1999. New Particle Formation, IGAC (International Global Atmospheric Chemistry Project), *IGACtivities Newslet.*, Issue No. 18, September 1999, 2pp.

31. Wexler A.S. and Potukuchi S., 1998. Kinetics and thermodynamics of troposperic aerosols. In Harrison R.M. and van Griecken R., (eds.) *Atmospheric Particles*, John Wiley, New York, 203-231pp.

32. Prospero J.M. and Savoie D.L., 1989. Effect of continental sources on nitrate concentrations over the Pacific Ocean. *Nature,* **339**, 687-689.

33. Savoie D.L. and Prospero J.M., 1989. Comparison of oceanic and continental sources of non-sea salt sulfate over the Pacific Ocean. *Nature,* **339**, 685-687.

34. Zang Y., 1994. *The chemical role of mineral aerosols in the troposphere in east Asia.* Ph.D. Thesis, Department of Chemical and Biochemical Engineering, University of Iowa. Iowa City.

35. Nishikawa M., Kanamori S., Kanamori N. and Misoguchi T., 1991a. Kosa aerosol as eolian carrier of anthropogenic material. *The Science of the Total Environ.*, **107**, 13-27.

36. Nishikawa M., Kanamori S., Kanamori N. and Misoguchi T., 1991b. Environmental significance of the Kosa aerosol (yellow sand dust) collected in Japan. *Proceedings of the 2nd IUAPPA Regional conference on Air Pollution, Seoul, Korea, 4 September*, 35-41pp.

37. Nishikawa M. and Kanamori S., 1991. Chemical composition of Kosa aerosol (yellow sand dust) collected in Japan. *Anal. Sci.*, **7**, 1127-1130.

38. Horai S., Minari T. and Migita Y., 1993. *Aerosol composition in Kagosima.* Annual Report of the Kagosima Prefectural Institute, 9.

39. Harkel M.J., 1997. The effects of particle-size distribution and chloride depletion of sea-salt aerosols on estimating atmospheric deposition at a coastal site. *Atmos. Environ.*, ***31***, 417-427.

40. Lacaux J., Carmichael G.R., Cieslik S., Galtier B., Hoepffner M. and Miller J., 1997. *ATELIER IDAF WORKSHOP*, Toulouse, 15-17 October 1997.

41. Song C.H. and Carmichael G.R., 1998. The aging process of naturally emitted aerosol (sea-salt and mineral aerosol) during long range transport. *Atmos. Environ.*, **33**, (1999) 2203-2218.

42. Andrea M.O. and Merlet P., 2001. Emissions of trace gases and aerosols from biomass burning. *Global Biogeochem. Cycles*, **15**, 955-966.

43. Hao W.M. and Liu M.H., 1994. Spatial and temporal distribution of tropical biomass burning. *Global Biogeochem. Cycles*, **8**, 495-503.

44. Schmid B., Redemann J., Russel P.B., Hobbs P.V., Hlavka D.L., Mcgill M.J., Holben B.N., Welton E.J., Campbell J., Torres O., Kahn R.A., Diner D.J., Helmlinger M.C., Chu D.A., Robles Gonzales C. and de Leeuw G., 2003. Coordinated airborne space borne, and ground based measurements of

massive thick aerosol layers during the dry season in Southern Africa. *J. Geophys. Res.*, **108** (D13), 8496.

45. Swap R.J., Annegarn H.J. and Suttles J.T., 2003. In: Africa burning. A thematic analysis of the Southern African Regional Science Initiative (SAFARI 2000). *J. Geophys. Res.*, **108**, D13, 8465.

46. Annegarn H.J., Turner C.R., Helas G., Tosen G.R. and Rorich R.P., 1996C. Gaseous Pollutants. In Held G., Gore B.J., Surridge A.D., Tosen G.R., Turner C.R. and Walmsley R.D., (eds), *Air Pollution and it's Impacts on the South African Highveld.* Environmental Scientific Association, Cleveland, 25-34pp.

47. Formenti P., Elbert W., Maenhaut W., Haywood J., Osborne S. and Andreae M.O., 2003. Inorganic and carbonaceous aerosols during the Southern African Regional Science Initiative (SAFARI 2000) experiment: Chemical characteristics, physical properties, and emission data for smoke from African biomass burning. *J. Geophys. Res.*, **108**, D13, 8488.

48. Warren D.R. and Seinfeld J.H. 1985. Simulations of aerosol size-distribution evolution in systems with simultaneous nucleation, condensation and coagulation. *Aerosol Sci. and Technol.*, **4**, 31-43.

49. Bessagnet B., Hodzic A., Vautard R., Beekmann M., Cheinet S., Horne C., Liousse C. and Rouil L., 2002. Aerosol modelling with CHIMERE – preliminary evaluation at the continental scale. *Atmos. Environ.*, **38**, 2803-2817.

50. Liousse C., Michel C., Bessagnet B., Cachier H. and Rosset R., 2005. 0-D-Modelling of Carbonaceous Aerosols over Greater Paris focusing on the Organic particle formation. *J. Atmos. Chem.*, **51** (2), 207-221.

51. DEBITS, 2007. [online]. [Accessed 11 September 2007]. Available from the World Wide Web: <http://medias.obs-mip.fr/idaf/maquette/presentation/Debits.html.

52. Van Velthoven P.F.J, and Kelder H., 1996. Estimates of Stratosphere-Troposphere Exchange: Sensitivity to model formulation and horizontal resolution. *J. Geophys. Res.*, **101**, 1429-1434.

53. Jeuken A., Veefkind J.P., Dentener F., Metzger S. and Gonzalez C.R., 2001. Simulation of the aerosol optical depth over Europe for August 2001 and comparison with observations. *J. Geophys. Res.*, **106**, 28295-28311.

54. Harrison R.M., *Pollution: Causes, Effects and Control, 4nd ed.*, 2001, The Royal Society of Chemistry, 1-2, 194pp.

55. Alloway B.J. and Ayres D.C., *Chemical Principals of Environmental Pollution, 2nd ed.*, 1997, Chapman & Hall, 3-4pp.

56. Dhammapala R., 1996. *Use of diffusive samplers for the sampling of atmospheric pollutants.* M.Sc. thesis, Potchefstroom University for CHE. Potchefstroom.

57. Ramaswamy. V., Boucher O., Haigh J., Hauglustaine D., Haywood J., Myhre G., Nakajima T., Shi G., Solomon S., Betts R.E., Charlson R., Chuang C.C., Daniel J.S., Del Genio A.D., Feichter J., Fuglestvedt J., Forster P.M., Ghan S.J., Jones A., Kiehl J.T., Koch D., Land C., Lean J., Lohmann U., Minschwaner K., Penner J.E., Roberts D.L., Rodhe H., Roelofs G.J., Rotstayn L.D., Schneider T.L., Schumann U., Schwartz S.E., Schwartzkopf M.D., Shine K.P., Smith S.J., Stevenson D.S., Stordal F., Tegen I., van Dorland R., Zang Y., Srinivasan J. and Fortunat J., 2001: Radiative forcing of climate change. In Houghton J.T., (eds.), *Climate Change 2001*: The Scientific Basis. Contribution of Working Group I to the Third Assessment Report of the Intergovernmental Panel on Climate Change, Cambridge University Press, Cambridge, United Kingdom and New York, NY, USA, pp. 349–416.

58. United States Environmental Protection Agency. 1996. *List of Designated Reference and Equivalence Methods.* Issue date: 31 May.

59. Code of Federal Regulations, 40. 1 July 1974. *Protection of Environment. Part 50*, Section 50.4-50.11, US Government Printing Office, Washington, D.C.

60. Fact Sheet, Final revisions to the national ambient air quality standards for particle pollution (Particulate matter) [online] [Accessed 17 February 2008]. Available from the World Wide Web: <http://epa.gov/air/particles/actions.html.

61. Pienaar J.J. and Sandham L.A., September 1995. Air Quality Management, A short Course in Environmental Management. Section for Training and Co-ordination, Potchefstroom University for Christian Higher Education. Potchefstroom.

62. van Loon G.W. and Duffy S.J., 2005. *Environmental Chemistry: A Global perspective, 2nd Ed.*, Oxford University Press, 536pp.

63. Arnnegarn H.J., Terblanche A.P.S., Sithole J.S., Rorich R.P. and Turner C.R., 1996B. Residential Air Pollution. In Held G., Gore B.J., Surridge A.D., Tosen G.R., Turner C.R. and Walmsley R.D., (eds.), *Air Pollution and it's Impacts on the South African Highveld*, Environmental Scientific Association, Cleveland, 47-57pp.

64. Rorich R.P., Croucamp P. and Galpin J., 1995. Results from the APOLCOM Air Quality Study at Witbank and the Long Term Pollutant Trends in the Central Mpumalanga Highveld, November 1995, *Proceedings of the 26th annual National Association for Clean Air conference*, Durban, South Africa.

65. Kellogg W.W., Cadle R.D., Allen E.R., Lazrus A.L. and Martell E.A. 1972. The Sulphur Cycle. *Science*, **175**, 587-596.

66. Campbell G.W., 1997. *Acid Deposition in the United Kingdom 1992-1994.* AEA Technology, London, 176pp.

67. Seinfeld J.H. and Pandis S.N., 1998. *Atmospheric Chemistry and Physics: From Air Pollution to Climate Change.* Wiley&Sons, Inc., New Jersey, 1326pp.

68. Meetham A.R., 1981. *Atmospheric Pollution: It's History, Origin and Preventions, 4th ed.*, Pergamon Press, Oxford, 219pp.

69. Finlayson-Pitts B.J. and Pitts J.N., 1986. *Atmospheric Chemistry: Fundamentals and Experimental Techniques*. John Wiley and Sons, New York, 1098pp.

70. Whelpdale D.M. and Kaiser M.S., 1996. *Global Acid Deposition Assessment.* WMO No. 106, Global Atmosphere Watch, World Meteorological Organization, Geneve.

71. Helas G. and Pienaar J.J., 1996. Biomass Burning Emissions. Chapter 3 in Held G., Gore B.J., Surridge A.D., Tosen G.R.,Turner C.R. and Walmsley R.D., (eds.), *Air Pollution and its impacts on the South African highveld*, Environmental Scientific Association, Cleveland, 12-15pp.

72. Cohen S., Chang S.G., Markkowitz S. and Novakov T., 1981. Role of fly ash in catalytic oxidation of S (IV) slurries. *American Chem. Soc.*, **15**, 1498-1502.

73. Raes F., Van Dingenen R., Vignati E., Wilson J., Putaud J.P., Seinfeld J.H. and Adams P., 2000. *Atmos. Environ.*, **34**, 4215.

74. Seinfeld J.H., 1986. *Atmospheric Chemistry and Physics of Air Pollution*, John Wiley and Sons Inc., New York, 738pp.

75. Crutzen P.J. and Carmichael G.R., 1993. Modelling the Influence of fires on Atmospheric Chemistry. In Crutzen P.J. and Goldammer J.G., (eds.), *Fire in the Environment: The Ecological, Atmospheric and Climatic Importance of Vegetation Fires*, John Wiley and Sons Ltd., Chichester, 89-104pp.

76. Blake D.R. and Rowland F.S., 1995. Urban Leakage of Liquefied Petroleum Gas and its Impact on Mexico City Air Quality. *Science*, **269**, 953-956.

77. World Meteorological Organization (WMO), 1986. Atmospheric Ozone 1985, Global Ozone Research and Monitoring Project, Report 16, Geneva.

78. World Meteorological Organization (WMO), 1990. Report of the international Ozone Trends Panel: 1988, *Global Ozone Research and Monitoring Project*, Report 18, Geneva.

79. Ferm M., 1979. Method for determination of atmospheric ammonia. *Atmos. Environ.,* **13**, 1385–1393.

80. Ashmore M.R. and Bell J.N.B., 1991. The Role of Ozone in Global Change. *Ann. of Botany*, **67**, 39-48.

81. ISO 10849 .January 1994. *NO_x Automated Measuring Systems*. Section A.4.2.2.2, Annex A, 24-26pp.

82. Binkley D., Driscoll C.T., Allen H.L., Schoeneberger P. and McAvoy D., (eds.), 1989. *Acidic Deposition and Forest soils: Context and case studies of the southern United states*, Springer-Verlag, New York, Inc., 149pp.

83. Linthurst R.A., (eds.), 1984. Direct and indirect effects of acidic deposition on vegetation, In *Acid Precipitation series Vol. 5*, American Chemical Society annual meeting, 27 March 1982, Los Vegas, NV, USA, Butterworth Publication.

84. Schindler D.W., 1988. Effects of acid rain on fresh water ecosystems. *Science* **239**, 149.

85. Charlson R.J., Lovelock J.E., Andrea M.O. and Warren S.G., 1987. Oceanic phytoplankton, atmospheric sulphur, cloud albedo and climate. *Nature*, **326**, 655.

86. Draajers G.P.J., Ivens W.P.M.F., Ross M.M. and Blouten W., 1989. The contribution of ammonia emissions from agriculture to the deposition of acidifying and eutrophying compounds into forest. *Environ. Pollut.*, **60**, 55.

87. Nihlgard B., 1985. The ammonium hypothesis: An additional explanation of the forest dieback in Europe. *Ambio*, **14**, 2.

88. Aber J.D., Nadelhoffer K.J., Steudler P. and Melillo J.M., 1989. Nitrogen saturation in northern forest ecosystems. *Bioscience*, **39**, 378.

89. Finlayson-Pitts B.J. and Pitts J.N., 2000. *Chemistry of the Upper and Lower Atmosphere*. Academic Press, San Diego.

90. Houghton J.T., Ding Y., Griggs D.J., Noguer M., van der Linden P.J., Dai X., Maskell K. and Johnson C.A., 2001. *Climate change 2001*: The Scientific Basis (Contribution of Working Group I to the Third Assessment Report of the Intergovernmental Panel on Climate Change). Cambridge University Press, Cambridge.

91. Lohmann U. and Feichter J., 2005. *Atmos. Chem. Phys.*, **5**, 715.

92. Pruppacher H.R. and Klett J.D., 1997. *Microphysics of clouds and precipitation.* Kluwer, Dordrecht.

93. Pöschl U., 2005. Atmospheric Aerosols: Composition, Transformation, Climate and Health Effects. *Atmos. Chem.*, **44**, 7520-7540.

94. Pandis S.N., Wexler A.S. and Seinfeld J.H., 1995. Dynamics of tropospheric aerosols. J. *Phys. Chem.*, **99**, 9646-9659.

95. Kgabi N.A., 2006. *Monitoring the levels of toxic metals of atmospheric particulate matter in the North West Province*, Ph.D thesis, North West University. Potchefstroom.

96. Lehtinen K.E.G. and Kulmala M., 2002, A model for particle formation and growth in the atmosphere with molecular resolution size. *Atmos. Chem. Phys. Discus.*, **2**: 1791-1807.

97. Meszaros E., 1981. *Atmospheric Chemistry: Fundamental Aspects.* Amsterdam: Elsevier Scientific. 90-160pp.

98. Kulmala M., Pirjola L. and Makela J.M., 2000. Stable sulphate clusters as a source of new atmospheric particles. *Nature*, **404**: 66-69.

99. Koch D.L. and Cohen C., 2000. Turbulent Coagulation of Aerosol Particles. (In Proceedings of the Fifth Microgravity Fluid Physics and Transport Phenomena Conference held in the NASA Glenn Research Center, Cleveland, CP-2000-210470, 1365-1367. August.

100. Hidy G.M. and Brock J.R., 1970. *The dynamics of aerocolloidal systems*, Oxford: Oxfordshire Pergamon Press.

101. Sateesh S.K., 2002. *Aerosols and Climate. Resonance*, 48-59. April.

102. Makela J.M., Maso M.D., Pirjola L., Keronen P., Laakso L., 2000. Characteristics of the atmospheric particle formation events observed at a boreal forest site in southern Finland. *Boreal Environ. Res.*, **5**, 299-313.

103. Dolazalek H., Reiter R. and Kroling P., 1985. Basic comments on the physics, occurrence in the atmosphere, and possible biological effects of air ions. *International Journal Biometeotology*, **29**, 207-242.

104. Tammet H., 1998a. In Raton B. and Arbor A, CRC Handbook of Chemistry and Physics 14, 79th edition. London, CRC Press, 32-34pp.

105. Raes F.J. and Anssens A., 1985. Ion-induced aerosol formation in a H_2O-H_2SO_4 system: Extension of classical theory and search for experimental evidence. J. Aerosol Sci., **16**, 217-227.

106. Yu F. and Turco R.P., 2000. Ultra fine aerosol formation via ion-mediated nucleation. *Geophys. Res. Let.*, **27**, 883-886.

107. University of Helsinki [online] [Accessed 27 October 2004]. Available from the World Wide Web: <http://atm.helsinki.fi/aerosols/ions/html.

108. Hidy G.M., 1984. *Aerosols: An Industrial and Environmental Science.* Academic Press, 757pp.

109. Hoppel W.A., Fitzgerald J.W., Frick G.M., Larson R.E. and Mack E.J., 1990. Aerosol size distributions and optical properties found in the marine boundary layer over the Atlantic ocean. *J. Geophys. Res.*, **95**, 3659-3686.

110. Laakso L., Grönholm T., Rannik U., Kosmale M., Fiedler V., Vehkamäki H. and Kulmala M., 2003. Ultra fine particle scavenging coefficients calculated from 6 years field measurements. *Atmos. Environ.*, **37**, 3605-3613.

111. Lee S.W., He I., Herage T., Young B., Razbin V., Kelly E. and Pomalis R., 2002. *Fuel sulfur effects on particulate emissions from fuel oil combustion systems under accelerated laboratory conditions*, Report CETC 02-09 (CF).

112. World Resources Institute. 1999. Urban Air: *Health Effects of Particulates, Sulphur Dioxide, and Ozone*. http://www.wri.org Accessed on the 12 April 2007.

113. USEPA. 1996a. Partiiculate Matter: An Introduction. United States Environmental Protection Agency (USEPA) Report.

114. Mar T.F., Norris G.A., Koenig J.Q. and Larson T.V., 2000. Associations between Air Pollution and Mortality in Phoenix, 1995-1997. *Environ. Health Perspectives*, **108** (4), April.

115. USEPA. 1996b. Particulate Matter Research Program Strategy, US Environmental Protection Agency, NHEERL MS-97-019, October.

116. Daisey J.M., 1980. Organic compounds in urban aerosols. *Ann. NY Acad. Sci.* **338**, 50-69.

117. Comfort B., Ewald W., Garner J.H.B., Grant L.D., Grantz D.A., Hemming B.L., Johnson D.W., Malm M. and Pinto J.P., 2004. *Charter 4: Environmental effects of particulate matter.* In Air quality criteria for particulate matter, Volume I, U.S. Environmental Protection Agency, Research Triangle Park, NC, EPA/600/P-99/002Af.

118. US EPA National Air Quality and Emissions Trends Report. 1997. EPA 454/R-98-016.

119. Smith W.H., 1984. *Pollutant uptake by plants.* In Treshow M., (eds.), Air pollution and plant life. New York, NY, John Wiley & Sons, Ltd, 417-450 pp.

120. Cape J.N., 1993. Direct damage to vegetation caused by acid rain and polluted cloud: definition of critical levels for forest trees. *Environ. Pollut.*, **82**, 167-180.

121. Hauhs M., 1989. *Lange Bramke: an ecosystem study of a forested catchment.* In Adriano D.C. and Havas M., (eds.), Acidic precipitation: volume 1, case studies. New York, NY: Springer-Verslag: 275-305.

122. Johnson D.W. and Lindberg S.E., (eds.), 1992a. *Atmospheric deposition and forest nutrient cycling: a synthesis of the integrated forest study*. New York, NY, Springer-Verslag. Inc.

123. Wesely M.L. and Hicks B.B., 2000. A review of the current status of knowledge on dry deposition. *Atmos. Environ.*, **34**, 2261-2282.

124. Clarke J.F., Edgerton E.S. and Martin B.E., 1997. Dry deposition calculations for the Clean Air Status and Trends Network. *Atmos. Environ.*, **31**, 3667-3678.

125. Pilinis C. and Seinfeld J.H., 1988. Continued development of a general equilibrium model for inorganic multicomponent atmospheric aerosols. *Atmos. Environ.* **21**, 2453-2466.

126. Swartz S.E., 1986. Mass-transport considerations pertinent to aqueous phase reactions of gases in liquid water clouds. In Jaeschke W. (eds.), *Chemistry of multiphase atmospheric systems*. NATO ASI Ser. Springer, Berlin.

127. Luria M. and Sievering H., 1991. Heterogeneous and homogeneous oxidation of SO_2 in the remote maritime atmosphere. *Atmos. Environ.*, **25**, 1489-1496.

128. Sievering H., Boatman J., Gorman E., Kim Y., Andersdon L., Ennis G., Luria M. and Pandis S., 1992. Removal of sulphur from the marine boundary layer by O_3 oxidation in sea-salt aerosol. *Nature*, **360**, 571-573.

129. Dentener F.J., Carmichael G.R., Zhang Y., Lelieveld J. and Crutzen P.J., 1996. Role of mineral aerosol as a reactive surface in the global troposphere. *J. Geophys. Res.*, **101**, 22, 869-889.

130. Ravishankara A.R., 1997. Heterogeneous and multiphase chemistry in the troposphere. *Science,* **275**, 1058-1065.

131. Kim Y.P. and Seinfeld J.H., 1995. Atmospheric gas-aerosol equilibrium: III. Thermodynamics of crustal elements Ca2+, K+, and Mg2+. *Aerosol Sci. Technol.*, **22**, 93-110.

132. Murphy D.M., Thompson D.S. and Middlebrook A.M., 1997. Bromine, iodine, and Chlorine in single aerosol particles at Cape Grim. *Geophys. Res. Lett.*, **24**, 3197-3200.

133. Parungo F., Kim Y., Zhu C., Harris J., Schnell R., Li X., Yang D., Fang X., Yan P., Zhou M., Chen Z., Qian F. and Park K., 1996. Asian Dust Storms and their Effects on Radiation and Climate Part II. STC Technical Report 2959, 34pp.

134. Zang J., Liu S.M., Lu X. and Huang W.W., 1993. Characterizing Asian wind-dust transport to the northwest Pacific Ocean. Direct measurements of the dust flux for two years. Tellus, **45B**, 335-345.

135. Hirai E., Miyazaki M., Chohji T., Lee M., Kitamura M. and Yamaguchi K., 1991. Effect of KOSA aerosol on inorganic ion components in rain water collected from circum-pan-Japan-sea area. *Proceedings of the 2nd IUAPPA Regional conference on Air Pollution*, Seoul, Korea, September 4, 27-34pp.

136. Dentener F.J. and Crutzen P.J., 1993. *J. Geophys. Resources*, **8**, 7149-7163.

137. Febo A., Perrino C. and Allegrini I., 1996. *Atmos. Environ.*, **30**, 3599-3609.

138. Andrés-Hernandés M.D., Notholt J., Hjorth J. and Schrems O., 1996. *Atmos. Environ.*, **30**, 175-180.

139. Neftel A., Blatter A., Hesterberg R. and Staffelbach T., 1996. *Atmos. Environ.*, **30**, 3017-3025.

140. Harrison R.M., Peak J.D. and Collins G.M., 1996. *J. Geophys. Resources*, **101**, 14429-14439.

141. Bongartz A., Kames J., Welter F. and Schurath U., 1991. *J. Phys. Chem.*, **95**, 1076-1082.

142. Bongartz A., Kames J., Schurath U., George C.H., Mirable P.H. and Ponche J.L., 1994. *J. Atmos. Chem.*, **18**, 149-169.

143. Schurath U. and Naumann K.H., 1998. Heterogeneous processes involving atmospheric particulate matter. *Pure Apl. Chem.*, **70**, 7, 1353-1361.

144. Nenes A., Pilinis C. and Pandis S.N., 1998. ISORROPIA: A new Thermodynamic Model for Multiphase Multicomponent Inorganic Aerosols. *Aquat. Geochem.*, **4**, 123-152.

145. Bassett M. and Seinfeld J.H., 1983. Atmospheric equilibrium model of sulphate and nitrate aerosols. *Atmos. Environ.*, **17**, 2237-2252.

146. Bassett M. and Seinfeld J.H., 1984. Atmospheric equilibrium model of sulphate and nitrate aerosols-ii. In Particle size analysis. *Atmos. Environ.*, **18**, 1163-1170.

147. Saxena P., Hudischewsky A.B., Seigneur C. and Seinfeld J.H., 1986. A Comparative study of equilibrium approaches to the chemical characterization of secondary aerosols. *Atmos. Environ.*, **20**, 1471-1483.

148. Kim Y.P., Seinfeld J.H. and Saxena P., 1993a. Atmospheric gas-aerosol equilibrium 1.Thermodynamic model. *Aerosol Sci. Technol.*, **19**, 157-181.

149. Kim Y.P., Seinfeld J.H. and Saxena P., 1993b. Atmospheric gas-aerosol equilibrium II. Analysis of common-approximations and activity coefficients calculations methods. *Aerosol Sci. Technol.*, **19**, 182-198.

150. Wexler A.S, and Seinfeld J.H., 1991. Second-generation inorganic aerosol model. *Atmos. Environ.*, **25A**, 2731-2748.

151. Bassagnet B. and Rosset R., 2001. Fractal modelling of carbonaceous aerosols-application to car exhaust plumes. *Atmos. Environ.*, **35**, 4751-4762.

152. Kulmala M., Laaksonen A. and Pirjola L., 1998. Parameterizations for sulfuric acid/water nucleation rates. *J. Geophys. Res.*, **103**, 8301-8308.

153. Gelbard R.J., Dabdub D. and Seifeld J.H., 1980. Sectional representations for simulating aerosol dynamics. J. *Colloid Interface Sci.*, **76**, 541-556.

154. Jacob D.J., 2000. Heterogeneous chemistry and tropospheric ozone. *Atmos. Environ.*, **34**, 2131-2215.

155. Odum J.R., Hoffman T., Bowman F., Collins D., Flagan R.C. and Seinfeld J.H., 1996. Gas-Particle partitioning and secondary aerosol yield. *Environ. Sci. Technol.*, **30**, 2580-2585.

156. Mallet M., Pont V., Liousse C., Roger J.C. and Dubuisson P., 2006. Simulation of aerosol radiative properties with the ORISAM-RAD model during a pollution event (ESCOMPTE 2001). *Atmos. Environ.*, **40**, 7696-7705.

157. Lurmann F.W., Loyd A.C. and Atkinson R., 1986. a Chemical mechanism for use in long range transport/acid deposition computer modelling. *J. Geophys. Res.*, **91**, 10905-10936.

158. Hanel G., 1976. The properties of atmospheric aerosol particles as a function of the relative humidity at thermodynamic equilibrium with the surrounding moist air. *Advance Geophys.*, **19**, 73-188.

159. Carmichael G.R., Peters L.K. and Kitada T., 1986. A second generation model for regional-scale transport/chemistry/deposition. *Atmos. Environ.*, **20**, 173-188.

160. KNMI, 2007. [Online]. [Accessed 15 November 2007]. Available from the World Wide Web: < http://www.knmi.nl/~velthove/tm.html>.

161. Schmidt H., Derognat C., Vautard R. and Beekmann M., 2001. A comparison of simulated and observed ozone mixing ratios for the summer of 1998 in Western Europe. *Atmos. Environ.*, **35**, 6277-6297.

162. Monteiro A., Vautard R., Borrego C. and Miranda A.I., 2005. Long-term simulations of photo oxidant pollution over Portugal using the CHIMERE model. *Atmos. Environ.*, **39**, 3089-3101.

163. Vautard R., Martin D., Beekmann M., Drobinski P., Friedrich R., Jaubertie A., Kley D., Lattuati M., Moral P., Neininger B. and Theloke J., 2003. Paris emission inventory diagnostics from ESQUIF airborne measurements and a chemistry transport model. *J. Geophys. Res.*, **108** (D17).

164. Russel G.L. and Lerner J.A., 1981. A new finite-differencing scheme for the tracer transport equations. *Journal of Applied Met.*, **20**, 1483-1498.

165. Houweling S., Dentener F. and Lelieveld J., 1998. The Impact of non-methane hydrocarbon compounds on tropospheric photochemistry. *J. Geophys. Res.*, **103**, 10673-10696.

166. Hertel O., Berkowicz R., Christensen J. and Hov O., 1993. Test of two numerical schemes for the use in atmospheric transport-chemistry models. *Atmos. Environ.*, **27A**, 2591-2611.

167. Ganzeveld L., Lelieveld J. and Roelofs G.J., 1998. A dry deposition parameterization for sulfur oxides in a chemistry and general circulation model. *J. Geophys. Res.*, **103**, 5679-5694.

168. Olson J.S., Watts J. and Allison L., 1983. *Carbon in live vegetation of major world ecosystems*. W-7405-ENG-26, U.S. Department of Energy, Oak Ridge National Laboratory.

169. Guillaume B., Liousse C. and Rosset R., 2007. a New global sectional multi-component aerosol model including SOA formation- Focus on carbonaceous BC and OC aerosols. *Tellus*, **59B**, 2, article 5. 126-146.

170. Whelpdale D.M. and Kaiser M.S., 1996. *Global Acid Deposition Assessment.* WMO No. 106, Global Atmospheric Watch, World Meteorological Organization, Geneve.

171. Frost P.G.H. and Robertson F.I., 1987. *The ecological role of fire in savannas.* In B.H. Walker B.H., (eds.), Determinants of tropical savannas, Oxford, IRL Press, 93-140pp.

172. Picketh S., Annegarn H.J. and Tyson P.D., 1999. Lower-tropospheric loading over South Africa: the relative contributions of aerolian dust, industrial emissions and biomass burning. *J. Geophys. Res.*, **104**, 1597-1607.

173. Cosijn C. and Tyson P.D., 1996. Stable discontinuities in the atmosphere over South Africa, *S. Afr. J. Sci.*, **92**, 381-386.

174. Annegarn H.J., Otter L., Swap R.J. and Scholes R.J., 2002. Southern Africa's ecosystem in a test-tube: A perspective on the Southern African Regional Science Initiative (SAFARI 2000), *SA J. Sci.*, **98**, 111-113.

175. Schulze B.R., 1965. *Climate of South Africa, Part 8, General Survey.* WB28, South African Weather Bureau, Department of Environment Affairs, Pretoria, 330pp.

176. Tyson P.D., Garstang M., Swap R.J., Edwards M. and Kallberg P., 1996. An air transport climatology for subtropical southern Africa. *International Journal of Climatology*, **16**, 151-163.

177. Preston-Whyte R.A. and Tyson P.D., 1977. *The atmosphere and weather of southern Africa.* Oxford University, Cape Town, 374pp.

178. Held G., Gore B.J., Surridge A.D., Tosen G.R., Turner C.R. and Walmsley R.D., 1996. Chemical transformations of atmospheric pollutants. In *Air Pollution and its Impacts on the South African Highveld*, Environmental Scientific Association, Cleveland, Johannesburg.

179. Tosen G.R. and Jury M., 1986. *The winter nocturnal wind jet over the Eastern Transvaal-a case study sequence.* TRR/N86/006, Eskom, Johannesburg, 20pp.

180. Piketh S. and Prangley A.R., 1998. Trajectory climatology of transboundary transport for the Highveld. TRR/T98/038, Eskom, Johannesburg, 24pp.

181. Crutzen P.J. and Andreae M.O., 1990. Biomass burning in the tropics: Impact on atmospheric chemistry and biogeochemical cycles. *Science*, **250**, 1669-1678.

182. Andreae M.O., Atlas H., Cachier W.R., Cofer III., Harris G.W., Helas G., Koppmann R., Lacaux J. and Ward D., 1996. Trace gas and aerosol emissions from savanna fires, in Levine J.S., (eds.), Biomass Burning and Global Change, MIT Press, Cambridge, Mass., 278-295pp.

183. Liousse C., Penner J.E., Walton J.J., Eddleman H., Chuang C. and Cachier H., 1996. *Modeling biomass burning aerosols*, In Levine J.S., (eds.), Biomass Burning and Global Change, MIT Press, Cambridge, Mass., 492-508pp.

184. Scholes M. C. and Andreae M. O., 2000. Biogenic and pyrogenic emissions from Africa and their impact on global atmosphere. *Ambio*, **29**, 23-29.

185. Dwyer E., Pereira J.M.C., Gregoire J.M. and Dacamara C.C., 2000. Characterization of the spatio-temporal patterns of global fire activity using satellite imagery for the period April 1992 to March 1993. *J. Biogeography*, **127** (1), 57-69.

186. Van der Werf G.R., Randerson J.T., Collatz G.J. and Giglio L., 2003. Carbon emissions from fires in tropical and sub-tropical ecosystems. *Global Change Biology*, **9** (4), 547-562.

187. Lacaux J.P., Cachier H. and Delmas R., 1993. Biomass burning in Africa. In Crutzen P.J. and Goldammer J., (eds.), An overview of its impact on atmospheric chemistry. *In Fire in the Environment: The Ecological Atmospheric and Climatic Importance of vegetation Fires*, John Wiley, New York, 159-191pp.

188. Sivertsen B., Matale C. and Pereira L.M.R., 1995. *Sulphur emissions and transfrontier air pollution in Southern Africa*. Southern African Development Community, Environmental and Land Management Sector, Report Series 34.

189. Garstang M., Tyson P.D., Swap R.J., Edwards M., Kallberg P. and Lindesay J.A., 1996. Horizontal and vertical transport of air over southern Africa. *J. Geophys. Res.*, **101**, 23, 721-23, 736.

190. Tyson P.D., Garstang M., Swap R.J., Browell E.V., Diab R.D. and Thompson A.M., 1996. Transport and vertical structure of ozone and aerosol distribution over southern Africa in Levine J.S.(eds.), *Biomass burning and Global change*, MIT Press, Cambridge, Mass., 403-421pp.

191. Swap R.J. and Tyson P.D., 1999. Stable discontinuities as determinants of the vertical distribution of aerosols and trace gases in the atmosphere. *S. Afr. J. Sci.*, **95**, 63-71.

192. Zunckel M., Robertson L., Tyson P.D. and Rodhe H., 2000. Modeled transport and deposition of sulphur over Southern Africa. *Atmos. Environ.*, **34**, 2797-2808.

193. Lindesay J.A., Andrea M.O., Goldammer J.G., Harris G., Annegarn H.J., Garstang M., Scholes R.J. and van Wilgen B.W., 1996. International Geosphere-Biosphere Programme/International Global Atmospheric Chemistry SAFARI-92 field experiment: Background and overview, *J. Geophys. Res.*, **101**, (D19), 23, 521-23, 530.

194. Fishman J., Brackett G., Browell E.V. and Grant W.B., 1996. Tropospheric ozone derived from TOMS/SBU measurements during TRACE-A. *J. Geophys. Res.*, **101** (D19), 24, 069-24, 082.

195. Garstang M., Ellery W.N., McCarthy T.S., Scholes M.C., Scholes R.J., Swap R.J. and Tyson P.D., 1998. The contribution of aerosol-and water-borne nutrients to the functioning of the Okavango Delta ecosystem, Botswana. *S. Afr. J. Sci.*, **94**, 223-229.

196. Swap R.J., Garstang M., Macko S.A., Tyson P.D., Maenhaut W., Artaxo P., Kallberg P. and Talbot R., 1996. The long-range transport of South African aerosols to the tropical South Atlantic. *J. Geophys. Res.*, **101**, 23, 777-23, 791.

197. Jaegle L., Steinberger L., Martin R.V. and Chance K., 2005. Global partitioning of NO_x sources using satellite observations: relative roles of fossil fuel combustion, biomass burning and soil emission. *Faraday Disc.*, **130**, 407-423.

198. Zunckel M., Venjonoka K., Pienaar J.J., Brunke E.G., Pretorius O., Koosailee A., Raghunandan A. and van Tienhoven A.M., 2005. Surface ozone over southern Africa: synthesis of monitoring results during the cross border Air Pollution Impact Assessment project. *Atmos. Environ.*, **38**, 6139-6147.

199. Dyson L.L., 2000. *A Dynamical Forecasting Perspective on Synoptic Scale Weather Systems over South Africa.* M.Sc. Thesis. University of Pretoria. Pretoria.

200. Tyson P.D., Garstang M. and Swap R.J., 1996. Large-scale re-circulation of air over southern Africa. *J. Appl. Meteorol.*, **35**, 2218-2236.

201. Brunke E.G. and Sheel H.E., 1995. *The new Cape Point Baseline Station and recent changes in trace gas trends.* Extended Abstracts of Papers presented at the WMO-IGAC Conference of the Measurements and Assessment of Atmospheric Composition Change. Report 107, World Meteorological Organization, Geneva, pp246-249.

202. Carmichael G., 1997. *Report of Diffusive Samplers for the Atmospheric Chemistry Measurements and their role in GAW*, WMO Report 122, WMO TD No. 829.

203. Allegrini I., De Santis F., Di Palo V., Febo A., Perrino C., Possanzini M. and Liberti A., 1987. Annular denuder method for sampling reactive gases and aerosols in the atmosphere. *Sci. Tot. Environ.*, **67**, 1–16.

204. US EPA, 1997. Determination of reactive acidic and basic gases and strong acidity of fine particles (<2.5 m). *Compendium of Methods for the Determination of Inorganic Compounds in Ambient Air*, Method IO-42. EPA-625/R-96/010a, Center for Environmental Research Information, Office of Research and Development, Cincinnati, OH.

205. Aslam M., Khalil K. and Rasmussen R.A., 2004. Changes in the Regional Emissions of Greenhouse Gases and Ozone-Depleting Compounds. *Environ. Sci. Technol.*, **38**, no. 2, 364-366.

206. Finnegan D.L., Kotra J.P., Hermann D.M. and Zoeller W.H., 1989. The use of 7LiOH-impregnated filters for the collection of acidic gases and analysis by instrumental neutron activation analysis. *Bull. Volcanol.*, **51**, 83– 87.

207. Miller T. H., Zoeller W.H., Crowe B.M. and Finnegan D., 1990. Variations in trace metal and halogen ratios in magmatic gases through an eruptive cycle of the Pu'u O'o vent, Kilauea, Hawaii: July – August 1985. *J. Geophys. Res.*, **95**, 12,607– 12,615.

208. Francis P., Horrocks L. and Oppenheimer C., 2000. Monitoring gases from andesitic volcanoes. *Philos. Trans. R. Soc.* London, Ser. A, **358**, 1567 – 1584.

209. Wagner J. and Leith D., 2001. Field tests of a diffusive aerosol sampler. *J. Aerosol Sci.*, **32**, Issue 1, 33-48.

210. DRI SOP #2-204.6, 2000. DRI Standard Operating Procedure. Thermal/Optical Analysis of Aerosol Filter Samples, Desert Research Institude Division of Atmospheric Sciences, 2215 Raggio Parkway, Reno, NV 89512.

211. Carmichael G.R., Ferm M., Thongboonchoo N., Woo J.H., Chan L.Y., Murano K., Pham H.V., Mossberg C., Bala R., Boonjawat J., Upatum P., Mohan M., Adhikary S.P., Shrestha A.B., Pienaar J.J., Brunke E.B., Chen T., Jie T., Guoan D., Peng L.C., Dhiharto S., Harjanto H., Jose A.M., Kimani W., Kirouane A., Lacaux J.P., Richard S., Barturen O., Cerda J.C., Athayde A., Tavares T., Cotrina J.S. and Bilici E., 2003. Measurements of sulfur dioxide, ozone and ammonia concentrations in Asia, Africa, and South America using diffusive samplers. *Atmos. Environ.*, **37**, 1293 -1308.

212. Ayers G.P., Keywood M.D., Gillet R.W., Mainins P.C. and Malfroy H., Bardsley T., 1998. Validation of passive diffusion samplers for SO_2 and NO_2. *Atmos. Environ.*, **32**, 3587-3592.

213. Ferm M. and Svanberg P.A., 1998. Cost-efficient techniques for urban and background measurements of SO_2 and NO_2, *Atmos. Environ.*, **32**, 1377-1381.

214. Aiuppa A., Bellomo S., Alessandro W.D., Federico C., Ferm M. and Valenza M., 2004. Volcanic plume monitoring at Mount Etna by diffusive (diffusive) sampling, *J. Geophys. Res.*, **109**, D21308.

215. Harper M. and Purnell C.J., 1987. Diffusive Sampling-a review. *Am. Ind. Hyg. Assoc. J.*, **48**, 214-218.

216. Ferm M., 2001. The theories behind diffusive sampling, paper presented at *International Conference Measuring Air Pollutants by Diffusive Sampling. Environ. Inst., Joint Res. Cent.*, Montpellier, France, 26– 28 Sept.

217. Ferm M., 1991. *A Sensitive Diffusional Sampler.* IVL publication B-1020, Swedish Environmental Research Institute, Box 47086, 402 58 Goteborg, Sweden.

218. Schwartz S.E. and Warneck P., 1995. Units for Use in Atmospheric Chemistry. *Pure and Appl. Chem.*, **67**, 1377-1406.

219. Koutrakis P., Wolfson J.M., Bunyaviroch A., Froehlich S.E., Hirano K. and Mulik J.D., 1993. Measurement of ambient ozone using a nitrite-coated filter. *Anal. Chem.*, **65**, 209-214.

220. Ferm M. and Rodhe H., 1997. Measurement of air concentrations of SO_2, NO_2 and NH_3 at rural and remote sites in Asia, *J. Atmos. Chem.*, **27**, 17-29.

221. Martins J.J., Dhammapala R.S., Lachmann G., Galy-Lacaux C. and Pienaar J.J., 2007. *S.A. J. of Sci.*, **103**, 1-7.

222. Tetlow J.A. and Wilson A.L., 1964. An absorptiometric method for determining ammonia in boiler feed water. *Analyst*, **89**, 453-465.

223. Pienaar J.J., 2005. DEBITS (Deposition of Biogeochemically Important Trace Species) enter Phase II as an IGAC task. *IGACtivities Newsl.* 31, 13-17.

224. Van der Walt H., Du Toit P., Pienaar J.J. and Julies A., 1998. Integration of diffusive sampler monitoring in non-electrified residential areas into a modern ambient air quality monitoring network. Paper No. 6G-4, Vol. 2, Proceedings,

11th World Clean Air and Environment Congress, Durban, 13-18 September 1998, 5pp.

225. Pienaar J.J. and Julies A.P., 2001. Present status and performance of passive samplers - theorogical considerations. In Proc. *Air Quality Workshop*, African Centre for Energy and Environment, Warmbaths, South Africa.

226. Manual Version 4.2c, 2001. *MiniVol Portable Sampler Operation Manual*, Airmetrics, 2121 Franklin Boulevard, 9, Eugene, OR 97403 U.S.A.

227. Baldauf W.R., Lane D.D., Marotz G.A. and Wiener R.W., 2001. Performance evaluation of the portable MiniVOL particulate matter sampler. *Atmos. Environ.*, **35**, 6087-6091.

228. AIRMETRICS, 2007. [Online]. [Accessed 27 October 2006] Available from the World Wide Web: <http//.w.w.w.airmetrics.com/products/minivol/index>.

229. WMO/GAW Aerosol Measurements Procedures: Guidelines and Recommendations. September 2003, TD No. 1178.

230. Zunckel M., Koosailee A., Yarwood G., Maure G., Venjonoka K., van Tienhoven A.M. and Otter L., 2006. *Modelled surface ozone over southern Africa during the cross Border Air Pollution Impact Assessment Project.* Environ. Modelling& Software, 21(7), 911-924.

231. Carmichael G.R., Street D.G., Calori G., Amann M., Jacobson M.Z., Hansen J. and Ueda H., 2002. Changing trends in sulphur emissions is Asia: Implications for acid deposition, air pollution and climate. *Environ. Sci. Technol.*, **36** (22), 4707-4713.

232. Zhang L., Brook R.J. and Vet R., 2003. A Revised parameterization for gaseous dry deposition in air-quality models. *Atmos. Chem. Phys.*, **3**, 2067-2082.

233. Peters N.E., Tilden P., Meyers and Aulenbach B.T., 2002. Status and trends in atmospheric deposition and emissions near Atlanta, Georgia, 1986-99. *Atmos. Environ.*, **36** (10), 1577-1588.

234. Lynch J.A., van Bowersox C. and Grimm J.W., 2000. Changes in sulphate deposition in eastern USA following implementation of Phase I of Title IV of the Clean Air Act Amendments of 1990. *Atmos. Environ.*, **34**, 1665-1680.

235. Guazzotti S.A., Suess D.T., Coffee K.R., Quinn P.K., Bates T.S., Wisthaler A., Hansel A., Ball W.P., Dickerson R.R., Neususs C., Crutzen P.J. and Prather K.A., 2003. Characterization of carbonaceous aerosols outflow from India and Arabia: Biomass/biofuel burning and fossil fuel combustion. J. *Geophys. Res.*, **108**, doi:10.1029/2002JD003277.

236. Andrea M.O., 1983. Soot carbon and excess fine potassium: Long range transport of combustion derived aerosols. *Science*, **220**, 1148-115.

237. Reddy M.S. and Venkataraman C., 2000. Atmospheric optical and radiative effects of anthropogenic aerosol constituents from India. *Atmos. Environ.*, **34** (26), 4511-4523.

238. Novakov T., Andrea M.O., Gabriel R., Kirchstetter T.W., Mayol-Bracero O.L. and Ramanathan V., 2000. Origin of carbonaceous aerosols over the tropical Indian ocean: Biomass burning or fossil fuels? *Geophys. Res. Let.*, **27** (24), 4061-4064.

239. Streets D.G. and Waldhoff S.T., 1999. Greenhouse gas emissions of biofuel combustion in Asia. *Energy*, **24**, 841-855.

240. Maenhaut W., Salma H., Caftneyer J., Annegarn H.J. and Andrea M.O., 1996. Regional atmospheric aerosol composition and sources in the eastern Transvaal, South Africa, and impact of biomass burning. *J. Geophys. Res.*, **101**, 23, 631-23, 650.

241. Tyson P.D. and D'Abreton P., 1998. Transport and recirculation of aerosols off southern Africa-Macroscale plume structure. *Atmos. Environ.*, **32**, 1511-1524.

242. Jost C., Trentmann J., Sprung D., Andrea M.O., Mcquaid J.B. and Barjat H., 2003. Trace gas chemistry in young biomass burning plume over Namibia:

Observations and model simulations. J. Geophys. Res., **108**, doi:10.1029/2002JD002431.

243. Drever J.I., 1982. *The geochemistry of Natural Waters*. Prentice-Hall, Inc., Englewood Cliffs, NJ, 388pp.

244. Ezcurra H., Casado H., Lacaux J.P. and Garcia C., 1988. Relationship between meteorological situations and acid rain in Spanish Basque country. *Atmos. Environ.*, **22**, 2779-2786.

245. Khwaja W.C., Pszenny A.A.P., Galloway J.N. and Hartley M.E., 1986. Sea-salt corrections and interpretation of constituent's ratios in marine precipitation. *J. Geophys. Res.*, **91**, 6647-6658.

246. Lee B.K., Hong S.H. and Lee D.S., 2000. Chemical composition of precipitation and wet deposition of major ions on the Korean peninsula. *Atmos. Environ.*, **34**, 563-575.

247. Andreae T.W., Annegarn H., Beer J., Cachier H., le Canut P., Elbert W., Maenhaut W., Salma I., Weinhold F.G. and Zenker T., 1998. Airborne studies of aerosol emissions from savanna fires in southern Africa: 2. Aerosol chemical composition. *J. Geophys. Res.*, **103**, 32, 119-32, 128.

248. Castro L.M., Pio C., Harrison R. and Smith DT.J., 1999. Carbonaceous aerosol in urban and rural European atmospheres: estimation of secondary organic carbon concentrations. *Atmos. Environ.*, **33**, 2771-2781.

249. NOAA, 2007. [online] [Accessed 27 November 2007]. Available from the World Wide Web: <http://noaa.gov.html.

250. Puxbaum H., Rendl J., Allabashi R., Otter L. and Scholes M.C., 2000. Mass balance of the atmospheric aerosol in a South African subtropical savanna (Nylsvley, May 1997). *J. Geophys. Res.*, **105**, D16, 20, 697–20, 706.

251. Lorenz R. and Murphy Jr., C.E., 1989. Dry deposition of particles to a pine plantation. *Boundry Layer Meteorology*, **46**, 355-366.

252. Allen A.G., Harrison R.M. and Nicholson K.W., 1991. Dry deposition of fine aerosol to a short grass surface. *Atmos. Environ.*, **25**, 2671-2676.

253. Anatolaki C.H. and Tsitouridou R., 2007. Atmospheric deposition of nitrogen, sulphur and chloride in Thessaloniki, Greece. *Atmos. Res.*, **85**, 413-428.

254. Tanner P.A., Law P.T. and Tam W.F., 2001. Comparison of aerosol and dry deposition sampled at two sites in Southern China. *Aerosol Sci.*, **32**, 461-472.

255. Mertes St. and Wahner A., 1995. *J. Phys. Chem.*, **99**, 14000-14006.

256. Liousse C., Junker C., Guillaume B. and Criqui P., 2007a. *An Emission Inventory of Carbonaceous Aerosol from documented and forecast data of Fossil Fuel and Biofuel consumption for the period 1950-2030.*

257. Zakey A.S., Solmon F. and Giorgi F., 2006. Implementation and testing of a desert dust module in regional climate model. *Atmos. Chem. Phys.*, **6**, 4687-4704.

258. Gong S.L., Barrie L.A., Blanchet J.P., von Salzen K., Lohmann U., Lesins G., Spacek L., Zhang L.M., Girard E., Lin H., Leaitch R., Leighton H., Chylek P. and Huang P., 2003. Canadian Aerosol Module: a size-segregated simulation of atmospheric aerosol processes for climate and air quality models. 1. Module development. *J. Geophys. Res.*, **108** (D1), 4007.

APPENDIX A

Site	Species	Year	Concentration in ppb per month											
AF	SO_2		Jan	Feb	Mar	Apr	May	Jun	Jul	Aug	Sep	Oct	Nov	Dec
		1995												
		1996												
		1997								4.07		2.74	3.35	4.15
		1998	3.81			2.09	2.28	2.55	3.00	3.65		2.75		
		1999	2.65					2.20	3.00		3.40	3.55	3.30	3.55
		2000	2.05	1.35	0.90	1.85	1.65		3.30	2.55			2.10	
		2001				2.50	2.35					1.60	1.20	1.05
		2002				1.50	2.65	2.45	4.25	3.05	2.60	4.00		3.85
		2003	0.85	4.88	0.79		2.98	3.73	1.28	1.95	0.61	0.38	0.98	1.22
		2004		3.06	1.71	2.34		1.13	1.15	1.56	1.47			1.43
		2005	2.69			2.85	5.43	5.50	4.84	4.93	4.55	6.33	4.69	2.76
LT	SO_2		Jan	Feb	Mar	Apr	May	Jun	Jul	Aug	Sep	Oct	Nov	Dec
		1995					0.86		0.77	0.94	0.90	0.72	0.58	0.15
		1996	0.26	0.45	0.31	0.79	0.94	2.04	0.67	0.44	1.31	0.65	0.57	0.60
		1997	0.45	0.27		0.32	0.75	1.71	0.71	1.65	0.32	0.28	0.65	1.12
		1998	1.03	1.28		2.39	2.10		2.90		3.95		0.15	0.20
		1999	0.20	0.35						1.70	0.75	0.35	0.35	0.25
		2000	0.40	0.75	0.20		0.55	0.40	0.60			0.25		
		2001			0.20	0.30	0.50	0.70	0.65	0.25		0.10		
		2002				1.35	0.90	1.05		0.30	1.25	0.20	0.35	0.34
		2003	0.19	0.10	0.11	0.10	0.14	2.18		0.10			0.12	0.10
		2004		0.27	0.61		0.37	0.15	0.21	0.15	0.34	0.19		0.68
		2005	0.73	0.80	0.24	0.30	0.86	1.25	0.22		0.40		0.44	0.35
CP	SO_2		Jan	Feb	Mar	Apr	May	Jun	Jul	Aug	Sep	Oct	Nov	Dec
		1995	0.58	0.49	0.17	0.50	0.78	0.96	0.68	0.76	0.45	1.06	0.30	
		1996	0.25	0.52	0.54	1.07	0.41	0.93	0.56	0.72		1.16	1.72	0.62
		1997	1.42	0.75	1.24	2.70	0.50		0.60	0.40	0.20	0.40	0.80	0.80
		1998	0.80	0.75	0.45	1.15	0.60	0.40	0.45	0.30	0.50		1.05	
		1999	0.30	0.60	0.40						0.45		0.95	
		2000	0.20	0.06	0.20	0.25				0.40		0.20	0.30	0.10
		2001	0.14	0.06	0.10	0.09	0.07	0.20	0.05	0.80	0.20	0.83		0.16
		2002		0.85		2.35		0.00		0.01			0.04	0.62
		2003	0.77		2.91		0.87	0.27	0.56		0.14	0.13	0.11	1.48
		2004	0.65	0.40	0.06	0.06	0.13		0.13	0.12	1.34	0.63	0.52	0.30
		2005	2.47	0.24	0.46	0.61	0.74	1.02	0.55		0.29	0.28	5.81	0.26
NA	SO_2		Jan	Feb	Mar	Apr	May	Jun	Jul	Aug	Sep	Oct	Nov	Dec
		1995	0.32	1.20	0.65	0.24	0.53	0.48	0.63	0.39	0.37	1.55	0.33	
		1996	1.40	0.31	0.25	0.29	0.67	0.73	0.34	0.50			0.39	0.77
		1997	0.63	0.80	0.43	1.41	0.61		0.40	0.25	0.55	0.50	0.75	0.75
		1998	0.55	0.35	0.35	0.10	0.30	0.20	0.25	0.35	1.00	0.65		
		1999	0.30	0.45	0.35						0.70		0.10	
		2000	0.55	0.10	0.35		0.30		0.40			0.40	0.50	
		2001	0.09	0.20	0.20	0.04	0.15	0.09	0.06	0.20	0.08	0.40	0.40	0.45
		2002		0.70		0.20		0.30		0.30		0.20	0.30	0.48
		2003			0.20	0.09		0.06	0.06	0.20		0.18	0.09	0.10
		2004	0.04	0.28	0.97	0.74	0.11	0.18	0.08	0.35	2.10		1.51	1.12
		2005	0.05	0.27	0.14	0.41	0.40	0.69	0.89		2.08	1.28	0.27	0.45

APPENDIX A

Site	Species	Year	Month Concentration in ppb per month											
AF	NO_2		Jan	Feb	Mar	Apr	May	Jun	Jul	Aug	Sep	Oct	Nov	Dec
		1995												
		1996												
		1997								4.33		3.32	4.03	3.52
		1998	2.79			2.28	2.10	2.55	2.18	3.30		3.75		
		1999	2.78					2.33	3.68		4.50	4.73	4.20	4.50
		2000	1.05	2.48	2.25	1.95	2.63		2.55	1.65			1.95	
		2001				1.20	0.98	3.75						0.45
		2002	0.30		0.15	0.38	1.58	1.65	0.68	1.35	0.98	1.35	2.18	1.73
		2003	1.50	1.84	4.49		3.50	3.18	2.18	4.21	2.72	3.14	3.94	
		2004		1.01	2.01	1.50	2.64	1.50	2.26	1.41				1.87
		2005	2.18	3.63		2.57	3.62	2.51	3.32	5.50		7.07	2.80	2.35
LT	NO_2		Jan	Feb	Mar	Apr	May	Jun	Jul	Aug	Sep	Oct	Nov	Dec
		1995					3.58		0.34	1.19	1.02	1.07	0.57	0.78
		1996	0.41	2.48	3.23	0.97	0.46	0.89	0.88	0.85	1.01	1.25	1.31	1.11
		1997	0.90	0.69		0.57	0.66	0.93	0.74	0.90	1.22	1.19	0.80	1.06
		1998	0.82	1.20		0.75	0.75		0.98		0.83		1.05	1.05
		1999	1.05	0.53						1.20	1.35	0.75	0.90	0.68
		2000	0.45	0.23	0.30		0.68	0.45	0.45			0.45		
		2001			0.30	0.30	0.30	0.75	0.83				0.10	0.06
		2002	0.14	0.13	0.14	0.23	0.60	0.30		0.08	0.38	0.14	0.30	0.68
		2003	0.09	0.06	0.39	0.52	0.69	0.40	1.30	0.69	1.17	1.34	0.84	0.71
		2004		0.47	0.73		0.31	0.50	0.24	0.19	0.71	0.83		0.77
		2005	0.79	0.21	0.11	0.27	0.13	0.67	2.61				1.07	0.66
CP	NO_2		Jan	Feb	Mar	Apr	May	Jun	Jul	Aug	Sep	Oct	Nov	Dec
		1995						2.37	2.20	2.03	1.25	0.55	0.40	0.68
		1996	1.29	1.04	4.89	2.18	2.91	2.91	2.90	1.69	2.14	1.18	1.04	0.78
		1997	0.60	1.21	1.17	3.11		2.93	2.87	1.79	1.05	0.85	0.73	0.85
		1998		1.09	0.77	2.20	1.20	2.94	1.35	1.35	0.75	0.60	0.60	1.20
		1999	0.53	0.68	0.98	1.05	2.18	2.78	2.33	2.03	0.75	0.75		
		2000	0.60	0.75		0.83	0.75					0.38	0.53	0.45
		2001	0.38	0.60	1.20	0.23		0.83	2.25	0.83				0.23
		2002						1.58		0.38	0.38	0.21	0.08	0.30
		2003	0.53	0.60	0.87		0.70	0.59	1.92	1.99	0.46	1.04		0.38
		2004	0.70	0.87	1.19	1.00	1.15	2.47	1.30	0.59	0.63	0.75	0.32	0.41
		2005	0.27	0.71	0.77	1.39	2.15	1.43	1.48	1.41	0.73	0.71	0.80	0.32
NA	NO_2		Jan	Feb	Mar	Apr	May	Jun	Jul	Aug	Sep	Oct	Nov	Dec
		1995						0.36	0.52	0.45	0.29	1.28	0.44	0.28
		1996	0.46	0.90	0.34	0.28	0.20	0.15	0.27	0.53	0.12	0.28	0.46	0.51
		1997	0.80	0.48	0.35	0.18		0.17	0.18	0.26	0.34	0.39	0.19	0.63
		1998	0.35	0.23	0.98	0.37		0.24	0.15	0.14	0.15	0.15	0.38	0.38
		1999	0.60	0.38	0.45	0.45	0.14	0.14	0.23	0.30	0.45	0.30		
		2000	0.30	0.21		0.30	0.75					0.75	0.45	0.90
		2001	0.60	0.30	0.60	0.38		0.45	0.68	0.60	1.13		0.30	0.15
		2002	0.45	0.05	0.11	0.05		0.20	0.19	0.07	0.30	0.05	0.06	0.05
		2003	0.45	0.60	0.75		1.74	0.69	0.26	0.14	0.35	0.09	0.29	0.25
		2004	0.32	0.27	0.23	0.29	0.40	0.08	0.11	0.13	0.09	0.05	0.15	0.36
		2005	0.42	0.10	0.28	0.10	0.25	0.14	0.11	0.07	0.25	0.39	0.41	0.25

APPENDIX A

Site	Species	Year	Concentration in ppb per month											
AF	O_3		Jan	Feb	Mar	Apr	May	Jun	Jul	Aug	Sep	Oct	Nov	Dec
		1995												
		1996												
		1997								35.9		36.5	34.6	42.9
		1998	29.3			24.2	21.5	24.1	23.4	30.6		38.4		
		1999	35.1					30.6	33.2		37.1	34.5	37.7	44.9
		2000	16.3	15.6	14.3	10.4	13.7		18.9	18.2			29.3	
		2001				17.6	15.0	23.4	16.9	44.9		43.6	25.4	23.4
		2002			18.2	29.3	26.7	16.9	24.1	37.7	32.5	24.1	13.0	
		2003			25.4		20.4	16.9	25.6	19.1	25.0	20.7	41.1	30.3
		2004		38.7	13.1	27.3	33.8	15.9	19.6	17.4	34.6			17.0
		2005	26.3	27.2		14.0	15.0	15.0	18.5	43.7		44.3	40.6	22.3
LT	O_3		Jan	Feb	Mar	Apr	May	Jun	Jul	Aug	Sep	Oct	Nov	Dec
		1995					36.2		43.2	35.8	37.6	41.5	43.0	37.1
		1996	29.1	22.0	30.9	49.9	32.6	42.5	43.8	46.0		57.2	52.5	46.0
		1997	35.1	25.1		40.7	28.8	43.8	51.2	21.0	52.3	38.1	37.2	37.8
		1998	41.8	52.0		28.0	41.0	0.0	39.7		42.9		42.9	28.6
		1999	28.6	24.1							36.4	33.8	33.2	25.4
		2000	18.2	38.4	37.1		22.8	23.4	29.9			27.3		
		2001		16.3	15.6	17.6	16.9	17.6		25.4			23.4	
		2002			21.5	25.4	34.5	31.2		37.1	46.2	46.8	49.4	53.3
		2003	29.9	1.2	41.6	36.6	43.6	27.7	38.8	30.9	24.0	28.0	21.0	30.9
		2004		17.6				19.2	23.3	29.0	36.0	29.6		26.6
		2005	25.4	23.8	20.2			46.2	52.8		24.7		25.5	21.5
CP	O_3		Jan	Feb	Mar	Apr	May	Jun	Jul	Aug	Sep	Oct	Nov	Dec
		1995	25.4	24.2	31.5	34.0	31.7	47.0	35.4	34.3	34.6	32.9	22.1	
		1996	20.8	21.9	29.3	30.3	43.4	33.2	30.2	30.6		29.9	18.8	15.8
		1997	15.5	23.1	31.5	19.8	30.2		39.3	36.1	28.6	38.5	17.9	31.2
		1998	10.8	13.1	48.1	27.1	30.6	34.5	30.6	28.0	27.3		11.7	
		1999	26.7	20.8	35.8						22.1		28.6	
		2000	22.1	11.1	11.7		13.0				18.9	24.1	22.8	
		2001	13.0	13.7	17.6	15.6	7.2	19.5	21.5	29.3	28.0	26.0		28.6
		2002		33.8		51.4		45.0		27.3			67.4	54.0
		2003	15.0		12.6	38.2		35.0	26.3	36.3		48.5	15.4	3.3
		2004	28.9	31.3	10.0	20.8	23.1	24.8	27.4	27.9	24.9	20.4	20.8	
		2005	16.2	21.4	22.9	15.6	27.1	26.3	27.5		27.1	29.4	34.7	23.0
NA	O_3		Jan	Feb	Mar	Apr	May	Jun	Jul	Aug	Sep	Oct	Nov	Dec
		1995	37.8	27.2	23.2	27.0	24.5	17.8	16.2	21.9	33.3	16.4	29.1	
		1996	37.9	29.8	30.6	22.7	29.2	32.1	32.2	33.1		37.3	31.6	46.1
		1997	23.6	28.2	24.0	28.8	21.9		26.0	22.8	15.6	26.7	23.4	25.4
		1998	20.2	24.7	26.0	20.2	20.2	26.0	22.1	22.8	22.1		21.5	
		1999	11.7	10.4	16.3						35.8		25.4	
		2000	20.2	18.9	18.9	15.0			18.2			29.9	18.9	
		2001	15.0	18.9	12.4	15.6	14.3	15.0	16.3	30.6	28.0	12.4		15.0
		2002		19.5		22.1		24.1		18.2			24.1	74.5
		2003	56.0		25.9	24.7			22.5	20.0		23.7	26.4	32.8
		2004	22.9	21.8	27.1	10.4	13.2	19.1	21.4	17.7		17.0	32.6	26.1
		2005	18.6	24.2	13.8	8.2	19.2	18.5	15.6		23.6	36.8	12.7	30.3

APPENDIX A

Site	Species	Year	Concentration in ppb per month											
AF	NH_3		Jan	Feb	Mar	Apr	May	Jun	Jul	Aug	Sep	Oct	Nov	Dec
		1995												
		1996												
		1997							2.33	2.42	3.14	2.58	1.57	2.33
		1998		1.83	1.68	1.50		1.68		1.60	2.20		2.13	
		1999	1.88		1.83					1.93	2.08	2.75	1.93	1.68
		2000	2.33	1.83	1.58		1.20	0.68	1.20				0.58	
		2001		0.40		0.25	0.23	0.58	0.30	0.50		0.35	0.50	0.30
		2002	0.23	0.28	0.55	0.65	1.00	2.63		1.18	0.20	1.43	1.23	0.39
		2003	0.56	2.81	0.30	1.13	0.42	0.34	1.12	0.93	0.62	0.60	0.50	
		2004	0.71	0.23		0.20	0.37	0.91	1.42	0.84	0.71		0.40	0.32
		2005	0.30	0.40	0.76	0.22	0.23	0.81	0.29		0.87		0.64	0.57
LT	NH_3		Jan	Feb	Mar	Apr	May	Jun	Jul	Aug	Sep	Oct	Nov	Dec
		1995					0.72		1.15	0.57	0.41	0.75	1.84	0.33
		1996	1.30	0.27	0.31		0.35	0.27	1.28	1.52	4.80	2.74	2.51	1.52
		1997		1.65	1.26	1.68	1.82	1.43	1.40	2.16	1.29	3.25	2.96	1.06
		1998		1.12	1.18	1.13		1.05	2.03	3.58			2.20	1.83
		1999			0.95					1.78	2.05	1.33	1.68	1.68
		2000	1.83	2.25	1.03		1.63	1.48	0.85			0.43		
		2001	0.40			0.25	0.75	0.53	0.25	0.23		0.20	0.73	0.60
		2002	0.58	0.53	0.28	0.40	0.40	0.60		1.10	0.20	0.13	0.65	1.50
		2003	2.67	0.47	1.74	0.64	0.60	0.20	1.01	2.10	0.91	0.52	0.40	0.60
		2004		0.88		1.00	0.45	0.52	0.33	0.41	0.64	1.06		0.89
		2005	0.23		0.24	0.29	0.37	0.89	0.22		0.26	0.69	0.69	0.72
CP	NH_3		Jan	Feb	Mar	Apr	May	Jun	Jul	Aug	Sep	Oct	Nov	Dec
		1995					0.78		0.47	1.45	1.33	0.91	0.73	1.33
		1996	1.61	1.60	1.68	0.67	1.45	1.37	1.48	1.94	1.77	1.58	2.82	2.73
		1997	3.62	1.88	2.17	1.68	2.39	1.38	1.58	1.90	2.44	2.16	2.23	1.65
		1998		3.66		2.22	2.82	1.37		2.00	3.20		2.88	
		1999	3.13		2.54					2.20	1.23	1.55	1.23	2.90
		2000	2.08	2.25	1.50		2.05	0.35	0.73			0.48		
		2001	0.28			0.90	1.60	1.40	4.40	4.25		4.25	0.78	1.20
		2002	1.10	1.15	2.53	1.33	1.63	2.23		3.35	3.68	3.88	4.83	0.95
		2003	1.17	5.48	6.95	4.27	1.13	1.42	1.49	2.67	1.75	1.60	2.17	0.20
		2004		1.08	1.35		2.71	3.64	1.55		0.79	1.61	0.88	0.58
		2005	0.67	1.12	0.66	0.47	3.93	1.19	0.91		1.06		1.59	1.06
NA	NH_3		Jan	Feb	Mar	Apr	May	Jun	Jul	Aug	Sep	Oct	Nov	Dec
		1995					0.40		0.74	0.45	1.56	1.38	2.27	1.96
		1996	1.13	2.22	0.59	0.98	0.92	2.27	3.10	2.12	1.67	2.34	1.11	1.50
		1997	1.74	1.09	3.45	2.48	3.22	2.45	3.06	0.91	1.23	2.58	1.47	2.45
		1998	3.08	2.43		5.00	3.83		2.53		2.63		1.65	1.23
		1999		1.40						1.73	1.93	2.55	2.03	1.33
		2000	2.03	2.05	4.35		2.23	2.18	0.58			1.35		
		2001	2.13			1.25	1.05	3.08	1.00	0.73		0.48	0.20	0.20
		2002	0.50	0.63	0.95	0.21	0.58	0.25		0.68	0.75	3.40	2.78	1.18
		2003	1.35	2.89	0.92	0.25	0.20	0.28	1.18	0.78	1.47	1.87	0.90	0.75
		2004		0.28		0.46	0.47	0.84	0.61	1.28	1.51	1.12		0.20
		2005	2.73	0.66	1.68	0.60	0.95	1.00	0.73		1.00		0.84	0.75

APPENDIX A

Site	Species	Year	Concentration in ppb per month											
AF	HNO_3		Jan	Feb	Mar	Apr	May	Jun	Jul	Aug	Sep	Oct	Nov	Dec
		2003					0.10	0.40	0.12	0.10	0.10	0.50	0.40	0.45
		2004	0.59	1.18	0.10	1.81	0.57	0.36	0.42	1.79	0.36	0.35	0.70	0.80
		2005	1.97	1.28	1.45	0.79	0.74	0.78	1.02	0.83	1.10	1.79	2.50	0.97
LT	HNO_3		Jan	Feb	Mar	Apr	May	Jun	Jul	Aug	Sep	Oct	Nov	Dec
		2003					0.10	0.10	0.12	0.26	0.10	0.12	0.49	0.10
		2004		0.10	0.39	0.36	0.23	0.26	0.57	0.50	0.20	0.20	0.23	0.30
		2005	0.45	0.10	0.10	0.10	0.36		0.41	0.44	0.35	0.33	0.32	0.10
CP	HNO_3		Jan	Feb	Mar	Apr	May	Jun	Jul	Aug	Sep	Oct	Nov	Dec
		2003					0.10	0.33	0.64	2.50	2.50	0.85	0.40	0.50
		2004	1.01	0.19	0.10	0.10	0.50	0.47	0.67	0.46	0.70	1.12	0.29	0.20
		2005	0.19	0.18	0.49	0.35	0.43	0.52	0.51	0.77	0.62	0.30	1.84	0.30
NA	HNO_3		Jan	Feb	Mar	Apr	May	Jun	Jul	Aug	Sep	Oct	Nov	Dec
		2003				0.10	0.10	0.10	0.10	0.10	0.10	0.10	0.33	0.31
		2004	0.10	0.11	0.13	0.11	0.10	0.15	0.23	1.21	0.86	1.42	0.35	0.44
		2005	0.10	0.72	0.65	0.10	0.27		0.16	0.20	0.38	0.18	0.10	

APPENDIX B

Date		Site	Size	CH_3COO^-	$HCOO^-$	Cl^-	NO_3^-	SO_4^{2-}	$C_2O_4^{2-}$	Na^+	NH_4^+	K^+	Mg^{2+}	Ca^{2+}	OC	BC
2005-08-30	2005-08-31	LT	2.5	0.01	1.02	0.19		4.23	0.48		1.25	0.62	0.06	0.12	4.24	1.85
2005-08-31	2005-09-01	LT	2.5		1.56	0.01	0.35	2.57	0.25	0.21	0.74	0.55	0.03	0.06	5.69	2.24
2005-09-01	2005-09-02	LT	2.5	0.06	0.87	0.05	0.93	2.06	0.59	0.39	0.56	1.20	0.05	0.10	1.08	2.20
2005-09-02	2005-09-03	LT	2.5	0.04	1.05		0.77	2.24	0.54	0.31	0.60	1.08	0.05	0.11	8.43	3.11
2005-09-03	2005-09-04	LT	2.5	0.01	0.79	0.02	0.83	1.77	0.56	0.41	0.42	1.02	0.04	0.10	8.36	2.49
2005-09-04	2005-09-05	LT	2.5	0.09	0.79	0.02	0.62	3.29	0.48	0.27	1.03	1.05	0.05	0.11	9.39	3.80
2005-09-05	2005-09-06	LT	2.5	0.04	0.72		0.38	4.49	0.52	0.18	1.43	0.97	0.05	0.13	8.05	3.03
2005-09-06	2005-09-07	LT	2.5	0.06	0.44	0.03	0.44	4.54	0.57	0.45	1.25	0.98	0.03	0.08	2.84	2.03
2005-09-07	2005-09-08	LT	2.5	0.02	1.17	0.01	0.27	1.56	0.22	0.17	0.50	0.36	0.01	0.03		
2005-09-08	2005-09-09	LT	2.5		0.57	0.02	0.37	2.46	0.24	0.28	0.79	0.44	0.02	0.05	3.77	5.32
2005-09-09	2005-09-10	LT	2.5	0.02	0.53	0.51	0.38	1.17	0.11	0.56	0.24	0.18	0.05	0.06	3.29	4.01
2005-09-10	2005-09-11	LT	2.5		0.38	0.50	0.66	2.11	0.12	0.68	0.64	0.19	0.04	0.05		
2005-09-11	2005-09-12	LT	2.5	0.01	0.35	0.11	0.32	1.13	0.08	0.29	0.26	0.17	0.03	0.04	2.10	2.90
2005-09-12	2005-09-13	LT	2.5	0.01	0.36	0.13	0.44	1.52	0.11	0.40	0.39	0.21	0.04	0.07	1.47	3.98
2005-08-30	2005-08-31	LT	10	0.00	0.81	0.03	0.91	3.89	0.36	0.54	1.17	0.61	0.05	0.07	4.05	2.08
2005-08-31	2005-09-01	LT	10	0.00	1.08	0.09	0.96	2.70	0.36	0.45	0.81	0.64	0.05	0.10	5.96	2.59
2005-09-01	2005-09-02	LT	10	0.09	0.99	0.03	1.67	2.41	0.70	0.59	0.64	1.27	0.08	0.17	8.83	2.91
2005-09-02	2005-09-03	LT	10	0.06	1.41	0.04	1.61	2.49	0.64	0.71	0.55	1.26	0.06	0.13	12.8	4.64
2005-09-03	2005-09-04	LT	10	0.09	0.93	0.10	1.99	1.99	0.70	0.91	0.45	1.10	0.09	0.17	6.77	2.44
2005-09-04	2005-09-05	LT	10	0.08	1.16	0.06	1.30	2.77	0.67	0.57	0.77	1.08	0.06	0.11	6.61	2.72
2005-09-05	2005-09-06	LT	10	0.03	0.60	0.05	0.80		0.19	0.29	0.20	0.27	0.01	0.02	2.69	2.82
2005-09-06	2005-09-07	LT	10	0.07	0.84	0.02	0.73	4.83	0.68	0.35	1.59	1.09	0.06	0.15	8.35	2.71
2005-09-07	2005-09-08	LT	10	0.00	0.47	0.11	1.13	1.74	0.30	0.58	0.54	0.40	0.03	0.06		
2005-09-08	2005-09-09	LT	10		1.37	0.12	1.04	1.68	0.26	0.53	0.25	0.48	0.04	0.08	6.52	7.18
2005-09-09	2005-09-10	LT	10		1.04	1.42	0.67	1.43	0.08	1.18	0.10	0.15	0.10	0.11	2.99	3.11
2005-09-10	2005-09-11	LT	10	0.01	0.40	1.66	1.31	2.35	0.14	1.56	0.68	0.22	0.11	0.12	0.82	1.28
2005-09-11	2005-09-12	LT	10	0.01	0.39	0.79	0.67	1.26	0.10	0.86	0.29	0.21	0.06	0.10	2.45	1.77
2005-09-12	2005-09-13	LT	10		1.07	1.28	0.93	1.56	0.09	1.15	0.09	0.27	0.11	0.15	0.63	3.49

Species concentration in $\mu g.m^{-3}$

APPENDIX B

Date		Site	Size	CH_3COO^-	$HCOO^-$	Cl^-	NO_3^-	SO_4^{2-}	$C_2O_4^{2-}$	Na^+	NH_4^+	K^+	Mg^{2+}	Ca^{2+}	OC	BC
2005-08-30	2005-08-31	AF	2.5	0.04	0.67	0.08	0.89	1.76	0.23	0.18	0.83	0.25	0.02	0.06	6.52	3.09
2005-08-31	2005-09-01	AF	2.5												7.59	3.52
2005-09-01	2005-09-02	AF	2.5	0.16	0.54	0.23	1.39	6.31	0.85	0.63	2.03	1.46	0.04	0.17	9.48	4.65
2005-09-02	2005-09-03	AF	2.5												18.5	6.00
2005-09-03	2005-09-04	AF	2.5	0.07	0.63	0.28	0.46	3.17	0.49	0.35	1.01	0.79	0.16	0.14	1.84	1.22
2005-09-04	2005-09-05	AF	2.5	0.08	0.65	0.10	0.92	2.85	0.50	0.23	1.01	0.88	0.04	0.51	8.13	5.83
2005-09-05	2005-09-06	AF	2.5	0.03	0.80	0.12	1.05	3.44	0.49	0.27	1.17	0.96	0.04	0.19	2.00	4.20
2005-09-06	2005-09-07	AF	2.5	0.04	1.23	0.05	0.07	2.63	0.18	0.13	0.85	0.36	0.02	0.08	2.25	1.94
2005-09-07	2005-09-08	AF	2.5	0.01	0.27	0.01	1.14	5.06		0.14	1.90	0.46	0.03	0.10	4.03	1.95
2005-09-08	2005-09-09	AF	2.5	0.05	0.39	0.01	0.32	1.82	0.15	0.14	0.60	0.28	0.02	0.07	10.5	4.43
2005-09-09	2005-09-10	AF	2.5	0.04	0.39		0.38	4.46	0.19	0.18	1.56	0.30	0.03	0.11	5.50	2.19
2005-09-10	2005-09-11	AF	2.5	0.09	0.38	0.02	0.56	2.57	0.24	0.18	0.95	0.37	0.04	0.11		
2005-09-11	2005-09-12	AF	2.5	0.18	0.30	0.02	0.77	1.06	0.15	0.09	0.66	0.32	0.03	0.08		
2005-09-12	2005-09-13	AF	2.5	0.11	0.25	0.03	0.42	1.63	0.24	0.06	0.70	0.48	0.03	0.12		
2005-08-30	2005-08-31	AF	10	0.04	0.68	0.15	0.93	3.11	0.36	0.39	1.02	0.51	0.06	0.21	8.27	4.15
2005-08-31	2005-09-01	AF	10	0.05	0.68	0.06	1.55	4.46	0.47	0.66	1.28	0.83	0.10	0.31	7.07	3.40
2005-09-01	2005-09-02	AF	10		0.55	0.03		1.39	0.13	0.10	0.44	0.24	0.02	0.07	7.97	3.04
2005-09-02	2005-09-03	AF	10	0.20	0.85	0.07	1.77	6.80	0.93	0.65	2.20	1.51	0.08	0.32	12.8	6.00
2005-09-03	2005-09-04	AF	10	0.12	0.71	0.03	1.33	3.45	0.62	0.33	1.18	0.84	0.15	0.27	1.84	1.22
2005-09-04	2005-09-05	AF	10	0.07	0.65	0.07	2.06	3.10	0.63	0.28	1.21	0.92	0.09	0.42	8.13	5.83
2005-09-05	2005-09-06	AF	10	0.08	0.84	0.17	1.93	3.79	0.66	0.49	1.33	1.07	0.08	0.30		
2005-09-06	2005-09-07	AF	10	0.02	0.47	0.03	0.28	2.69	0.24	0.17	0.87	0.32	0.02	0.09	2.25	1.94
2005-09-07	2005-09-08	AF	10	0.07	0.45	0.04	1.79	5.14	0.30	0.35	1.83	0.48	0.07	0.23	4.03	1.95
2005-09-08	2005-09-09	AF	10	0.05	0.41	0.14	1.02	2.05	0.21	0.36	0.70	0.30	0.05	0.15	10.5	4.43
2005-09-09	2005-09-10	AF	10	0.08	0.39	0.08	1.53	4.75	0.27	0.37	1.74	0.33	0.09	0.22	5.50	2.19
2005-09-10	2005-09-11	AF	10	0.13	0.26	0.13	1.50	2.73	0.34	0.41	1.07	0.42	0.07	0.20		
2005-09-11	2005-09-12	AF	10	0.14	0.36	0.06	0.74	1.17	0.23	0.19	0.56	0.32	0.04	0.15		
2005-09-12	2005-09-13	AF	10	0.19	0.35	0.07	1.74	1.70	0.36	0.10	1.05	0.51	0.07	0.22		

***Species concentration in $\mu g.m^{-3}$**

APPENDIX B

Date		Site	Size	CH_3COO^-	$HCOO^-$	Cl^-	NO_3^-	SO_4^{2-}	$C_2O_4^{2-}$	Na^+	NH_4^+	K^+	Mg^{2+}	Ca^{2+}	OC	BC
2006-07-24	2006-07-25	LT	2.5	0.03		0.09	0.36	2.93	0.20	0.14	0.95	0.47	0.01	0.01	2.51	0.99
2006-07-25	2006-07-26	LT	2.5	0.03	0.05	0.11	0.32	2.68	0.22	0.18	0.84	0.54	0.01	0.01	3.44	1.15
2006-07-26	2006-07-27	LT	2.5	0.02	0.06	0.05	0.32	2.94	0.19	0.20	0.96	0.35	0.01	0.01	2.42	1.06
2006-07-27	2006-07-28	LT	2.5			0.10	0.28	3.21	0.17	0.31	1.16	0.31	0.01		3.00	2.06
2006-07-28	2006-07-29	LT	2.5	0.03	0.09	0.09	0.52	3.28	0.18	0.14	1.15	0.31	0.01	0.04	1.90	1.47
2006-07-29	2006-07-30	LT	2.5	0.03	0.03	0.04	0.25	2.41	0.15	0.15	0.83	0.24	0.01	0.02	1.92	0.47
2006-07-30	2006-07-31	LT	2.5	0.04	0.12	0.13	0.30	0.51		0.24	0.19	0.25	0.01	0.01	2.20	1.01
2006-07-31	2006-08-01	LT	2.5	0.03	0.08	0.10	0.30	0.63	0.15	0.17	0.19	0.30	0.02	0.01	3.05	1.48
2006-08-01	2006-08-02	LT	2.5	0.04		0.09	0.33	0.95	0.18	0.14	0.25	0.41	0.01	0.01	3.30	3.70
2006-08-02	2006-08-03	LT	2.5	0.02	0.09	0.03	0.30	0.59		0.13	0.10	0.36	0.01	0.02	0.65	0.35
2006-08-03	2005-10-09	LT	2.5			0.03	0.33	0.85	0.15	0.15	0.35	0.38	0.00	0.01	1.00	0.16
2006-08-04	2006-08-04	LT	2.5	0.03	0.12	0.06	0.21	0.27	0.18	0.12	0.13	0.31	0.01	0.01		
2006-08-05	2006-08-05	LT	2.5	0.03	0.07	0.07	0.34	2.01	0.18	0.14	0.76	0.43	0.01	0.01	2.87	0.53
2006-08-06	2006-08-07	LT	2.5	0.03	0.07	0.06	0.31	1.76	0.10	0.11	0.64	0.40	0.01	0.01	1.20	0.47
2006-07-24	2006-07-25	LT	10	0.07	0.03	0.04	0.52	3.06	0.26	0.22	0.99	0.51	0.03	0.10	4.97	1.69
2006-07-25	2006-07-26	LT	10	0.06	0.02	0.04	0.75	2.93	0.30	0.26	0.92	0.59	0.03	0.11	5.08	1.50
2006-07-26	2006-07-27	LT	10	0.05	0.02	0.04	0.43	3.01	0.25		0.99	0.40	0.02	0.08	3.16	1.06
2006-07-27	2006-07-28	LT	10	0.03	0.04	0.05	0.54	3.32	0.22	0.23	1.02	0.34	0.03	0.09	3.16	1.31
2006-07-28	2006-07-29	LT	10	0.04	0.19	0.15	1.15	4.11	0.26	0.51	1.40	0.37	0.03	0.09	4.47	1.31
2006-07-29	2006-07-30	LT	10	0.04	0.30	0.31	0.96	2.71	0.21	0.54	0.91	0.28	0.05	0.08		
2006-07-30	2006-07-31	LT	10	0.02	0.85	0.86	0.38	0.70		0.69	0.23		0.07	0.07	1.45	0.75
2006-07-31	2006-08-01	LT	10	0.05	0.56	0.58	1.08	0.90	0.21	0.70	0.25	0.41	0.08	0.15	3.65	1.20
2006-08-01	2006-08-02	LT	10	0.06	0.10	0.12	0.87	1.03	0.24	0.33	0.31	0.45	0.05	0.15		
2006-08-02	2006-08-03	LT	10	0.01	0.08	0.09	0.56	0.29			0.12		0.01	0.08	1.45	0.31
2006-08-03	2006-10-09	LT	10		0.03	0.04	0.81	0.94		0.43	0.39	0.44	0.01	0.06	1.78	0.44
2006-08-04	2006-08-04	LT	10	0.01	0.01			0.32		0.67	0.16	0.19	0.01	0.12	1.47	0.66
2006-08-05	2006-08-05	LT	10	0.03	0.02		0.32	2.22	0.10	0.09	0.84	0.56	0.01	0.05	1.85	0.72
2006-08-06	2006-08-07	LT	10	0.04	0.14	0.21	0.69	1.98	0.13	0.36	0.70	0.18	0.05	0.07	1.12	0.16

***Species concentration in $\mu g.m^{-3}$**

APPENDIX B

Date		Site	Size	CH_3COO^-	$HCOO^-$	Cl^-	NO_3^-	SO_4^{2-}	$C_2O_4^{2-}$	Na^+	NH_4^+	K^+	Mg^{2+}	Ca^{2+}	OC	BC
2006-07-24	2006-07-25	AF	2.5	0.05	0.04	0.07	1.85	5.88	0.35	0.12	2.32	0.93	0.01	0.10	8.32	3.38
2006-07-25	2006-07-26	AF	2.5	0.06	0.03	0.06	1.25	4.14	0.30	0.11	1.60	0.80	0.01	0.03	9.65	2.34
2006-07-26	2006-07-27	AF	2.5	0.05	0.04	0.14	1.11	2.84	0.24	0.09	1.14	0.69	0.01	0.09	5.77	4.50
2006-07-27	2006-07-28	AF	2.5												6.00	1.88
2006-07-28	2006-07-29	AF	2.5	0.03	0.02	0.04	0.31	3.95	0.18	0.12	1.37	0.42	0.01	0.06	4.31	1.45
2006-07-29	2006-07-30	AF	2.5	0.04	0.03	0.03	0.19	2.64	0.14	0.10	0.93	0.30	0.00	0.02	5.36	1.97
2006-07-30	2006-07-31	AF	2.5	0.03	0.02	0.04	1.28	5.91	0.19	0.09	2.30	0.50	0.02	0.03	5.15	1.95
2006-07-31	2006-08-01	AF	2.5	0.02	0.02	0.04	1.16	3.73	0.16	0.10	1.54	0.35	0.02	0.04	2.30	1.57
2006-08-01	2006-08-02	AF	2.5	0.01	0.01	0.05	0.34	0.97	0.10	0.33	1.69	0.46	0.10	0.32	0.73	0.58
2006-08-02	2006-08-03	AF	2.5	0.00	0.00	0.02	0.04	0.71	0.02	0.03	0.28	0.02	0.00	0.02	2.20	0.50
2006-08-03	2006-10-09	AF	2.5	0.00		0.01	0.04	0.45	0.02	0.03	0.17	0.01		0.00		
2006-08-04	2006-08-04	AF	2.5	0.01	0.01	0.15	0.08		0.02	0.11	0.06	0.04		0.01	2.09	1.12
2006-08-05	2006-08-05	AF	2.5	0.01	0.01	0.02	0.61	1.73	0.05	0.06	0.75	0.08	0.00	0.02	0.49	0.52
2006-08-06	2006-08-07	AF	2.5													
2006-07-24	2006-07-25	AF	10	0.05	0.05	0.11	1.51	2.85	0.24	0.07	1.15	0.69	0.01	0.08		
2006-07-25	2006-07-26	AF	10	0.07	0.07	0.05	2.25	6.83	0.43	0.17	2.48	0.99	0.03	0.19	7.64	1.05
2006-07-26	2006-07-27	AF	10	0.12	0.07	0.19	1.87	6.07	0.45	0.24	2.84	0.86	0.06	0.22	4.64	1.03
2006-07-27	2006-07-28	AF	10	0.09	0.06	0.12	1.98	5.29	0.40	0.19	1.73	0.84	0.05	0.26	3.61	2.72
2006-07-28	2006-07-29	AF	10	0.11	0.04	0.07	0.60	4.19	0.23	0.16	1.45	0.46	0.03	0.14	5.60	2.15
2006-07-29	2006-07-30	AF	10	0.04	0.03	0.05	0.42	2.68	0.19	0.14	0.97	0.32	0.02	0.11	3.51	1.71
2006-07-30	2006-07-31	AF	10	0.05	0.03	0.10	2.18	6.00	0.25	0.15	2.41	0.56	0.07	0.29	4.10	1.89
2006-07-31	2006-08-01	AF	10	0.05	0.03	0.21	2.32	4.02	0.22	0.33	1.68	0.45	0.10	0.32		
2006-08-01	2006-08-02	AF	10	0.03	0.02	0.08	0.65	1.11	0.14	0.19	0.37	0.26	0.06	0.14		
2006-08-02	2006-08-03	AF	10												4.85	1.30
2006-08-03	2006-10-09	AF	10												5.80	2.22
2006-08-04	2006-08-04	AF	10												4.45	0.79
2006-08-05	2006-08-05	AF	10	0.03	0.01	0.07	0.89	1.76	0.06	0.08	0.79	0.06	0.01	0.11		
2006-08-06	2006-08-07	AF	10	0.01	0.01	0.05	0.08	0.28	0.02	0.04	0.12	0.02	1.70	0.03		

Species concentration in $\mu g.m^{-3}$

APPENDIX B

Date		Site	Size	CH_3COO^-	$HCOO^-$	Cl^-	NO_3^-	SO_4^{2-}	$C_2O_4^{2-}$	Na^+	NH_4^+	K^+	Mg^{2+}	Ca^{2+}	OC	BC
2007-04-09	2007-04-10	LT	2.5		0.03	0.13	0.10	4.32	0.03	0.14	1.33	0.01	0.01	0.11	1.40	0.40
2007-04-10	2007-04-11	LT	2.5	0.02	0.03	0.01	0.04	4.47	0.07	0.11	1.30	0.03	0.01	0.04	1.73	0.68
2007-04-11	2007-04-12	LT	2.5	0.02	0.04	0.02	0.10	4.38	0.14	0.13	1.47	0.05	0.01	0.03	2.04	0.68
2007-04-12	2007-04-13	LT	2.5	0.02	0.04	0.01	0.04	6.08	0.14	0.09	1.92	0.05	0.01	0.02	3.33	0.82
2007-04-13	2007-04-14	LT	2.5	0.01	0.04	0.01	0.04	1.63	0.05	0.04	0.57	0.01		0.01	1.34	0.52
2007-04-14	2007-04-15	LT	2.5	0.02	0.02	0.04	0.06	1.21	0.06	0.07	0.43	0.01	0.00	0.01	0.82	0.65
2007-04-15	2007-04-16	LT	2.5	0.02	0.03	0.04	0.06	1.53	0.12	0.09	0.59	0.02	0.00	0.01		
2007-04-16	2007-04-17	LT	2.5	0.02	0.04	0.01	0.08	6.57	0.15	0.16	1.68	0.04	0.01	0.02	2.84	
2007-04-17	2007-04-18	LT	2.5	0.01			0.04	3.88	0.19	0.10	1.24	0.03	0.02	0.01	2.90	0.87
2007-04-18	2007-04-19	LT	2.5			0.01	0.04	5.01	0.17	0.18	1.31	0.06	0.02	0.01		1.08
2007-04-19	2007-04-20	LT	2.5	0.03	0.06	0.02	0.13	3.33	0.21	0.15	1.13	0.06	0.01	0.04	2.70	1.17
2007-04-20	2007-04-21	LT	2.5	0.03	0.04	0.05	0.02	8.44	0.10	0.08	1.85	0.04	0.01	0.01	0.79	0.65
2007-04-21	2007-04-22	LT	2.5	0.03	0.05		0.02	9.37	0.13	0.07	2.51	0.03	0.01	0.02	2.49	1.62
2007-04-22	2007-04-23	LT	2.5	0.02	0.05	0.01	0.01	4.46	0.06	0.03	1.07	0.02	0.00	0.05	1.94	1.08
2007-04-09	2007-04-10	LT	10	0.02	0.05	0.81	0.26	4.03	0.05	0.59	1.15	0.05	0.06	0.15	1.85	0.49
2007-04-10	2007-04-11	LT	10	0.01	0.02	0.12	0.53	4.28	0.10	0.38	1.16	0.07	0.04	0.10	1.01	0.51
2007-04-11	2007-04-12	LT	10	0.03	0.05	0.05	0.58	4.41	0.18	0.31	1.41	0.06	0.04	0.09		0.82
2007-04-12	2007-04-13	LT	10	0.02	0.03	0.06	0.35	4.65	0.20	0.25	1.03	0.06	0.03	0.08	3.28	1.22
2007-04-13	2007-04-14	LT	10	0.02	0.04	0.05	0.23	2.59	0.06		0.54	0.04	0.01	0.26	1.10	0.40
2007-04-14	2007-04-15	LT	10	0.01	0.03	0.07	0.30	0.93	0.08	0.15	0.35	0.04	0.02	0.11	0.94	0.16
2007-04-15	2007-04-16	LT	10			0.04	0.78	3.04	0.06	0.11	0.24	0.02	0.01	0.10	1.69	0.52
2007-04-16	2007-04-17	LT	10	0.05	0.11	0.06	0.17	5.64	0.26	0.35	1.76	0.07	0.05	0.06	2.16	
2007-04-17	2007-04-18	LT	10												2.01	0.52
2007-04-18	2007-04-19	LT	10	0.04	0.05	0.11	0.54	3.45	0.23	0.46	1.16	0.09	0.05	0.10	1.33	0.73
2007-04-19	2007-04-20	LT	10	0.02	0.04	0.11	0.61	3.87	0.21	0.36	0.99	0.08	0.04	0.37	1.22	0.45
2007-04-20	2007-04-21	LT	10			0.01	0.19	7.64	0.15	0.20	1.68	0.05	0.02	0.04	0.99	0.51
2007-04-21	2007-04-22	LT	10	0.02	0.00	0.02	0.21	8.45	0.19	0.14	2.26	0.05	0.02	0.07		
2007-04-22	2007-04-23	LT	10	0.03	0.04	0.02	0.18	6.86	0.15	0.09	1.68	0.04	0.02	0.08	1.03	0.49

Species concentration in $\mu g.m^{-3}$

APPENDIX B

Date		Site	Size	CH_3COO^-	$HCOO^-$	Cl^-	NO_3^-	SO_4^{2-}	$C_2O_4^{2-}$	Na^+	NH_4^+	K^+	Mg^{2+}	Ca^{2+}	OC	BC
2007-04-09	2007-04-10	AF	2.5	0.00	0.00		0.08	3.92	0.03	0.03	1.40	0.03		0.00	3.38	1.41
2007-04-10	2007-04-11	AF	2.5	0.01	0.01	0.04	0.21	3.65	0.08	0.11	1.31	0.12	0.00	0.02	2.34	0.94
2007-04-11	2007-04-12	AF	2.5	0.01	0.00	0.05	0.06	2.37	0.06	0.05	0.86	0.08	0.01	0.03	4.74	1.71
2007-04-12	2007-04-13	AF	2.5	0.01	0.00	0.01	0.15	4.85	0.11	0.09	1.68	0.11	0.01	0.02	0.65	0.44
2007-04-13	2007-04-14	AF	2.5												1.24	0.84
2007-04-14	2007-04-15	AF	2.5	0.01	0.01	0.04	0.17	5.88	0.08	0.04	2.21	0.05	0.01	0.04	1.85	1.13
2007-04-15	2007-04-16	AF	2.5	0.01	0.01	0.01	0.24	4.01	0.07	0.04	1.34	0.05	0.01	0.02	1.45	0.73
2007-04-16	2007-04-17	AF	2.5			0.02	0.09	2.63	0.06	0.04	0.97	0.03	0.01	0.03	3.75	1.45
2007-04-17	2007-04-18	AF	2.5	0.02	0.02	0.03	0.42	4.36	0.12	0.08	1.64	0.09	0.01	0.03	1.57	1.36
2007-04-18	2007-04-19	AF	2.5	0.01	0.01	0.10	0.79	5.29	0.07	0.11	1.94	0.15	0.02	0.08	1.24	1.10
2007-04-19	2007-04-20	AF	2.5	0.01	0.00	0.07	0.43	5.81	0.06	0.06	2.21	0.10	0.01	0.02	0.37	0.26
2007-04-20	2007-04-21	AF	2.5												1.26	0.92
2007-04-21	2007-04-22	AF	2.5	0.02	0.01	0.05	0.10		0.04	0.05	0.18	0.06	0.01	0.05	1.22	0.44
2007-04-22	2007-04-23	AF	2.5	0.02	0.01	0.08	0.20	2.03	0.07	0.09	0.78	0.10	0.01	0.02		
2007-04-09	2007-04-10	AF	10		0.00	0.01	0.11	4.13	0.05	0.06	1.35	0.05	0.01	0.03	2.55	0.54
2007-04-10	2007-04-11	AF	10	0.02	0.01	0.06	0.40	4.08	0.11	0.18	1.47	0.13	0.01	0.05	3.19	1.59
2007-04-11	2007-04-12	AF	10	0.01	0.01	0.04	0.22	2.47	0.10	0.04	0.89	0.15	0.02	0.10	4.38	1.47
2007-04-12	2007-04-13	AF	10	0.02	0.01	0.02	0.53	5.19	0.15	0.19	1.64	0.13	0.03	0.10	1.22	0.66
2007-04-13	2007-04-14	AF	10												2.16	1.66
2007-04-14	2007-04-15	AF	10	0.02	0.02	0.05	0.22	5.68	0.10	0.07	1.90	0.06	0.03	0.09	3.79	1.55
2007-04-15	2007-04-16	AF	10	0.01	0.01		0.36	4.39	0.11	0.08	1.39	0.07	0.02	0.05	0.92	0.82
2007-04-16	2007-04-17	AF	10	0.01	0.01	0.02	0.27	2.79	0.08	0.06	1.02	0.08	0.02	0.10	4.29	1.74
2007-04-17	2007-04-18	AF	10	0.02	0.01	0.09	0.24	5.21	0.08	0.12	1.93	0.14	0.03	0.13	1.45	1.17
2007-04-18	2007-04-19	AF	10	0.01	0.01	0.07	0.09	5.49	0.06	0.08	1.89	0.10	0.01	0.04	1.59	1.24
2007-04-19	2007-04-20	AF	10	0.03	0.01	0.12	0.82	4.41	0.14	0.22	1.65	0.18	0.03	0.09	1.54	0.65
2007-04-20	2007-04-21	AF	10	0.03	0.02	0.04	0.39	3.65	0.10	0.08	1.37	0.08	0.03	0.10	1.03	1.10
2007-04-21	2007-04-22	AF	10	0.00		0.03	0.16	3.47	0.08	0.06	1.32	0.05	0.01	0.05	2.32	1.15
2007-04-22	2007-04-23	AF	10	0.02	0.02	0.06	0.37	2.08	0.11	0.12	0.80	0.08	0.03	0.06		

Species concentration in $\mu g.m^{-3}$

APPENDIX B

Date		Site	Size	CH_3COO^-	$HCOO^-$	Cl^-	NO_3^-	SO_4^{2-}	$C_2O_4^{2-}$	Na^+	NH_4^+	K^+	Mg^{2+}	Ca^{2+}	OC	BC
2007-07-05	2007-07-06	LT	2.5	0.03		0.09	0.06	1.98	0.11	0.03	0.20	0.06	0.00	0.02	1.92	0.99
2007-07-06	2007-07-07	LT	2.5	0.03	0.03		0.07	2.00		0.06	0.76	0.06	0.01	0.01	1.41	0.66
2007-07-07	2007-07-08	LT	2.5	0.05	0.04	0.25		2.13	0.09	0.04	0.82	0.05	0.01	0.01	1.52	0.76
2007-07-08	2007-07-09	LT	2.5	0.03	0.02	0.33	0.47	2.36	0.10	0.21	0.87	0.14	0.01	0.03	4.37	1.72
2007-07-09	2007-07-10	LT	2.5	0.04	0.04	0.37	0.46	1.30	0.10	0.41	0.46	0.14	0.04	0.04	1.35	0.76
2007-07-10	2007-07-11	LT	2.5	0.04	0.01	0.22	0.30	1.91	0.11	0.28	0.20	0.22	0.03	0.02	1.16	0.87
2007-07-11	2007-07-12	LT	2.5													
2007-07-05	2007-07-06	LT	10	0.03	0.03	0.09	0.10	0.45	0.13	0.04	0.19	0.06	0.00	0.02	1.66	1.06
2007-07-06	2007-07-07	LT	10	0.02	0.03	0.06	0.19	1.62		0.08	0.63	0.05	0.01	0.04	0.75	0.84
2007-07-07	2007-07-08	LT	10	0.05	0.02	0.89		2.46	0.15	0.61	0.89	0.08	0.09	0.16	1.59	1.85
2007-07-08	2007-07-09	LT	10	0.03	0.04	0.02	0.84	2.51	0.14	0.04	0.95	0.19	0.02	0.06	5.72	1.16
2007-07-09	2007-07-10	LT	10	0.05	0.04	1.46	1.09	1.51	0.12	1.20	0.47	0.16	0.18	0.13	1.52	1.19
2007-07-10	2007-07-11	LT	10	0.07	0.05	1.03	0.76	0.75	0.12	0.90	0.24	0.17	0.13	0.08	1.14	0.86
2007-07-11	2007-07-12	LT	10													
2007-07-05	2007-07-06	AF	2.5	0.02	0.03	0.04	0.26	2.32	0.05	0.03	0.31	0.08	0.00	0.02	1.30	1.13
2007-07-06	2007-07-07	AF	2.5	0.03	0.02	0.04	0.46	3.28	0.08	0.03	1.60	0.09	0.01	0.11	1.52	1.19
2007-07-07	2007-07-08	AF	2.5	0.03	0.04	0.04	0.35	2.25	0.06	0.04	0.93	0.07	0.01	0.04	1.80	1.47
2007-07-08	2007-07-09	AF	2.5	0.03	0.03	0.03	0.24	1.31	0.10	0.06	0.54	0.11	0.01	0.03	2.02	0.88
2007-07-09	2007-07-10	AF	2.5	0.06	0.04	0.07	0.44		0.07	0.04	0.30	0.06	0.01	0.02	6.11	2.11
2007-07-10	2007-07-11	AF	2.5	0.06	0.06	0.19		2.46	0.15	0.05		0.20	0.05	0.01	4.78	2.52
2007-07-11	2007-07-12	AF	2.5												1.91	1.18
2007-07-05	2007-07-06	AF	10	0.03	0.03	0.13	0.71	1.48	0.06	0.07	0.71	0.17	0.05	0.08	1.25	1.17
2007-07-06	2007-07-07	AF	10	0.04	0.03	0.10	0.61	3.30	0.09	0.06	1.65	0.10	0.01	0.18	1.07	2.06
2007-07-07	2007-07-08	AF	10	0.04	0.02	0.10	0.72	2.37	0.14	0.10	1.02	0.21	0.07	0.14	1.15	2.16
2007-07-08	2007-07-09	AF	10												1.54	1.10
2007-07-09	2007-07-10	AF	10	0.16	0.09	0.38	1.55	2.63	0.28	0.43	1.02	0.39	0.21	0.42	9.08	2.24
2007-07-10	2007-07-11	AF	10	0.09	0.11	0.32		2.52	0.28	0.25	0.99	0.41	0.24	0.52	8.12	3.61
2007-07-11	2007-07-12	AF	10												1.75	1.23

Species concentration in $\mu g.m^{-3}$

Acknowledgements

Herewith I would like to offer my deepest acknowledgement and appreciation to the following entities:

My GOD - for good health and guidance during the course and completion of my studies.

My supervisor (Prof. J.J. Pienaar) and co-supervisor (Dr. C. Galy-Lacaux) for their support and knowledge making this study possible.

My parents, whose support and encouragement never faltered.